Production of bio-oil by catalytic pyrolysis of microalgae using Li-LSX-zeolite and alkali silicates

Nur Adilah Abd Rahman

Submitted for the degree of Doctor of Philosophy

Heriot-Watt University

Institute of Mechanical, Process and Energy Engineering

School of Engineering and Physical Sciences

JULY 2019

Abstract

Microalgae are promising feedstock for bio-fuels due to high productivity, fast growth rate, and for not being in competition with food crops. Also, catalytic pyrolysis couples a cost effective thermo-chemical conversion process to produce fuels and chemicals from biomass. In this work, different species of microalgae were investigated to assess their potential as pyrolysis feedstock. Pyrolysis of *Isochrysis* sp. produced the largest bio-oil yield (37 wt.%) with a low content in aromatics and N-compounds compared to the other microalgae bio-oils, suiting the requirements for producing bio-oil. *Isochrysis* microalgae therefore selected for catalysts screening study; Evaluation of Li-LSX-zeolite, micro-silica, LiNa-FA and Na-FA for the bio-oil upgrading. The bio-oil yield reduced but its quality improved in the presence of the catalysts. Li-LSX-zeolite showed a good catalytic performance, principally for bio-oil denitrogenation and good activity for olefins and aromatics production. Since the catalyst resulted the most promising material for enhancing the quality of *Isochrysis* pyrolysis, a detailed parametric study was carried out. The optimum conditions for producing bio-oil include temperatures close to 500 °C, residence time of ~ 8 secs and a catalyst: microalgae ratio of 1:1. However, N content in bio-oil can be reduced from 3.9 wt.% (non-catalytic) to barely 0.8 wt.% by increasing the catalyst ratio to 3:1, which also boosts the aromatics to five-fold those non-catalytically obtained. Due to high ash contents in the microalgae, chemical pre-treatment was carried out before pyrolysis. Pre-treatment of the algae in acid able to increase the bio-oil yield (38 wt.%) while base pre-treatment favoured gas production (61 wt.%). The acid pre-treated microalgae increased the formation of aliphatic in bio-oil simultaneously reduce N-compounds. The use of catalyst over several regeneration cycles on *Isochrysis* sp. microalgae was studied. The pre-treatment greatly affects the catalyst activity over cycles by enhanced the bio-oil yield and tuned the composition of the bio-oil with high aliphatic compounds. However, the denitrogenation capacities wasd low due to the deactivation of the acid sites of the Li-LSX-zeolite. In conclusion, Li-LSX-zeolite showed a very good denitrogenation activity, with mild deoxygenation capacity which can be useful for the production of olefins and aromatics from microalgae. **Keywords:** Microalgae, Catalytic pyrolysis, zeolite, bio-oil, Li-LSX-zeolite, denitrogenation.

Mission accomplished.

"For indeed, with hardship [will be] ease.

Indeed, with hardship [will be] ease" Quran, 94:5-6

Acknowledgements

Declaration

Academic registry
Research Thesis Submission

Name:	NUR ADILAH ABD RAHMAN		
School:	SCHOOL OF ENGINEERING AND PHYSICAL SCIENCES (EPS)		
Version: *(i.e. First, Resubmission, Final)*	Final	Degree Sought:	PhD

Declaration

In accordance with the appropriate regulations I hereby submit my thesis and I declare that:

1)   the thesis embodies the results of my own work and has been composed by myself

2)   where appropriate, I have made acknowledgement of the work of others and have made reference to work carried out in collaboration with other persons

3)   the thesis is the correct version of the thesis for submission and is the same version as any electronic versions submitted*.

4)   my thesis for the award referred to, deposited in the Heriot-Watt University Library, should be made available for loan or photocopying and be available via the Institutional Repository, subject to such conditions as the Librarian may require

5)   I understand that as a student of the University I am required to abide by the Regulations of the University and to conform to its discipline.

6)   I confirm that the thesis has been verified against plagiarism via an approved plagiarism detection application for example; Turnitin.

*   *Please note that it is the responsibility of the candidate to ensure that the correct version of the thesis is submitted.*

Signature of Candidate:		Date:	03/07/2019

Submission

Submitted By *(name in capitals)*:	
Signature of Individual Submitting:	
Date Submitted:	

For Completion in the Student Service Centre (SSC)

Received in the SSC by *(name in capitals)*:	
Method of Submission *(Handed in to SSC; posted through internal/external mail)*:	
E-thesis Submitted (mandatory for final theses)	
Signature:		Date:	

Table of contents

List of Publications

The work submitted in this thesis is, to the best of my knowledge, original and has not been submitted for any other degree.

Journal Papers

1. N. A. Abd Rahman, J. Fermoso and A. Sanna, "Effect of Li-LSX-zeolite on the in-situ catalytic deoxygenation and denitrogenation of *Isochrysis* sp. microalgae pyrolysis vapours," Fuel. Process. Technol., vol. 173, January, pp. 253-261, 2017.

2. T. Aysu, N. A. Abd Rahman, and A. Sanna, "Catalytic pyrolysis of *Tetraselmis* and *Isochrysis* microalgae by nickel ceria-based catalysts for hydrocarbon production (2016)," Energy, 103, 205-214.

Book chapter

1. Sanna, N. Adilah, and A. Rahman, "Conversion of Microalgae Bio-oil into Bio-diesel," in Algal Biorefineries, A. P. et Al., Ed. Springer International Publishing Switzerland, 2015, pp. 493–510.

Conferences Presentation

1. "Micro-algae bio-oil denitrogenation by in-situ catalytic pyrolysis with Li-LSX-zeolite", VENICE 2016, Venice, Nov 2016.

2. "Chemical pre-treatment on microalgae *Isochrysis* sp. for bio-oil production", 1st International Conference Bioresource Technology for Bioenergy, Bioproducts & Environmental Sustainability, Sitges, Oct 2016.

3. "Catalytic pyrolysis of microalgae *Isochrysis* sp. with Li-LSX-zeolite", IMPEE conference, Edinburgh, Jul 2016.

4. "Characterisation and pyrolysis of microalgae for biofuel production", 1st Biomass Emission conference, Leeds, Sept. 2015.

5. "A study on the effect of Li-LSX-zeolite catalyst on pyrolysis of marine microalgae *Isochrysis* sp.", 1st Chemistry on Energy (CEC), Edinburgh, Jul 2015.

6. "A study on the effect of metal silicate catalyst on pyrolysis of wood chips, lignin, and cellulose",23rd European Biomass conference & exhibition (EUBCE), Vienna, June 2015.

Award and grant

1. Winner for poster presentation 2014 under IMPEE, School of EPS, Heriot-Watt University.

2. Santander Travel grant for the International Conference "Bioresource Technology for Bioenergy, Bioproducts & Environmental Sustainability, 2016".

Journal Papers (In preparation)

1. N. A. Abd Rahman and A. Sanna "Lithium-sodium fly ash derived catalyst for the in-situ deoxygenation of *Isochrysis* sp. microalgae bio-oil". Submitted to: Journal of Energy Chemistry.

2. N. A. Abd Rahman and A. Sanna "Effects of aqueous pre-treatments on pyrolysis oil characteristics of microalgae *Isochrysis* sp.". Will be submitted to: Journal of Biomass and Bioenergy.

3. N. A. Abd Rahman, J. Fermoso, and A. Sanna, "Deactivation and regeneration of Li-LSX-zeolite in catalytic pyrolysis of microalgae". Will be submitted to: Journal of Energy Conversion and Management.

List of Figures

xii

List of Tables

xvi

Abbreviations

BET	Brunauer–Emmett–Teller
DTG	Derivative thermogravimetric
EA	Elemental analysis
EDX	Energy-dispersive X-ray spectroscopy
FA	Fly ash
FCC	Fluid catalytic cracking
FID	Flame ionisation detector
GC	Gas Chromatography
HHV	High heating value
Li	Lithium
Li-Na	Lithium-sodium
LSX	Low silica X-type
MS	Mass spectrometry
MW	Molecular weight
NMR	Nuclear magnetic response
PAH	Polycyclic aromatic hydrocarbons
SEM	Scanning Electron Microscopy
TGA	Thermal gravimetric analysis
TPD	Temperature programme desorption
VM	Volatile matter
XRD	X-ray diffraction
ZSM-5	Zeolite Socony Mobile-5

Chapter 1

Introduction

1.1 Background and significance of the research

Currently, there is a global focus on the transformation of the energy system from fossil sources to low carbon options, such as biofuels, hydrogen and electrical vehicles to overcome global climate change and shortage of oil reserves (Demirbas, 2011; Sacha Alberici and Gemma Toop, 2013; Mohan *et al.*, 2014). Paris climate agreement pledge to keep global temperature below two-degree Celsius above pre-industrial levels to fight the global climate change. Energy (bioenergy) and chemicals from biomass can help balance the net production of CO_2 to the atmosphere while meeting future energy and chemical demands on a sustainable basis (Yue, You & Snyder, 2014).

Bioenergy is the renewable energy which is derived from biological matter or "biomass". Biomass can be anything from plants, crops, various waste that can be converted into energy used for electricity, heat and transport fuel. Figure 1-1 illustrates the UK renewable energy resources. Currently, about 70.72% of renewable energy comes from bioenergy such as bio-diesel, bio-ethanol and bio-gas. Wind energy contributes about 20.8% to renewable energy followed by solar (4.2%) and hydro (3.25%)(Energy and Climate Change Committee, 2016). In 2017, the UK produced about 368 million litres of liquid biofuels, which is consumed as transportation fuels. The bioethanol consumption in 2017 accounted for approximately 190 million litres followed by biodiesel consumption (178 million litres) (DEFRA: Department for Environment Food & Rural Affairs, 2017). The UK has established a goal of 10% of transport fuels to come from renewable sources by 2020 (Energy and Climate Change Committee, 2016). Accomplishing this goal would require an increase in biomass use and efficient conversion technologies.
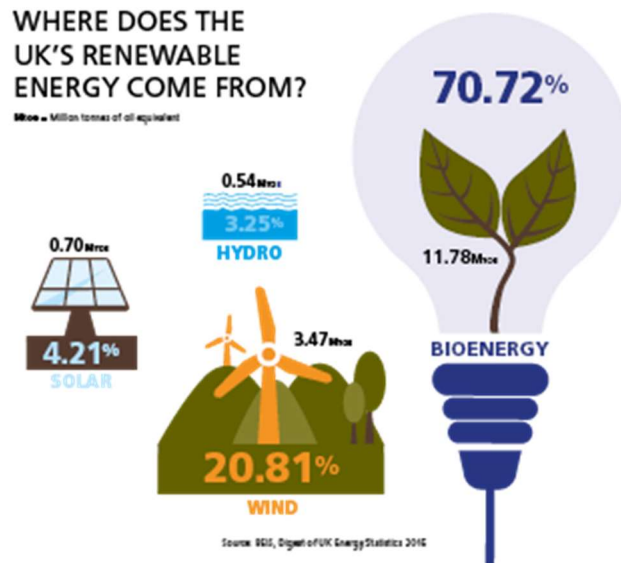
Figure 1-1 UK's bioenergy resources. (Energy and Climate Change Committee, 2016).

First-generation biofuels such as bioethanol and biodiesel, are produced from sugar, starch and plant oils; meanwhile, biogas, including biomethane was obtained from anaerobic digestion of plant matter. However, there are concerns about the first-generation biofuels because of the competition with food supply and for the use of arable land. Alternatively, "advanced biofuels" which come from a second generation (lignocellulose biomasses) and 3rd generation (algal feedstock) are being considered as promising feedstock for biofuel production (Naik *et al.*, 2010; Jones & Mayfield, 2012; Sanna & Abd Rahman, 2015).

There have been worldwide research interests, efforts and investments in microalgae-based biofuel technologies due to their capability of all year round production, higher photosynthetic activity, high biomass productivity (microalgae double their biomass in as short as 3.5 h time), easy to adapt in different growing conditions (avoiding the use of arable lands), ability to fix higher oils (20-50%), and ability to bio-mitigate CO_2 (1 kg dry algal biomass utilize 1.83 kg of CO_2) (Sanna & Abd Rahman, 2015; Brennan & Owende, 2010). Moreover, the alternative application of microalgae to reduce the CO_2 emission for industrial processes or gas power plant offers more attractive opportunities.

Despite the strong interests and investments in bio-fuels from microalgae from the academic world and the industry, there are still technical and economic issues that need to be addressed for their widespread utilisation in the near future. This work wants to contribute to enlarge the knowledge on microalgae to biofuels through thermo-chemical conversion technologies such as pyrolysis.

1.2   Problem statement

Among the various routes investigated for the conversion of biomasses into fuels, pyrolysis is a promising and relatively simple alternative. Pyrolysis convert biomasses into bio-oil, bio-char and gas at temperatures between 400 and 600°C in inert conditions (Bridgwater, 2012; Sanna & Abd Rahman, 2015). On one hand, the bio-oil can be exploited for the production of higher value fuels including bio-fuels and chemicals. On the other hand, the two co-products from fast pyrolysis bio-char and gas have potential applications in energy production (French & Czernik, 2010; Sanna & Abd Rahman, 2015).

Many studies from pyrolysis of microalgae reported that algal bio-oil has better qualities in many aspects than that produced from lignocellulose biomasses. Despite this, microalgae pyrolysis oils are still a complex organic mixture, consisting high of N-and O-compounds such as amides, ketones, phenols and carboxylic acids and further upgrading is necessary to match their quality to crude derived fuels. N-compounds represent the main technical limitation for the algae bio-oil implementation as bio-fuels. Perhaps, methods or catalysts that able to remove nitrogen (N) from bio-oil during or after its production can be developed.

Catalytic pyrolysis is a system where catalysts are incorporated directly into the pyrolysis process either mixing with catalyst (in-situ) or used downstream the pyrolysis to upgrade the pyrolysis vapours (ex-situ) (Dickerson & Soria, 2013). Most of the prior works on algal catalytic pyrolysis have focused on using zeolites such as HZSM-5, which have

been found to be very effective for deoxygenation and production of aromatic hydrocarbons (Du *et al.*, 2013b; Thangalazhy-Gopakumar *et al.*, 2012; Wang & Brown, 2013; Dong *et al.*, 2013; Campanella *et al.*, 2012). However, other zeolites and oxide catalysts can potentially be used for the pyrolysis of microalgae. In this research, a series of acid (Li-LSX-zeolite), basic (LiNa-FA and Na-FA) and neutral catalysts (micro-silica) were selected and evaluated for the denitrogenation of *Isochrysis* sp. by in-situ pyrolysis.

Another alternative approach to upgrade the bio-oil quality is through pre-treatment of the microalgae feedstock. Microalgae contain significantly high ash content, which comes from the macro minerals and trace elements (Bae *et al.*, 2011; Bi & He, 2013). Ash content affects the pyrolysis process design and operations as well as the product purification process. As a result, the removal of inorganics from microalgae can benefit their intrinsic bio-oil quality. Therefore, one of the objectives of this work is to investigate the removal of alkali and alkaline earth metals through chemical pre-treatment for the improvement of the microalgae bio-oil quality as well as the products yield.

Moreover, the addition of catalysts to pyrolysis can results in several issues such as catalyst deactivation due to coking and polymerisation of oxygenates on the catalyst surfaces and catalysts poisoning (Hernando *et al.*, 2017b; Zhang *et al.*, 2015). Since most of the tested zeolite catalysts suffer from coke-induced deactivation, new materials are developed/tested as potential catalysts for the pyrolysis of biomass. Catalyst regeneration need to be assessed to test the stability and effectiveness of the catalyst over cycles and how their activity varies after a number of cycles (López *et al.*, 2011; Shao *et al.*, 2018). Currently, to the best of my knowledge, no such studies have been reported in the literature on the catalyst regeneration/recycling from pyrolysis of microalgae. Overall, the focus has been given to the upgrading of bio-oil derived from microalgae *Isochrysis* sp. via catalytic pyrolysis.

1.3   Research scope

In this research, microalgae *Isochrysis* sp. is to be assessed as a feedstock for bio-oil production through the catalytic pyrolysis process. *Isochrysis* sp. is a small marine flagellate widely used in as food sources for marine aquaculture. *Isochrysis* sp. has been identified among the microalgae species that are suitable candidates for multiple-product algae-crop, due to their variety of fatty acids that offer a broad scope for several bio-products in a biorefinery approach (O'neil *et al.*, 2012). *Isochrysis* sp. also presents a relatively low N content compared to other species which is beneficial for the conversion process. Only a few studies currently investigate and report the effect of specific pyrolysis process parameter (Wang *et al.*, 2015; Dong *et al.*, 2014; Aysu, Abd Rahman & Sanna, 2016; Derrien *et al.*, 1998). In order to fully explore the potential of the *Isochrysis* sp. for bio-oil production, there is a need to evaluate the combined effects of the most critical process parameters on the pyrolysis products distribution, which is one of the goals of this research.

Catalyst Li-LSX-zeolite have been used widely in industrial air separation processes where the catalyst preferable to adsorb N_2 than O_2 during separation process. The application of the catalyst into pyrolysis in this research is to study the ability of the catalyst in denitrogenation of the bio-oil. Meanwhile, sodium and lithium fly ash derived sorbents/catalysts (Na-FA and LiNa-FA) have been used in the carbon capture studies. The literature suggest that Na-and Li/Na silicates derived from coal fly ash have could also be good performing catalysts for the catalytic pyrolysis of microalgae by converting them in carbon monoxide and hydrocarbon-rich gas. There is no work available in the literature using both type of catalyst and detailed study on their potential activity since they have not been investigated yet for the pyrolysis of microalgae. This can be monitored through the catalyst activity in enhancing the quality of the produced bio-oil.

1.4   Aim and objectives

The research study aims focused on the viability of Li-LSX zeolite as a catalyst for the upgrading of *Isochrysis* sp. microalgae bio-oil to high-grade fuel or chemicals. The specific objectives of this research can be summarised as:

1. To explore the potential of the *Isochrysis sp.* for bio-oil production via pyrolysis in terms of yield and qualities of products.

2. To evaluate the potential and activity of different catalysts (Li-LSX-zeolite, micro-silica, Na-FA, LiNa-FA) on the microalgae pyrolysis in terms of denitrogenation and deoxygenation power, products yield and quality.

3. To identify the effects of operating conditions, product distribution and physicochemical properties of bio-oil and the other products from the pyrolysis of *Isochrysis* sp. in the presence of Li-LSX-zeolite.

4. To investigate the influence of acid and basic chemical pre-treatment of *Isochrysis* sp. microalgae on the pyrolysis products.

5. To evaluate the recyclability of Li-LSX-zeolite catalyst in the presence of both chemicals treated and non-treated microalgae.

1.5   Research approach

The experimental research will be the evaluation of pyrolysis products distribution and bio-oil properties in comparison to other microalgae species and catalyst type. Results from the previous study will be taken as the reference, and new results will be compared with research. The approach is as follows:

- Screen microalgae species based on suitability and the yield from pyrolysis conversion for bio-oil production.

- Analyse different type of catalyst for evaluation of potential and activity of the catalyst during pyrolysis process.

- Optimise the pyrolysis parameters to develop a pilot scale of pyrolysis process.

- Analyse the profile of microalgae after pre-treatment and investigate the effects on bio-oil properties after pyrolysis.

- Perform regeneration tests to investigate the performance of the catalyst after three cycles and the effect on the pyrolysis products.

The objective of this research is only achievable when the selected catalyst can enhance the bio-oil quality produced from the pyrolysis of microalgae. The catalyst performance and bio-oil properties are only possible when all other steps in microalgae species and catalyst selection have been performed. A pilot scale test can be carried out on selected microalgae and catalyst; thus, physicochemical and chemical composition of all products (gas, bio-oil and char) can be evaluated using analytical instruments. Moreover, chemical pre-treatment on microalgae using different solvents were carried out to investigate the potential difference in their effects on pyrolysis products. Finally, catalyst recyclability or regeneration was investigated experimentally through catalyst activity and products characterisation. The details of the research are shown in Figure 1-2.
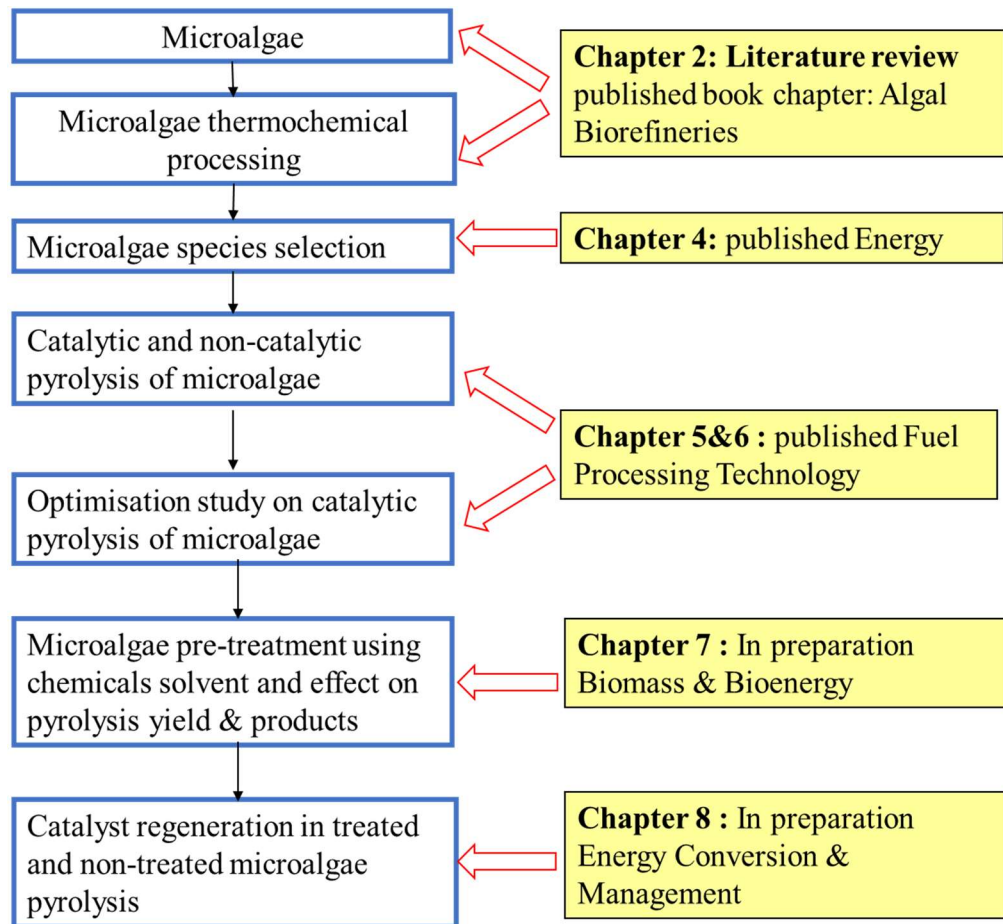
Figure 1-2 Conceptual flow chart of research approach.

1.6 Thesis overview

The thesis is organised in nine chapters including this chapter. The following topics and contents within the Chapters are as set out below:

Chapter 1   This current chapter presents an overview and motivations for the work. The objectives and outline of this thesis are also given in details.

Chapter 2   A general introduction to the key themes of the thesis, which are microalgae biomass, pyrolysis, the main liquid products (bio-oil), catalyst and the relationship between these three themes. It discusses

the criteria of the quality bio-oil assessed, examines the methods used to upgrade the quality, and evaluate the important parameters for bio-oil upgrading. Also, this chapter encompasses a literature review of various catalysts employed in catalytic pyrolysis.

Chapter 3   This chapter describes the set-ups employed, ranging from analytical equipment to bench-scale reactors. It includes an overview of the thermogravimetric analyser (TGA), TGA-pyro, EA, GC-MS and other equipment that been used in this study. The mass balance methodology is also discussed. Additionally, the methodology used for the characterisation of the microalgae, pyrolysis products and catalyst are presented in this chapter.

Chapter 4   This chapter discusses Objective 1. In order to address the objective, a series of characterisation analyses including proximate, ultimate and HHV analyses and preliminary-TGA were carried out on three microalgae species *(Isochrysis, Nannochloropsis and Tetraselmis)*. The characteristics of the microalgae and their pyrolysis products are discussed and compared to *Chlorella vulgaris*, microalgae that have been widely used in literature. The pyrolysis yield and products decomposition from three microalgae were quantified and compared to select suitable feedstock for biofuel production.

Chapter 5   This chapter discusses Objective 2. To address the objective, two commercial catalysts were employed (Li-LSX-zeolites and micro-silica), and other two were synthesised by solid state impregnation method (LiNa-FA and Na-FA). The catalytic activity of the four catalysts was characterised by a series of techniques (BET analyses, TGA-Basicity, Ammonia-TPD), then evaluated using a thermogravimetric (TG) analyser and tested in a semi-fixed bed reactor. The effect of different type of catalyst on the products yield

and characterisation are discussed. Further, the comparison between catalytic and non-catalytic pyrolysis are presented.

Chapter 6	This chapter analyses and discuss on the parameters that affect the catalytic pyrolysis to address Objective 3. A series of pyrolysis tests using a fixed bed reactor was carried out under different pyrolysis conditions, such as temperatures (400 to 700 °C), residence times (2 to 12 secs), catalyst: microalgae ratios (0.5:1, 1:1, and 3:1) and the reactor setup (in-situ and ex-situ).
Chapter 7	This chapter investigates the effect of chemical pre-treatment on microalgae to address Objective 4. Different solvents (NaOH, H_2SO_4 and water) were used to remove alkali and alkaline earth metals presence in the microalgae. This chapter includes the comparison of the fast pyrolysis results obtained from non-treated and pre-treated microalgae, in terms of pyrolysis products yields and chemical distribution on bio-oil. The influence of pre-treatment methods on bio-oil quality is also examined.
Chapter 8	In order to establish the recyclability of the best performing catalyst in both presence of the deashed and non-deashed microalgae, three different pyrolysis-regeneration cycles were carried out and are reported in this chapter. Discussion on the background to this study, including reviews of relevant published works that have influenced this work were included.
Chapter 9	The final chapter of the thesis discusses the conclusions derived from this research and highlights the findings from this study. Also, some recommendations for future works are presented in this chapter.

Chapter 2
Literature Review

2.1 Introduction

Renewable and nuclear power are the world's fastest growing forms of energy. At present, there are different renewable resources available such as wind, solar, hydropower and bioenergy. These renewable resources can satisfy energy demand in power sector, but transportation sector mainly depends on the liquid fuels, which cannot be produced from other renewable sources except biomass (Ferrell & Sarisky-Reed, 2010). The world energy outlook projected to meet 5% of world demand for transportation fuel by biofuels in 2030. As a result, many countries have set national biofuels targets and provide incentives and supports to expand the bioenergy industry.

The UK target to share 15% of energy consumption in 2020 comes from renewable sources. The overall obligation includes three sub-targets; 30% in electricity, 12% in heat and 10% in transport (Energy and Climate Change Committee, 2016). It is reported that the UK is three-quarters in meeting the 30% of electricity sub-target by 2020; however, the heat and proportion of renewable energy in transport is way behind the target. The renewable transport fuel proportion fell from 4.93% to 4.23% between the year 2014 and 2015, way below the level needed to meet the 2020 target. Figure 2-1 illustrate the UK Renewable Energy statistics in the year 2015. In order to achieve the 10% target in transport fuel, the government urged to increase the Renewable Transport Fuel Obligation (RTFO) to 9% by 2020. The current policy sets a minimum quota of 4.75% for the proportion of biofuels (Energy and Climate Change Committee, 2016). On the other hand, introducing E10 fuels (90% petrol, 10% bio-ethanol) could help the UK to reach 2020 transport target.

How close is the UK to its 2020
RENEWABLE ENERGY
TARGETS?

30% Target

22.31%

12% Target

5.64%
HEAT

10% Target

4.23%
TRANSPORT

ELECTRICITY

Source: BEIS, Digest of UK Energy Statistics 2015
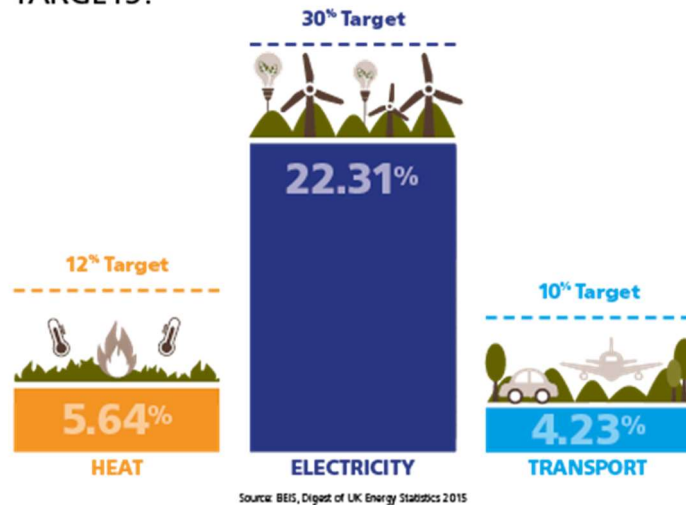
Figure 2-1 UK Renewable Energy statistics 2015. (Energy and Climate Change Committee, 2016)

2.2 UK Biofuels scenario

Biomass energy is amongst the most promising, most hyped and most heavily subsidised renewable energy sources. Biomass can be sustainable, environmentally benign and economically sound. It can provide heat, power and transportation fuels in an environmentally friendly manner, by reducing GHG emissions and thus can aid in achieving renewable energy targets (Phukan *et al.*, 2011; Brennan & Owende, 2010).

Biofuels are derived from biomass feedstock rich in carbon and oxygen and with the presence of hydrogen and nitrogen. Biofuels offer the perspective to reduce the dependence on the fossil fuels and greenhouse gaseous emissions, at the same time provide a sustainable economy and related jobs (Sanna, 2013; Huber & Corma, 2007). The main biofuels available in the UK are bioethanol and biodiesel. The total volume of UK biofuels produced in 2015/16 was 386.3 million litres; a sudden decrease of 22% from the year of 2014/15. The biodiesel and bioethanol decreased to 188.3 million litres

(22%) and 195 million litres (23%) respectively (DEFRA: Department for Environment Food & Rural Affairs, 2017). The UK grown energy crops come from rapeseed (converted into biodiesel), wheat and sugar beet (converted into bioethanol by fermentation), miscanthus and wood (burned to produced heat and power). On another note, waste products can also be turned into energy or fuels, for example straw and forestry waste converted into heat and power or used vegetable oil/tallow into bio-diesel. Wheat is the major precursor, supplying 33% for biofuels production in the UK, followed by used cooking oils, 32% and maize 20% (DEFRA: Department for Environment Food & Rural Affairs, 2017).

However, the increasing demand creates competition between food and fuel crops production in terms of usage of arable land, high water and fertiliser requirement, and biodiversity conservation. Typically, the use of first-generation biofuels has generated a lot of controversies, mainly in the food-versus-fuel, where the food price increase as the biofuel production increase (Naik *et al.*, 2010; Patil, Tran & Giselrød, 2008; Sanna, 2013). Therefore, biofuels from food crops are not socioeconomically advantageous to meet current and future energy demands. Second-generation biofuel feedstock materials, referred to lignocellulosic biomass have progressed to solve some of the problems associated with first-generation biofuel sources. However, this generation faces challenges related to technological performance and consistency, cost-effectiveness, and biomass collection networks.

Microalgae have been widely researched as a suitable feedstock with the capacity to solve significant challenges of first- and second-generation biofuel feedstock. Microalgae represent as third-generation biofuel feedstock with a vast diversity of photosynthetic species and are either heterotrophic or autotrophic in nature (Sanna & Abd Rahman, 2015).

Microalgae have gained significant attention as third-generation biofuel feedstock for several reasons, including:

- Microalgae biomass productivity and oil yield are very high compared to other oil-based feedstocks.

- Microalgae are not in competition with food crops.

- Microalgae can be cultivated in freshwater, brackish water or even wastewater.

- Microalgae can be fully utilized for biofuels or chemicals production, attracting investments worldwide, for the research and development in a biorefinery system.

2.3 Microalgae

Microalgae are unicellular micro-organisms, which convert sunlight, water and carbon dioxide into algal biomass(Dillon, 2009). The size of microalgae, depending on the species can vary from 1 to 100 micrometres (μm). Microalgae do not have roots, stems and leaves like higher plants and can be grown in freshwater, brackish, or seawater in a range of temperatures(Ferrell & Sarisky-Reed, 2010). A typical green microalga is shown in Figure 2-2.
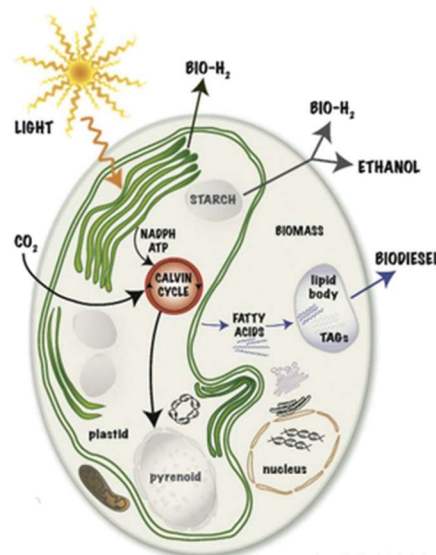
Figure 2-2 A schematics of typical green microalgae cell. (Beer *et al.*, 2009)

14

There are vast species of microalgae estimated around 30, 000 to 40, 000 species which have been identified and classified in group such as green algae (*Chlorophyta*), red algae (*Rhodophyta*), cyanobacteria (*Cynaophyceae*), yellow-green algae (*Xanthophycae*), brown algae (*Phaeophyceae*) and diatoms (*Bacillariophyta*) (Brennan & Owende, 2010; Jones & Mayfield, 2012). In this research, only green microalgae are considered, so a further reference to microalgae refers to green microalgae only.

2.3.1 *Microalgae cell composition*

Microalgae can be cultivated by different methods which are phototrophic (growth in light without additional nutrients), heterotrophic (growth in the dark with additional nutrients) and mixotrophic (growth in either light or dark with additional nutrients) (Sawangkeaw & Ngamprasertsith, 2013). Manipulating growing conditions such as light intensity, nutrient sources (organic carbon and nitrogen), temperature and pH influence the growth rate and lipid content of microalgae.

The structure of microalgae is crucial since it affects the decomposition behaviour during pyrolysis. The three main components of microalgae biomass are lipid, carbohydrate and protein; additionally, it contains small amounts of organic extractives and inorganic materials. The proportion of these components varies depending on the microalgae species. A list of lipid, carbohydrate and protein contained in different microalgae species is shown in Table 2-1.

From where it can be seen microalgae *Botryococcus, Chlorella vulgaris, Isochrysis, Neochloris oleoabundansand* and *Nannochloropsis* are among species contain high content in lipids. According to Chisti, microalgae with high lipid contents are suitable for producing bio-diesel (Chisti, 2007). Researchers have focused on production of bio diesel from microalgae by utilising the algae lipid content. Lipids are extracted from microalgae cells and undergo conventional esterification and trans-esterification processes; while the

remnant biomass (mainly proteins and cellulose) is considered as waste (Luque *et al.*, 2010; Serrano-ruiz & Dumesic, 2012).

Table 2-1 Chemical composition of different species of microalgae based on % dry matter.

Algal species	% of dry weight		
	Proteins	Carbohydrates	Lipids
Botryococcus braunii	8 - 17	8 - 20	25 - 75
Chlorella vulgaris	51 - 58	12 - 17	14 - 22
*Isochrysis sp.	31 - 51	11 - 14	20 - 22
Neochloris oleoabundans	20 - 60	20 - 60	35 - 54
Scenedesmus quadricauda	48	17	21
Spirulina maxima	60 - 71	13 - 16	6 -7
*Tetraselmis suecica	63	11	11
*Nannochloropsis	62	9	18

*Microalgae species used in this research

Data adapted from (Sawangkeaw & Ngamprasertsith, 2013; Raveendran *et al.*, 2017; Wijffels *et al.*, 2010).

2.3.1.1   *Lipids*

Microalgae lipids serve as energy reserves and structural components (membranes) of the cell (Maity *et al.*, 2014). The simple fatty acid triglycerides are important energy reserves. Membranes are mainly constructed from phospholipids and glycolipids, where the hydrophilic polar phosphate or sugar moieties and the level of saturation of the fatty acyl chains determine the fluidity of the membranes (Mohan *et al.*, 2014; Singh & Gu, 2010).

Most of the microalgal oils have similar fatty acid constitutions to conventional vegetable oils. The similarity makes microalgal lipid is a promising source for fossil fuel replacement. A study reported lipid compounds such as monogalactosyldiglyceride, digalactosyldiglyceride, phosphatidylethanolamine, phosphatidylglycerol were found in the *Chlorella vulgaris* (Phusunti, 2012). Each of these lipids contained fatty acids in a range from C12 to C24, the common saturated straight chain fatty acids such as lauric (C12), myristic (C14), palmitic (C16) and stearic (C18) are found in microalgae (Phusunti, 2012). Figure 2-3 illustrated structure of lipids and fatty acids that are typically contained in the microalgae.

(a) Myristic Acid, SAFA

(b) Palmitoleic Acid, MUFA

(c) Arachidonic Acid, PUFA

(d) Linoleic Acid, PUFA

(e) Docosahexaenoic Acid, HUFA

(f) Eicosapentaenoic Acid, HUFA

(g) alpha-Linoleic Acid, PUFA
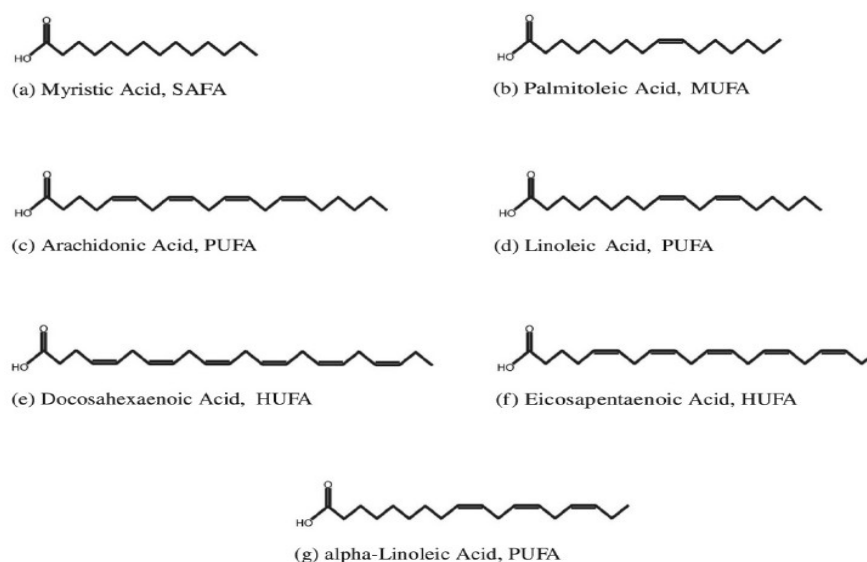
Figure 2-3 Some structure of lipids and fatty acids which are available in microalgae.(Phusunti, 2012)

The composition of fatty acids present in oils from microalgae determines the quality of the produced biodiesel. The level of unsaturated fatty acids affects biodiesel properties. For example, fuels with a higher level of unsaturation of the acyl chains have a higher cloud point, which is desirable but is also much more susceptible to oxidation (Lee & Wilson, 2014). The highly unsaturated fatty acids found in algae may need to be hydrogenated to improve their potential fuel properties. Furthermore, a high level of

unsaturated fatty acids in fuel increases the danger of polymerisation in the engine oil and can cause problems with oxidative stability of the fuel (O'Neil *et al.*, 2014).

2.3.1.2   *Carbohydrates*

Similar to lipids, algae and plant crops differ significantly in their carbohydrate fraction composition. Carbohydrates serve both structural and metabolic functions and, as the early products of photosynthesis, they serve as the starting point for the synthesis of the other biochemicals (Foley, Beach & Zimmerman, 2011; Singh & Gu, 2010). Different classes of algae produce specific types of polysaccharides. For example, green algae produce starch as an energy store, consisting of both amylose and amylopectin, like higher plants. Other algae, for example, many brown algae and diatoms, accumulate carbohydrates such as laminarin, mannitol, or fucoidan as food reserves(Foley, Beach & Zimmerman, 2011).

Since algae can accumulate significant amounts of carbohydrates (mainly referred to as starch) inside their cells, the potential to utilise the carbohydrate for bioethanol production is high (Raheem *et al.*, 2015). However, the extracted carbohydrates need to be further processed (hydrolyse) into simple sugars (i.e., glucose) for the yeast to convert to sugar during the fermentation process (Raheem *et al.*, 2015), adding complexity and costs of the conversion process. On the other hand, direct conversion approaches, such as pyrolysis or liquefaction do not require the extraction of the sugars from the algae cells.
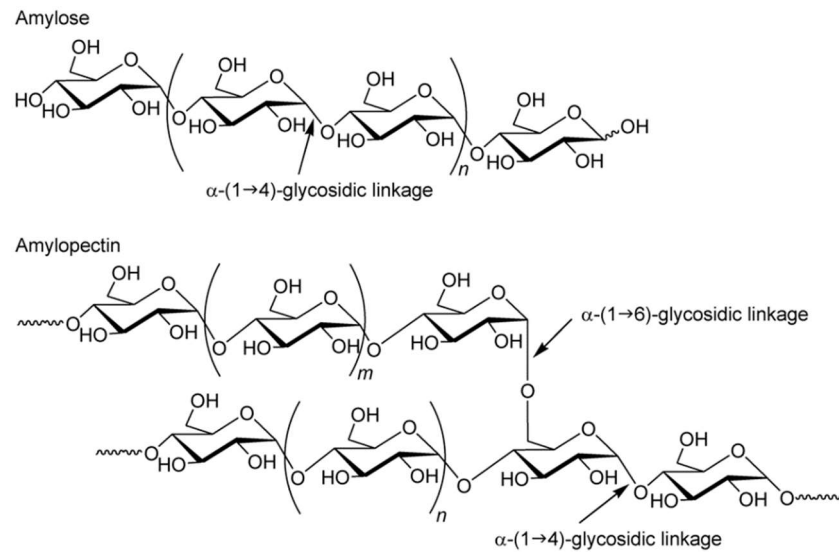
Figure 2-4 Amylose and Amylopectin structures in carbohydrates.

2.3.1.3   *Proteins*

Proteins facilitate cell growth and cell metabolism of microalgae. The high protein content of various microalgal species is one of the main reasons to consider them as an unconventional source of protein (Foley, Beach & Zimmerman, 2011). Some algae contain up to 60% of protein such as *Spirulina maxima* and *Chlorella vulgaris* (Luque *et al.*, 2010). Some well-known algae that is currently cultivated for its protein content are the cyanobacterium species *Athrospira*, or better known as *Spirulina* (Suganya *et al.*, 2016). From Table 2-1, it shows that microalgae *Chlorella*, *Nannochloropsis*, *Tetraselmis* and *Spirulina* among species that contained high protein in the microalgae composition (50 to 60 dry wt.%).

Protein is the main component of nitrogen fraction. The cellular nitrogen includes inorganic-, free α-amino-, free amino, volatile and protein nitrogen. In some algae, as much as 40% of the total amino acids may be found in the free form within the cell, with varying degrees of enrichment components (Hannon *et al.*, 2010; Foley, Beach & Zimmerman, 2011). Amino acids, the building blocks of proteins, have high commercial value (for use in food, pharmaceuticals and cosmetics) relative to most other fractions of

19

biomass. Besides, the amino acid pattern of almost all algae compares favourably with that of other food proteins. As the cells can synthesise all amino acids, they can provide the essential ones to humans and animals (Spolaore *et al.*, 2006). A list of amino acids contained in different microalgae species is shown in Table 2-2. Different microalgae species have a different composition of amino acids. From the table, it shows that aspartic and glutamic acid constitute a relatively large proportion of the total amino acids followed by proline. Aspartic acid can be found in protein supplements as energy boosters. Meanwhile, glutamic acid contributes to the health of the immune and digestive systems, as well as energy production.

Table 2-2 Amino acids composition in different microalgae species (% d.wt.)

Amino acid (%)	*Isochrysis galbana*	*Nannochloropsis*	*Tetraselmis suecica*	*Chlorella vulgaris*
Aspartic acid	10.36	9.4	8.95	4.7
Serine	3.86	4.31	3.71	2
Glutamic acid	11.42	15.48	17.59	5.8
Glycine	6.78	7.11	5.93	3.1
Histidine	0.23	0.61	0.19	1.1
Arginine	4.39	4.57	4.59	3.3
Threonine	4.88	5.28	4.4	
Alanine	7.55	1.54	7.62	4.3
Proline	12.48	15.2	6.47	2.5
Tyrosine	2.84	1.06	1.84	n.a.
Valine	5.49	6.9	5	3.2
Methionine	3.79	2.64	2.55	1.3
Lysine	6.96	9.07	8.2	n.a.
Isolucine	1.11	1.47	0.97	2.3
Leucine	6.87	11.57	7.94	4.7
Phenylalanine	8.52	1.92	3.51	2.8

2.3.2 *Microalgae for biofuels*

The production of liquid fuels from biomass or bio-fuels can be accomplished through several different methods. These processes typically run at a moderate temperature within shorter residence times with fast heating rates. Previously, microalgal biomass has been promising feedstock for biodiesel production. The process involved lipid extraction and get through transesterification process to produce biodiesel (Ahmad *et al.*, 2011; Demirbas, 2011). The microalgal residues obtained after conventional transesterification are mainly composed of proteins, carbohydrates, and a fraction of unutilised lipids, which can be employed to generate liquid and gaseous fuels, and biochar solids, depending on the temperature used. This method of conversion is an alternative progression for low-lipid or post-extraction residues of high-lipid microalgal streams. Microalgae for biodiesel suffers from the costly extraction of algal oils (lipids) by organic solvents due to the microalgal different physicochemical characteristics, such as the small cells size and cell wall chemistry (Sawangkeaw & Ngamprasertsith, 2013; Gouveia, 2011). Moreover, only the lipid fraction of microalgae used for biodiesel, while the carbohydrates and proteins are considered as waste.

Algal biomass conversion to fuel in the form of liquid or gas is generally classified into two categories and identified as biochemical (fermentation involvement of microbes) or thermochemical (liquefaction, pyrolysis and gasification), involving catalysts and high temperature to produce char, oil, and gas. Many factors influence the conversion process selection, such as type and quantity of biomass feedstock, economic consideration, the desired form of energy and end-products (McKendry, 2002). Figure 2-5 shows the conversion processes in converting microalgae into bio-oil with operating parameters and key products. Some of the microalgae with high lipid contents are suitable for biodiesel and glycerine production via transesterification. Meanwhile, the bio-chemicals reaction produced bioethanol via fermentation and biogas from anaerobic digestion.

21

Thermochemical conversion appears to be a promising technology to produce various biofuels compared to bio-chemical processing (time-consuming to produce biofuels). The bio-oil produce can be directly implemented for power and electricity plant, or the refining bio-oils can be used as transportation fuels (for example; diesel and gasoline). Furthermore, thermochemical technology can be applied to any types of biomass feedstock without the use of toxic or chemicals in the process. Besides, the conversion utilises the whole algae biomass for bio-fuel production, where the biomass is thermally decomposed into bio-oil under specific conditions (Chiaramonti *et al.*, 2015). The relative fractions of various solids, liquids and gaseous products are highly dependent on the operating conditions including temperature, pressure, heating rate and residence time (refer to Figure 2-5).
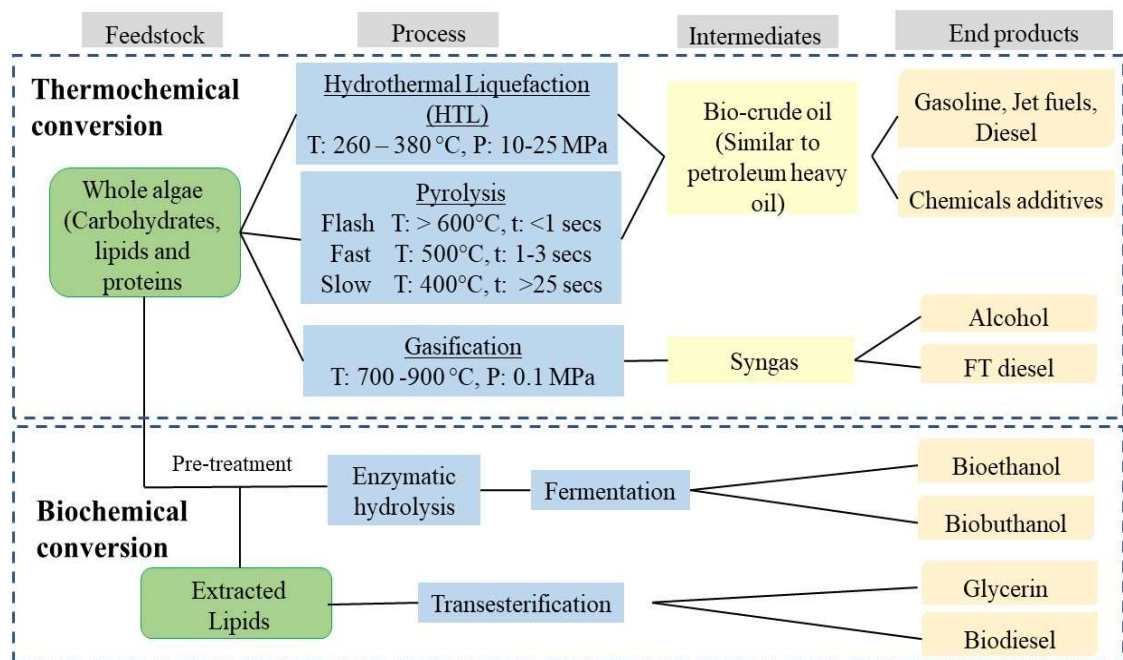
Figure 2-5 Scheme of microalgae conversion for energy production from microalgae. (Raheem *et al.*, 2015)

Hydrothermal liquefaction (HTL) can be carried out at a low temperature range between 260 to 380 °C, however, required high-pressure system (10 to 25 MPa). Meanwhile, pyrolysis can be carried out at moderate temperature 400 to 600 °C, in inert condition and

depends on the residence time of reactions. Gasification runs at a higher temperature >700 °C, cracking and promoting the production of gaseous hydrocarbons and syngas. Bio-oil from pyrolysis and HTL need to be upgraded through deoxygenation and hydrocracking/ cracking process to produce products with same properties as gasoline, jet fuels and diesel (Chiaramonti *et al.*, 2015; Raheem *et al.*, 2015). Although recent work on HTL has shown promising results, it is currently a nascent technology with high capital costs due to the high pressures required, while pyrolysis has been already demonstrated at industrial scale (for example BTG Biomass Technology Group in Netherland) and present lower capital costs compared to liquefaction and gasification (Lehto *et al.*, 2014; Chiaramonti *et al.*, 2015).

Although HTL crude oil contained low O and N-compounds and high HHV compared to pyrolysis oil, the bio-oil shows some advantages such as lower viscosity and comparable with the vegetable oil (Chiaramonti *et al.*, 2015; Lehto *et al.*, 2014). Pyrolysis liquid final product can be transported and upgraded to fuels and valuable products such as fertilisers, resins, and other speciality chemicals that are fully compatible with existing petroleum infrastructure by downstream processing in a similar way as crude oil is processed in an oil refinery. Furthermore, all pyrolysis products can be utilised in the pyrolysis system. Gas and bio-char can be burned to help dry the incoming biomass and operate the reactor while char and ash are considered promising soil amendments and a potential C sink (Yu *et al.*, 2017).

However, the production of bio-oil from microalgae requires large quantities of biomass. The process takes place either in dry or wet conditions. Microalgae contain high water content (80-90%), and this is a significant drawback for the direct implementation conversion (gasification or pyrolysis) of microalgae. Therefore, like the terrestrial biomasses, water content needs to be reduced before processing the raw algae, through energy-intensive separation processes. There are a variety of methods for dewatering microalgae such as flash-drying, rotary dryers, incinerator and the low-cost method; sun-drying.

Microalgae characteristics introduce another problem to the process design. The technologies available this day carried out using lignocellulosic biomass which is different compared to the microalgae. Microalgae contained higher inorganic and ashes content, the peculiar state of aggregation depending on the harvesting methods (Chiaramonti *et al.*, 2015; Ross *et al.*, 2008). The use of salty water for algae cultivation increase problem such as corrosion and solid deposition, especially for HTL due to more critical pressure and temperature operating conditions. Thus, a pre-treatment on the microalgae before the conversion could be an advantage on tackling the issues.

2.4   Pyrolysis

2.4.1   *Definition*

Pyrolysis is a thermo-chemical decomposition process which organic material or biomasses is converted into carbon-rich solid and volatile matter by heating the absence of oxygen. The solid usually termed as char, bio-char or coke is generally contained high carbon content. The volatiles can be partly condensed produced liquid fraction or known as bio-oil, while the non-condensable vapours released out as gaseous or bio-gas (Sanna & Abd Rahman, 2015; Bridgwater, 2012). The process is represented in Figure 2-6. Each of the products from pyrolysis (Bio-char, bio-oil and gas) have high property values which can be applied in many sectors. The production of bio-oils through pyrolysis of microalgae is attractive since the whole biomass can be converted to fuel products.
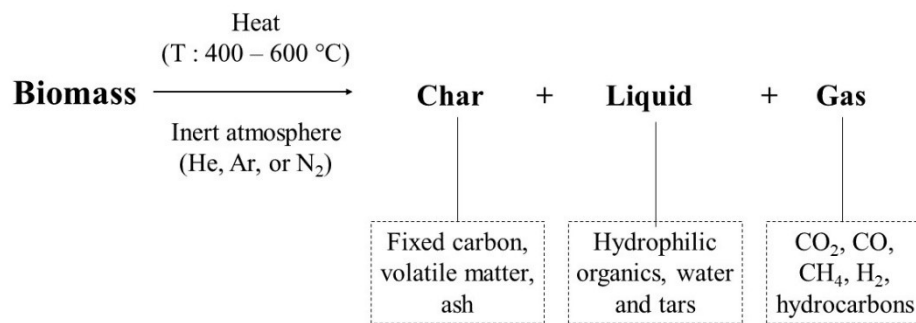
Figure 2-6 Pyrolysis process representation (Bridgwater, 2012).

Pyrolysis can be classified depending on the heating rate and the presence of catalysts. These parameters segregate the pyrolysis into four modes of operations: slow pyrolysis, fast pyrolysis, catalytic pyrolysis and microwave (MW) assisted pyrolysis (Fermoso *et al.*, 2017a). Slow pyrolysis consists of slow heating rates with residence time varying from minutes to hours and temperature ranging from 400 to 600 °C. Slow pyrolysis has been widely used for the production of charcoals for centuries. Fast pyrolysis is a promising technology involving a high liquid yield produced at very short residence times of <3 s, with rapid heating rates >1000 °C/s.

Catalytic pyrolysis is a system where both catalyst and biomass are incorporate and mixed, undergo pyrolysis reactions (for example using fixed, fluidised or circulating bed reactors) at the same time (generally known as in situ upgrading) or setting up an upgrading fixed bed at the outlet of the pyrolysis reactor to treat the pyrolysis vapours/gaseous (ex-situ configuration) (Du *et al.*, 2013b). Other than that, microwave assisted pyrolysis is a promising technology, which is still under research for commercialisation. The yield of bio-oil can be increased by operating the microwave at lower frequencies and higher output power of microwave (Bu *et al.*, 2012).

2.4.2 *Key factors on fast pyrolysis*

Fast pyrolysis of microalgae has lately received great attention to produce liquid biofuels from microalgae. The yield of bio-oil depends on several parameters such as biomass composition, heating rate, pyrolysis temperature, vapour residence time and inorganic compositions (Fahmi *et al.*, 2008). The mass yields and HHV of microalgae bio-oil found in literature vary in a wide range with values between 18-72 wt.% and 18-41 MJ/kg, respectively, depending on the operation conditions: temperature (300-600 °C), heating rate (600-1000 °C/s) and residence time (1.5-3 s).

2.4.2.1 *Temperature*

Temperature is considered as the most important parameter influencing the pyrolysis products yield and distributions. Biomass decomposition occurs when the temperature exceeds above the activation energies breaking the bonds, resulting in the formation of free radicals and fragmented species. Low temperature is not sufficient for complete biomass decomposition and leads to char, while at high temperature, cracking take place forming small compounds in the gas phase (Aysu & Sanna, 2015; Wang & Brown, 2013).

Many studies have been done on evaluating the effect of pyrolysis temperature towards product distribution. A study conducted on pyrolysis of blue-green algae blooms (BGAB) at different pyrolysis temperature ranges (300 to 700 °C) (Hu *et al.*, 2013). The yield of the bio-oil increased up to 55 wt.% at 500 °C but reduced drastically to 40 wt.% at 700 °C. Another study was done by Aysu et al. (2015) on the catalytic pyrolysis of *Nannochloropsis* using ceria-based catalyst found the maximum yield at 500 °C using a NiCe/ZrO$_2$ catalyst (Aysu & Sanna, 2015). Aysu also investigated the catalytic pyrolysis of *Pavlova* by using titania-based catalyst. The pyrolysis was set up at different temperatures (400, 500 and 550 °C). From the work, it can be seen that the maximum

bio-oil yield (22.6 wt.%) was obtained at temperature of 500 °C using Ni/TiO$_2$ catalyst (Aysu *et al.*, 2017a).

The effect of temperature on pyrolysis yields for catalytic pyrolysis follows the same trend as for the non-catalytic experiments. The bio-oil yields reach a maximum at approximately 500 °C, and further temperature increase results in a reduction of liquid yields. In contrast, gas yields increase with rising temperature. The opposite trend is observed with char yields.

2.4.2.2   *Sweep gas flow rate*

The sweep gas flow rate in the system determine the time required to process one reactor volume of fluid based on entrance conditions. The use of nitrogen gas is common practice for rapid purging of hot pyrolysis vapours. The nitrogen flow removes the volatiles from the hot zone to minimise secondary reactions and to maximise the liquid yield. The increase of gas flow rate results in an increase of the thermal cracking of pyrolysis vapours.

As reported by Hu et al. (2013) the bio-oil yield increased from 20.4 wt.% to 54.9 wt.% when the nitrogen flow rate was increased from 50 to 100 ml/min (Hu *et al.*, 2013). However, the bio-oil yield decreased to 45 wt.% when nitrogen flow rates was further increased to 400 ml/min. Another study work on the catalytic pyrolysis of cottonseed by changing the sweeping gas flow rate. The maximum bio-oil yield was obtained at nitrogen flow rate of 200 ml/min and decreased when the gas flow rate increased (Pütün, 2010). Similarly, a study showed that during the pyrolysis of green-blue algae the bio-oil yield increased (from 38 wt.% to 44 wt.%) when the gas flow rate increase (from 50 to 250 ml/min) and decreased when the flow rate was further increased (Campanella & Harold, 2012). Therefore, a high rapid gas flow rate leads to low conversion to bio-oil.

2.4.2.3 *Microalgae: catalyst ratio*

For heterogeneous catalytic systems, the contact between catalyst and biomass/vapour is an important issue and poses practical challenges. The contact can be improved by increasing the catalyst to biomass ratio. Nowadays high catalyst to feed ratio is getting more attention for producing high-quality fuel directly from microalgae. Wang and Brown (2013) investigated the production of aromatic hydrocarbons from catalytic pyrolysis of *Chlorella vulgaris* using HZSM-5 (Wang & Brown, 2013). The study increased the biomass to catalyst ratios of 5, 10 and 20 and it shows that the aromatic hydrocarbons yield increased with the increasing catalyst ratio. High catalyst loading increased the contact of vapours into the catalyst pores, where the aromatisation reaction occurs.

In another study done on the catalytic pyrolysis of *Nannochloropsis* sp. residue using HZSM-5 catalyst (Pan *et al.*, 2010), it was observed that the gaseous products (from 24.5 to 29.8 wt.%) was increased, and the bio-oil yield reduced (from 25.1 to 20.7 wt.%), when the catalyst to material ratio increased from 0.2:1 to 1:1. The increasing of catalyst amount in the reaction enhanced the direct contact between vapours and catalyst pores, promoting the primary and secondary cracking reactions, which resulted in high gaseous products. Another research studied the catalytic pyrolysis of microalgae using HZSM-5 by varying the catalyst: microalgae ratios between 1:1, 1:4 and 1:9 (Thangalazhy-Gopakumar *et al.*, 2012). The study reported a decrease of nitrogen content in the bio-oil when the catalyst load was four times that of biomass. Also, the aromatic hydrocarbons increased at the expenses of alkanes compounds when the catalyst ratio increased. Meanwhile, Zeng reported that the yield of bio-oil decreased as the catalyst: biomass ratio arose from 0:1 to 1.5:1 (Zeng *et al.*, 2013). The study was done using nickel phosphide catalyst for the pyrolysis of natural algae and reported the decreasing of O-compounds to 18.6% and an alkane increase of 9 times (to 59.4%) when the catalyst amount was doubled.

The catalyst to microalgae ratio influences the overall product distribution, elemental distribution and the characteristics of the products. An increase of ratio enhanced the conversion of pyrolysis vapours and improved the bio-oil quality. Therefore, the microalgae: catalyst ratio is a factor that can be used to optimise the catalytic pyrolysis process.

2.4.2.4 *Inorganic compounds or ash*

Algal biomass harvested from wastewater typically contain 5 to 35 wt.% (dry weight basis) ash content (Bi & He, 2013). Microalgae contains significantly high levels of macro-minerals (Na, K, Ca, P) and trace elements (Al, Cu, Fe and Mn) compared to non-marine biomasses such as wood, straws, miscanthus and willow coppice (Bi & He, 2013; Ross *et al.*, 2008). It is well established that alkali and alkaline metals in biomass affect the mechanism of pyrolysis and decrease the pyrolysis oil yield (Ross *et al.*, 2009; Fahmi *et al.*, 2008). Ash content affects the pyrolysis process design and operations (causing fouling, slagging and corrosion in the reactors), as well as the product purification process. As a result, the removal of inorganics from microalgae would benefit their intrinsic quality. Reduction of these inorganic components via a pre-treatment step before the pyrolysis process will go a long way in improving the quality of the oil and life span of the equipment.

2.4.3 *Pyrolysis products*

The constituents of microalgae are thermally degraded into smaller units that can be liquids, gaseous and solids. Microalgae then can be densified into intermediate bio-oil. The primary products can be used directly or can be converted further into even higher quality and valuable fuel or chemical products. The composition and properties of the derived products depend on the pyrolysis conditions, i.e. pyrolysis temperature and heating rate, as previously discussed.

Lipid, carbohydrate and protein are strongly interconnected by physio-chemical bonds, and pyrolysis oil is a complex combination of the thermal degradation products of each biomass constituent. Primary pyrolysis products react with the original biomass components, as well as inter-reactions between primary products, resulting in the production of secondary products. Also, studies have found that metal compounds in biomass, both as ash and contaminants, behave as catalysts and influence the decomposition behaviour of biomass.

2.4.3.1   *Bio-oil*

2.4.3.1.1   *Bio-oil characteristics*

The present interest in deoxygenated liquid products from pyrolysis are driven by their potential for further applications of heat and electricity generation and upgrading to premium-grade fuels. Bio-oils are complex mixtures that contain more than 300 compounds including aliphatic, aromatics hydrocarbons together with a high amount of oxygenated and nitrogenated hydrocarbons. Compounds in bio-oils can be classified into ten different broad categories; aliphatic, aromatics, aldehydes, alcohols, ketones, esters, ethers and carboxylic acids. Table 2-3 describes the complex compounds found in microalgae bio-oil.

The hydrocarbons such as aliphatic and aromatics generally present valuable chemicals. Meanwhile, oxygenates compounds such as aldehydes, ketones and acids are responsible for deleterious properties of bio-oil such as thermal instability, corrosivity, high viscosity and immiscibility with hydrocarbon fuels (Xiu & Shahbazi, 2012). Nitrogenate compounds such as amine, amide and pyridine originated from the decomposition of proteins. Therefore, bio-oils must be upgraded before being used as transportation fuels.

Table 2-3 Groups of compounds found in the microalgae bio-oils.

Groups	Compounds
Acids	Acetic acid, propanoic acid, carbamic acid
Aliphatic	Heptadecane, Octadecane, Butene, Nonene
Esters	Hexanoic acid, 2-ethyl-, octyl ester, Hexanoic acid, 2-ethyl-, octyl ester
Alcohols	Ethanol, Heptanol, Hexanol
Ketones	Octanone, Pentanone, Octadecanone
Aldehydes	Formaldehyde, Acetaldehyde
Aromatics	Benzene, Toluene, Xylenes, Naphthalene, PAH
Nitrogenated compounds	Propenamide, pyrazine, pentadecanitrile

Table 2-4 compares the properties of bio-oil from microalgae those of heavy fuel oil. Bio-oils have high moisture contents (15 to 30 wt.%) and low high heating values (HHV) (16 to 19 MJ/kg). Besides, bio-oil has high acidity that causes instability and corrosivity during its handling and storage (Dickerson & Soria, 2013). The low pH mainly comes from carboxylic acids in bio-oils, mainly formic and acetic acids. A study reported there are about 0.3% to 3.0% suspended solids found in the bio-oil, which can cause plugging and deposits on pipes and reactors (Lehto *et al.*, 2014). The viscosity of bio-oil increases due to secondary condensation and polymerisation of high concentration of reactive components such as ketones, aldehydes and phenols. Therefore, the development of

technologies to stabilise the bio-oil functionalities converting them into more stable ones, are needed.

Table 2-4 The comparison between the properties of bio-oil from pyrolysis of Chlorella vulgaris sp. and heavy fuel oil.

Properties	*Bio-oil from Chlorella vulgaris	Heavy fuel oil
Elemental composition (wt.%)		
C	51.4	85
H	10.4	11
N	12.4	0.3
O	24.8	1
Ash	1.0	0.1
HHV (MJ/kg)	18.6	40
Moisture content (wt.%)	15-30	0.1
pH	2.8 - 3.8	n.a.

*Adapted from (Thangalazhy-Gopakumar *et al.*, 2012)

In the petrochemical industry, higher quality products contain low O/C ratio and high H/C ratio. These ratios are important if the bio-oil is to be a substitute for demanding petrochemical application such as transportation fuels (Dickerson & Soria, 2013). Therefore, bio-oil must be upgraded by removing/reducing unwanted compounds such as oxygen and nitrogen. Besides, sulphur contents in bio-oils are typically lower than in crude oil. Microalgae bio-oil has lower oxygen contents compared to the terrestrial biomass, which led to considerably high HHV. Figure 2-7 illustrate Van Krevelen diagram, which comparing biomass and fossil fuels in terms of the O/C and H/C ratios. The lower the respective ratio means the higher energy content of a material. It is shown

that microalgae bio-oil fall in the same region as biodiesel. Microalgae bio-oil has lower oxygen content than biomass bio-oil and closer in nature to heavy oil. However, as reported in Table 2-4, the N-content in microalgae is very high, and this represents a limitation in terms of bio-fuels production.
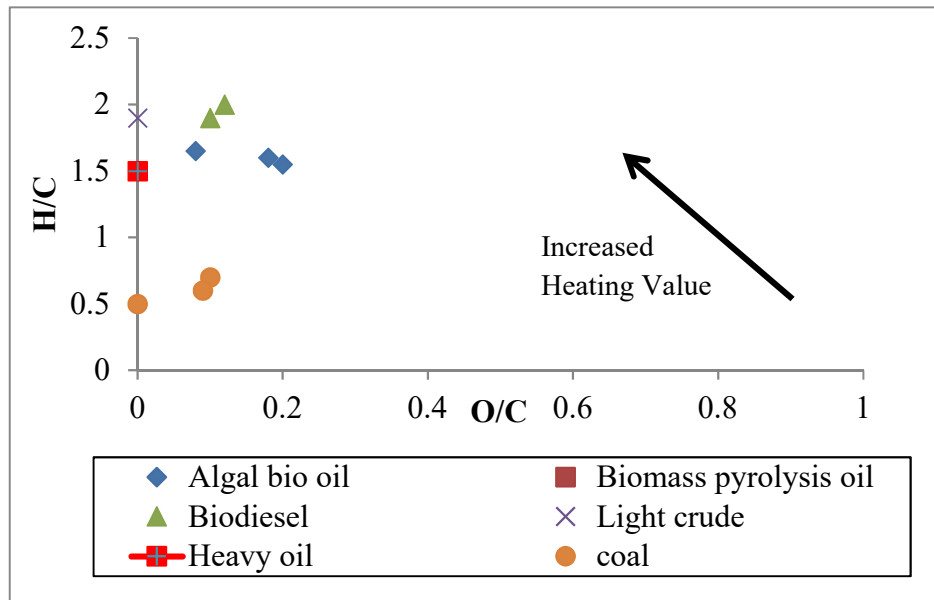
Figure 2-7 Van Krevelen diagram for fuel and bio-oils. (Sanna & Abd Rahman, 2015)

2.4.3.1.2   *Application of bio-oil*

Potential applications of bio-oil are to produce higher value fuels, including biofuels and chemicals. Bio-oil can be used directly in boilers, furnaces, engines and gas turbines as a fuel, but modifications of the existing systems are required. Applications of bio-oils have been the focus of several reviews. An extensive review of bio-oil characteristics and the problems that were reported with the use of bio-oil for heat and power and biofuels was published by Bridgwater (Bridgwater & Watkinson, 2015).

Another potential application of fast pyrolysis and consequently of bio-oil could be within a biorefinery system. Figure 2-8 below shows a scheme of biorefinery concept, where

microalgae are used as a feedstock to produce value-added chemicals, such as amino acids, omega fatty acids and iodine. Production of chemicals needs to be able to meet product specification requirements for market acceptability. These may be oxygenated (such as acetic acid or phenol), whereby the requirement is less on the de-oxygenation and more on delivering a product that is sufficiently high concentration, to justify separation and refining into a marketable chemical. Hydrocarbon chemicals are also of interest and maybe produced along with biofuels from de-oxygenation process.
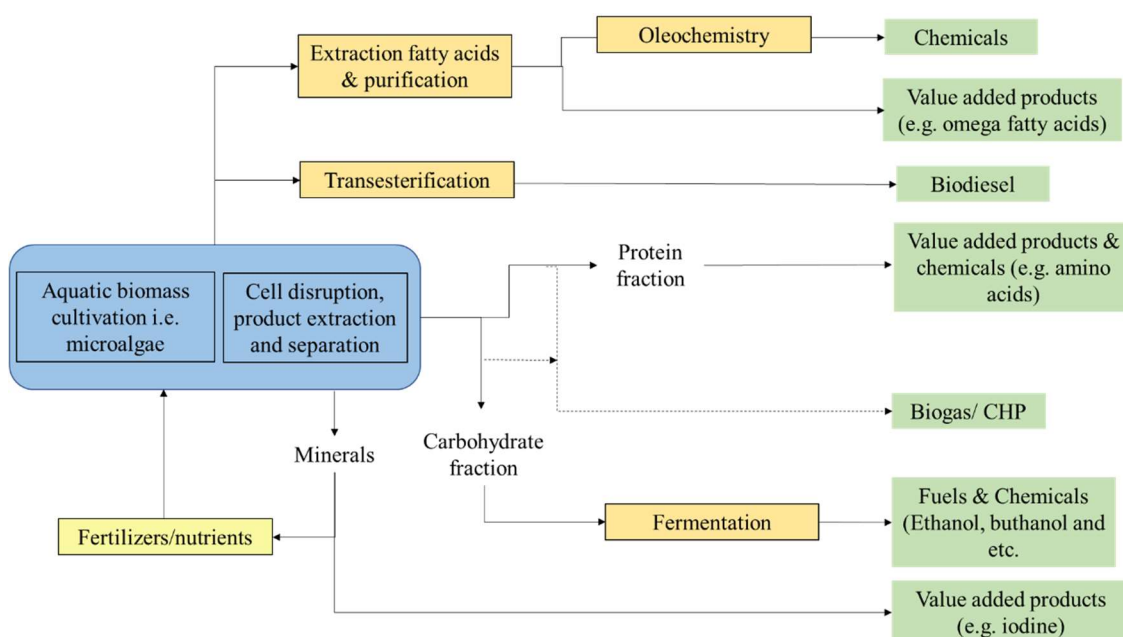
Figure 2-8 An example of a microalgae biorefinery concept. (Suan *et al.*, 2017)

2.4.3.1.3 *Quality bio-oil*

Before bio-oil can effectively be used in any application as a fuel or chemicals, there are several inherent properties that require consideration. Biofuels require well defined and carefully specified products. These are either completely compatible with conventional fuels, such as gasoline or synthetic diesel or can be sufficiently controlled in quality to be blend able in some proportions, such as ethanol or a partially de-oxygenated product that is miscible with conventional fuels. Production of dedicated biofuels such as ethanol,

methanol or DME is possible, but only through gasification to syngas and synthesis of the required product. This route is not considered further for the purpose of present thesis.

The most important general quality requirements of the bio-oils are:

1. All direct uses of bio-oil require a consistent and homogenous product, which homogeneity is the most important for storage, handling and processing.

2. Low solids are important to avoid potential blockage of injectors, filters and catalyst beds.

3. Low alkali metals and other impurities such as traces of sulphur and chlorine are important in catalytic systems.

Other than that, the quality requirements for the production of transport fuels and chemicals are water content, acidity and the bio-oil composition; oxygen and nitrogen content.

2.4.3.2 Bio-char

Bio char is the solid product from pyrolysis and has typically carbon content over 50%. Bio-char ash and oxygen content is higher compared to coal, and usually, its structure is more disordered. Char can be used to produce activated carbon, as solid fuel or to produce carbon nanotubes (Laird, 2010). Alternatively, the application of bio char as agricultural soils amendment is an immediate and easily quantifiable means of carbon sequestration, which leads to GHG reduction. Soils low in organic matter exhibit greatest increase in C after the addition of biochar. Besides, the use of biochar as soil amendment offers the opportunity to recycle nutrients as well as improve the soil quality and sequester carbon (Laird, 2010).

When the pore structure and surface area of bio-char are appropriate, they can be prepared for activated carbon applications. Activated carbon is widely used as an adsorbent in many applications such as toxic metal removal from water, taste- and odour-causing compound removal or reduction of gaseous pollutants from the exhaust gas and removal of volatile organic compounds (Park *et al.*, 2013).

2.4.3.3 *Gas*

Gas from pyrolysis of microalgae mainly contains light hydrocarbons (range from C1 to C4), CO, CO_2, H_2, NH_3, and HCN. Through pyrolysis process, CO_2 is the major gas products which is about 50 -60% followed by CO that ranges from 30 to 40%. Besides, other light hydrocarbons such as methane, ethane and hydrogen can be found in pyrolysis gas. The gas composition mainly depends on the feedstock type, temperature and residence time (Amin, 2009). However, most syngas production focused on the gasification process, where operating conditions at high temperature support the gas formation. The gaseous products can be utilised into combined heat and power to produce electricity and heat.

2.5 Pyrolysis of microalgae

Various microalgae species have been investigated for pyrolysis in terms of bio oil yield and composition under different reaction condition and operation modes. A large number of researches on microalgae pyrolysis have been carried out in recent years.

2.5.1 *Pyrolysis mechanism and reaction pathways*

Pyrolysis is a complex thermal degradation process composed of numerous reactions resulting in the production of a huge number of chemical compounds. However, basically, the reaction products are often lumped into three groups: gas, pyrolytic liquid (bio-oil) and char. Most of the catalytic pyrolysis studies focused primarily on the influence of process variables on the quantity and quality of algal bio-oil. There are only a few

literatures reported on the pyrolysis mechanism of microalgae (Du *et al.*, 2013a; Aysu, Maroto-Valer & Sanna, 2016; Kumar *et al.*, 2017; Aysu *et al.*, 2017a). Different from terrestrial biomass, microalgae biomass primarily made up of lipids, carbohydrates and proteins. Figure 2-9 shows the proposed mechanism of microalgae catalytic pyrolysis.
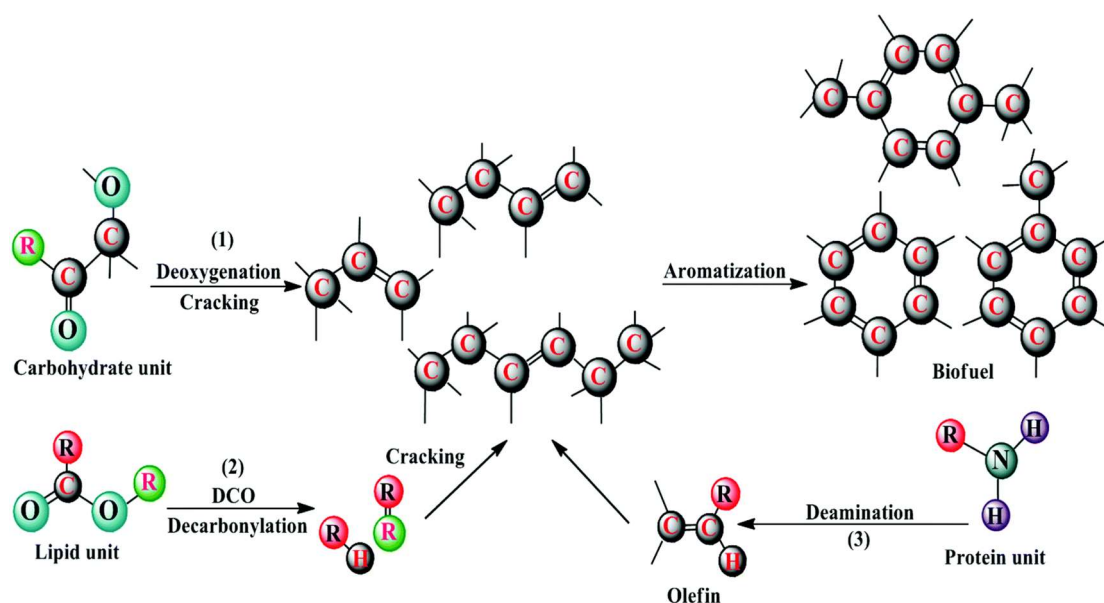
Figure 2-9 Postulated pathways catalytic pyrolysis of microalgae. (Kumar *et al.*, 2017)

When microalgae are heated, their constituents thermally degrade and vapourise. As the temperature and heating rate increase, the complexity of pyrolysis increase, and a variety of products are released as vapour and gas species. When pyrolysis vapours enter the pores of the catalyst, they may undergo a complex series of reactions such as cracking, aromatisation, ketonisation, aldol condensation, isomerisation, oligomerisation and dehydrogenation, among others. Deoxygenation may occur via removing water (dehydration), CO (decarbonylation) and CO_2 (decarboxylation). In addition, some carbon and hydrogen are lost during coke formation over the catalyst and the production of gaseous hydrocarbons because of cracking of the bio-oil vapours. To simplify the degree of complexity and understand the reactions involved in the depolymerisation of biomass, the use of model compounds is typically employed.

2.5.1.1 Lipids

The neutral lipids or fatty acids can be thermally decomposed to long-chain ketones, aldehydes, and esters, which are then converted to alkanes and alkenes through thermal and catalytic processes, as shown in Figure 2-9. These alkanes and alkenes, in turn, could be cracked to generate light olefins, while aromatic hydrocarbons may be produced in the pores of the zeolite catalysts through a series of reactions such as oligomerisation, cyclisation, and aromatisation (Kumar *et al.*, 2017).

2.5.1.2 Carbohydrates

Volatiles from carbohydrates formed during the decomposition in contact with the zeolite catalyst and produce light olefins and other liquid products. Carbohydrates thermally decompose to anhydrosugars and other condensable oxygenated products, such as furans and smaller aldehydes after dehydration and rearrangement reactions. These oxygenate then diffuse into the pores of the catalyst where they undergo a series of dehydration, decarbonylation, decarboxylation and oligomerisation to form aromatics and olefins compounds. For example, phenols and benzene compounds resulted from decomposition of carbohydrates.

2.5.1.3 Proteins

Figure 2-10 shows the reaction pathways for the degradation of a protein unit. Compounds including amines, nitriles, pyridine and indole have been detected in the pyrolysis products of microalgae. Protein degradation proceeds through aldol condensation reaction forming free radicals resulting in pyridine and pyrroles. The researcher suggested that decarboxylation, deamination and rupturing of C-C bonds (radical formation) pathways exist during the primary decomposition of phenylalanine and tyrosine (Li *et al.*, 2014a). Other than that, protein degradation also produced

aromatic hydrocarbons such as toluene, styrene and phenols as illustrated (Kumar *et al.*, 2017).
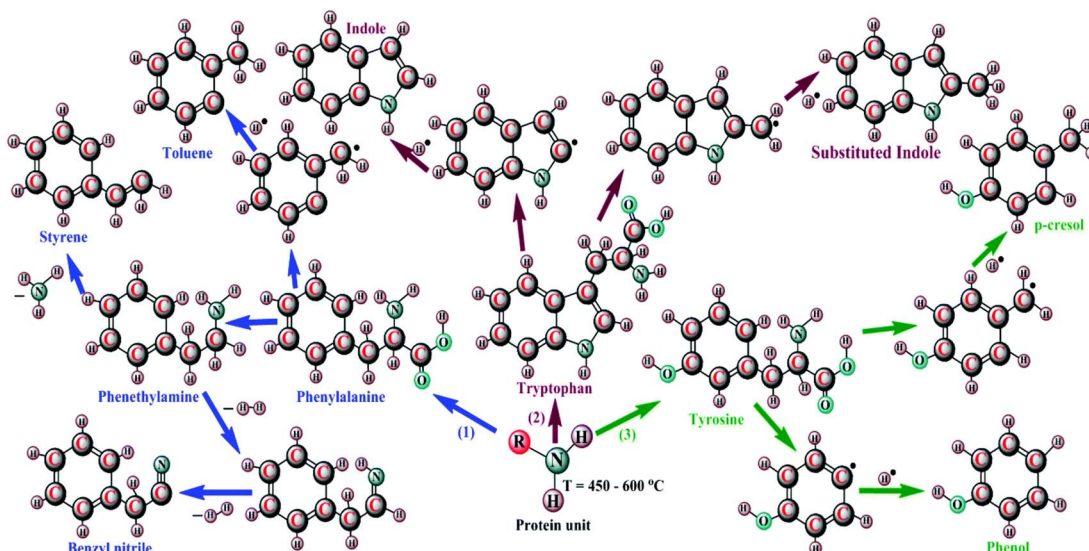
Figure 2-10 Postulated pathways of protein pyrolysis for the formation of several major products. (Kumar *et al.*, 2017)

2.6   Upgrading of bio-oil

Bio-oil from microalgae pyrolysis is a complex mixture consisting predominantly of oxygenated and nitrogenated compounds, light hydrocarbons, phenolics and sulphur containing compounds. The high level of the oxygenated and nitrogenated compound in the bio-oil is responsible for its poor physicochemical characteristics such as low calorific value, corrosivity, instability under storage and transportation conditions, and high viscosity. These properties make it unsuitable in most cases for direct application as fuel or feedstock for quality fuel production and chemicals; therefore, require further processing.

The present study investigates two different ways of improving the quality of bio-oil:

- Upgrading pyrolysis vapours in the presence of the catalyst. The catalytic pyrolysis is used in this study to improve bio-oil in terms of heating value, deoxygenation and denitrogenation, and chemical compositions.

- Improvement of bio-oil quality via chemical pre-treatment of feedstock. The process is used mainly to improve bio-oil in terms of chemical distribution. Different type of chemical solvents been used in this study for comparison and the effect of pre-treatment on the composition of the products can be analysed.

One of the main limitations of bio-oils derived from microalgae is the high N content. Microalgae show higher nitrogen content, which can be as high as 10 wt.%, far more than the terrestrial biomass. This represents an important issue when microalgae want to be converted to fuels due to the downstream potential emission of N-containing compounds, such as HCN and NO_x. The in-situ denitrogenation of microalgae pyrolysis bio-oils is somehow a new investigation topic with few works available in literature since nitrogen is typically removed via hydro-processing. Studies on nitrogen removal from catalytic upgrading is scarce; therefore, catalysts that able to remove nitrogen (N) from the bio-oil during or after its production must be developed.

2.6.1 *Bio-oil upgrading*

Catalytic cracking and HDO are two of the most promising chemical methods to upgrade bio-oils into liquid biofuels. The catalytic upgrading is performed with the aid of catalyst through series of chemical reactions such as dehydration, decarbonylation, decarboxylation where oxygen is removed in the form of H_2O, CO and CO_2 prior to condensation of volatiles. In this process, the catalyst is mixed or separated with the biomass or arranged in a packed bed together in the pyrolysis reactor. Volatiles from the pyrolysing biomass pass through the catalyst bed where the reactions take place.

2.6.1.1 *Catalytic pyrolysis of microalgae*

Catalytic pyrolysis technology has been extensively investigated as a technique for producing high-quality bio-oil. Most researches of microalgae pyrolysis evaluated *Chlorella sp.* as marine biomass because this family of microalgae is high in lipid content. Since catalytic upgrading is an attractive process to enhance the quality of algae bio-oil, it has been widely investigated using different catalysts.

A wide array of heterogeneous catalysts has been investigated for catalytic pyrolysis of biomass, the most common being a microporous acidic zeolite. Catalyst ZSM-5 seems to be the most promising catalyst for the process, mainly due to its relatively low number of acid sites with high strength and medium-sized channel pore system and enhancing aromatics selectivity. However, ZSM-5 suffered with high coke formation during pyrolysis. The zeolite supported metals are another-zeolite class of catalysts for biomass conversion, such as nickel, cobalt, iron and gallium substituted with ZSM-5. The presence of metal is suggested to affect the mode of deoxygenation by producing more carbon oxide and less water, thus providing more hydrogen available for the formation of hydrocarbon molecules. Metal modified catalysts have been studied for the catalytic pyrolysis as an attempt to produce a higher yield of hydrocarbons and less coke compared to non-metal modified zeolite catalysts. Therefore, the acidity of the zeolite catalysts can be optimised to achieved higher catalyst activity and lower coke formation.

Figure 2-11 shows a summary of the catalyst activities from several studies on catalytic pyrolysis. Most of the studies focused on product distributions and bio-oil quality from the catalytic pyrolysis. Overall, the bio-oils derived from the catalytic pyrolysis of microalgae present a higher energy density and able to reduce oxygen and nitrogen concentration in the bio-oil. Other than that, the presence of catalyst able promoting production of aromatics in the bio-oils. Among the catalyst, only metal oxides able to accelerate the decomposition of microalgae at low temperature. The summary implies that improved quality bio-oil can be obtained in the presence of the adequate catalyst, although these benefits also imply the production of a lower amount of this liquid fraction.

41

The literature also indicates that there is still low understanding on microalgae catalytic pyrolysis due to the different intrinsic composition compared to better-studied terrestrial biomasses. Another clear observation emerging from the current literature is the fact that acid zeolites are the most investigated class of catalyst in algae pyrolysis, while medium acids/basic materials received little attention so far. Therefore, this work wants to reduce knowledge gap on base/acid catalysts behaviour of microalgae conversion.
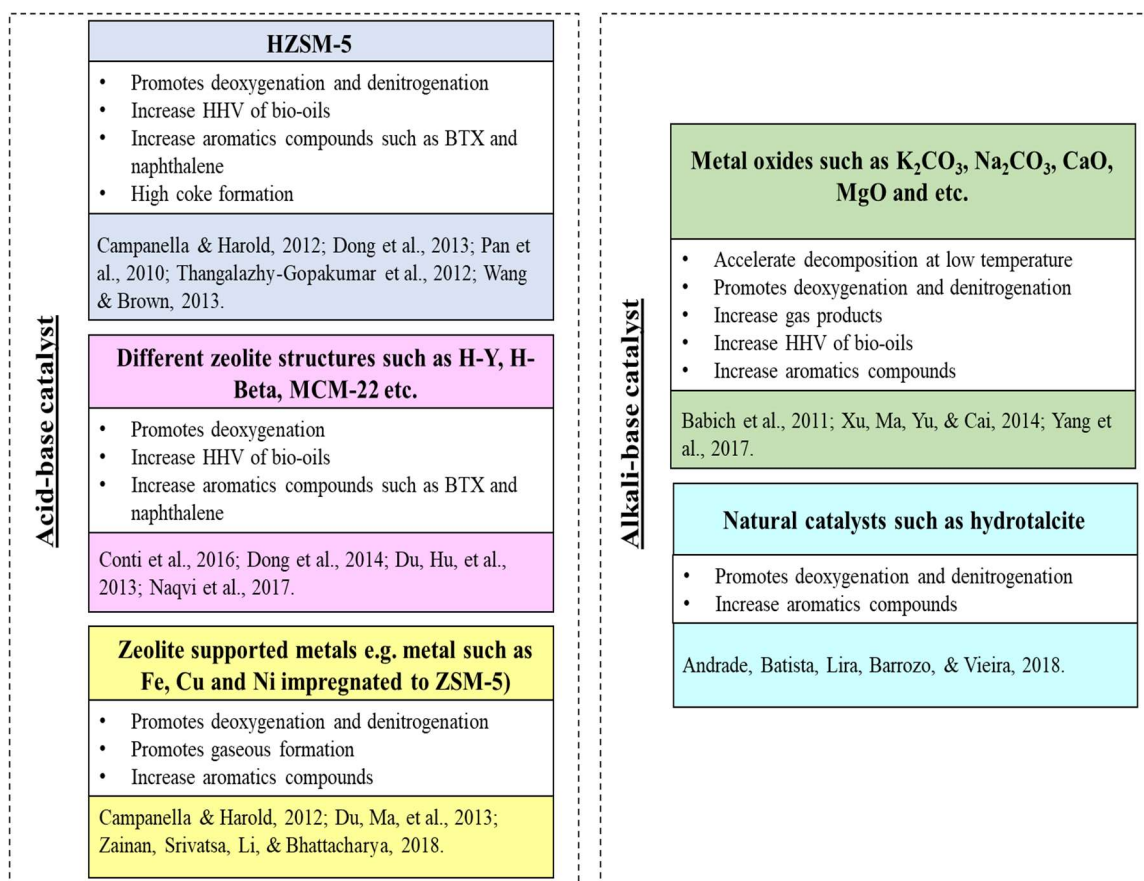
Figure 2-11 Summary of findings on catalytic pyrolysis of microalgae.

In the present study, two different types of catalysts (acid and alkali based) will be used to enhance the quality of the bio-oil. Micro silica which is neutral will be used for comparison between the catalyst type.

i.   *Li-LSX-zeolites*

Li-LSX-Zeolites catalyst contains a low Si/Al ratio (1.0) with a pore size between 7 to 12Å. The addition of a metal such as lithium in LSX zeolite enhances its hydrocracking and isomerisation activity by providing a large surface area. Li-LSX-Zeolite has been widely used for industrial air separation processes for oxygen production. Since the Li cations preferentially adsorb nitrogen over oxygen (Zanota *et al.*, 2011), its affinity to nitrogen could be beneficial for the denitrogenation of microalgae bio-oils. Studies on using Li-LSX-zeolite in pyrolysis has not been reported in the literature, which is part of one of the objectives of this research. Therefore, there is a need for further investigation to establish more detailed information on the yield and characteristic of pyrolysis oil from the catalytic upgrading of microalgae.

ii.   *Sodium and lithium fly ash derived sorbents*

The literature shows that sodium and lithium fly ash derived sorbents has been investigated for high temperature post-combustion CO_2 capture applications. The use of waste materials such as fly ash as precursors of the sorbents was considered for being widely available and cost-effective. A novel Li_4SiO_4 based sorbents from FA was synthesised by Olivares-Marin (Olivares-Marin, Drage & Maroto-Valer, 2010). The study compared the use of Li-FA derived sorbents with pure Li_4SiO_4 sorbents on the CO_2 sorption. The novel sorbent was able to maintain its sorption capacities after 10 cycles; meanwhile the pure Li_4SiO_4 sorbent attains no equilibrium capacity for CO_2 sorption. Meanwhile, another study showed that the Li-Na-FA had a CO_2 uptake comparable to other high temperature sorbents such as pure Li_4SiO_4 sorbents. The sorbents maintained their capacity and absorption/desorption rates after 10 cycles at high temperatures (Sanna, Ramli & Mercedes Maroto-Valer, 2015).

The above literature on using basic catalysts for pyrolysis of microalgae and CO_2 capture purposes, suggest that Na-and Li/Na silicates derived from coal fly ash have could also be good performing catalysts for the catalytic pyrolysis of microalgae by converting them

in carbon monoxide and hydrocarbon-rich gas. However, there is a lack of knowledge on their potential activity since they have not been investigated yet for the pyrolysis of microalgae.

2.6.1.2 *Hydrodeoxygenation (HDO)*

Hydrodeoxygenation (HDO) is an effective bio-oil upgrading technique using a variety of heterogeneous catalysts at high hydrogen pressure (7.5–30 MPa) and moderate temperatures (250 to 450 °C) (Rogers & Zheng, 2016). Various noble and transitional metal catalysts supported on carriers of alumina, silica, titania, zirconia, magnesium oxide, active carbon, and HZSM-5 have been tested on bio-oil and model HDO compounds (Laskar *et al.*, 2014; Fermoso *et al.*, 2017b). During the bio-oil HDO process, multiple reactions including hydrogenation, hydrogenolysis, hydrodeoxygenation, decarboxylation, decarbonylation, cracking/hydrocracking, and polymerization reactions occurred. HDO removes oxygen in bio-oil as H_2O, CO, and/or CO_2. This results in the production of stable hydrocarbon biofuel with higher energy content. An efficient HDO catalyst should effectively remove oxygen with low hydrogen consumption and suppress the coke formation that leads to catalyst deactivation.

2.6.2 *Pre-treatment of microalgae and subsequent pyrolysis*

The presence of impurities in the biomass and microalgae, such as alkali, sulphur and nitrogen species disrupt the catalyst activity. There are several biomass pre-treatment methods depending on the conversion route and the desired product. For thermochemical conversion process, hydrothermal, torrefaction and chemical pre-treatment are the most commonly used. In this study, chemical pre-treatment will be carried out on microalgae to investigate the influence on the pyrolysis process.

2.6.2.1   *Chemical pre-treatment*

The chemical pathway involves the use of either mild solutions of acids (hydrochloric acid and sulphuric acid) or bases (lime and sodium hydroxide), which present minimal toxicity in the applied mild concentrations (Harun & Danquah, 2011). Acid and alkaline pre-treatments are those technique that require lower operating cost when compared to other pre-treatments. Acid treatments have been widely studied and predominantly used in raw materials with high carbohydrate content, while alkaline treatments are best applied to raw materials with a high concentration of proteins which recently applied to microalgae.

So far, only a limited number of works have been done for pyrolysis purposes. A study investigated the effect of treatment on bio-oil production by pyrolysis of macroalgae *Undaria pinnatifida,* which contained high ash content (38 wt.% on dry basis) (Bae *et al.*, 2011). Treatment by acid washing (2M hydrochloric acid, mix on the hot stirrer at 60 °C for 6 h) was able to remove most of the ash content to 0.76 wt.%. As a result, the bio-oil yield from pyrolysis increased after acid treatment from 40 wt.% to 46 wt.% at 500 °C. In another work, Choi et al. showed that sulphuric acid treatment of brown macroalgae (*Saccharina Japonica*) was able to remove active inorganic minerals by reducing the ash content from 18.3 wt.% to 3.3 wt.% (Choi *et al.*, 2014). The treatment did not modify the bio-oil quality, with a minor HHV increase from 12.1 MJ/kg to 14.4 MJ/kg after treatment. The data in the literature show that microalgae pre-treatment improves the thermal decomposition behaviour as well as enhance the bio-oil conversion. Consequently, fundamental studies on pre-treatment of microalgae, product characterisation and their impacts on pyrolysis products distribution have not been reported widely in the literature, which is one of the objectives of this research.

2.7 Catalyst deactivation

Even though catalytic upgrading is a very promising route for the conversion of microalgae into bio fuels and chemicals, catalyst deactivation represents a challenge. Although advances have been achieved, the deactivation and regeneration of catalysts remained a challenge. Catalyst deactivation is a big concern in the industrial catalytic process. Oxygen-containing chemical species such as aromatic and nitrogenated compounds in the pyrolysis oil are perceived to result in coke formation during upgrading due to their instability and deficiency in molar balance (Bartholomew, 2001; French & Czernik, 2010). The coke precursors are said to undergo polymerisation and polycondensation on the catalyst surface, fill up the in inner pores, build-up trap compounds and eventually result in catalyst deactivation.

Studies have suggested that lipid-derived compounds are more susceptible to char and coke formation during cracking and upgrading of bio-oil compared to carbohydrates (acid, aldehyde, ketones and sugars) (Gai *et al.*, 2013). This was attributed to the complex structures of lipid and the bulkiness of the lipid derivatives, which make them too large for the pores of the ZSM-5 catalyst. Other than that, by-products from proteins cracking contributed to the coking process causing catalyst deactivation.

Coke deposition on the catalyst during catalytic pyrolysis has been classified into two groups; catalytic carbon and thermal carbon as shown in Figure 2-12. The catalytic carbon is formed as a result of chemisorption of poisons such as amines and nitrogen-containing heterocyclic compounds, and other heavy hydrocarbons on the catalyst structure due to reactions such as condensation, hydrogen transfer and dehydrogenation reactions. Meanwhile, the thermal carbon is the coke formation on the catalyst surfaces as a result of the high reaction temperature. Both catalytic and thermal carbon lead to either partial or complete loss of catalytic activity (Mortensen *et al.*, 2011).
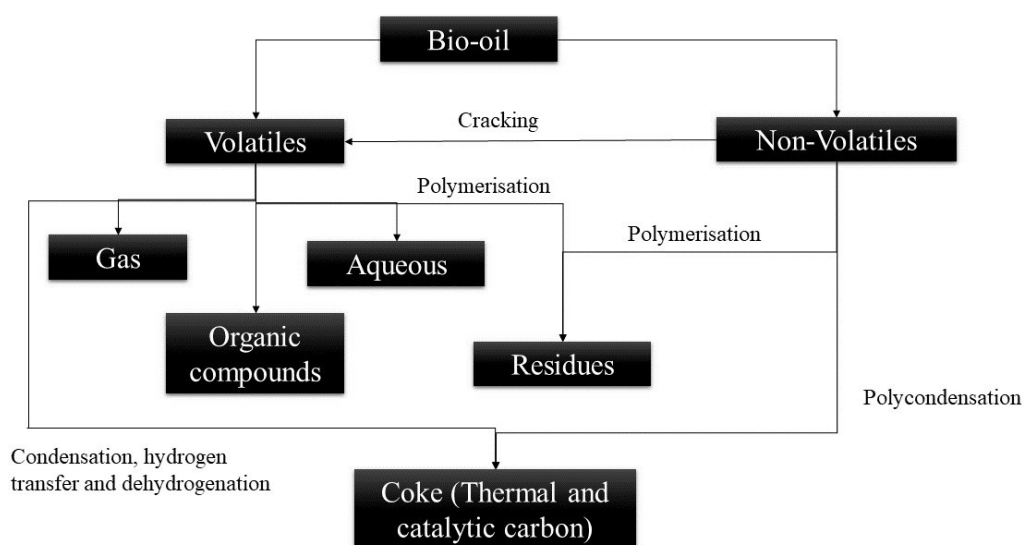
Figure 2-12 Coke formations from bio-oil deoxygenation. (Mortensen *et al.*, 2011).

2.7.1 *Zeolite deactivation*

Fouling or coking is the main reason for zeolite deactivation in catalytic cracking (Cheng *et al.*, 2016). Catalyst deactivation on zeolite occurs due to coke formation and strong adsorption of oxygenates compounds on the surface of catalyst support (Pütün *et al.*, 2014; Zhang *et al.*, 2015). Acid zeolites perform the best to deoxygenate pyrolysis vapours as well as increasing hydrocarbon production, mostly forming aromatics compounds. However, this acid catalysed transformation usually results in polymerisation of oxygenates and formation of large polyaromatic hydrocarbons (PAH) known as coke on the catalyst. This coke remained trapped on the pores sites or covered on the active surface of the catalyst. Thus, reduced the catalysts activity, selectivity and life cycle time and hindered the production of high valued chemicals (hydrocarbons) from catalytic pyrolysis. Studies aimed at minimising catalyst deactivation and searching for long-lasting solutions are in progress to ensure the sustainability of industrial process scale-up. Structural modification of zeolite is considerable attention in recent time as a solution to reduce coke formation.

2.7.2 *Catalyst regeneration and recycling in catalytic cracking*

In order to improve catalyst lifetime and reduce operation cost on the catalyst, the regeneration or recycling of catalyst becomes essentials. Zeolite catalyst can be recovered by oxidation regeneration at high temperature through coke combustion. The catalyst regeneration temperature should not exceed the catalyst calcination temperature because it will destroy the catalyst structure or if the temperature is too low, coke cannot be removed completely. The performance of the catalyst during the pyrolysis depends on its successful regeneration.

A lot of attention has been paid to the kinetic study of coke formation and catalyst regeneration in various processes (Zhang *et al.*, 2013; Paasikallio *et al.*, 2017; Shao *et al.*, 2018). A study on the fresh, spent and regenerated ZSM-5 catalyst during catalytic pyrolysis was carried out by (Zhang *et al.*, 2015). The study was conducted on the pyrolysis of corn Stover using Py-GC/MS at 500 °C. The catalysts in this study were indicated as; FZ (fresh catalyst), SZ (spent catalyst) and RZ (regenerated catalyst). From the catalyst characterisation, FZ had the highest value of total acid sites and BET surface area compared to other catalysts. The results show that the catalyst produced vapour yield in the following order: (FZ > RZ > SZ). Besides, the highest coke yield was obtained by FZ followed by RZ and SZ. Opposite patterns observed with the production of hydrocarbons and oxygenation removal, where catalyst SZ and RZ favoured both reactions compared to the FZ. Moreover, the production of aromatics, such as BTX and PAHs were investigated where it resulted that SZ catalyst effective in producing these aromatics compounds followed by RZ and FZ. The study concluded that pre-coking was a useful method in minimising the coke yield and induce the selectivity hydrocarbons formation.

Shao et al. studied the regeneration of catalyst ZSM-5 in the combined oxygen and steam atmosphere used for catalytic pyrolysis (Shao *et al.*, 2018). The study was carried out to

study the relationship between oxygen concentration of regeneration and performance of the catalyst during pyrolysis. The results show that the optimal oxygen concentration (15%) was enough to keep the catalyst works for 30 cycles. However, when 15% oxygen/5% steam was combined for regeneration atmosphere, the yield of hydrocarbons boosted by 31.3% compared with only 15% of oxygen. The study also investigated on the regeneration of catalyst by retaining some coke (partially regeneration). The results showed that by retain coke (2.18%), the yield of olefins promoted by 27.4% compared to the completely regenerated catalyst. This show that retaining coke changed the products distribution by forming more hydrocarbons such as ethylene, propylene, butylene and BTX. The study concluded that the combined oxygen/steam atmosphere and controlled on the regeneration able to create stable-catalysis regeneration products and tuned end-products for hydrocarbons production.

The overall effect of continued regeneration reduced the effectiveness of the catalyst in converting biomass pyrolysis oils to aromatic products. Regarding the pyrolysis product yields, the replication of regeneration amplified the oil yields and lowered the aqueous yields. Also, the use of H-ZSM-5 after several regeneration cycles suggested that its aromatisation power was reduced after each regeneration. Although numerous studies have been done to investigate on the ZSM-5 catalyst regeneration on lignocellulose biomasses, fewer studies are available in the literature for the regeneration of other catalysts on pyrolysis of microalgae. Therefore, the investigation on the regeneration of other zeolites such as LSX-zeolites could give an important contribution to the understanding of the deactivation process and in defining strategies to reduce it.

2.8   Summary

Vast of studies have been carried out on catalytic pyrolysis of microalgae. However, collective evaluation of pyrolysis process parameters on products distribution derived from microalgae biomass and subsequent assessment of bio-oil, bio-char and gaseous are

needed in order to fully examine the biomass potential for bioenergy production. Indeed, no study currently available on the catalytic upgrading of bio-oil using Li-LSX-zeolite and sodium and lithium fly ash derived sorbents. Therefore, in the following chapters, this study provides a comprehensive assessment of pyrolysis of selected microalgae biomass and pyrolysis products in the presence of the catalysts. Other than that, the study on parameter optimisation for optimal bio-oil production from catalytic pyrolysis will be carried out. The effect of pre-treatment of microalgae on pyrolysis product distribution and characteristics will be evaluated. Finally, the catalyst regeneration will be evaluated in comparison of treated and non-treated microalgae.

Chapter 3
Methodology

3.1   Overview

The overall experimental work of the research is summarised in Figure 3-1. Chapter 4 reports on the selection of microalgae biomasses based on their bio-chemical compositions (i.e. lipid and protein content) and characterisation analyses including elemental and proximate analyses. The selected microalgae then underwent pyrolysis experiments to evaluate their potential direct upgrading through catalytic pyrolysis. Chapter 5 mainly focuses on the selection and evaluation of different catalysts for the microalgae pyrolysis. Various types of catalysts were used to investigate their effects on the in-situ catalytic pyrolysis and evaluate their bio-oil/bio-gas upgrading activity. In Chapter 6, a selected microalgae species and catalyst were then subjected to further catalytic pyrolysis studies under different operating parameters for the optimisation of the catalytic activity the operating parameters. Different conditions such as residence time, catalyst: biomass ratio, temperature and reactor configuration were evaluated. The product yields from using the different parameters then were calculated and all products characterised. Various analyses were carried out for the products characterisation, such as ^{1}H NMR, GC-MS, FT-IR and EA analyses, which are further discussed in the next sub-chapter.

Chapter 7 mainly focuses on microalgae pre-treatment using a different kind of chemicals; Sulphuric acid (H_2SO_4) and Sodium hydroxide (NaOH) solutions (in different concentrations) and water, with the intent to partially remove the alkali species presence in the microalgae. Then, the treated microalgae were pyrolysed in the presence of the selected catalyst to examine the influence of the chemical pre-treatment on the pyrolysis product yields and quality. Finally, Chapter 8 reports on the catalyst regeneration, where the selected catalyst (Li-LSX-zeolite) was subjected to pyrolysis and regeneration cycles for evaluating the catalyst deactivation during pyrolysis.
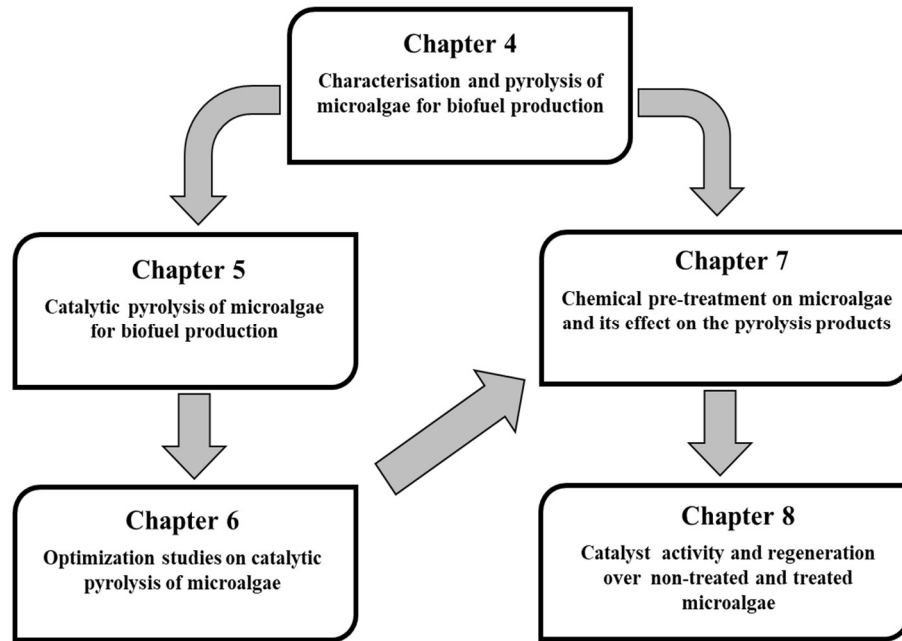
Figure 3-1 Experimental work carried out in this research.

3.2 Procurement and preparation of samples

3.2.1 *Microalgae procurement*

In this study, several algae strains were purchased from Varicon Aqua Solutions Ltd. Selected microalgae species were *Nannocholoropsis 3600, Tetraselmis 3600* and *Isochrysis 1800*. All purchased algae were in liquid form in 1L bottles. The selection of these specific microalgae strains as potential biofuel source was done through the investigations of the open literature and data obtained in previous works, as discussed in the literature review. In short, it has been ensured that all the selected microalgae have good global distribution, high productivity and there were fewer works available on their pyrolysis behaviour with and without catalysts.

3.2.2 *Microalgae preparation*

The received microalgae samples were received in liquid form. The microalgae were dried at 60 °C in an oven for 1 week to remove about 90% of the moisture. This temperature was selected to maintain its structural integrity. After the drying process, the samples were milled for 1 minute using a Fristch Pulverisette 2 to a particle size less than 177 μm and stored in a desiccator for further use.

3.2.3 *Catalyst procurement*

In this research, different types of catalyst were used: Li-LSX-zeolite (acid), Na-FA and LiNa-FA (basic) and micro silica (inert). Li-LSX-zeolites was acquired (in pellets form) from Shanghai Hengye Chemical Industry Co. Ltd. This catalyst was then grounded using a pestle and mortar. Micro powder SiO_2 was purchased from Sigma Aldrich (product code 805890), while the basic catalysts were synthetized as described below.

3.2.4 *Catalyst synthetisation*

The other two catalysts, Na-FA and LiNa-FA were instead synthesised in the lab by following the method reported by Sanna (2015) (Sanna, Ramli & Mercedes Maroto-Valer, 2015). The catalysts (Na-FA and LiNa-FA) were prepared using a solid-state method, by mixing Li_2CO_3 and/or Na_2CO_3 (both from Arcos Organics) with coal fly ash rich in SiO_2. The fly ash, obtained from a coal power plant, had the following composition: SiO_2 49.8%, Al_2O_3 23%, Fe_2O_3 7.1%, CaO 4.9%, K_2O 2.3%, MgO 2.2%, TiO_2 1%, Na_2O 0.8% (Sanna, Aimaro, Maroto-Valer, 2016). The chemicals were mixed using mortar and pestle for 10 minutes until the solid mixture achieved homogeneity. Then, the mixtures were calcined for 8 hours at 800 °C. After calcination, the materials were homogenised using a Mortar Grinder (Pulverisette 2, Fritsch) for 1 minute to eliminate any potential large agglomeration. The catalysts were kept in bottles until further used. Figure 3-2 shows the catalysts used in this research.
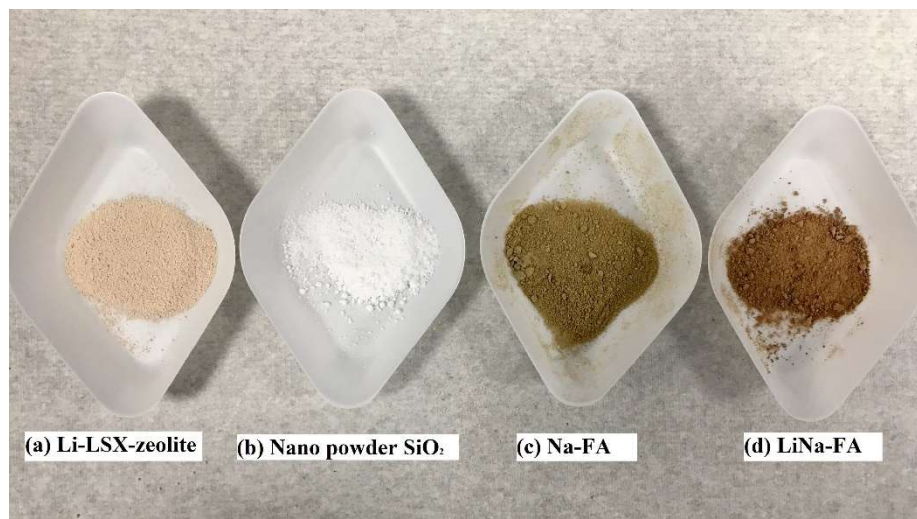
Figure 3-2 Types of catalyst used in this research.

3.3 Biomass and Pyrolysis products characterisation

Biomass characterisation is important to determine the composition and predisposition of the fuel feedstock towards the production of bio-fuel. Microalgae biomasses contain high oxygen and nitrogen, which could lead to poor properties of bio-oil. A quality biofuel can be produced by removing the oxygen and the nitrogen content through catalytic upgrading. Therefore, the characterisation of the starting materials and reactions products is important to track the potential improvements of the bio-oil produced. A detailed description of the techniques employed is discussed in the following sections.

3.3.1 *Thermogravimetric analysis (TGA)*

3.3.1.1 *Background of TGA*

Thermo-gravimetric analysis (TGA) is an analytical equipment used for material characterisation. A thermo-gravimetric analyser TA Q500 was used. As shown in Figure 3-3, TGA compromises a furnace, a vertical precision thermal balance, a gas system to maintain the atmosphere and a computer to control the programme selected.

Details:

1. Furnace
2. Pan holder
3. Thermal balance
4. Gas system
5. Computer monitoring

Figure 3-3 TGA Q500

3.3.1.2   *Experimental procedure using TGA*

3.3.1.2.1   *Proximate analysis*

Proximate analysis was carried out to characterise the microalgae used in this research. The decomposition profile of biomass can provide information on the microalgae depolymerisation, that assists in predicting the best conditions for recovering bio-oil and used to compare the activity of the catalyst. For example, the volatile matter (VM) profile shows the potential amount of bio-fuels (bio-oil + gas) produced. Ash content in the biomass also needs to be considered, whereby high ash content can affect the yield and quality of the bio-oil.

Figure 3-4 depicts the proximate analysis method that was used in this research. Before each run, the crucibles were tared and loaded within 20 mg of sample. Each sample was heated up in nitrogen atmosphere with a flow rate of 100 ml/min. The samples were normally running in duplicates. The programme used was 15 °C/min from 30 °C to 105 °C in nitrogen and held for 15 minutes at 105 °C for evaluating the residual moisture content in the microalgae, then, the temperature was increased at 20 °C/min from 110 to 800 °C and held at 800 °C in oxygen-free atmosphere for 40 minutes. At this temperature, the atmosphere was changed from nitrogen to oxygen, and the temperature was cooled down at 50 °C/min from 800 to 600 °C and held for 40 minutes to permit the complete combustion of the sample and determine the fixed carbon and ash content in the microalgae. Finally, the system was cooled down from 550 °C to 30 °C at 50 °C/min.
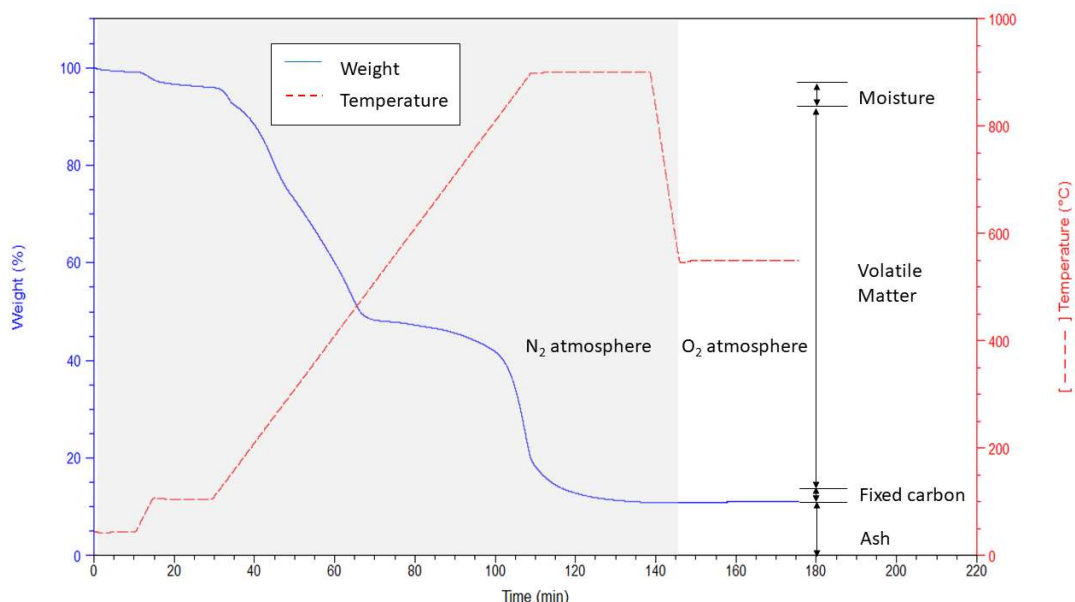
Figure 3-4 Proximate analysis method using TGA.

3.3.1.2.2   *TGA-pyro analysis*

TGA was used to simulate the pyrolysis of microalgae on their own and in the presence of different catalysts. Preliminary pyrolysis in micro-scale was done for the

characterisation of microalgae. About 0.5 g of sample (of each microalgae) was mixed with the catalyst with a ratio of 1:1 using a pestle and mortar for consistency in the pyrolysis tests when catalysts were used. Then, about 10 mg of each sample (microalgae on their own or microalgae/catalyst mixtures) was then placed in a platinum pan and loaded into the TGA furnace. The analysis was performed under a nitrogen gas atmosphere. The program used was heated 100 °C/min from 25 °C to 500 °C. The temperature was hold for 20 mins at 500 °C to permit the complete conversion of the sample. Finally, the system was cooled down from 500 °C to 25 °C at 50 °C/min. In many tests, the incondensable gaseous released during the pyrolysis were directly sent to an MKS Cirrus MS for their characterisation. This is discussed in Section 3.3.7.

3.3.2   *Elemental analyser*

3.3.2.1   Background of Elemental analyser

Elemental analysis (EA) is an analytical tool specifically designed to simultaneously analyse and quantify Carbon, Hydrogen, Nitrogen and sulphur (CHNS) in organic and related materials. These elemental compounds are important to determine the quality of the pyrolysis products and can be used to calculate their calorific values. There are various types of elemental analysers manufacture by different companies with different configurations, which include CHN, CHNS and CNS depending on the elements intended to analyse. The sample was introduced in the analyser furnace at temperature between 950 °C and 1800 °C, where all samples are combusted and vapourised to CO_2, N_2, N_xO_y, H_2O and other by-products. The gaseous are then swept out of the combustion chamber by an inert carrier gas such as helium and passed through the thermal conductivity detector (TCD), where the amount of each gas, CO2, H2O, N2 and He (carrier gas) are detected. From the readings, the percentage of C, H, S and N can be determined.
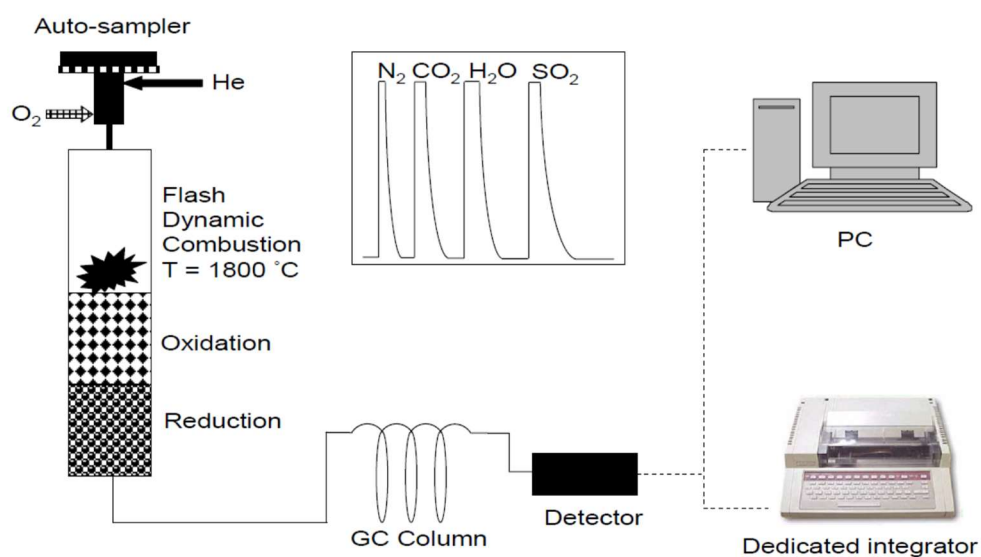
Figure 3-5 Schematic diagram of a CHNS Elemental analyser (EA). (Thompson, 2008)

3.3.2.2   *Experimental procedure of Elemental analyser*

The elemental composition was determined by Elemental analysis (EA) following ASTM E777, ASTM E778, ASTM E775, respectively. This technique allows the tracking of the variation of oxygen in the samples. The elemental analysis of the biomass samples and the solid/liquid products from pyrolysis reaction was determined using an Exeter CE-440 Elemental analyser.

The oxygen (O) content was determined by difference using the following formula:

$$Owt\%_{DAF} = 100 – (Cwt\%_{DAF} + Hwt\%_{DAF} + Nwt\%_{DAF} + Swt\%_{DAF}) \qquad (3.3.1)$$

where C is carbon, H is hydrogen, N is nitrogen and S is sulphur. The Dry Ash Free (DAF) values were calculated by the ASTM method:

$$Cwt\%_{DAF} = Cwt\% * 100 / (100 – (moisture \% + ash \%) \qquad (3.3.2)$$

58

$$Nwt\%_{DAF} = Nwt\% * 100 / (100 - (moisture \% + ash \%)) \qquad (3.3.3)$$

$$Hwt\%_{DAF} = (Hwt\% - 0.0111 * moist.) * 100 / (100 - (moisture \% + ash \%)) (3.3.4)$$

The tests were carried out duplicates for each sample and the average calculated.

3.3.3 *Energy content (HHV)*

The higher heating values (HHV) of the feedstocks and liquid/solid products were calculated based on equation 3.3.5 (Parikh, Channiwala & Ghosal, 2005; Channiwala & Parikh, 2002).

$$HHV \ (MJ/kg) = (0.3491*C) + (1.1783*H) + (0.1005*S) - (0.1034*O) - (0.015N)$$

$$- \quad (0.0211A) \qquad\qquad (3.3.5)$$

Where C, H, S, O, N and A represent the mass percentages on a dry basis of carbon, hydrogen, sulphur, oxygen, nitrogen and ash contents of biomass, expressed in mass percentages on a dry basis, respectively obtained from the elemental analyses.

3.3.4 *Gas chromatography mass spectrometry (GC-MS)*

3.3.4.1 Background GC-MS

Gas-Chromatography Mass Spectrometry is a useful technique for the identification and quantification of organic compounds with the molecular weight (MW) ranging from 50 to about 400 a.m.u. Gas chromatography separate different volatile components of liquid mixture coupled with the mass spectrometry to identify each volatile organic compound that produced.

3.3.4.2   *Experimental procedure*

The obtained bio-oil samples were dried in the vials together with the acetone. In this research, GC-MS analysis was performed by a Shimadzu GCMS QP2010 SE equipped with a Restek RXI-5HT column. The column (length: 30m, inner diameter: 0.250; film: 0.25 μm) had temperature limits between 40 °C to 300 °C. The oven was programmed to hold at 40 °C for 10 min, ramp at 5 °C/min to 200 °C and hold for 10 min, ramp at 10 °C/min to 250 °C and hold for 10 min, ramp at 10 °C/min to 295 °C and hold for 10 min. Helium was used as the carrier gas with a constant flow rate of 1.7ml/min and injector split ratio at 1:20 ratio. The end of the column was directly introduced into the ion source detector of VG Trio 1000 series. Typical mass spectrometer operating conditions were as follows: transfer line 270 °C, ion source 250°C, electron energy of 70 eV. The chromatographic peaks were identified according to the NIST library to identify bio-oil components. Since the maximum operating temperature of the combined technique was lower than 300°C, the "picture" of the bio-oils composition provided by the GC-MS is only partial (about 40-50%) and can be quantify in 80% (average value) by evaluating the fraction of volatiles released up to 300°C during the pyrolysis of the bio-oils.

3.3.4.3   *Quantification*

All relative quantification was performed by first checking the peak area percentage. The peak area of each analysis was integrated using the available system and software and double checked by using Microsoft Excel. Firstly, the percentage area below 0.1% were not considered relevant and eliminated. Next, the identified compounds in each sample were categorised into the following chemical functional groups: aliphatic hydrocarbons, aromatic hydrocarbons, ketones, nitrogenated compounds, alcohols, ethers, esters, carboxylic acids, aldehydes. Table 3-1 describes the main compounds of each group category detected in the bio-oil.

Table 3-1 Main compounds in the functional groups.

Group	Compounds
Alcohols	Dodecanol, Hexadecanol, Phytol, Methanol
Aldehydes	7-Hexadecenal, 9-Octadecenal
Aliphatic hydrocarbons	Nonadecene, Octadecene, Heptadecane, Tetracosane
Aromatic hydrocarbons	Benzene, Phenols, Naphthalene, p-Cresol
Carboxylic acids	Pentanoic acid, Propionic acid, n-Hexadecenoic acid
Ester	Heneicosanoic acid-methyl ester, Butyric acid-2-phenyl-, Decyl ester, Fumaric acid-butyl 1-naphthyl ester
Ether	Hexadecen-1-ol- acetate, Tetradecyl trifluoroacetate
Ketones	2-Decanone, 2-Nonadecanone, 3-Hexadecanone
Nitrogen compounds	Hexadecanamide, Indole, Propanamide, Olea nitrile

3.3.5 *Nuclear Magnetic Resonance (^{1} H NMR)*

3.3.5.1 *Background of NMR analysis*

The Nuclear Magnetic Resonance (NMR) is a device based on the quantum mechanical magnetic properties of elements such as ^{13}C and ^{1}H. Each ^{13}C and ^{1}H has a specific magnetic moment, and angular momentum defined by its neighbours that is detected during NMR spectroscopy.

3.3.5.2 *Experimental procedure of NMR*

In this work, Proton NMR (^{1}H NMR) was selected to give an overall picture of the bio-oil composition in terms of the proton distribution in the different chemical functionalities. The ^{1}H NMR of the bio-oils was analysed using a Bruker Avance III operating at 400MHz. The machine was equipped with 60 samples position autosampler, with a 5 mm dual ^{1}H/^{12}C pyro probe. For samples preparation, bio-oils were diluted in 99.9% of Dichloromethane ($CDCl_3$) (Merck, Germany) with ratio 1:1 by volume and poured into 5 mm NMR tubes. All the acquired NMR spectra were processed through Topspin version 2.1 software. The chemical shifts in ^{1}H spectra were integrated to quantify various components based on their hydrogen bonding behaviour. Table 3-2 describes the type of protons that are present in the chemical shift regions from the integrations. The total area integrations are expressed as a percentage.

Table 3-2 ^{1}H NMR based on the integration of chemical shifts region.

Chemical shift region (ppm)	Type of protons
0.0 - 1.6	CH3. -CH2-
1.6 - 2.2	-CH2-, aliphatic OH
2.2 - 3.0	-CH3OC, -CH3-Ar, -CH2Ar
3.0 - 4.2	CH3O-, -CH2O-, =CHO
4.2 - 6.4	=CHO, ArOH, HC=C (nonconjugated)
6.4 - 6.8	HC=C (nonconjugated)
6.8 - 8.0	ArH, HC=C (conjugated)
8.0 - 10.0	-CHO, -COOH, downfiled ArH

3.3.6 *Fourier Transform Infrared spectroscopy (FT-IR)*

3.3.6.1 *Background of FT-IR*

Fourier Transform infrared spectroscopy (FT-IR) is a fast, non-destructive and easy method analysis of the chemical structure of samples. The operation based on the analysis of the interaction of infrared light with matter. When infrared radiation is directed at a sample, it is partially absorbed/transmitted due to the vibrations of chemical bonds of the molecules. The sample can be analysed via either transmittance or absorbance mode. There is a correlation between the wavenumber at which each compound absorbs IR radiation and its chemical structure (Sawant, Baravkar & Kale, 2011).

In FT-IR instrument, the source energy submitted through an interferometer and onto the sample (Gable, 2013). In every scan, all source radiations are passed through the sample. The light passes through a beam splitter, which sends the light in two directions at right angles. One beam goes to a stationary mirror, which reflects the beam back to the beam splitter. Meanwhile, the other goes to a moving mirror, and the motion of the mirror reflects the beam to the beam splitter. Both beams recombine at the beam splitter, however, the difference in the path lengths creates an interferogram (constructive and destructive interference). The recombined beam passes through the sample. The sample absorbs all the different wavelengths characteristic of its spectrum and remove specific wavelengths from the interferogram. The detector then reports variation of energy versus time for all wavelengths simultaneously. A mathematical function called Fourier transform converts an intensity vs. time spectrum into an intensity vs. frequency spectrum. The output of the detector is connected to the computer. Next, the transformation was automated by the software, followed by mathematical refinement of the data. Figure 3-6 illustrates the FT-IR instrumentation setup.
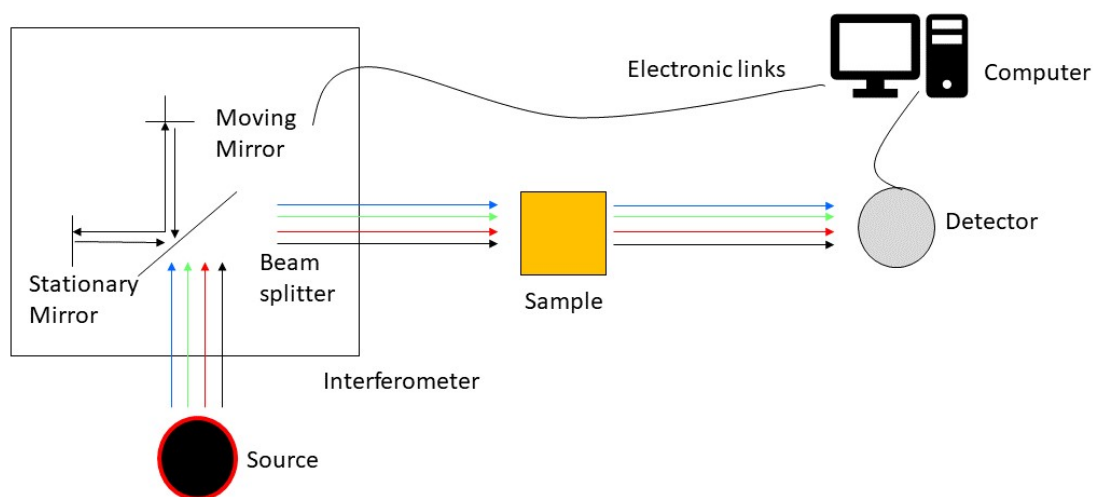
Figure 3-6 FT-IR instrumentation setup (Gable, 2013).

3.3.6.2 *Experimental procedures of FT-IR for bio-char*

In this research, FT-IR analysis was performed using a Perkin Elmer Frontier assisted with Spectrum 10 software to acquire and process data. The first step of the tests was to collect background spectra that can be subtracted from the sample spectra. Next, the sample was placed directly on the crystal plates for the analysis. The samples then produced its own spectra, and the peaks were compared with catalogued spectra to identify components for the known materials. All samples were analysed in duplicate in the range 4000-400 cm^{-1} for consistency, with four scans per run set in the instrument configuration. The absorbance spectra showing the unique chemical bonds, thus, both the chemical components present in the sample and their molecular state can be determined. Absorbance peaks on the spectrum indicate functional groups (for example alkanes, ketones or alcohols).

3.3.7 *Mass spectrometry*

3.3.7.1 *Background of Mass Spectrometry*

Mass spectrometers use the difference in mass to charge ratio (m/z) of ionised atoms or molecules to separate them. Therefore, mass spectroscopy allows quantitation of atoms or molecules and provides structural information by the identification of distinctive fragmentation patterns. Figure 3-7 illustrates the building blocks of a MS system. All mass spectrometer contains a vacuum system to maintain the low pressure (high vacuum) condition, required for the operation. This condition minimises ion molecules reactions, scattering and neutralisation of ions. The inlet transfers the sample into the vacuum chamber of the mass spectrometer. In the gaseous ion source, neutral sample molecules are ionised and then accelerated into the mass analyser. The mass analyser will separate ions, either in space or in time, according to their mass to charge ratio. After the ions are separated, they are detected by ion transducer, and the signal is transferred to the data system for analysis.
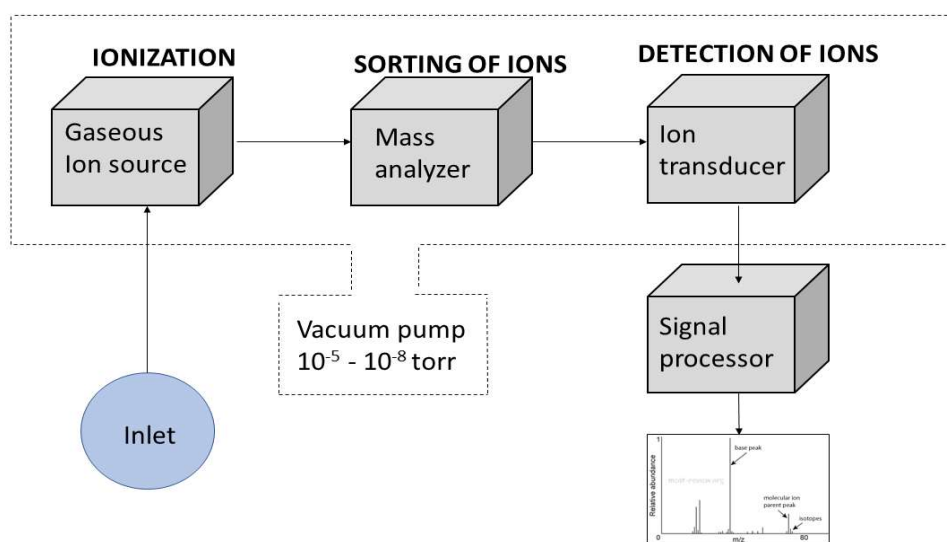
Figure 3-7 MS instrumentation setup.

The Cirrus MKS MS is an on-line gas analysis system, which is able to analyse gas at atmospheric pressure. The Cirrus is built around a Microvision plus IP Residual Gas Analyser. The RGA is quadrupole mass spectrometers, incorporating a closed ion source, a triple mass filter and a dual (Faraday and Secondary Electron Multiplier) detector system. This configuration offers long-term stability performance and optimises the sensitivity. The RGA is placed in a small stainless-steel chamber, pumped by a turbo molecular pump, which is in turn backed by a dry diaphragm pump. A capillary inlet is used to achieve a suitable pressure differential between the atmospheric sample and the RGA itself. The diaphragm pump served as a by-pass pump for the capillary inlet. The Cirrus unit operates using "Process Eye" software. The operation of the gaseous analyses can be monitored online and recorded using this software.

3.3.7.2   Experimental procedure of Cirrus MKS spectrometry

During the pyrolysis, the non-condensable gaseous such as CO, CO_2, NH_3, and HCN. were sent and collected in a 10 L gas bag. The gas samples then were analysed using a Cirrus MKS Mass Spectrometer controlled by Process Eye view software. Before starting the analysis, the capillary heater and system heater were switched on at least 1 day in advance to achieve stable conditions and remove any potential moisture from the capillary. Then, the gas bag was attached to the MS capillary inlet and then. The gas transferred into the MS by a vacuum through the heated capillary inlet. The analysis of the gaseous was run until the gas bags were almost empty and the gas reading stable (about 1 hour). Using Process Eye View software, the partial pressures of the gaseous were monitored recording mass spectra between 1 and 100 a.m.u.

3.3.7.3   Analysing and diagramming a mass spectrum

The pyrolysis of biomass involving several reactions and producing a large number of products. The evolved gaseous emitted from the decomposition of biomass were monitored by Mass spectrometry. However, there is similarity of each evolved gas profile

in case of the peak temperatures and shape, the fragmentation in the mass spectrometer, as well as the general main products from pyrolysis. For the data analysis, calculations on the same molecular masses were carried out since several compounds can present overlapping peaks. The molecular masses reported as m/z were 2, 12-18, 26-32, 39-44 and 57. The identification of each m/z can be observed in Table 3-3. The main products of this sample are H_2O, CO, CO_2, CH_4, NH_3, H_2 and some light hydrocarbons.

Table 3-3 Relation between mass per charge ratio (m/z), fragment and probable molecule

m/z	Fragment	Probable molecule
2	H_2^+	H_2
14	CH_4^+	CH_4
17	NH_3^+	NH_3
18	H_2O^+	H_2O
26	$C_2H_4^+$	C_2H_4
28	CO^+	CO
44	CO_2^+	CO_2

3.4   Catalyst characterisation

The catalyst characterisation was required to understand the catalyst functionalities, thus was used to understand the catalytic behaviour. The surface, pore volume and pore sizes of the catalysts were investigated by Micromeritics Gemini VII, while the acid/base characteristics were studied by ChemBET TPD and ChemStar, their morphology and

67

surface elemental composition by SEM-EDS, and their mineral composition by XRD analyses.

3.4.1 *Surface adsorption analyses*

The surface area and pore volume are important physical properties that influence the quality and utility of the catalyst. Therefore, it is important that these characteristics be accurately determined and controlled. In this research, catalyst characterisation was carried out through physisorption analysis using a Micromeritics Gemini VII. In this study, the total surface area (BET), external surface area, micropore volume and micropore area were all calculated using the software supplied with the Micrometrics Gemini VII 2390 V3.03 surface area/porosity analyser. Firstly, the catalysts were degassed for 12 hours at 200 °C under N_2 gas using a Micromeritics Flowprep 060. About 0.2 to 0.4 g of materials were weighed before and after degassing. Then, the catalysts underwent analysis using nitrogen as an adsorption gas. Sample evacuation was conducted at a rate of 760.9 mmHg/min and equilibrated for 5 min. The BET surface area was analysed on the adsorption isotherm using ten data points within the P/P_o range of 0.05 to 0.3 as illustrated in Figure 3-8. External surface area, micropore volume and micropore opening were calculated using the method of t-plot theory. The quantitative micropore volume was calculated by choosing a reference isotherm (either Halsey or Harkin-Jura equation).
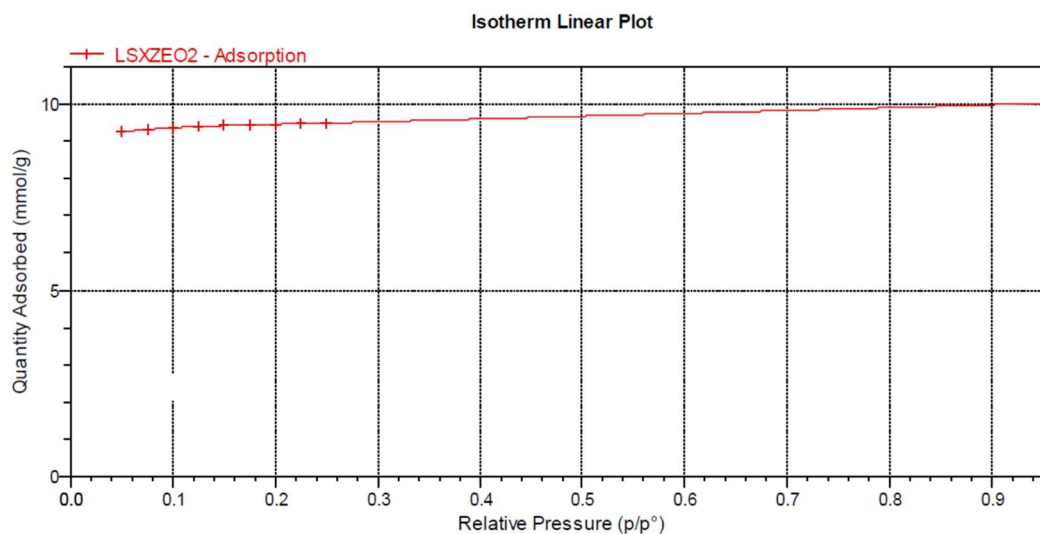
Figure 3-8 Isotherm linear plot for catalyst Li-LSX-zeolite.

3.4.2 *Temperature programme desorption (TPD)*

The Li-LSX-zeolite catalyst underwent temperature programmed desorption (TPD) to determine its surface acid sites strength.

3.4.2.1 *Ammonia Temperature Programme desorption (NH₃-TPD)*

In this work, ammonia Temperature programme desorption (NH_3-TPD) was performed using a ChemBET PULSAR TPR/TPD from Quantachrome instruments, fitted with a thermal conductivity detector (TCD) and a TPRWin version 3.5 software for data analysis. Figure 3-9 illustrate the ChemBET PULSAR used in this research.

Figure 3-9 ChemBET PULSAR for TPD/TPO/TPR (Micromeritics, 2012)

The analysis was carried out to determine the overall acidity of the catalyst. TPD of ammonia is widely used for characterisation of site densities in solid acids. The small molecular size of ammonia allows it to penetrate all pores of the solid, whereas larger molecules only have access to large micro and mesopores. On another note, ammonia is a very basic molecule that us capable of titrating weak acid sites without reacting with the catalyst sites.

Approximately 0.5 g of catalyst sample was weighed and placed in quartz U-tube with an internal diameter of about 4 mm. The catalyst sample was degassed at 100 °C with a heating rate of 20 °C/min for one hour under continuous flowing helium. This is to remove water vapour and to avoid pore damage which will alter the structure of catalysts. The samples were then pre-treated up to 500 °C with a ramp rate of 10 °C/min and were held for two hours to remove strongly bound species and to activate the sample.

Subsequently, the sample was saturated by pulsing the ammonia into the loop with a rate of 10% NH_3/90% He stream (25 mL/min) at 120 °C (about 10 minutes). This temperature is used to minimise physisorption of ammonia or organic amines. Pulsing the ammonia

helps to compare the quantity of ammonia adsorbed to the quantity desorbed for the subsequent TPD. After being saturated, the samples were exposed to helium gas (25 mL/min) at 50 °C for 2 hours to remove any physically bound ammonia from the surface.

Desorption studies were carried out under helium flow (40 ml/min) at a heating rate of 10 °C/min by ramp the temperature from 50 °C to 500 °C. The TPD spectrum was obtained from continues monitoring the amount of ammonia in the exit gas stream by the TCD detector as the temperature was changed. The TCD will monitor the concentration of the desorbed species (Micromeritics, 2012).

3.4.2.2 *Pyridine TPD (Py-TPD)*

The determination of the weak and strong acid sites by pyridine desorption was carried out at the Quantachrome Materials Characterisation Laboratory in Florida, USA using a Chemstar Chemisorption Instrument. The Li-LSX-zeolite was degassed at 100 °C for one hour in flowing helium to remove water vapour and avoid pore damage from steaming, which may alter the structure of the zeolite. The sample was then temperature programmed to 500 ºC at a ramp rate of 10 °C/minute and held at that temperature for two hours to remove strongly bound species and activate the sample. Finally, the sample was cooled to 120 °C in a stream of flowing helium. Next, the sample was saturated with pyridine at 120°C. This temperature was used to minimise the physisorption of the pyridine. The temperature-programmed desorption was performed by ramping the sample temperature at 10 °C/minute to 500 °C. During the TPD of the non-reactive probes (pyridine), the built-in thermal conductivity detector (TCD) monitored the concentration of the desorbed species.

3.4.2.3 *Pyridine FT-IR for catalyst*

The selection between the Lewis or the Brønsted acidic sites was determined by performing FT-IR of pyridine (Py) adsorbed samples (at 150 °C) using a Harrick made

Praying Mantis cell attached to a PerkinElmer Spectrum GX instrument. The samples were dried in situ at 150 °C under a nitrogen flow. Then, pyridine was injected into the sample by saturating the carrier nitrogen gas for 60 min at room temperature. Excess pyridine was flushed by flowing nitrogen at 150 °C before recording the spectra. The pyridine adsorbed on Lewis and Brønsted acid sites gives characteristic FT-IR bands at 1450 and 1540 cm^{-1}, respectively.

3.4.3 *TGA-Basicity characterisation*

Basic sites were characterised using a TGA (TA, Q500) by CO_2 adsorption/desorption. Potential adsorbed species in the catalysts were removed by heating in Helium at 50°C/min to 550°C and holding the final temperature for 50 min. Then, the temperature was decreased to 60°C and the CO_2 is flushed in the TGA for 30 minutes to allow its adsorption on the catalysts surface. Next, the gas in the TGA was switched back to Helium at 60°C and for 20 min, to allow the physisorbed CO_2 to be desorbed. Finally, the temperature was ramp to 600°C at 10°C/min to determine the chemisorbed CO_2.

3.4.4 *X-ray diffraction (XRD) analyses*

3.4.4.1 *Background of XRD analysis*

XRD is a versatile and non-destructive technique used for phase identification of crystalline materials. The schematic of an XRD is illustrated in Figure 3-10. A powdered sample is placed in the diffractometer and bombarded with X-rays generated by copper X-ray tube. XRD peaks are produced by constructive interference of a monochromatic beam of X-rays diffracted at certain angles from each set of lattice planes in a sample. The peak intensities were determined by the distribution of atoms within the lattice. The diffracted X-ray was then collected by a detector and was sent to a computer. The computer then converted them to digital data, produced diffraction pattern and matched the pattern against a database using specialised identification software.
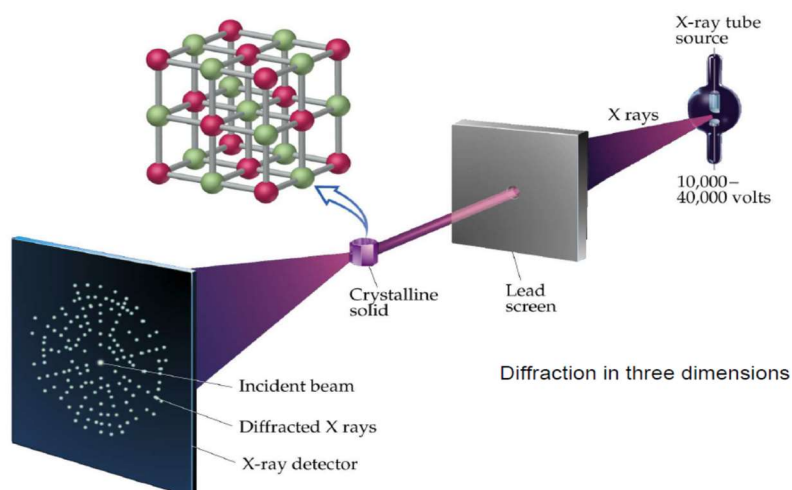
Figure 3-10 Schematic of an XRD (Scott A Speakman, 2009).

3.4.4.2 Experimental procedures of XRD analysis

In this research, XRD analyses were carried out by the instrument operator in the School of Engineering and Physical Sciences in Heriot-Watt University using a Bruker D8 Advance powder diffractometer, operating with Ge-monochromated copper $K\alpha 1$ radiation with a wavelength of 0.15406 nm and a LynxEye linear detector in reflectance mode. Prior to the analysis, the catalyst sample were ground using pestle and mortar and oven-dried at 110 °C overnight. The dried powdered catalyst sample was transferred into a sample holder made up of a rectangular aluminium cavity, which was covered with a clean, transparent glass. The sample in the sample cavity holder was gently pressed making the sample packed compactly within the cavity, then labelled with sample number and used for the XRD analysis. Data were collected over the angular range 5° to 85° in two-theta under atmospheric pressure. Diffraction patterns were analysed using EVA, a software package used for the qualification of crystalline compounds. The error range of XRD measurements was between 2 to 3%.

3.4.5 *SEM-EDS analysis*

3.4.5.1 *Background of SEM analysis*

Scanning Electron Microscope (SEM) - Energy-dispersive X-ray spectroscopy (EDS) was used to characterise the morphology as well as the chemical composition of the catalyst used in this research. Figure 3-11 illustrates SEM schematic diagram, which comprises basic parts of SEM, namely an electron gun, vacuum chamber, lenses, samples chamber and detectors. The SEM was connected to the computer for controlling and viewing of the microscopic images generated.

At the initial stage of scanning a sample using SEM, a beam of electrons is generated by an electron gun, heated by high voltage. When the heat is enough, electrons are emitted, resulting in a strong electric force between the electron gun and anode plate in the vacuum chamber. The electron beam generated was focused on the samples, resulting in an energy transfer, which creates primary electrons. These electrons reflected a secondary electron from the samples. The secondary electrons were then collected by a positive detector and were translated into a signal. Then, the signal produced from secondary electron were amplified, analysed and translated into SEM images. Images were captured based on their surface characteristics and image magnification.

The EDS x-ray detector measures the relative abundance of emitted x-rays versus their energy. When an incident x-ray strikes the detector, it creates a charge pulse then converted into a voltage pulse by a charge sensitive preamplifier. The signal then submits to a multichannel analyser, which sorted the pulses by voltage. The energy as determined from voltage measurement, send to a computer for display and further data evaluation.
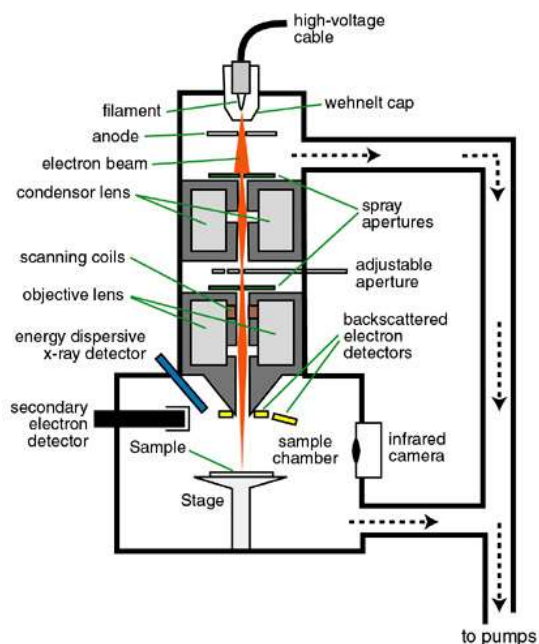
Figure 3-11 SEM schematic diagram.

3.4.5.2   *Experimental procedures of SEM analysis*

The SEM facilities located in the School of Geosciences, University of Edinburgh. The SEM/EDS analyses were carried out using Carl Zeiss Sigma HD VP Field Emission SEM and Oxford Aztec ED X-ray analysis and electron backscatter Diffraction (EBSD) system. The patterns were imaged and analysed using an Oxford instrument software to perform the compositional analysis on the catalyst. The prepared catalyst samples deposited at the edge of a conductive double-sided sticky conductive carbon pad attached to an aluminium stub. The samples were labelled with sample numbers at the bottom of the stub. For efficient conductivity during morphological analysis, the catalyst was coated with carbon.

SEM-EDS facilities consisted of an electron gun, condenser lens, objective lens, sample stage, secondary electron detector and a display unit. All procedure for SEM-analysis was computerised. Firstly, samples with stub were mounted on sample holder according to the

75

numbers. Then, the samples holder was placed to sample stage following the track. Next, the air inside the chamber was pumped out to achieve vacuum condition inside the chamber. After vacuum condition was achieved, the sample stage was moved to the inspection location, which is about 7 cm from the end of the electron column to prevent the samples from hitting the column. The positioning of the sample stage was done on the computer and assisted by a video camera located inside the chamber, allowing real-time observation of the stage movement.

3.5   Coke analyses

The coke formed on the catalysts was analysed by thermal treatment of the catalyst after the pyrolysis tests. The analysis was carried out using TA TGA Q500. The burning of coke was carried out in a 70 mL/min oxygen atmosphere. About 10 mg of catalyst sample was placed in the platinum pan and loaded into the furnace. The programme used was heated from ambient temperature to the final temperature of 900 °C at a rate of 15 °C/min. The amount of coke deposited on the catalysts was determined by the weight change during oxidisation.

3.6   Bench scale pyrolysis reactors

Desirable criteria for a laboratory pyrolysis reactor are simplicity, ease of operation and handling, scale-up potential, cost-effective and a compact design. In this study, two fixed bed reactors with different configuration were used. The details of both reactors will be explained in the following sections.

3.6.1   *Horizontal reactor*

A schematic diagram of the horizontal pyrolysis set-up that was used in this work is presented in Figure 3-12. The reactor consists of different sections: (1) Gas injection

system, (2) Pyrolysis reactor and furnace, (3) Stage condenser consisting of two different systems; a) ice + sodium chloride condenser (-20 °C) b) liquid nitrogen condenser (-65 °C), where the condensable gaseous were trapped; (4) sample injection system composed of a sample-crucible that is first kept outside the heating zone and then inserted into the hot area when the required temperature is constant. The reactor (1-inch diameter) is made of 316 stainless steel, with an operating temperature limit of 1000 °C.

The flow and distribution of gas are regulated manually by using valves and rotameter. The temperature into the reactor is measured by a K-type thermocouple connected from the reactor exit. All dreschel bottles are connected with high temperature resistant 6709-Viton rubber tubing. A compact horizontal tube furnace (Model GHA12/1200 from Carbolite) with a maximum heating rate of 100 °C and maximum operating temperature of 1000°C was used to pyrolyse the microalgae. With this reactor, about 3 g of samples (or samples mixed with catalyst) were loaded into a crucible boat with 7 cm length and width of 2 cm and placed into the reactor. When the desired temperature was achieved, the crucible boat was pushed inside the furnace. This configuration was principally selected to increase the heating rate of the devolatilisation stage to resemble those required for fast pyrolysis to take place.

3.6.1.1   *Flow meter calibration*

The flow meter used in the experiments with the horizontal reactor was designed to work with water. Thus, a calibration was required, since the gas used in the experiments was nitrogen gaseous (N_2). To measure the exact flow rate used in the experiments and the corresponding residence time of the gas into the reactor, the time required for fill in a 1L gas bag was recorded, t. The experiments were run in duplicates.

i)   Gas flow rate, Q = 30 cm^3/min (calibrated for H_2O)

where t_1= 78 sec, t_2= 80 sec, t_{avg} = 79 sec

$Q = V/t = 1000/79 = 12.66 \text{ cm}^3/\text{sec}$

$= 760 \text{ cm}^3/\text{min of } N_2 \text{ gas}$

ii)   Gas flow rate, $Q = 40 \text{ cm}^3/\text{min}$

where $t_1 = 60$ sec, $t_2 = 58$ sec, $t_{avg.} = 59$ sec

$Q = V/t = 1000/59 = 16.95 \text{ cm}^3/\text{sec}$

$= 1017 \text{ cm}^3/\text{min of } N_2 \text{ gas}$
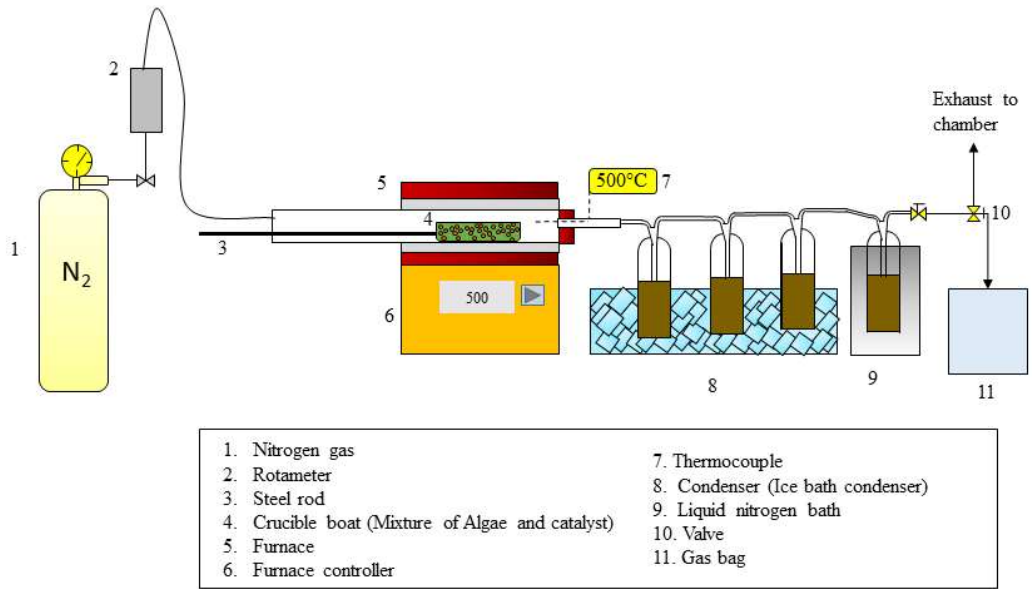
Figure 3-12 (a) Schematic diagram. (b) Real set-up of the horizontal pyrolysis

The schematic labels shown in the figure:

1. Nitrogen gas
2. Rotameter
3. Steel rod
4. Crucible boat (Mixture of Algae and catalyst)
5. Furnace
6. Furnace controller
7. Thermocouple
8. Condenser (Ice bath condenser)
9. Liquid nitrogen bath
10. Valve
11. Gas bag

3.6.2 *Vertical reactor*

The vertical configuration setup was the same as in the horizontal one (as described in section 3.5.1) with the differences of having the reactor-tube (1.27 cm of diameter, 15 cm of height) in a vertical position. The reactor tube had an operating temperature limit of 1000 °C. The furnace used was a Vertical tube furnace GVA/GVC from Carbolite with a maximum heating rate of 100 °C/min. In the down-stream configuration, the carrier gas (N_2) was introduced from the top side of the furnace. The gas flow rate was regulated manually by using rotameters. The temperature inside the furnace was measured by a K-type thermocouple connected from the top side of the reactor and was connected to a PC for log the temperature profiles during the experiments. The condensation system was the same used as in the horizontal configuration, with all Dreschel bottles connected with high temperature resistant Viton tubing.

The sample inside the reactor was hold by a sample holder (stainless steel tube), a SS316 wire mesh (with 0.45mm wire diameter) and quartz wool. The vertical reactor set-up was used to carry out in-situ and ex-situ pyrolysis experiments. For in-situ pyrolysis, both samples and catalyst were mixed following the desired algae: catalyst ratio and placed in the sample holder. Meanwhile, for ex-situ pyrolysis, the metal mesh and quartz wool were alternated between samples and catalyst to avoid mixing of the two materials and allowing only the devolatilisation gaseous/aerosols to flow across the catalyst bed. A schematic diagram of the vertical pyrolysis set-up used in this work is presented in Figure 3-13.

3.6.2.1 *Flow meter calibration*

A different type of flow meter and gas bag were used for the calibration of flow meter. The calibration was carried out using the same method used for the horizontal reactor.

> i) Gas flow rate, Q = 40 ml/min where t_1= 8.2 min, t_2= 7.8 min, t_{avg} = 8.0 min.

$Q = V/t = 10000/8.0 = 1250$ ml/min

$= 1250$ ml/min of N_2 gas

ii)   Gas flow rate, $Q = 15$ ml/min where $t_1 = 28$ min, $t_2 = 30$ min, $t_{avg} = 29$ min

$Q = V/t = 10000/29 = 344.83$ ml/min

$= 345$ ml/min of N_2 gas

1. Nitrogen gas	6. Furnace controller
2. Rotameter	7. Computer connect to thermocouple
3. Furnace	8. Condenser (water ice bath)
4. Catalyst-microalgae mixture	9. Liquid nitrogen bath
5. Sample holder	10. Valves
	11. Gas bag
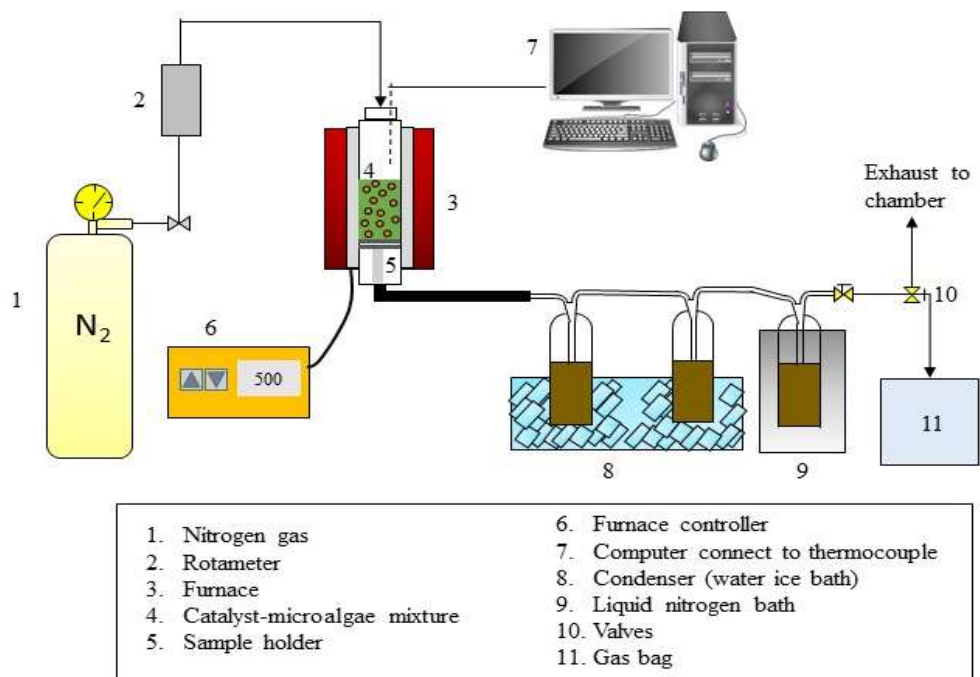
Figure 3-13 (a) Schematic diagram. (b) Real set-up of the vertical pyrolysis set-up

3.6.3 *Pyrolysis experiments method*

Before each experiment, the reactor was purged with nitrogen for 10 minutes in order to remove the remaining impurities in the reactor. The reactor was electrically heated to the desired temperature. The decomposition of the sample produced pyrolysis vapour (a gas composed of condensable and non-condensable components) and char (left in the crucible into the reactor or on the sample holder in the vertical set-up). The reaction was run for 20 minutes. This is to ensure maximum decomposition of all microalgae during pyrolysis. The produced pyrolysis vapours then pass through the condenser system with the aid of flowing N_2.

In the stage condenser, the condensable vapour condensed and remained into the Dreschel bottles in the form of liquid/tar. The liquid products (bio-oil) were recovered by washing with 50 ml acetone. Then, the liquids were transferred into small bottles and stored in the fridge for further characterisation. The non-condensable gaseous were sampled in gas-bag and then analysed by mass spectrometry analysis (detailed in section 3.3.6). While the solids left behind in the reactor were taken out, weighed and recorded as bio-char yield (considering the amount of catalyst).

The products mass balances of the pyrolysis experiments were calculated considering the weight difference between the Dreschel bottles before and after the experiments (section 3.6.1). The char yield was found by the weight difference between the weight of the biomass before the experiment, and the weight char left after the experiments (section 3.6.3).

The bio-oil collected is calculated by the equation;

$$M_{bio\text{-}oil} = M_{bottle\ after} - M_{bottle\ before}$$ (3.6.1)

The bio-oil yield is calculated as below;

$$Bio\text{-}oil\ yield = \frac{M\ bio-oil}{M\ sample} \times 100\% \tag{3.6.2}$$

Where M_{sample} is the initial mass of biomass used for the pyrolysis. Meanwhile, the bio-char retained is calculated by the equation;

$$M_{bio\text{-}char} = M_{boat\ after} - M_{boat\ before} \tag{3.6.3}$$

If the reaction were carried out with catalyst, the weight of catalyst needs to be considered by deducting the catalyst after the reaction.

The bio-char yield is calculated as below:

$$Bio\text{-}char\ yield = \frac{M\ bio-char}{M\ sample} \times 100\% \tag{3.5.4}$$

Finally, the gas yield was calculated by difference, as shown in equation 3.5.5.

$$Gaseous\ yield = 100\% - bio\text{-}char\ yield - bio\text{-}oil\ yield \tag{3.5.5}$$

It was noticed that some condensable gaseous went through the vent, trapped and adhere in the tube (turns yellowish after the experiment). However, the gaseous was considered negligible since some of it were trapped in the gas bag for analysis.

Table 3-4 shows the different operating conditions such as temperature, sweep gas flow rate and catalyst ratio used in this research study. The experiment then was repeated three times and the average reading was recorded.

Table 3-4 Operating conditions for pyrolysis experiments.

Temperature (°C)	Catalyst: microalgae ratio	Sweep gas flow rate (ml/min)	Catalysts	Reactor Configuration
400, 500, 600,700	1:0, 0.5:1, 1:1, 3:1	1250, 345 and 210	Li-LSX-zeolite, $NaSiO_2$, $LiNaSiO_2$, nano-powder SiO_2	In-situ, ex-situ, horizontal and vertical fixed bed

3.6.4 *Regeneration studies of catalysts*

The catalysts were regenerated to examine the activity and deactivation of the catalyst after a number of cycles. In the regeneration studies, the vertical reactor was used to separate the catalyst from the microalgae in an ex-situ configuration. Figure 3-14 illustrates the close-up diagram of regeneration studies. After the pyrolysis tests, the catalysts were separated and sieved using standard sieves (stainless steel mesh with sieves opening of 0.125 mm (mesh 115) and 0.25mm (mesh 60)) from Cole Parmer. One-quarter of the catalyst was separated and submitted to SEM-EDS analysis; meanwhile the rest of the catalysts was calcined to remove the coke from the catalyst's surface. The catalysts were heated up in the muffle furnace (Carbolite) at 500 °C for 1 hour in the presence of air. Then, the catalysts were kept in the desiccator for the second cycle of pyrolysis. The same method was applied to the third cycle regeneration. The experiments described in Chapter 7 were obtained using this method in the presence of the pre-treated and non-pre-treated microalgae. Moreover, a set of calcinations at 700°C and 950°C were carried out to evaluate the maximum temperature for calcining the Li-LSX zeolite and their effect in removing coke.
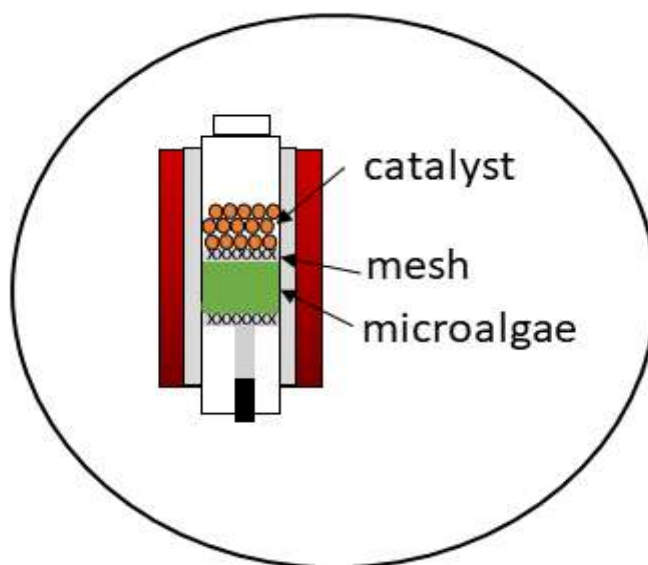
Figure 3-14 Schematic diagram of catalyst regeneration studies.

3.7 Chemical pre-treatment on Microalgae

3.7.1 *Microalgae pre-treatment*

Microalgae contain significantly high levels of macro-minerals (Na, K, Ca, P) and trace elements (Al, Cu, Fe and Mn). A pre-treatment process was proposed to partially remove these elements to improve the intrinsic quantity and quality of the pyrolysis products. The pre-treatment of microalgae (*Isochrysis* sp.) was performed with different chemicals: (i) Sulfuric acid (H_2SO_4) solution; (ii) Water; (iii) Sodium hydroxide (NaOH) solution. The method was selected due to the good result in removing alkali metals from kelp macroalgae biomass (Choi *et al.*, 2014). Different concentrations were used for the acid and basic pre-treatment (0.4%, 1%, 4%). The treatment was performed by mixing the dried microalgae (3 g) with the chemicals (30 ml) (solid to liquid ratio of 100 g/1L) for 30 min at mixing speed of 350 rpm and temperature of 25 °C. After the treatment, the mixture was rinsed with DI water to achieve a pH of 7 and centrifuged for 2 hours using Thermo Fischer centrifuge to separate the water solution (top of centrifuge vial) from the leached microalgae (bottom of the vial). The residual solid was then oven-dried at 60 °C

to obtain a constant weight. In the meantime, the liquid obtained was collected for ICP analysis.

3.7.1 *Ash content*

The ash content yield in raw and treated microalgae was determined by recording the weight change during combustion using a high-temperature muffle furnace (Carbolite Model CWF 1100). The ash content was determined following ASTM E175-01(2015). About 1 g of sample was placed in small crucibles and heated from 25 °C to the final temperature of 800 °C for 8 hours at a rate of 50 °C/min. The weight left was associated with the inorganic materials or ash. Triplicates analyses were then carried out.

3.7.2 *ICP analysis of wastewater*

The wastewater obtained after treatment were wet digested in HNO_3 in a volumetric flask. 2 ml of raw samples were filtered using 0.22 μm MF-Millipore MCE Membrane (MILLEX HA Filter units), to remove suspended solids (microalgae). Then, 1 ml of wastewater was acidified with 2 ml of 70% HNO_3 (Trace metal grade, Fischer Scientific) and diluted with distilled water to 100 ml. The wastewater was then analysed for metals (Na, K, Mg and Ca) by inductively coupled plasma spectrometry-optical emission spectroscopy (ICP-OES), using Optima 5300 DV (Perkin Elmer) with a maximum output power of 1400 W. Argon (99.99%) was used as the carrier gas at a constant flow rate of 15, 0.2 and 0.75 L min^{-1} for plasma, auxiliary, and nebuliser flows, respectively. The instrument was operated in the axial mode for elements. The ICP analysis was carried by Dr. Lorna Eades in the School of Chemistry, University of Edinburgh.

A range of multi-element calibration standards were prepared using single element 1000 mg/l standards (Fisher Scientific), diluted with 2% HNO_3 v/v. A 100-fold dilution of Merck ICP Multi element standard solution IV CertiPUR® was employed as a reference standard for each of the elements.

3.7.3 *X-ray Fluorescence spectroscopy (XRF)*

3.7.3.1 **Background of XRF**

XRF is a non-destructive technique to analyse the inorganic composition of a sample qualitatively and quantitatively. Similar to XRD, X-ray is used in this analysis to irradiate on the sample. As a result of the irradiation step, x-ray fluorescence is generated which possess energy characteristic to each element in the sample. The x-ray fluorescence is then collected by a detector before converted into digital signals. The digital signal is then amplified to be analysed of its elemental composition using spectrometry analysis software.

3.7.3.2 **Experimental procedure of XRF**

In this research, XRF analyses were carried out to quantify the elemental composition and were performed by the instrument operator in the LPD Lab Services Limited in Blackburn using a Philips PW1480 XRF spectrometer and SemiQ semi-quantitative analysis software. Approximately 5 mg of sample was placed between two layers of mylar film, mounted into a two-part holder system are normally used for liquid samples. The x-ray scans identified and quantified the elements phosphorus, sulphur, chlorine, potassium and calcium in all the samples.

Chapter 4

Characterisation and pyrolysis of microalgae for biofuel production

4.1 Introduction

Microalgae are attracting worldwide attention as an alternative resource for fuels and chemicals production (Serrano-Ruiz *et al.*, 2012). Although lignocellulosic biomass is currently the most advanced choice for bio-fuel production, microalgae are very rapidly becoming a key player since they absorb CO_2 during growth, present a high production yield per hectare compared to terrestrial plants and can row in a land not suited for agricultural crops (Luque *et al.*, 2010).

Microalgae consist of a vast number of aquatic species that contain different chemical constituents, such as lipids, proteins, carbohydrates, which differ from terrestrial biomass composition, rich in lignin and cellulose. Fast pyrolysis consists in the decomposition of organic materials between 400 and 600°C in absence of oxygen, resulting in a liquid bio-oil, a solid char and gas products (Bridgwater, 2012; Sanna, 2013). The condensable gas/vapours condensed into a liquid, which is known as bio-oil. Yields and properties of the products are based on the conditions of pyrolysis system, such as heating rate, temperature and gas flow rate (Bridgwater, 2012; Dickerson & Soria, 2013; French & Czernik, 2010; Jahirul *et al.*, 2012). The bio-oils produced can potentially be used for direct combustion in energy generation, or can be upgraded further into liquid transport fuels and bio-chemicals (Grierson *et al.*, 2009). Bio-char is another product from pyrolysis and has carbon content over 50%. Bio-char has highly porous structure, and the addition of bio-char to soil could improve water retention and increase the efficiency of nutrient use (Chaiwong *et al.*, 2013).

Therefore, the potential of microalgae as biofuels and chemicals source need to be explored. A large number of microalgae exist and can be considered as potential feedstock

for a biorefinery system. In this work, three species of microalgae (*Nannocholoropsis, Tetraselmis* and *Isochrysis)* have been selected and studied due to their abundance and availability. The purpose of this study is to understand the physical and chemical properties of the selected microalgae and their pyrolysis products, which will represent the comparative base for the critical design and evaluation of different catalysts and their effect in the microalgae pyrolysis in the following chapters.

4.2   Proximate analysis of feedstocks

Table 4-1 shows the characterisation of microalgae and comparison with selected microalgae, *Chlorella vulgaris* sp. using data taken from the literature. *Chlorella vulgaris* sp. is the reference species been used in pyrolysis of microalgae. Among the microalgae studied, *Isochrysis* sp. (76.9 wt.%) and *Tetraselmis* sp. (69.7 wt.%) have higher volatile matter than *Chlorella vulgaris* sp. (66.6 wt.%). Meanwhile, *Nannocholoropsis* sp. has a lower VM (62.0 wt.%). The high amount of volatile matter in biomass strongly influences its combustion behaviour and thermal decomposition (Phukan *et al.*, 2011).

Ash content for *Isochrysis* and *Tetraselmis* sp. (16.3 wt.% and 19.6 wt.%) are also higher compared to *Chlorella vulgaris* sp. (15.6 wt.%). High ash yield leads to coking reaction and increased formation of char. This has been observed in particular for cellulose decomposition, while ash was less effective on modifying the thermo-chemical decomposition of lignin and hemicellulose (Mayer, Apfelbacher & Hornung, 2012). There is a lack of knowledge on the effect of alkali/hearth alkaline metals on the behaviour of proteins. Overall, the high ash content inhibits the bio-oil production, but at the same time leads to improved quality of bio-char as a soil amendment due to high inorganic nutrient contents in ash (Hyung, Chul & Jin, 2014). Microalgae with a high percentage of volatile matter and low ash content are required with respect to their application in gasification and pyrolysis processes.

Table 4-1 Proximate analyses of different microalgae.

	Weight (wt.%)			
	Isochrysis	*Nannochloropsis*	*Tetraselmis*	**Chlorella vulgaris*
Moisture	5.79	6.88	9.35	6.18
Volatile matter	76.88	62.02	69.74	66.56
Fixed carbon	1.00	17.20	1.30	11.62
Ash	16.33	13.90	19.61	15.64l

*Adapted from (Wang & Brown, 2013).

4.3   Ultimate analysis of microalgae

The ultimate analyses (Table 4-2) show that the selected microalgae species have carbon contents between 44.9 and 47.5 wt.%, which makes them suitable feedstocks for biofuel production. Their C content are lower than *Chlorella* sp. (50.7 wt.%). *Isochrysis* sp. N content (4.77 wt.%) is lower compared to that of *Nannochloropsis* (7.10 wt.%), *Tetraselmis* (6.41 wt.%) and *Chlorella vulgaris* sp. (7.91 wt.%). High nitrogen content is undesirable due to the potential formation of NO_x species during combustion. In particular, *Isochrysis* sp. presents a relatively low N content, which is still higher compared to lignocellulose biomasses (for example red oak 0.06 wt.%) and organic wastes (for example camelina straw waste, 0.3 wt.%)(Wang & Brown, 2013; Hernando *et al.*, 2017a). Compared to lignocellulose biomasses, microalgae species contain less oxygenated compounds, but deoxygenation and denitrogenation are required to process them in conventional crude-oil facilities.

Microalgae contain a variety of lipids, proteins and extractives depending on the species and cultivation condition (Sanna & Abd Rahman, 2015). In this study, *Isochrysis* (19 wt.%), *Nannochloropsis* (18 wt.%) and *Tetraselmis* (11 wt.%) have lower lipid content than *Chlorella vulgaris* (28.8 wt.%). Microalgae containing higher lipid contents will produce higher yields of bio-diesel (Chisti, 2007; Campanella *et al.*, 2012), so that these

three species are more suitable to "whole-conversion" technologies such as pyrolysis than *Chlorella*. *Nannochloropsis* and *Tetraselmis* are particularly rich in proteins (62 wt.% and 63 wt.%), while *Isochrysis* has a balanced distribution of proteins, lipids and carbohydrates.

Table 4-2 Ultimate analyses of different microalgae.

	Isochrysis	*Nannochloropsis*	*Tetraseslmis*	**Chlorella vulgaris*
Ultimate analysis (wt.%)				
C	45.58	47.51	44.96	50.70
H	5.84	6.50	6.08	8.07
N	4.77	7.10	6.41	7.91
O	43.80	38.89	42.56	33.31
Biochemical composition (wt.%)				
Protein	44	62	63	43.2
Lipid	19	18	11	28.8
Carbohydrate	25	9	11	9.5

*Adapted from (Wang & Brown, 2013).

4.4   Thermogravimetric analysis

Three main degradation stages were observed during the thermochemical conversion of *Isochrysis, Nannochloropsis* and *Tetraselmis* sp. in agreement with other literature

thermal degradation studies of macro-and microalgae (Campanella *et al.*, 2012; Ross *et al.*, 2008). The weight loss and corresponding derivative curves of both species are shown in Figure 4-1. The first stage that occurred at the temperature between 25 to 105 °C was characterised by a small weight loss. During this stage, 5 to 7% weight loss was related to the release of absorbed water. The second stage occurred at temperature between 110 to 550 °C where most of the organic material decomposed (VM in Table 4-1). The final stage occurred at temperature above 550 °C, showing the gradual mass loss related to the solid residue decomposition.

According to Figure 4-1, the thermal decomposition occurring between 125 to 500 °C involves four defined steps (a, b, c, d), which correspond to the volatilisation of proteins (a, b), carbohydrates (c) and lipids (d). The small release of volatiles at about 180°C was associated to short compounds originated from proteins. The highest peak (b) was assigned to the decomposition of proteins, which occurred between 250 to 310 °C. This agrees with the biochemical composition of microalgae, where *Nannocholoropsis* sp. has higher protein content (62 wt.%) compared to *Isochrysis* sp. (44 wt.%). The decomposition of the carbohydrate fraction was associated with the decomposition between 330 and 360 °C (c) as reported in the literature (Huang, 2012). As shown in Table 4-2, *Isochrysis* (25 wt.) has a larger carbohydrate content compared to *Nannocholoropsis* and *Tetraselmis* (9 and 11 wt.%). Finally, the long chain lipids decomposition took place between 350 and 500 °C (d). Both *Nannocholoropsis* and *Isochrysis* are rich in saturated palmitic (16:0) and stearic acid (18:0), monounsaturated palmitoleic (16:1 n-7) and oleic acid (18:1 n-9), eicosapentaenoic acid (20:5 n-3) and omega-3 acids. It has been shown that fatty acids are stable to thermal degradation up to about 325°C even in the presence of solvents and high pressure (Shin *et al.*, 2011).
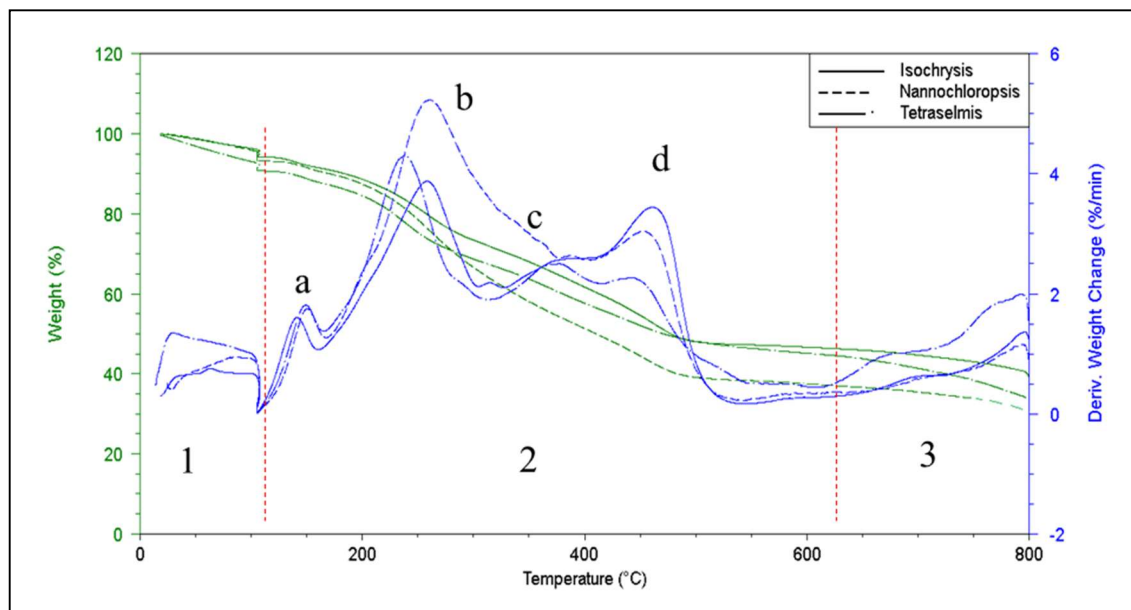
Figure 4-1 DTG profile of different microalgae species.

4.5 Standard pyrolysis of microalgae species

Three different species of microalgae have been pyrolysed with the intention to add value to the future integrated biorefinery. The samples were pyrolysed at a temperature of 500 °C and ambient pressure with a fixed bed reactor. The distribution of the products obtained from the pyrolysis of the different microalgae is shown in Figure 4-2. The pyrolysis of *Isochrysis* produced the highest bio-oil yield (37.2 wt.%) followed by *Tetraselmis* (26.6 wt.%), while the lowest bio-oil yield derived from *Nannochloropsis* (21.8 wt.%). The bio-oil yields reported are in good agreement to bio-oil yields reported for the pyrolysis of microalgae by other researchers (22 to 36.6 wt.%) (Pan *et al.*, 2010; Lorenzetti *et al.*, 2016). Conversion to gas species was favoured for *Tetraselmis* and *Nannocholoropsis* with yield of 54 wt.% and 48.6 wt.%, respectively, as compared to *Isochrysis* (27.9 wt.%). High gas yield was linked to microalgae biochemical compositions, were both *Tetraselmis* and *Nannocholoropsis* contain high protein content (refer to Table 4-2), which decomposes at temperatures < 500 °C and lead to the formation of gas species (for example CO, CO_2, NH_3).

The amount of bio-char generated was different for each microalgae species. The pyrolysis of *Isochrysis* produced more bio-char (34.8 wt.%), followed by *Nannochloropsis* (29.6 wt.%) and *Tetraselmis* (20.2 wt.%). Bio-char formation can be related to the microalgae content in lipids, which is the lowest in *Tetraselmis*. The complex microalgae structure with fatty acids and amino acids compounds is partly converted to bio-char during pyrolysis. Table 4-2 shows that *Isochrysis* has the highest lipid content (19 wt.%), which contributed to higher bio-char production.
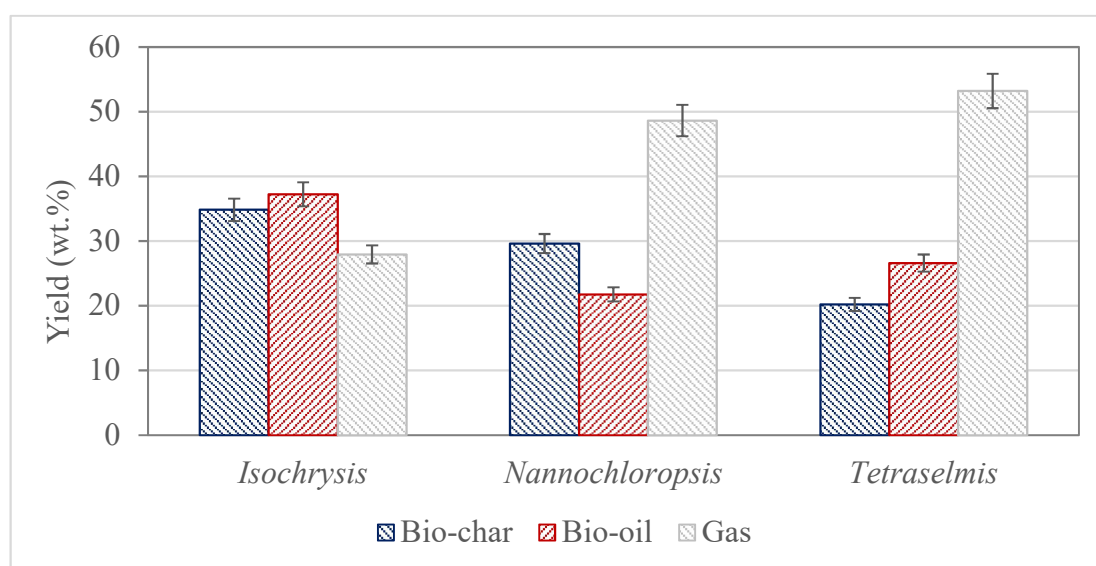
Figure 4-2 Microalgae pyrolysis products yields.

4.6   Energy distribution

In terms of energy recovery, a remarkable fraction of the starting microalgae energy was recovered in the bio-oils. Figure 4-3 shows the energy distribution from the pyrolysis of the different microalgae species. For *Tetraselmis*, about 76.9% of the starting energy was retained in the bio-oil, followed by *Isochrysis* (75.1%) and *Nannochloropsis* (51.5%). The least energy was retained in the gas with ~4% for *Isochrysis* and *Tetraselmis* species.
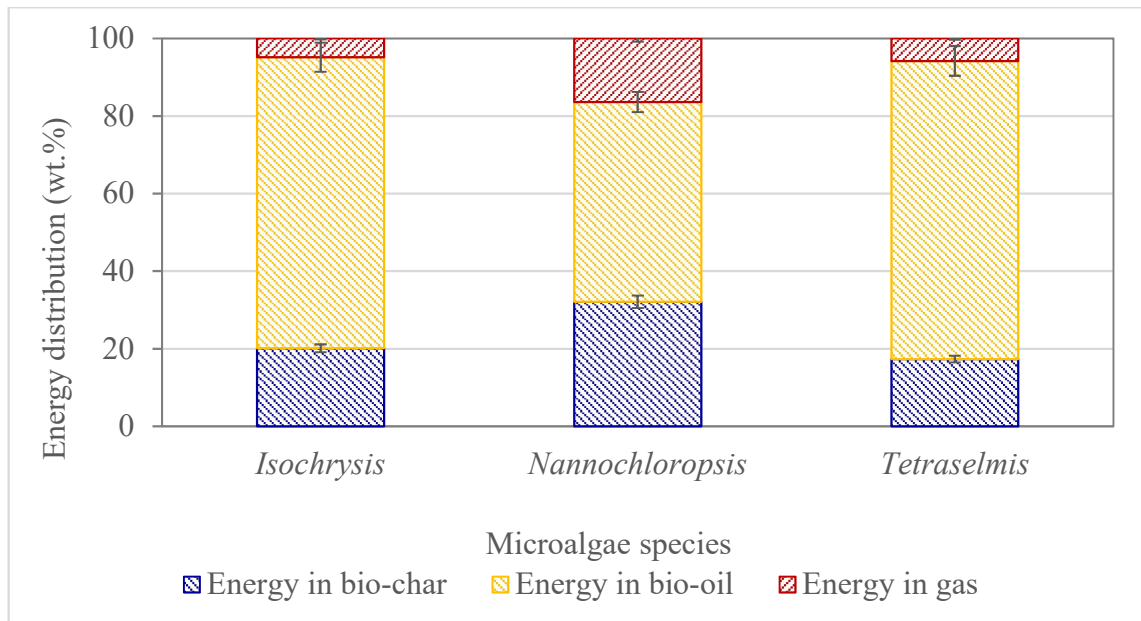
Figure 4-3 Energy distribution on pyrolysis of different microalgae.

4.7 Characterisation of pyrolysis products

4.7.1 *Elemental analyses of bio-chars and bio-oils*

The elemental analyses of the bio-chars and bio-oils obtained from the pyrolysis of the different microalgae are shown in Table 4-3. The bio-chars obtained from *Tetraselmis* had lower calorific value (10.4 MJ/kg) than those obtained from *Isochrysis* (13.2 MJ/kg) and *Nannochloropsis* (14.8 MJ/kg). Also, *Tetraselmis* bio-chars yielded higher carbon content (48.1 wt.%) than *Isochrysis* (45.4 wt.%) but lower than *Nannochloropsis* (55.3 wt.%). All bio-chars had high ash and nitrogen contents (3.2 to 5.4 wt.%), which make them suitable for utilisation as a soil amendment.

The C content of *Isochrysis* and *Tetraselmis* bio-oils was almost 70 wt.%, resulting in higher than that of *Nannocholoropsis* (65.6 wt.%), as can be seen in Table 4-3. All the bio-oils presented a low O/C ratio (0.1 to 0.2), which indicates deep deoxygenation as compared to the corresponding starting materials (see Table 4-1). Deoxygenation can be

attributed to deoxygenation reactions such as reduction of oxygen in the form of carbon monoxide, carbon dioxide and water during pyrolysis. Bio-oil from pyrolysis of microalgae has lower oxygen content than bio-oils from pyrolysis of lignocellulose biomass, which makes it more suitable for fuel use. Furthermore, the N content in bio-oil for *Nannochloropsis* and *Tetraselmis* are quite high (6.8 wt.% and 8.1 wt.%) compared to *Isochrysis* (3.9 wt.%). High nitrogen content of bio-oils comes from chlorophyll and proteins in the microalgae. However, the content of oxygen and nitrogen in microalgae bio-oil were still higher than fossil oil. Therefore, further removal of oxygen and nitrogen in the bio-oils is necessary for their application as biofuels.

The HHVs of bio-oils were between 32.2 to 35.5 MJ/kg, which resulted higher than the HHVs of lignocellulosic bio-oils and microalgae bio-oils produced using Chlorella vulgaris (28 MJ/kg) and blue-green algae blooms (31.9 MJ/kg) that had proteins content (60%) comparable to *Tetraselmis* (Du *et al.*, 2013b; Hu *et al.*, 2013).

Table 4-3 Elemental analysis of the bio-oils obtained at 500 °C.

Elemental analysis	*Isochrysis*	*Nannochloropsis*	*Tetraselmis*
Bio-chars			
Carbon	45.41	55.34	48.14
Hydrogen	2.91	1.96	1.65
Nitrogen	3.44	5.16	4.25
Oxygen	48.24	37.54	45.96
H/C molar ratio	0.77	0.42	0.42
O/C molar ratio	0.80	0.50	0.73
HHV (MJ/kg)	13.18	14.77	10.37

Bio-oils			
Carbon	71.69	65.59	69.55
Hydrogen	10.01	9.26	9.48
Nitrogen	3.89	6.81	8.07
Oxygen	14.41	18.34	12.90
H/C molar ratio	1.68	1.69	1.63
O/C molar ratio	0.15	0.20	0.14
HHV (MJ/kg)	35.54	32.24	34.88

4.7.2 *Oxygen/Carbon (O/C) and Hydrogen/Carbon (H/C) ratios of bio-oils*

The bio-oils O/C molar ratios are shown in Figure 4-4. The oxygen content of oils was significantly lower than the original feedstock, indicating that the pyrolysis process has partially deoxygenated the microalgae. The O/C ratio from *Isochrysis* and *Tetraselmis* was the lowest, with 0.14 and 0.15, respectively. This suggests that these two microalgae species are viable for the pyrolysis process. Therefore, the use of catalyst able to further reduce the O and N contents during the bio-oil production stage may enhance the quality of the bio-oils.

Meanwhile, the H/C molar ratios of the bio-oils are compared with the starting materials in Figure 4-5. The trend indicates that the hydrogen/carbon ratio increased after pyrolysis reaction. The H/C of the bio-oil which range between 1.63-1.68 are closer to the H/C ratio of petroleum fuel (1.80) and diesel (2.0), compared to the starting material. A catalytic upgrading is required to improve the H/C ratios of bio-oil.
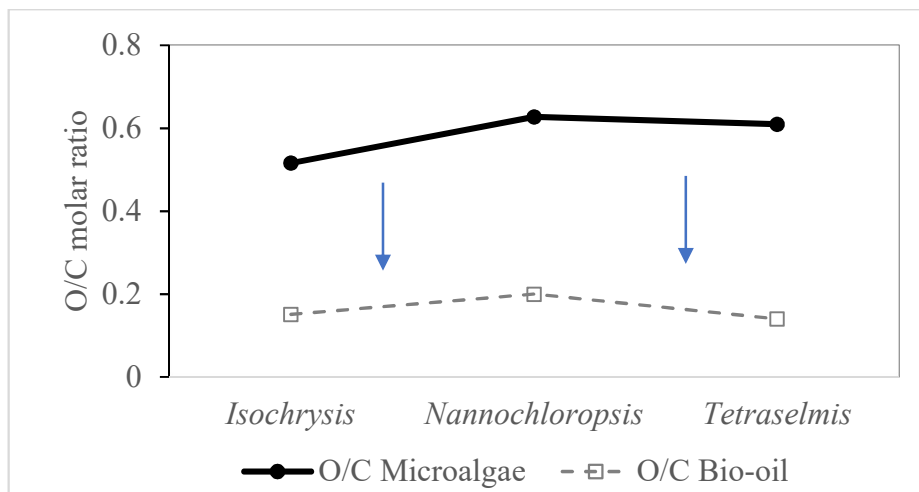
Figure 4-4 Oxygen/Carbon ratios of different microalgae species.
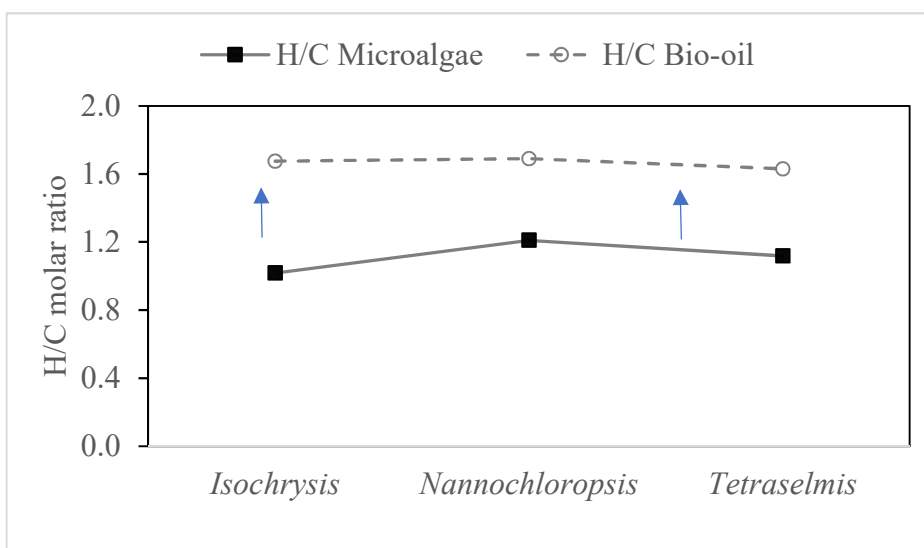
Figure 4-5 Hydrogen/Carbon ratios of different microalgae species.

4.7.3 *Nitrogen distribution*

Nitrogen content represents a limitation to implement bio-oil as a transportation fuel. The distribution of nitrogen (N) in the pyrolysis products is presented in Figure 4-6. About 42 wt.% of the starting N is retained in the *Tetraselmis* bio-oil; meanwhile, 24.2 wt.% and 27.3 wt.% were retained in *Nannochloropsis* and *Isochrysis* bio-oils, respectively. The N

content for *Nannochloropsis* was lower due to the lower yield of the bio-oil obtained during pyrolysis (22 wt.%). The N transferred in gas phase ranged between 41.7 (*Tetraselmis*) to 50.7 wt.% (*Nannochloropsis*). The N compound was released in the gas phase as NH_3 and HCN, which is be discussed further in section 4.9.5. The study on nitrogen evolution during algae pyrolysis is important to control the emission of N-containing pollution (for example, NH_3, HCN and NO_x). Further upgrading is necessary to reduce the nitrogen content in bio-oil, which will be discussed in Chapter 5. On the contrary, N rich bio-char could be used as soil amendment.
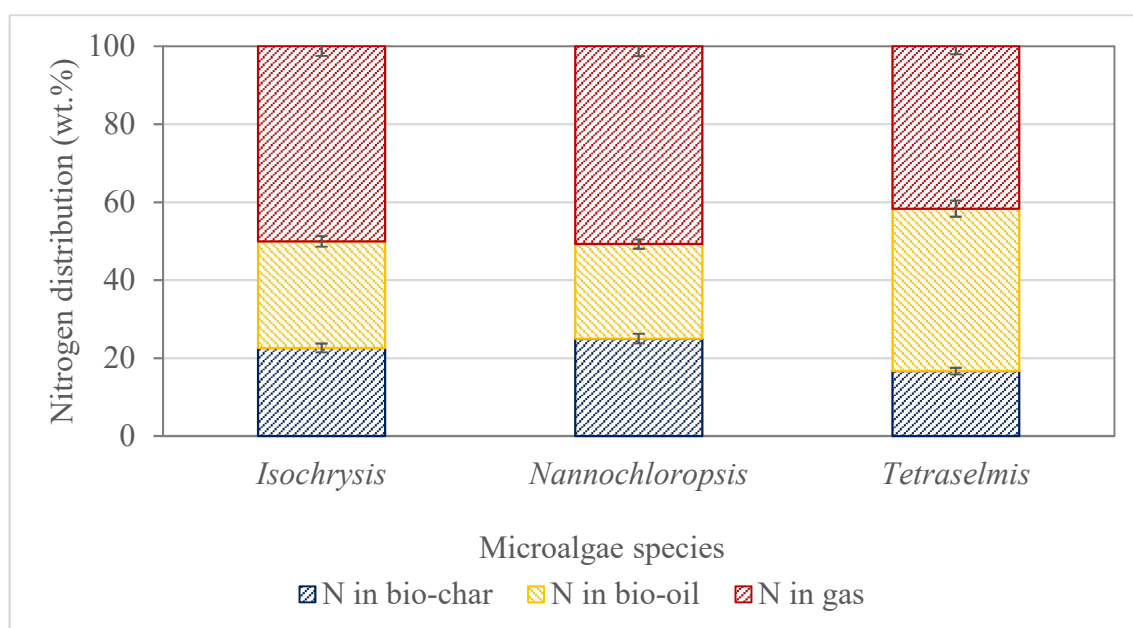
Figure 4-6 Nitrogen content distribution in the pyrolysis products.

4.7.4 *^{1}H NMR*

^{1}H-NMR analysis was carried out to evaluate the overall composition of the bio-oils, since it gives an overall distribution of protons in the oil. The integration of the proton NMR spectra of the three-different bio-oils is presented in Table 4-4. The first region of the spectra (0 to 1.6 ppm) representing aliphatic protons, was the most abundant (>50%) for all the bio-oils indicating their higher aliphatic content. *Nannochloropsis* (60.4%) and *Isochrysis* (60.2%) had the largest content of aliphatic protons, compared to *Tetraselmis*

(53.7%). Aliphatic compounds mostly derived from the microalgae fatty acids and the larger content of aliphatic protons in *Nannochloropsis* and *Isochrysis* can be explained by their larger lipid content (see Table 4-2).

This composition resulted very differently from that obtained using zeolites catalysts (for example ZSM-5 and HY), where oxygenates and aromatics were the main products from the pyrolysis of *Chlorella vulgaris* and *Laminaria japonica* (Du, 2013; Harman-Ware *et al.*, 2013). The regions from 1.6 to 2.2 ppm and from 2.2 to 3.0 ppm represent protons on aliphatic carbon atoms bonded to a C=C double bond (olefinic or aromatic) or two bonds away from a heteroatom. Bio-oils obtained from *Nannochloropsis* had the lowest number of protons (~21 % of all) in these regions.

The next integrated region of the spectra (3 - 4.2 ppm) characterises the aliphatic alcohol/ether protons, or a methylene group joining two aromatic rings. The bio-oils from *Nannochloropsis* and *Isochrysis* microalgae showed similar percentage (46%) of protons, while *Tetraselmis* presented a larger content of protons linked to oxygenated molecules. The region between 4.2 and 6.4 ppm represents the aromatic ether protons, such as methoxy phenols and hydrogen atoms of carbohydrate-like molecules. The percentages of protons in this region were found to be in small amounts (~2.4 to 4.1%) in all bio-oils. *Isochrysis* presents the most numerous protons in this group (4.1%), which can be explained by a large amount of carbohydrates in the starting material (see Table 4-2). The low protons in this region indicate that the carbohydrates were converted in different classes of compounds.

The aromatic region of the spectra (6.4-6.8 and 6.8-8 ppm) contained between ~8.1 to 11.2% of the protons in the bio-oils represent aromatic compounds and heteroaromatics containing nitrogen (from proteins) and oxygen, such as indoles. *Isochrysis* bio-oil had lower aromatics (8.1%) compared to the other microalgae bio-oils. The aromatic content can be explained by the intermediate pyrolysis conditions, that allow the aromatisation reaction of small chain aliphatic. *Isochrysis* was the least rich in proteins and therefore

N-compounds, which explains the low content in aromatics. Protons from aldehydes and carboxylic acids (8-10 ppm) were only detected in *Isochrysis* bio-oil in minimal amount (0.3%). This is a distinctive difference with lignocellulosic bio-oils, which are particularly abundant in the latter compounds. Overall, the proton NMR analyses results indicate that higher percentages of the aliphatic protons (compounds) exist in the bio-oils obtained from pyrolysis of the microalgae species.

Table 4-4 ^{1}H NMR Integrations of microalgae bio-oils from pyrolysis versus specific chemical shift ranges.

Chemical shift region (ppm)	Type of protons	*Isochrysis*	*Nannochloropsis*	*Tetraselmis*
		Proton abundance, %		
0.0 – 1.6	-CH$_3$, -CH$_2$-	60.17	60.36	53.73
1.6 – 2.2	-CH$_2$-, aliphatic OH	14.19	13.19	14.57
2.2 – 3.0	CH$_3$OC-, CH$_3$-Ar, -CH$_2$Ar	8.73	7.92	12.63
3.0 – 4.2	CH$_3$O-, -CH$_2$O-, =CHO	4.38	4.05	6.81
4.2 – 6.4	=CHO, ArOH, HC=C (nonconjugated)	4.12	3.25	2.43
6.4 – 6.8	HC=C (nonconjugated)	0.43	1.62	0.65
6.8 – 8.0	ArH, HC=C (conjugated)	7.65	9.61	9.18
8.0 – 10.0	-CHO, -COOH, downfield ArH	0.33	0	0

4.7.5 *GC-MS analyses*

GC-MS analysis of the different microalgae bio-oils produced at 500 °C was carried out in order to determine the bio-oils composition and to compare the three microalgae species. The list of the functionalities representing the compounds identified by GC-MS from pyrolysis is presented in Table 4-5. Bio-oils from microalgae contain a complex mixture of different compounds grouped into eight functionalities; aliphatic, aromatics, aldehydes, ketones, alcohols, carboxylic acids, esters and nitrogenates.

The different products distributions reflect the different compositions of the starting microalgae. *Isochrysis* produced a bio-oil rich in aliphatic hydrocarbons (34.1%) and esters (5.3%), while *Nannochloropsis* and *Tetraselmis* bio-oils contained more aromatics (8-11%), carboxylic acids (5-6%) and N-compounds (20-2%) due to the original microalgae large content in proteins. Tridecane, pentadecane, cyclohexane substitutes, cyclotetradecane, hexadecane and heptadecane were among the most abundant aliphatic, while phenols, cresols and benzenes (for example benzenepropoanenitrile) were the most abundant aromatics, which were produced by catalytic cracking of fatty acids and proteins (Du *et al.*, 2013a). Indole, amines, amides, pyridine, imidazole, piperidone and pyrrolidine were the prominent N-heteroatoms, originated by the pyrolysis of proteins (Huang *et al.*, 2017; Chen *et al.*, 2017b). Finally, hexadecane nitrile and pentadecanenitrile were the main N-compounds.The abundance of N-compounds in the bio-oils were in agreement with the elemental analysis (Table 4-3) and the ^{1}H-NMR (Table 4-4), where *Nannochloropsis* and *Tetraselmis* bio-oils are shown to contain high N content and heterocyclic compounds.

High oxygenates are undesirable as the compounds are reactive and not stable and tend to change rapidly during condensation or under storage conditions. Oxygenated compounds identified in pyrolysis bio-oils are represented with a wide range of functionalities, which include carboxylic acids, alcohols, esters, aldehydes, ethers and ketones. Pentanones, pentadecanone, hexadecanone and heptadecanone were the main

identified ketones, hexadecenal and octadecenal were the most abundant aldehydes, while carbamic acid, propionic acid and pentanoic acid are the most abundant carboxylic acids.

Isochrysis produced less aldehydes and carboxylic acids amount the three microalgae. The bio-oils from pyrolysis of microalgae had larger content in alcohols but overall lower oxygen content than bio-oil from wood and a lower content in aldehydes and carboxylic acids, which make them more stable.

Table 4-5 GC-MS products distribution from different microalgae pyrolysis bio-oils.

Groups	*Isochrysis*	*Nannochloropsis*	*Tetraselmis*
Aldehydes	3.44	5.78	6.35
Aliphatic hydrocarbons	34.08	27.72	23.18
Alcohols	16.99	15.05	15.88
Aromatics	3.39	8.10	11.39
Carboxylic acids	3.31	5.75	5.31
Esters	5.31	0.00	0.00
Ketones	16.42	14.86	16.99
Nitrogenated compounds	17.06	22.74	20.90

4.8   Summary

Three different species of microalgae (*Isochrysis*, *Nannochloropsis* and *Tetraselmis*) were evaluated as feedstock for the production of bio-fuels. The samples were pyrolysed at 500°C, atmospheric pressure in a fixed bed reactor. This work aim to establish if any of the selected microalgae could be used as a source for bio-fuels through thermos-chemical processing and also to evaluate their potential direct upgrading by catalytic pyrolysis. Their relatively high carbon contents (44.9 to 47.5 wt.%) and their decomposition profiles make them suitable feedstock for biofuel production. *Isochrysis*,

Nannochloropsis and *Tetraselmis* volatile matter (gas + oil) were 77, 62 and 70%, respectively. The pyrolysis of the microalgae produced different bio-oil yields, where *Isochrysis* produced the largest bio-oil fraction (37.2 wt.%). This indicates that *Isochrysis* is the most suitable as feedstock for pyrolysis.

H/C bio-oil ratios from three different species ranged between 1.61 and 1.69 and were closer to those of diesel and gasoline, rather than the original microalgae. *Tetraselmis* microalgae oil retained 41.7% of the original nitrogen content, meanwhile *Isochrysis* and *Nannochloropsis* bio-oil contained about 1/4 of the raw microalgae nitrogen. The bio-char yields of *Tetraselmis* were lower than that of obtained with *Isochrysis* and *Nannochloropsis*. This indicates that proteins (less abundant in *Isochrysis*) are less prone to form char deposits and are preferentially converted in gas species (CO and NH_3).

From the ^{1}H-NMR analyses, the bio-oils from pyrolysis of microalgae contained high abundance of aliphatic groups, mainly derived from the lipids in microalgae. In agreement to ^{1}H-NMR data, the GC-MS analyses indicate higher aromatics and N-heterocyclic compounds in the *Tetraselmis* and *Nannochloropsis* bio-oil, which is linked to its higher protein content, while *Isochrysis* bio-oil had lower aromatics, aldehydes and N-compounds compared to the other microalgae bio-oils.

Overall, the pyrolysis of *Isochrysis* sp. shows a high bio-yield and a better quality compared to the *Tetraselmis* and *Nannochloropsis*. Therefore, *Isochrysis* was selected for further work on catalytic upgrading by pyrolysis (Chapters 5 and 6) for the removal of O and N from the bio-oil and its qualitative enhancement. Also, the microalgae characterisation indicated the presence of alkali minerals in microalgae, which is detrimental for their thermo-chemical conversion in industrial scale. Therefore, a demineralisation pre-treatment of selected microalgae was studied (Chapter 7) to evaluate its effectiveness in the catalytic pyrolysis process.

Chapter 5

Catalytic pyrolysis of microalgae *Isochrysis* sp. to fuels and chemicals

5.1 Introduction

In the previous chapter, the conversion of different microalgae species through pyrolysis was described. The non-catalytic pyrolysis of the microalgae led to a bio-oil that is still rich in oxygen and nitrogen, so that further upgrading is necessary for deoxygenation and denitrogenation to obtain fuel similar to that derived from crude oil, with the aim to integrate the bio-oil into existing crude oil refinery settings. Several researches investigated the effect of catalyst for upgrading pyrolysis bio-oils. Most of the studies have been carried out using zeolites such as HZSM-5 for their acid properties and pores size in the range 5-6 nm (Thangalazhy-Gopakumar *et al.*, 2012).

This chapter investigates the use of different catalysts for the in-situ upgrading of the bio-oils during their production by pyrolysis process. Different types of catalysts were selected: Li-LSX-zeolite (strong acid zeolite), micro silica (weak acid), Na-FA and LiNa-FA derived from fly ash (basic silicates). The pyrolysis experiments and their interpretation are reported in the first part of the chapter together with the characterisation of the catalysts. The second part of the chapter focuses on the characterisation of the reaction products to establish the catalysts effect on the bio-oil yield and quality.

5.2 Selection of catalysts

The selection of the catalysts for the pyrolysis experiments was based on the literature review in Chapter 2. The catalysts were selected because of their characteristics and potential availability. To the best of my knowledge, there are no studies on pyrolysis of microalgae using Li-LSX-zeolite catalyst. Also, works on the metal silicate catalysts are

still scarce. Therefore, evaluation of different type of catalysts on the pyrolysis of microalgae can inform on their potential for bio-oil upgrading.

5.3   Catalyst characterisation

The principal of using the zeolite and non-zeolite catalysts was to determine the extent (performance) to which they could upgrade bio-oil to hydrocarbon-rich liquid products since no information on the performance of these catalysts is available. In addition to conversion to hydrocarbon-rich products, the catalysts were chosen so that an investigation into the role of catalyst acidity, pore size and structure on the upgrading could be made possible.

Li-LSX-zeolite catalysts were purchased from Shenghye Chemicals while micro silica was purchased from Sigma Aldrich chemicals. The LiNa-FA and Na-Fa used were synthesised following procedure describe by Sanna et al (Sanna, Ramli & Mercedes Maroto-Valer, 2015). The detailed preparation procedure is outlined in Chapter 3. In the following sections, the structure of the catalysts is described. Following these, the characterisation by BET surface area, pore volume, and pore size measurements are provided.

5.3.1   Catalyst surface area

BET surface area measurements, pore size and pore volume distributions were conducted with Gemini VII analyser equipped with multi-tasking software control and a single and dual controls. The pore sizes and micropore area were calculated using the Harkin and Jura equations. Table 5-1 summarises the textural properties of the Li-LSX-zeolite, Micro silica, Na-FA and LiNa-FA. The specific surface area (BET), and total pore volume of Li-LSX-zeolite were 662.02 m^2 g^{-1} and 0.27 cm^3 g^{-1}, respectively. The catalyst is a low silica X type (LSX) zeolite with of Si/Al ratio of 1.0. Instead, the specific surface area (BET) and total pore volume of micro silica were 640 m^2 g^{-1} and 0.40 cm^3 g^{-1},

respectively. Meanwhile, the Na-FA and LiNa-FA have low surface area of 1.57 m^2 g^{-1} and 0.86 m^2 g^{-1}, respectively. The micropore volume is too small at 0.000013 and 0.000023 cm^3 g^{-1}.

Table 5-1 Physical data of catalysts used in this research.

Sample	Li-LSX-zeolite	Micro silica	Na-FA	LiNa-FA
BET Surface area (m^2/g)	662.02	640.00	1.57	0.86
Micropore volume (cm^3/g)	0.309	0.40	0.000013	0.000023

5.3.2   *Catalyst acidity and basicity*

The aim for studying the acid and basic properties for catalysts is to find out how the sites are affecting the pyrolysis products. Therefore, it is important to determine the amount of basic or acid sites in the catalyst and to study whether strong or weak acidic sites or even both are present on the catalyst surfaces. Each catalyst presents different kind of acidity and basicity. The Li-LSX-zeolite considered as a strong acid zeolite, micro silica is a weak acid catalyst while, Na-FA and LiNa-FA derived from fly ash are basic silicates catalyst.

5.3.2.1   *TGA-Basicity*

The basicity test for the catalyst was done using TGA and the procedure has been discussed in Chapter 3. The basicity test was carried out using CO_2 on Li-LSX-zeolites and the two metal silicates catalysts. Figure 5-1 shows the different profiles obtained from the basicity test. The results show that the Li-LSX-zeolites absorb high CO2 which is about 8.845% during CO_2 flushing followed by Na-FA (0.009%) and LiNa-FA (0.007%). Meanwhile, during desorption of CO_2, about 3.22% of CO_2 were released from Li-LSX-zeolite surface. The Na-FA catalyst release about 1.14% of CO_2 during desorption reaction followed by LiNa-FA (0.286%) at temperature 500 °C. The order of the basicity

of the catalyst are Li-LSX-zeolites > Na-FA > LiNa-FA. The basicity samples show good correlation to the fraction of silica: The higher silica ratio in the samples, the higher amounts of desorbing CO_2. The presence of the alkali metals in the catalyst increased the basicity of the catalyst. However, due to the small surface area of the catalyst, the metal silicates are unable to absorb CO_2 during the analyses.
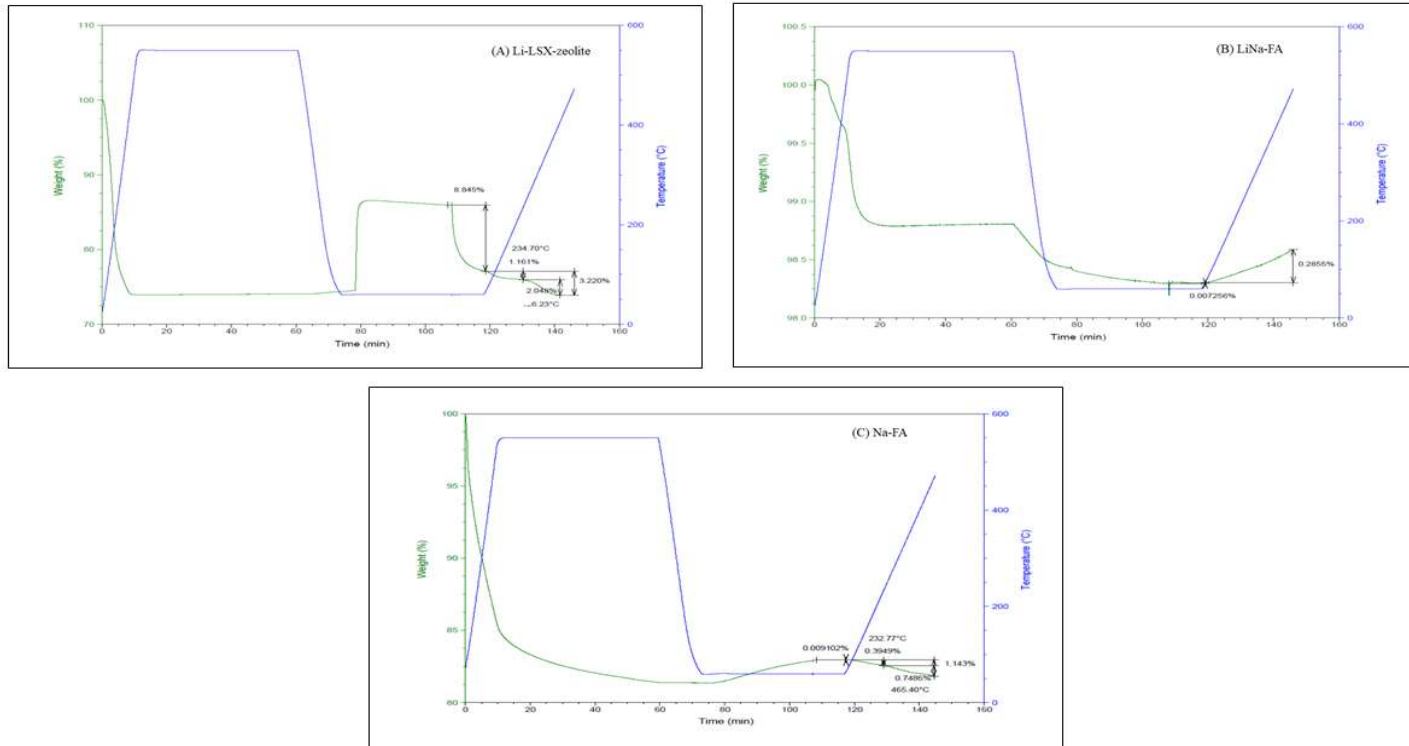
Figure 5-1 TGA Basicity test on (A) Li-LSX-zeolite (B) LiNa-FA (C) Na-FA catalysts.

5.3.2.2 *Ammonia (NH₃) and TPD pyridine*

NH$_3$-TPD was carried out to determine the acidity of the Li-LSX-zeolite. Figure 5-2 shows the NH$_3$-TPD profile of the Li-LSX-zeolite catalyst. It can be observed that there are two main peaks at different temperatures, which indicate desorption of ammonia from the catalyst. Figure 5-2 shows the catalyst contained weak and moderate acids sites. From the profile of the Li-LSX-zeolite catalyst resulted in a total acidity of 4.68 mmol of NH$_3$ g^{-1}.
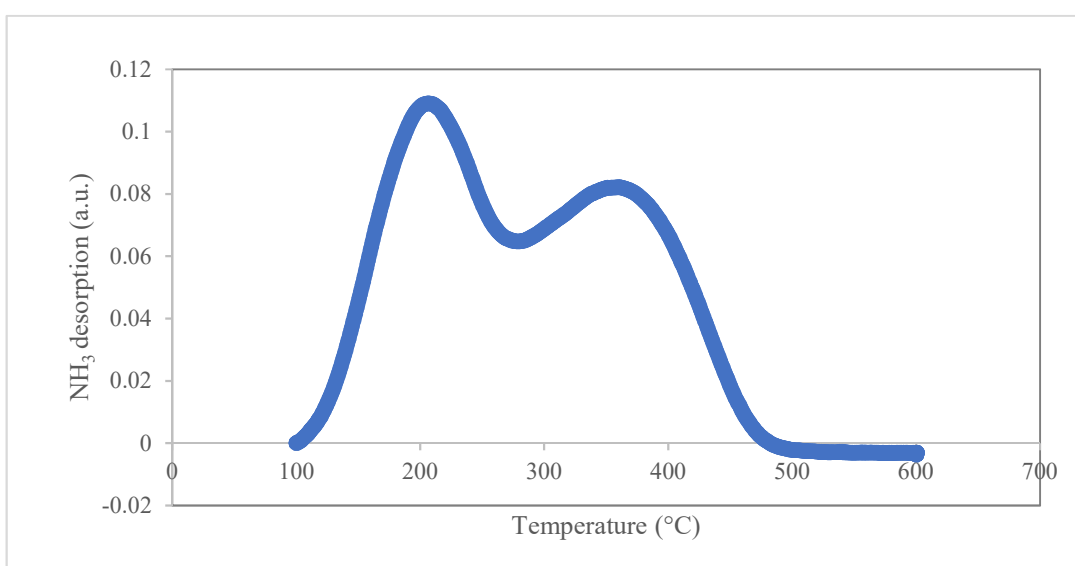
Figure 5-2 Profiles of TPD ammonia for Li-LSX-zeolites.

Since NH$_3$-TPD can only be used to calculate the total acidity of a solid catalyst, pyridine-TPD was used to quantify the presence of weak, moderate and strong acid sites. Fig. 5-3 shows the desorption profile of pyridine from the Li-LSX-zeolite, which clearly indicates the presence of weak acid sites (peak at 237 °C) and strong acid sites (peak at 498 °C). Also, the presence of moderate strength acid sites is suggested by the shoulder between the two main peaks. From the quantification of these acid sites, it can be observed that the abundance of weak and strong acid sites is quite similar. Thus, the weak acid sites concentration (180–280 °C) was 2.39 mmol pyridine g−1, while that of strong acid sites

(290–500 °C) was 2.21 mmol pyridine g^{-1}. Therefore, Li-LSX-zeolite possesses acidic properties.

Since the catalytic activity of the Li-LSX-zeolite may be explained by the acid sites type, the catalysts were investigated via pyridine adsorption on the catalyst surface using FT-IR spectroscopy. Since pyridine is larger than NH_3, it can adsorb only on the main zeolite channels (> 0.7 nm), which are also the pores range required for catalytic cracking reactions and titrate only to medium and strong acid sites. Fig. 5-3 shows the infrared spectra of Li-LSX-zeolite (dotted line) and pyridine adsorbed on the Li-LSX-zeolite at 150 °C (solid line). After the pyridine adsorption, the bands corresponding to the Lewis acid sites (L): 1450 cm^{-1}, and Brønsted acid sites (B)1540 cm^{-1} were detected together with another strong band at 1595 cm−1 (denoted as H), which can be assigned to weak hydrogen bonds between pyridine and the surface silanol groups of zeolites (Dong *et al.*, 2016). The band at 1492 cm^{-1} can be attributed to both Lewis and Brønsted acid sites. The ration between bands associated to Lewis acid and Brønsted acid sites suggests that the latter is less abundant. The generation of Lewis acidity could be linked to the Li incorporation in the tetrahedral coordination within the silica framework as observed for other zeolites (Dong *et al.*, 2016). In summary, the acid sites characterisation indicates that the Li-LSX-zeolite can be considered as an acid catalyst and its catalytic activity linked to those properties.
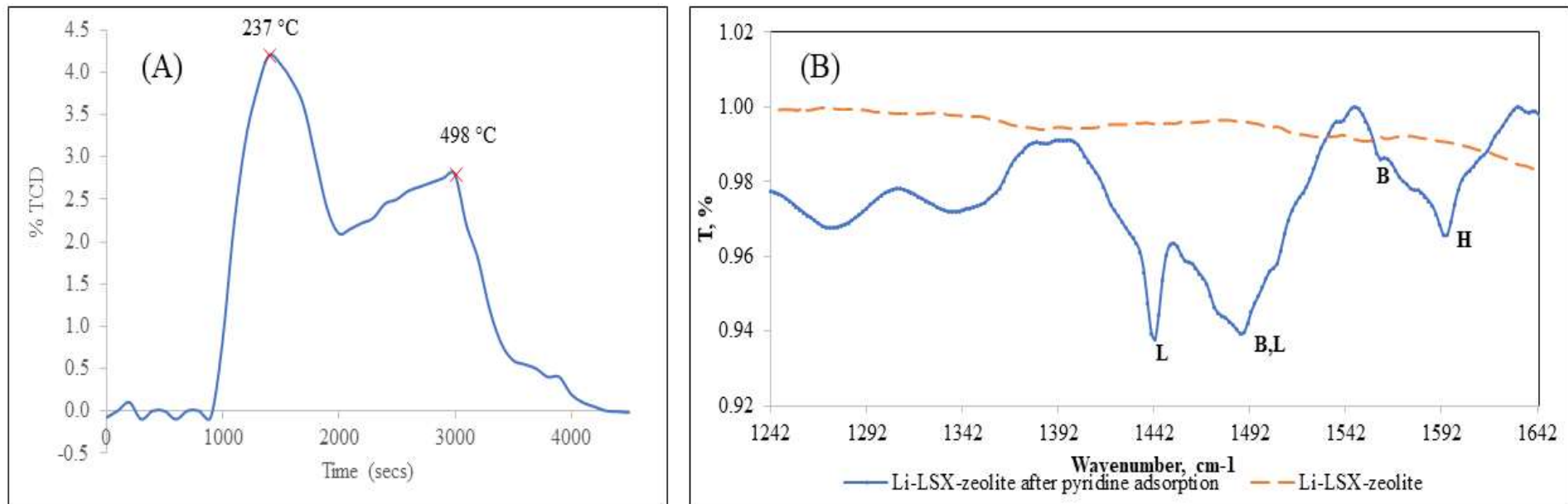
Figure 5-3 Pyridine-TPD (A), and FT-IR after pyridine adsorption (B) for Li-LSX-zeolite.(Abd Rahman, Fermoso & Sanna, 2017).

5.4 Evaluation by TGA-pyrolysis

The first step was to screen the catalysts by TGA-pyrolysis, to determine whether the catalysts had activity on microalgae depolymerisation and the resulting pyrolysis products distribution.

5.4.1 *TGA pyrolysis*

Isochrysis sp. underwent pyrolysis in the presence of three different catalysts at 500 °C. The catalysts used were Li-LSX-zeolite, Na-FA and LiNa-FA. The profiles obtained from the TGA-pyrolysis with the different types of catalyst are presented in Figure 5-4. Based on the figure, it can be observed that each catalyst had different effect on the microalgae pyrolysis. The volatile matters (VM) obtained in the use of Li-LSX-zeolite recorded the highest yield which is 35.3 wt.% followed by Na-FA (31.9 wt.%), while LiNa-FA resulted the lowest 25.9 wt.%. Li-LSX resulted the most effective in cracking the microalgae to gas and bio-oil compounds and predicted to produce high bio-oil yield.

5.4.2 *DTG of different catalyst*

Figure 5-5 shows that the first derivative of the *Isochrysis* weight changed in the presence of the different catalysts and the main decomposition temperatures. The derivative weight change profiles can be divided into three different decomposition, whose temperatures are reported in Table 5-2. An initial release of adsorbed water is associated to the peak at about 73-78 °C. The Phase I decomposition occurred around 180-200 °C and depicts the decomposition of protein compounds. This findings agrees with Babich (2011) and Wang (2016) that reported the decomposition temperature tend to shift to lower temperature in the presence of metals catalyst (Wang *et al.*, 2006; Babich *et al.*, 2011). Phase II, which was associated to the decomposition of carbohydrates, ranged between 250-360 °C. The decomposition peaked at 290-296 °C except in the presence of Li-LSX-zeolites, 273.2 °C. Finally, Phase III occurred at higher temperature, >350 °C and represents the

decomposition of lipids and protein compounds (350–500 °C). Overall, the *Isochrysis* decomposition rates (Table 5-2) decreased in the order: Li-LSX-zeolite > LiNa-FA> Na-FA. The rates associated to the decomposition of the proteins (Phase I) when Li-LSX-zeolite was used, were found to be faster (12.8 wt.%/min), compared to the LiNa-FA (7.44 wt.%/min) and Na-FA (4.69 wt.%/min). However, the decomposition rates of Li-LSX-zeolite were lower in Phase II and III, 5.88 wt.%/min and 5.33 wt.%/min respectively. Meanwhile, both metal silicate catalysts decomposed faster during Phase II and III as reported in Table 5-2. This shows that both metals silicate catalysts were active at higher temperature when the decomposition rate is higher.
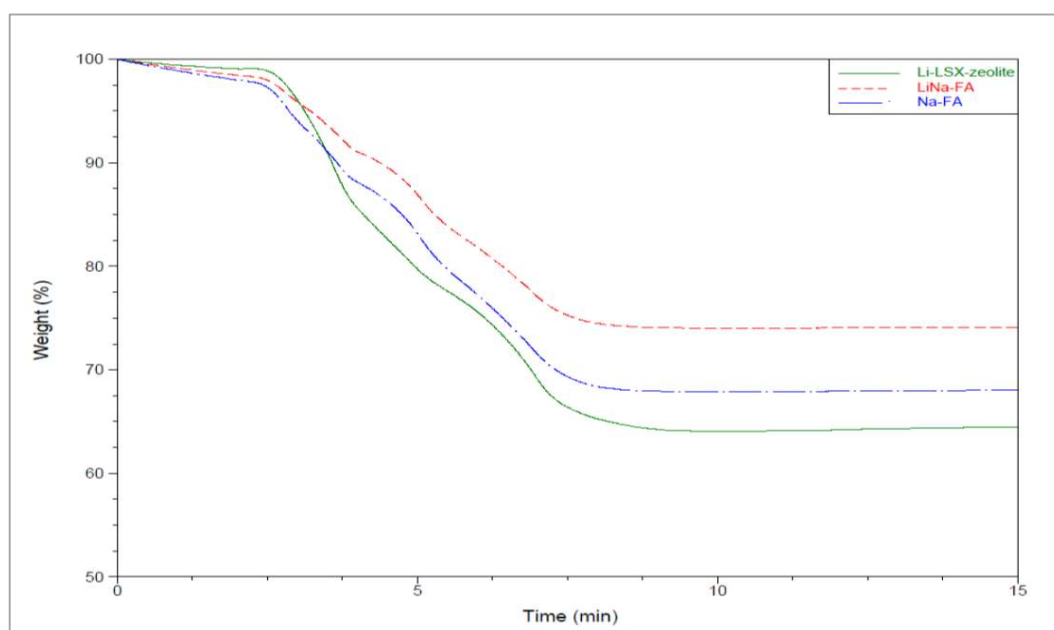
Figure 5-4 TGA profile on pyrolysis using different catalyst type.
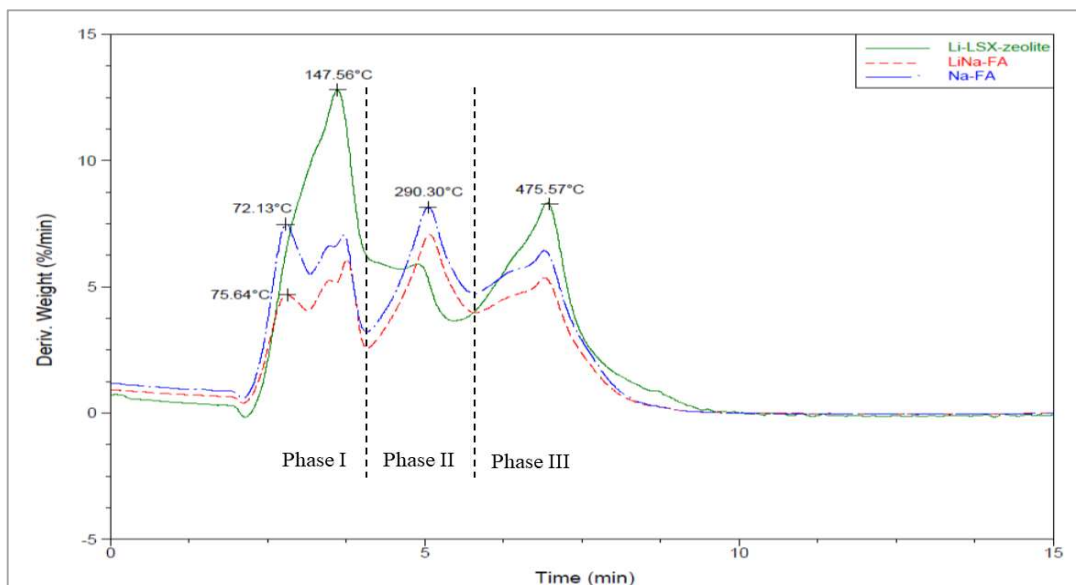
Figure 5-5 DTG of pyrolysis microalgae with and without catalysts.

Table 5-2 Temperature at maximum decomposition of microalgae from DTG of experiments carried out at 500 °C.

	Li-LSX-zeolite	LiNa-FA	Na-FA
		Decomposition Temperature. (°C)	
Phase I	147.03	170.27	163.5
Phase II	279.1	296.26	290.14
Phase III	475.99	475.99	476.99
		Decomposition Rate, wt.%/min	

Phase I	12.77	7.435	4.691
Phase II	5.875	8.159	7.014
Phase III	5.329	6.435	8.325

5.5 Catalytic pyrolysis of *Isochrysis*

Catalytic pyrolysis was used to investigate the effect of the different catalyst on the yield and quality of the pyrolysis products. The pyrolysis of *Isochrysis* sp. were ran at 500 °C in a fixed bed reactor with N_2 as carrier gas using Li-LSX-zeolite, micro silica, Na-FA and LiNa-FA with a catalyst: biomass ratio of 1:1. Non-catalytic pyrolysis was running for comparison purpose.

Figure 5-6 shows the product distribution from the catalytic and non-catalytic pyrolysis of *Isochrysis* sp. A remarkable reduction in the oil yield from 37 wt.% without catalyst to 28-29 wt.% with the acidic catalysts (Li-LSX-zeolite and micro-silica) and to ~31 wt.% in the presence of the basic alkali metal silicate catalysts, were observed. This shows that the presence of both the acidic and basic catalysts influenced the products yield. Previous work done by Chen (2008) showed that both alkaline Na_2SiO_3 and acidic HZSM-5 increased yields of solid products greatly and decreased yields of gaseous products when used for pyrolysing pine wood. However, the yields of liquid products (bio-oil) were not subjected to dramatic change (Chen *et al.*, 2008b).

Both metal silicate catalysts produced a slightly higher bio-oil yield than acidic catalyst and did not promote gas formation during pyrolysis. Using Na_2CO_3 and K_2CO_3 for gasification of biomass, Demirbaş et al. (2001) reported that both sodium (Na) and potassium (K) influenced the products yield. The presence of alkali metals weakened the intermolecular chain of polymer compounds, and catalysed the dehydration and promotes the condensation of products (Demirbaş, 2001). This can explain the tendency of both

Na-FA and LiNa-FA in producing a higher char yield compared to the non-catalytic run and to the presence of Li-LSX-zeolite and micro silica.

Bio-char formation related to the microalgae content, lipids and proteins. Lipids, which is complex with fatty acids and amino acids compounds, can be partly converted into bio-char during pyrolysis (Bi & He, 2013). On the contrary, the acid sites of the Li-LSX-zeolite and the micro silica (in minor extent) promoted a series of reactions such as dehydration, decarboxylation, decarbonylation and aromatisation thus enhancing the *Isochrysis* cracking to small molecular weight species (Jae *et al.*, 2011; Foster *et al.*, 2012). The cracking activity of pyrolytic vapours over Li-LSX-zeolite resulted in an increase in the gas yields from 28 wt.% (without catalyst) to 36 wt.%. The same trend was shown when using micro silica with gas yield of 36.8 wt.%.
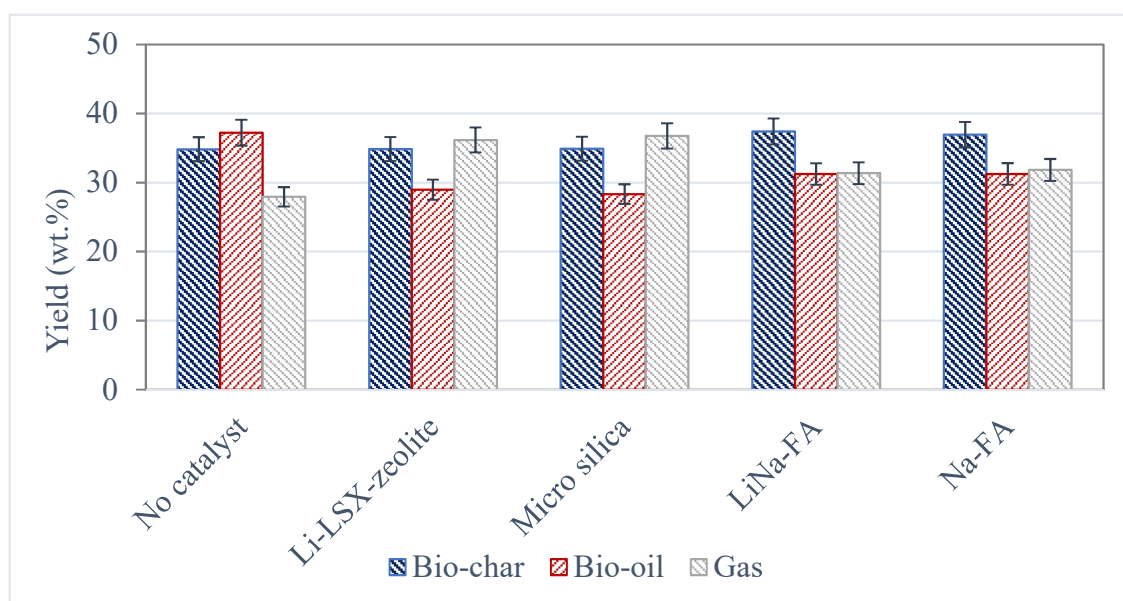
Figure 5-6 Product distribution from catalytic and non-catalytic pyrolysis.

5.6   Characterisation of pyrolysis products

5.6.1   *Elemental analyses of bio-chars and bio-oils*

Further indication of the catalytic activity of the microalgae using different catalyst can be extrapolated from the EA and the HHV data. Table 5-3 reports the elemental analyses and high heating value (HHV) of the bio-chars and bio-oils obtained from the catalysts screening. As expected, the usage of catalysts caused the EA and HHV to improve, compared to when catalysts are absence. The bio-chars obtained from the catalytic pyrolysis using Li-LSX-zeolite had high calorific values (23.0 MJ/kg), higher than those obtained from the non-catalytic pyrolysis (14.3 MJ/kg). Also, the bio-char was enriched in H and C. In particular, the H/C molar ratio suffered a dramatic increased from 0.8 to 1.7, with the latter being close to the coal. Instead, N-content was increased from 3.4 wt.% (non-catalytic) to 4.7 wt.% in the presence of Li-LSX-zeolite. However, the N content increased when other catalysts were used, indicating that the protein decomposition were condensed and retained in the bio-char. Both C and N compounds are good for soil amendment application (Grierson, Strezov & Shah, 2011). Catalytic bio-chars can be used as soil amendment only if the catalysts are efficiently separated and recovered.

The comparison of the EA of the bio-oils obtained using the different catalysts suggest that the only Li-LSX-zeolite reduce O in the bio-char and that the other catalysts, produce a char with very high oxygen content (39.1 to 53.6 wt.%). Compared to the non-catalytic test, the Li-LSX-zeolite and LiNa-FA silicate were the most effective in increasing the C content in the bio-oil of 4.3% and 2.2%, respectively; and in decreasing the O content of 8% and 25%, respectively. However, only Li-LSX-zeolite was able to dramatically reduce the N content in the bio-oil, with a 46% reduction, compared to the non-catalytic run. In the presence of catalyst, the oxygen is removed through several reactions such as decarboxylation, decarbonylation and dehydration, resulting a high gas yield and low bio-oil yield compared to the non-catalytic pyrolysis (Fermoso *et al.*, 2017b; French & Czernik, 2010; Babich *et al.*, 2011).

119

A great reduction of nitrogen content in the bio-oil would be benefited for the conversion process. However, there are no changes in nitrogen content (~5.0 to ~5.8 wt.%.) when the two alkali metal silicate catalysts were used. Same trend was shown when the HZSM-5 catalyst was used, where there is no significant reduction of nitrogen content at 1:1 ratio. (Pan *et al.*, 2010; Thangalazhy-Gopakumar *et al.*, 2012).

Overall, the results in Table 5-3 clearly show that presence of Li-LSX-zeolite catalyst improves the elemental composition and physical properties of the bio-oil from pyrolysis. Moreover, LiNa-FA catalyst is able to deoxygenate the bio-oil (10.77 wt.%) and retains a large fraction of the O in the bio-char. This suggests that the lithium (Li) and sodium (Na) mixture has chemically adsorbed carbon dioxide formed during the pyrolysis process in form of alkali carbonates. Differently, the Na-FA silicate was not able to adsorb CO_2 under the studied conditions. Previous work show that similar materials were able to capture about 2 wt.% (LiNa-FA) and < 1 wt.% (Na-FA)(Sanna, Ramli & Mercedes Maroto-Valer, 2015; Sanna, Aimaro, Maroto-Valer, 2016). Therefore, LiNa-FA was able to partially chemisorb CO_2 in form of carbonates on its surface. Since the biochar and the catalysts were analysed together in the elemental analyser, the carbonate derived O is accounted in the bio-char.

Table 5-3 Elemental analysis, H/C and O/C molar ratios and HHV of bio-chars and bio-oils obtained with catalyst and no-catalyst.

	Catalyst type				
Elemental analysis	No catalyst	Li-LSX-zeolite	Micro silica	LiNa-FA	Na-FA
Bio-chars					
Carbon	45.41	52.00	48.56	42.45	55.87
Hydrogen	2.91	7.36	4.34	0.20	1.00
Nitrogen	3.41	4.72	4.12	3.74	4.01
Oxygen	48.24	35.91	42.98	53.61	39.11

H/C molar ratio	0.77	1.70	1.07	0.06	0.22
O/C molar ratio	0.80	0.52	0.66	0.95	0.52
HHV (MJ/kg)	14.25	23.04	17.56	7.90	15.25
Bio-oils					
Carbon	71.69	74.77	71.80	73.31	70.70
Hydrogen	10.01	9.86	9.71	10.04	9.42
Nitrogen	3.89	2.11	3.47	5.88	5.02
Oxygen	14.41	13.26	15.02	10.77	14.86
H/C molar ratio	1.68	1.58	1.62	1.64	1.60
O/C molar ratio	0.15	0.13	0.16	0.11	0.16
HHV (MJ/kg)	35.27	36.32	34.90	36.33	34.23

5.3.3 *Oxygen/Carbon (O/C) and Hydrogen/Carbon (H/C) ratios of bio-oils*

One of the most important parameters to evaluate the upgrading effect of the studied catalyst is the oxygen content of bio-oils in terms of oxygen/carbon molar ratios. Figure 5-7 shows the O/C and H/C molar ratios of the bio-oils from the catalytic pyrolysis of *Isocrhysis*. It can be observed that the bio-oils suffered a mild deoxygenation by using Li-LSX-zeolite, with the O/C ratio reduced from 0.15 to 0.13. LiNa-FA showed the highest catalytic activity towards oxygen removal with the O/C ratio reduced to 0.11. This can be related to the presence of eutectic mix of Li and Na cations and their combined activity. There was a negative effect with increased O/C molar ratios (~1.60) when micro-SiO_2 and Na-FA catalysts were used, indicating they are not effective in oxygen removal.

Previous work had evaluated the effect of Na_2SiO_3 on the pyrolysis of lignocellulosic biomass showing the increased of char yield compared to non-catalytic runs (Chen *et al.*, 2008a). However, the deoxygenation power was not discussed. Regarding the H/C molar

ratios, all the catalysts had tendency to reduce it, with Li-LSX-zeolite showing the lowest ratio of ~1.58. A similar trend was shown by *Pavlova* bio-oils obtained with Titania based catalyst, where the H/C molar ratio dropped from 1.55 (without catalyst) to 1.46 - 1.53 (in the presence of metal doped TiO_2 catalyst) (Aysu *et al.*, 2017b).
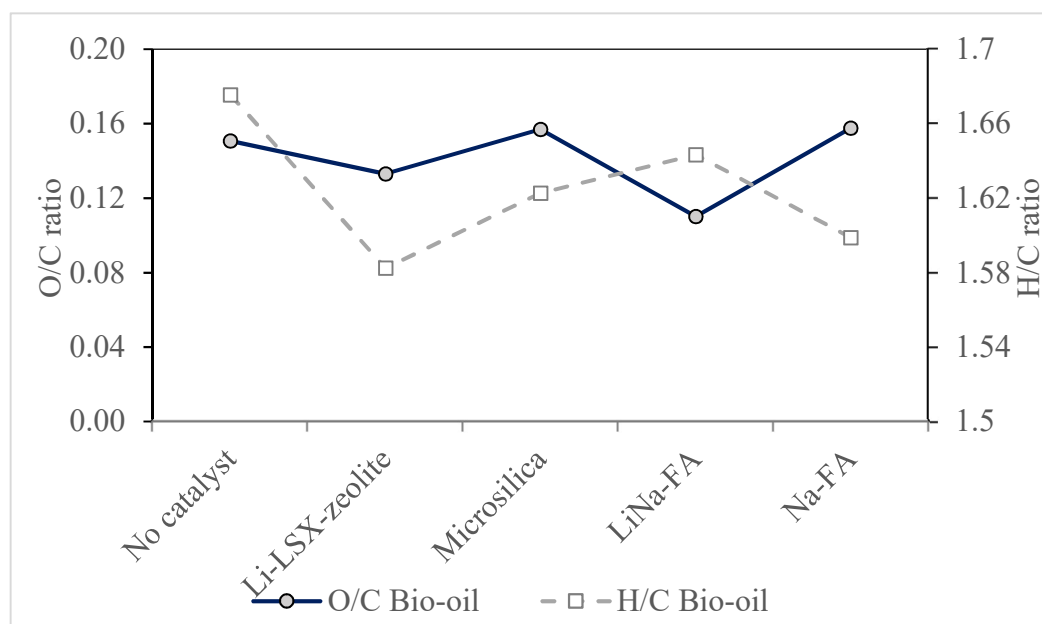
Figure 5-7 Oxygen/Carbon (O/C) and Hydrogen/Carbon (H/C) ratios of bio-oils using different catalysts.

Figure 5-8 compares the energy content with the respective oxygen contents of the bio-oils. As expected, there is an inverse relationship between energy content and oxygen level of bio-oils. Li-LSX-zeolite and LiNa-FA were able to promote the greatest enhancement in oil quality with HHV of about 36.7 MJ/kg and 36.3 MJ/kg, respectively. Differently, SiO_2 and Na-FA were not able to enhance the energy content compared to that of the non-catalytic one. Overall, Li-LSX-zeolite and LiNa-FA showed a positive effect on the bio-oil quality, owing to the reduction in oxygen content and the increased energy content.
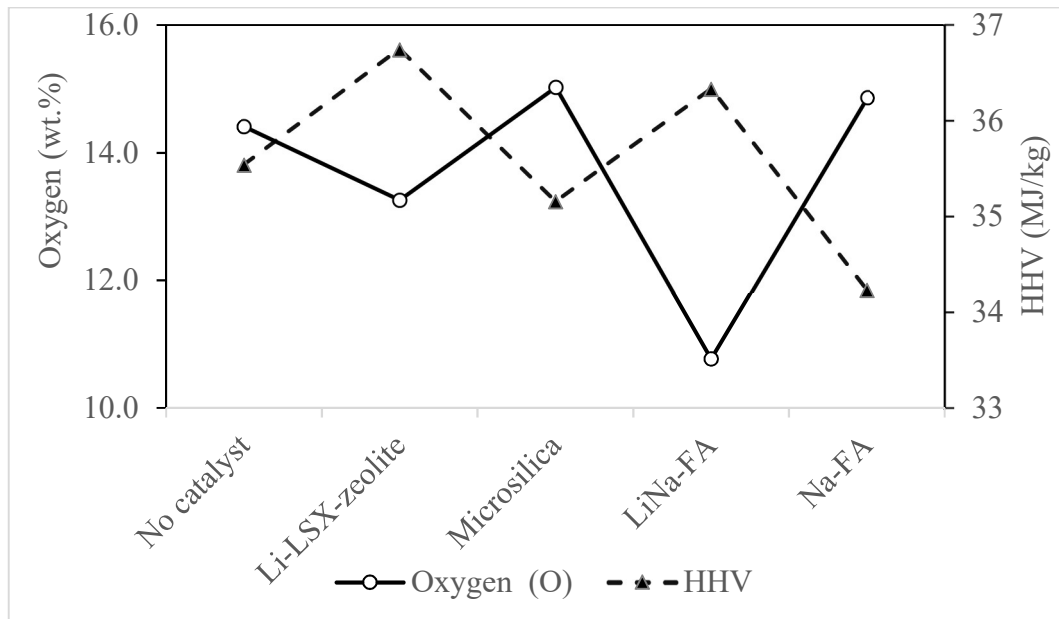
Figure 5-8 Bio-oils HHV and oxygen content relation; using different catalysts.

5.3.4   Nitrogen distribution

The bio-oil from pyrolysis of microalgae contained high nitrogen content reflects the high starting protein content of the feedstock. Microalgae *Isochrysis* sp. had a N content of 5.3 wt.%, which is detrimental in terms of fuels applications. Therefore, methods towards the N-content reduction in the bio-oils need to be developed. The addition of catalysts for the microalgae pyrolysis was therefore evaluated. The nitrogen distribution in the products of the catalytic and non-catalytic pyrolysis of *Isochrysis* sp. at 500 °C is shown in Figure 5-9. The bio-oil obtained without the catalyst contained about 27.3 wt.% of the nitrogen, while 22.6 wt.% remained in the solid bio-char and 50.1 wt.% went into gas products.

Acidic Li-LSX-zeolite and the weak acidic micro silica were the only catalysts that were able to lower the nitrogen content in the bio-oils to about 11.5 wt.% and 18.6 wt.%, respectively. Most of the N was removed in the gas phase (57.3 wt.% and 54.3%) and the remnant in the bio-char (31 wt.%). Meanwhile, pyrolysis using metal silicate catalysts increased the relative N-content in the bio-oils. Only 38.9 wt.%-42.3 wt.% of the N was

released in the gas phase, suggesting that only the acid catalysts could promote the removal of N in gas phase. Therefore, Li-LSX-zeolite was the only catalyst that is able to simultaneously reduce the content of N and O in the bio-oil and enhancing its energy content.
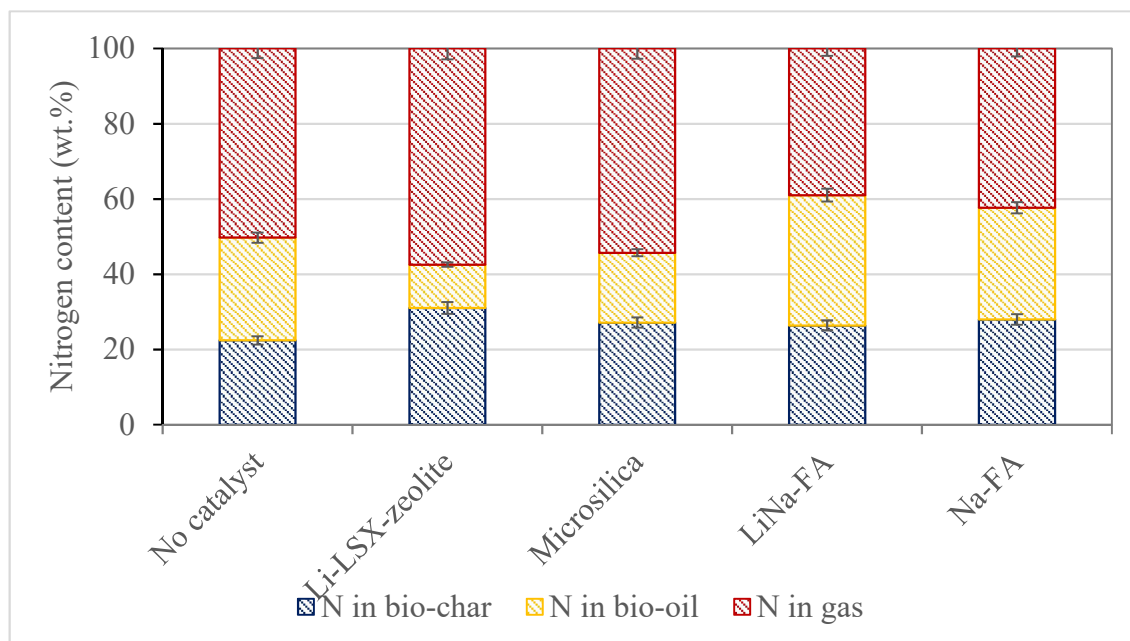
Figure 5-9 Nitrogen distribution in the products of catalytic pyrolysis.

5.3.5 ^1H NMR

The ^{1}H NMR analyses was carried out to understand the overall chemical functionalities of the bio-oils and at the same time the effect of the different catalysts. Table 5-4 reports the integration of the ^{1}H NMR spectra of the *Isochrysis* bio-oils that were obtained without and with catalysts. Clearly, there were differences in the overall protons' distribution in the bio-oils when different catalysts were used. The integrated region (0-1.6 ppm), which represents aliphatic protons was the most abundant for the bio-oils, indicating higher aliphatic content. Bio-oils obtained in the presence of Li-LSX-zeolite contained highest percentage of aliphatic protons (67.4%), followed by metal silicate catalysts (63.1%-63.5%), micro silica (61.1%) and no catalyst (60.2%). The aliphatic

compounds were mostly derived from the microalgae fatty acids and carbohydrates degradation. The next integrated region from 1.6 to 2.2 ppm, which is associated to alcohols and N-H in amines/amides indicates that Li-LSX-zeolite reduce these two functionalities in the bi-oil, while the other catalysts only slightly enhanced their abundance compared to the non-catalytic bio-oil. Resonance between 2.2 to 3.0 ppm (aliphatic protons bonded to C=C double bond (aromatic or olefinic) or H two bonds away from a heteroatom) did not show relevant differences, although Li-LSX-zeolite had the lowest amount (6.0%) of protons in this region.

The region of the spectra (3.0-4.2 ppm) that characterises the aliphatic alcohol/ether protons, or methylene groups joining two aromatic rings were less in the presence of all the catalysts (1.5-1.7%) than without catalyst (4.4%). The protons in the carbohydrates/aromatic ether (4.2-6.4 ppm) region were found to be in small amounts (~1.4-4.1 %) in all bio-oils, with lower levels in the presence of all catalysts. The overall decrease (more marked when Li-LSX zeolite was used) of protons linked to oxygenated species (3.0-6.4 ppm) compared to the non-catalytic test, can be associated to the partial O removal in the presence of the catalysts. These results are in accordance to the elemental (Table 5-2) and GC-MS (Table 5-5) analyses of bio-oils, which show lower oxygen contents when the catalysts were used. The protons linked to olefins (6.4-6.8 ppm) increased only in the presence of Li-LSX-zeolite, when compared to the test run in absence of catalyst. A similar trend was noticed for the aromatic region of the spectra (6.8-8.0 ppm) with Li-LSX-zeolite resulting in the highest protons abundance (12.96%) indicating the propension of this acidic catalyst in producing aromatics. This region represents hydrogen atoms both in benzenoid aromatic compounds and in heteroaromatics which contain oxygen and nitrogen such as furan and pyridine. Negligible amount (~0.7%) of aldehydes and carboxylic acids (9.0-10.1 ppm) were detected in bio-oils with and without catalyst, with Li-LSX-zeolite showing a decrease of the protons from 0.33% to 0.13%.

Table 5-4 ^{1}H NMR integrations of Isochrysis bio-oils for med at 500 °C versus specific chemical shift ranges.

Chemical shift region (ppm)	Type of protons	Hydrogen content (% of all hydrogen)				
		No catalyst	Li-LSX-zeolite	SiO_2	LiNa-FA	Na-FA
0.0 - 1.6	CH3. -CH2-	60.17	67.43	61.07	63.06	63.57
1.6 - 2.2	-CH2-, aliphatic OH	14.19	10.01	17.67	15.56	17.01
2.2 - 3.0	-CH3OC, -CH3-Ar, -CH2Ar	8.73	6.01	7.55	8.51	7.16
3.0 - 4.2	CH3O-, -CH2O-, =CHO	4.38	1.74	1.54	1.60	1.60
4.2 - 6.4	=CHO, ArOH, HC=C (nonconjugated)	4.12	1.35	3.01	3.06	2.70
6.4 - 6.8	HC=C (nonconjugated)	0.43	0.61	0.21	0.27	0.35
6.8 - 8.0	ArH, HC=C (conjugated)	7.65	12.96	8.70	7.65	7.01
8.0 - 10.0	-CHO, -COOH, downfiled ArH	0.33	0.13	0.24	0.29	0.62

5.3.6 GC-MS analyses

Proton NMR analyses were carried out to evaluate the overall composition of the bio-oils, which is not detectable by the GC-MS technique, are usually able to identify about 40% of bio-oil. However, GC-MS analyses give important contribution to the understanding of the reactions involved in the catalytic pyrolysis, since single compounds and chemical functionalities quantities can be tracked. The GC-MS analyses revealed that microalgae bio-oil is an extremely complex mixture of numerous compounds. Among the compounds identified in Table 5-5, main components in the bio-oil were classified into different groups: alcohols, aldehydes, aliphatic hydrocarbons, aromatics, nitrogenated compounds, and ketones.

Among these chemical classes, aliphatic the most valuable component in bio-oil from the point of view of fuel application. Straight chain alkanes such as hexadecane and dodecane are compounds found in diesel and aviation fuel. Meanwhile, aromatic hydrocarbons are important industrial chemicals and fuel additives to increase octane number in petrol. Table 5-5 shows that the addition of all the catalysts increased the aliphatic hydrocarbons compared to the non-catalytic pyrolysis in the following order: Na-FA silicate > Li, Na-FA silicate. > Micro silica > Li-LSX-zeolite. Aliphatic hydrocarbons are mainly derived from the catalytic decarbonylation and decarboxylation of the microalgae fatty acids. Figure 5-10 (A) suggests that the acidic catalysts were able to crack the long chain fatty acids more easily than the basic catalysts, producing C9-C15 hydrocarbons, while the basic catalysts were less efficient. This can be seen by the larger relative abundance of the dodecane, when Li-LSX-zeolite and micro silica were used. The acid catalysts also reduced the content in ketones and aldehydes.

Table 5-5 shows that only Li-LSX-zeolite was able to promote the formation of aromatic compounds from 2.9 rel.% (non-catalytic) to ~11.8 rel.%, while the other catalysts were not effective in aromatisation. In Figure 5-10 (C) it can be appreciated that both monoaromatics and polyaromatics were formed in the presence of Li-LSX-zeolite.

127

Benzene content, which has great commercial value for fuel productions, was doubled from 0.9 rel.% (non-catalytic) to 1.8 rel.% in the presence of Li-LSX-zeolite, but in the same time PAH such as naphthalene increased consistently. Meanwhile, other catalysts showed a decreasing trend for benzene compounds. Also, phenols (not shown in Figure 5-10) were reduced from 0.8% to 0.5% in the presence of Li-LSX-zeolites. Acid catalyst produced high aromatic compounds due to polymerisation that occurred inside the catalyst pores. Cheng et al. (2012) suggested that large pore zeolites tend to have severe coke formation due to polymerisation of larger compounds and block active sites in catalysts (Cheng *et al.*, 2012).

In general, bio-oil generated from pyrolysis of microalgae were found to contain high abundance of nitrogenated compounds which came from chlorophyll and proteins in microalgae. Although the determination of the nitrogenates by GC-MS (for denitrogenation evaluation purpose) can be misleading, since high molecular weight heterocyclic compounds are mostly undetectable by GC, showing deviation from the elemental analyses. However, the comparison of single compounds can give insight to the catalytic activity towards nitrogen rich compounds. Figure 5-10-(D) shows the relative abundance of two nitrogen rich compounds; (1) a linear Olea nitrile derived from oleic acid; and (2) a heterocyclic aromatic compound, Indole, produced by cyclisation reactions or protein-derived compounds. As can be seen, the catalyst rich in acid sites (Li-LSX-zeolite) promoted cyclisation reactions, while the basic catalysts (LiNa-FA and Na-FA silicates) formed only nitriles compounds. Also, the relative abundance of catalytic compared to the non-catalytic run suggests that the basic catalysts and Li-LSX-zeolite partially cracked the long chain nitrile into smaller compounds. A different trend was found for weak acid micro silica, which promoted formation of nitriles, possibly owing to the large surface available.

Oxygenated compounds were present in all bio-oils. From Table 5-5, it can be seen that the basic LiNa-FA and Na-FA silicates dramatically promoted esterification reactions, with formation of almost three times the content of esters obtained in the absence of catalyst. Alcohols were reduced in the presence of catalysts as compared to the non-

catalytic test, where the strong acid (Li-LSX-zeolite) and micro silica have the lowest content of 2.93 rel.% and 4.51 rel.%. Overall, the GC-MS indicates that the composition of the bio-oil obtained from pyrolysis of *Isochrysis* microalgae can be consistently modified depending on the catalyst used.

Table 5-5 Relative proportions (area%) of the main compounds of microalgae bio-oil from catalytic and non-catalytic pyrolysis.

Group families	c (rel.%)				
	Catalyst type				
	No catalyst	Li-LSX-zeolite	Micro silica	LiNa-FA	Na-FA
Alcohol	12.35	2.93	4.51	13.94	7.06
Aldehydes	1.67	0.73	0.9	3.39	2.7
Aliphatic	26.49	23.13	29.94	38.95	45.49
Aromatics	2.89	11.84	2.02	3.24	5.08
Carboxylic acids	2.27	2.07	0.93	1.94	1.45
Esters	3.67	3.25	1.97	13.28	12.77
Ethers	0.84	1.31	0.78	4.60	2.79
Ketones	9.33	3.43	3.73	13.85	14.93
Nitrogen compounds	12.42	5.52	8.35	8.75	9.18
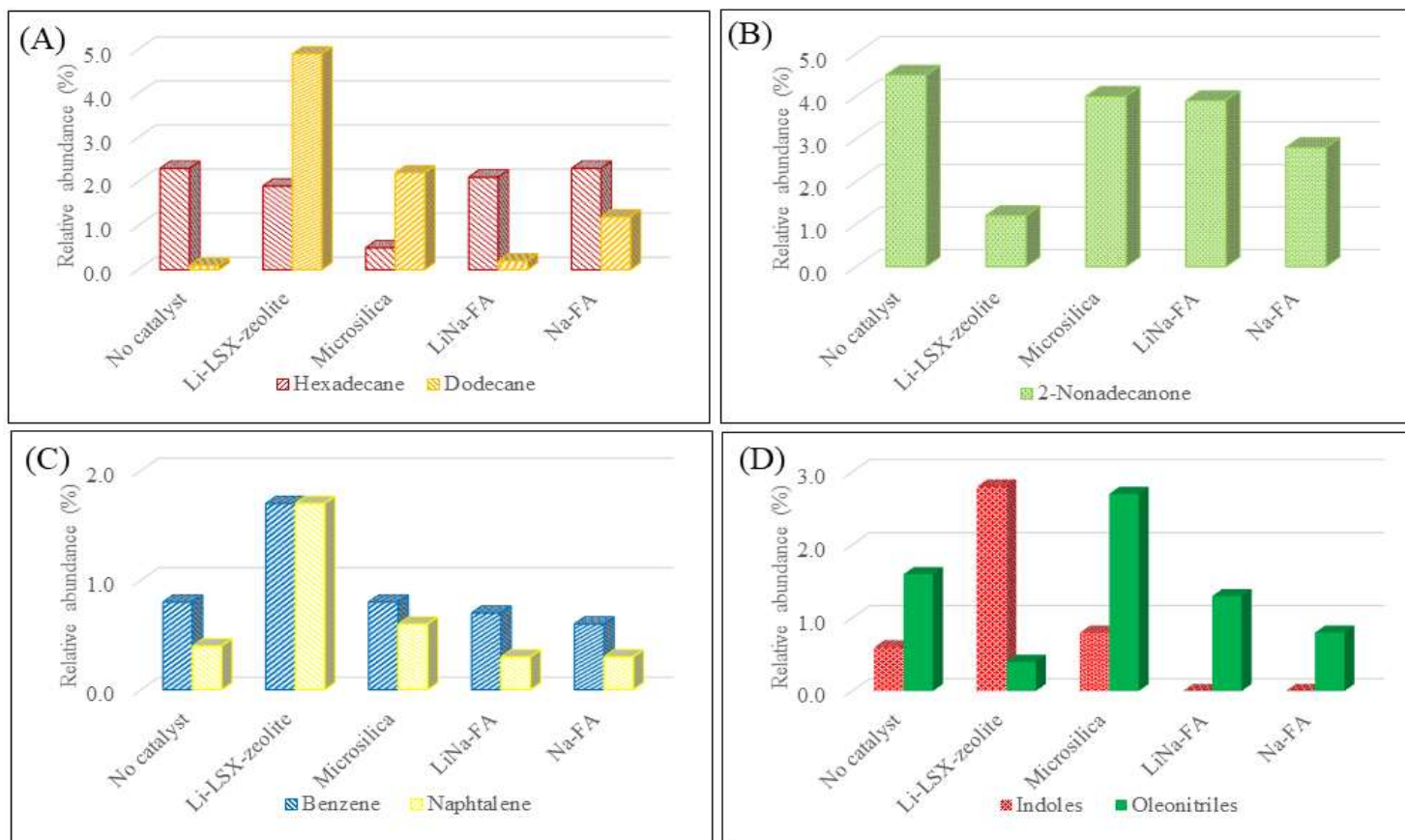
Figure 5-10 GC-MS distribution of selected bio-oil compounds. (A) alkanes (B) aldehydes (C) aromatics (D) N-compounds.

5.3.7 *Gaseous analyses*

Adding catalyst in pyrolysis reduces the bio-oil yield, enhancing the production of gaseous, whereas and water formation are less affected. The analyses of the composition of the gas fractions obtained from the catalytic and non-catalytic pyrolysis of *Isochrysis* at 500°C is presented in Table 5-6. In the presence of catalysts, the olefins and alkanes yield were increased more than two folds. All catalysts had cracking activity on the microalgae producing C_2H_4, C_2H_3, and CH_4.

The deoxygenation of the bio-oils took place by decarbonylation, dehydration and decarboxylation reactions. Almost all catalysts enhanced the deoxygenation by decarbonylation (8.1 to 23.0 wt.%) compared to the non- catalytic reaction. The same trend was observed for decarboxylation where all catalysts enhanced the CO_2 removal except Li-LSX-zeolite. The catalysts also promoted the formation of hydrogen (0.68-1.73 wt.%) and methane (1.7-3.9 wt.%). Micro silica was the less effective on H_2 and CH_4 formation. Previous work showed that alkaline sodium compounds (NaOH, Na_2CO_3, and Na_2SiO_3), promoted H_2 formation in microwave pyrolysis of pine wood (Chen *et al.*, 2008c).The main difference in the gas composition when Li-LSX-zeolite was represented by the increase in the NH_3 and HCN yield compared to the non-catalytically obtained gas, supporting the EA and ^{1}H-NMR data that showed a propension of the Li-LSX-zeolite to remove mostly in form of ammonia the protein derived nitrogen.

Figure 5-11 illustrates the deoxygenation activity with different catalyst. Clearly, the highest level of deoxygenation activity comes from dehyration reactions, by releasing water to the gas, followed by decarbonylation and finally decarboxylation. The distribution of the oxygen initially contained in the biomass among the different fractions is shown in Table 5-2. While in the non-catalytic reactions, a large fraction of the oxygen was retained in the bio-oil, this trend drastically changed when the catalysts were added to the pyrolysis, in particular with the basic catalysts. Thus, in agreement with the promotion of decarbonylation and decarboxylation, there was a drastic increase in the

oxygen contained in the gas phase, which was reflected in the reduction of the oxygen in the bio-oil fraction.

Table 5-6 Gas product distributions with different type of catalysts.

Gas compounds	C (wt.%)				
	Catalyst type				
	No catalyst	Li-LSX-zeolite	Micro silica	LiNa-FA	Na-FA
H_2	0.11	0.91	0.68	1.61	1.73
CO	5.22	8.12	21.83	24.69	23.04
CO_2	1.26	0.87	1.38	1.13	1.58
CH_4	0.87	1.17	1.75	2.93	3.91
H_2O	12.93	19.74	21.66	14.29	18.8
HCN, NH_3	1.63	12.05	0.98	0.56	0.49
Olefins (C_2H_4, C_2H_3, C_3H_6, C_4H_8)	17.14	26.98	41.1	42.68	34.36
Alkanes (C_3H_8, C_2H_6, C_4H_{10}, C_5H_{12})	3.56	8.63	6.96	10.15	14.38
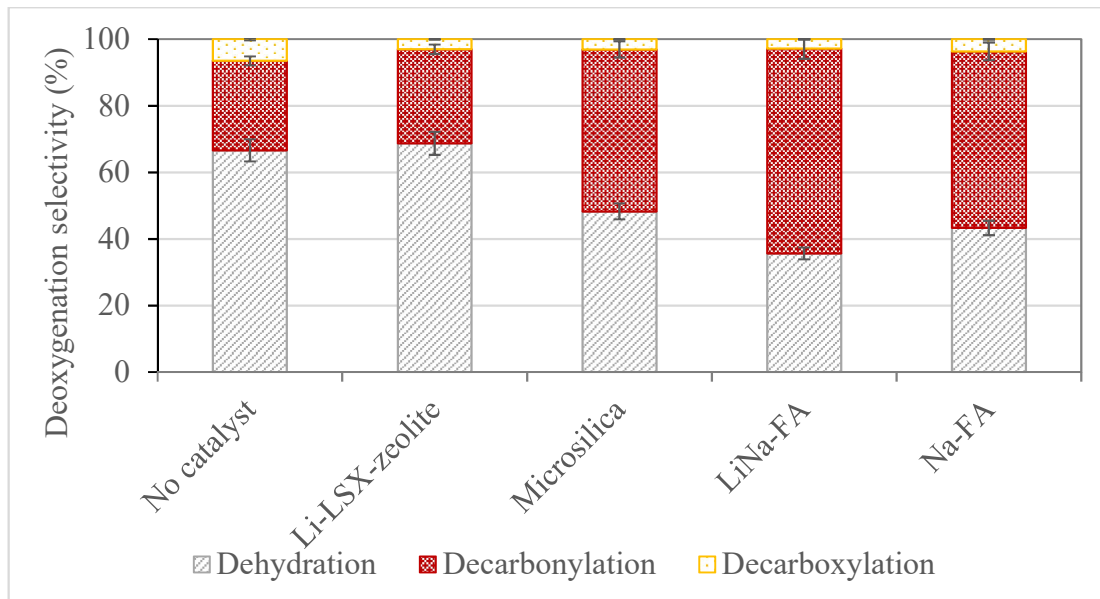
Figure 5-11 Catalytic deoxygenation activity with different catalysts.

5.7 Summary

In this chapter, the chemical transformation of *Isochrysis* sp. microalgae by pyrolysis using different catalysts was investigated. The yield of bio-oils was lower when catalysts were added into the pyrolysis of microalgae. Overall, the maximum yield of bio-oil was found to be in the following order: No catalyst > LiNa -FA > Na-FA > Li-LSX-zeolite > Micro silica. Overall, Li-LSX zeolite promoted the cracking of microalgae at lower temperature compared to other catalyst.

Two important criteria for the bio-oil to be implemented as bio-fuel are (1) removal of oxygen; and (2) nitrogen from bio-oil. The deoxygenation of the biomass starting material with deoxygenation power decreasing in the following order: LiNa-FA > Li-LSX-zeolite > Na-FA > Micro silica. Meanwhile, the denitrogenation power was different with Li-LSX-zeolite > SiO_2 and the other two catalysts does not change the N composition. Compared to the non-catalytic test, Li-LSX-zeolite and LiNa-FA and Na-FA silicate were the most effective in increasing the C content in the bio-oil of 4.3 wt.% and 2.2 wt.%, respectively and in decreasing the O content of 8 wt.% and 25 wt.%, respectively.

However, only Li-LSX-zeolite was able to dramatically reduce the N content in the bio-oil, with a 46 wt.% reduction, compared to the non-catalytic run. This was also supported by the decrease in protons abundance in the integrated area 1.6-2.2 ppm of the ^{1}H-NMR, associated to N-H in amines/amides. The ^{1}H NMR analysis also suggested that the bio-oils obtained using Li-LSX-zeolite contains more aromatics and aliphatic than other catalysts.

The GC-MS, in agreement to the ^{1}H-NMR, indicated that the addition of all the catalysts increased the aliphatic hydrocarbons compared to the non-catalytic pyrolysis in the following order: Na-FA silicate > LiNa-FA > Micro silica > Li-LSX-zeolite. The acidic catalysts where able to crack the long chain fatty acids to C9-C15 hydrocarbons and reduced the content in unstable ketones and aldehydes. Only Li-LSX-zeolite was able to promote the formation of aromatic compounds from 2.89 rel.% (non-catalytic) to ~11.84 rel.%. Almost all catalysts enhanced the deoxygenation through decarbonylation (22-23.5 wt.%) compared to the non- catalytic reaction, while decarboxylation is promoted only by Li-LSX zeolite, with a 38% CO_2 compared to the non-catalytic run. Li-LSX-zeolite was able to increase by 4.5 folds the yield of NH_3 and HCN in gas, compared to the non-catalytically obtained gas, supporting the EA and 1H-NMR data that showed a propension of the Li-LSX-zeolite to remove protein-derived nitrogen in gas phase.

Overall, it is possible to produce bio-oil with less oxygen and nitrogen retaining high energy content in the liquid using Li-LSX-zeolites. Therefore, this catalyst was selected for further assessment on catalytic pyrolysis to enhance the upgrading process.

Chapter 6

Optimisation studies on catalytic pyrolysis of *Isochrysis* sp. using Li-LSX-zeolite catalyst

6.1   Introduction

Following the marine biomass and catalysts selection in the previous chapters, microalgae *Isochrysis* sp. and Li-LSX-zeolite catalyst were selected for further catalytic pyrolysis due to the promising bio-oil yield and chemical composition of the former and the simultaneous denitrogenation and deoxygenation propension shown by the latter. The chemical composition of bio-oils varies with the properties of biomass and pyrolytic environment (reaction temperatures, gas flow rates, catalyst: biomass ratio, and the pyrolysis set-up).

Since, to the best of my knowledge, no previous studies reported the influence of these parameters on the bio-oil yield, bio-oil composition as well as other products obtained in the presence of Li-LSX-zeolite and in view of its potential as O and N removal agent, this study fill the gap in the literature by systematically investigating the pyrolysis products composition by changing process parameters such as pyrolysis temperature, catalyst: biomass ratios, residence time and pyrolysis reactor set-up. The summary of the various parameters used in this study are shown in Table 6-1. The pyrolysis products were analysed through different methods. The C, H, N content in bio-oil and bio-char were determined by elemental analysis. Besides, the bio-oils undergo GC-MS and ^{1}H-NMR analysis to determine their chemical compositions. Meanwhile, gaseous products were trapped in gas bag and analysed using Cirrus MKS MS spectrometer.

Table 6-1 Summary of process parameters used in this study.

Operating conditions	
Temperature (°C)	400, 500, 600, 700
Catalyst: Microalgae ratio	0.5:1, 1:1, 3:1
Reactor setup	In-situ vs. Ex-situ

6.2   Effect of reaction temperature

Temperature is considered as the most important parameter influencing products yields and distributions. Biomass decomposition occurs when the temperature exceeds the activation energies breaking the bonds, resulting in formation of free radicals and fragmented species. Low temperature is not sufficient for biomass decompositions, while high temperature lead to cracking of large compounds to smaller ones, producing gas (Aysu & Sanna, 2015; Wang & Brown, 2013).

6.2.1   *Pyrolysis yield and mass balance*

The catalytic screening showed that Li-LSX-zeolite is able to denitrogenate and partially deoxygenate the *Isochrysis* sp. bio-oil and promoted the production of aromatics and aliphatic. Therefore, Li-LSX-zeolite was further investigated to establish the effect of temperature and catalyst: microalgae ratio on the products distribution and quality. The yields of bio-char, bio-oil and gaseous obtained from the catalytic pyrolysis of *Isochrysis* between 400 to 700 °C are presented in Figure 6-1. With increasing temperature from 400 to 700 °C, the gaseous yield increased steadily from 34 wt.% to 48 wt.%, at the expenses of the bio-char, which decreased from 46 wt.% to 28 wt.%. The bio-char yield decreased at higher temperature due to the increasing cracking activity at 600 and 700°C.

Within temperature range of 400-500 °C, the bio-oil yield increased significantly from 19.6 wt.% to 28.9 wt.%. However, as temperature varied from 500 to 700 °C, the bio-oil yield declined gradually to 23.9 wt.%. Therefore, the maximum bio-oil yield was obtained at 500 °C (29 wt.%). The bio-oil yield decreased as the temperature increased because pyrolysis vapours undergo secondary cracking reactions at high temperature leading to increase in the gas yield. The result led to the selection of 500 °C as the reaction temperature for the other tests, which will be discussed on the next subchapter.

Figure 6-1 Product distribution from catalytic pyrolysis of *Isochrysis* sp. at different temperature.

6.2.2 *Elemental analyses*

Table 6-2 shows the elemental analysis of the bio-chars and bio-oils from the catalytic pyrolysis at different temperatures. As expected, the C content in the bio-chars increased according to the increase in temperature to a maximum of 71.2 wt.% at 700°C. However, Zainan et al. (2015) showed a decreasing trend on C content in bio-char (43.2% to 41.9 %) with increasing temperature from 300 to 600 °C (Zainan, Srivatsa & Bhattacharya,

2015). The authors used catalyst HZSM-5 on catalytic pyrolysis of microalgae *Tetraselmis* sp. Meanwhile, compounds like H, N and O content appeared to follow the trend from this study, where these compounds reduced as the temperature increased. The bio-oil produced between 500 and 700°C contained the lowest N content of 2.1-2.3 wt.%. The highest HHV value (37 MJ/kg) was obtained at 500 °C and was comparable to that of petroleum derived fuels (42 MJ/kg) and diesel (43 MJ/kg) (Mortensen *et al.*, 2011). The decrease of HHV at 700°C is due to high transfer of C in the solid phase.

Table 6-2 Elemental analysis, H/C and O/C molar ratios and HHV of bio-chars and bio-oils obtained at different temperature.

	Temperature (°C)			
Elemental analysis	400	500	600	700
Bio-chars				
Carbon	41.88	52.00	63.22	71.23
Hydrogen	7.65	7.36	7.51	7.07
Nitrogen	4.45	4.72	2.99	0.11
Oxygen	46.01	35.91	26.28	21.59
H/C molar ratio	2.19	1.70	1.43	1.19
O/C molar ratio	0.82	0.52	0.31	0.23
HHV (MJ/kg)	18.82	23.04	28.16	30.96
Bio-oils				
Carbon	70.43	74.77	74.27	71.45
Hydrogen	9.05	9.86	8.85	9.25

Nitrogen	3.07	2.11	2.12	2.28
Oxygen	17.46	13.26	13.76	17.02
H/C molar ratio	1.54	1.58	1.43	1.55
O/C molar ratio	0.19	0.13	0.14	0.18
HHV (MJ/kg)	33.39	36.32	34.90	34.05

6.2.3 *Nitrogen distribution*

Figure 6-2 illustrates nitrogen distribution in pyrolysis products. The graph shows that pyrolysis temperature affects the N distribution in pyrolysis products. At 400 °C, only about 49.9% of nitrogen was released in gaseous phase, while 38.7% was found in the bio-chars. As temperature increased, the amount of nitrogen in the bio-char or residue dropped dramatically to 31% at 500 °C and only 0.6% at 700 °C. Correspondingly, the amount of nitrogen released in gaseous phase as ammonia and HCN increased with temperature. The highest N removal was recorded at high temperature (700 °C), where 89.1% of N released in gaseous phase. The same trend showed by Wang et al. (2013) where the amount of ammonia increased as the temperature increased, from 2% at 400°C to 53% at 800 °C. Meanwhile, the amount of HCN increased from 1% to 15% at temperature 400 °C and 800 °C, respectively (Wang & Brown, 2013). About ~10.3 to 11.5 % of N remained in the bio-oil, which indicates that temperature does affect the nitrogen content in the bio-oil. The N distribution in bio-oil will be discussed on next subchapter.
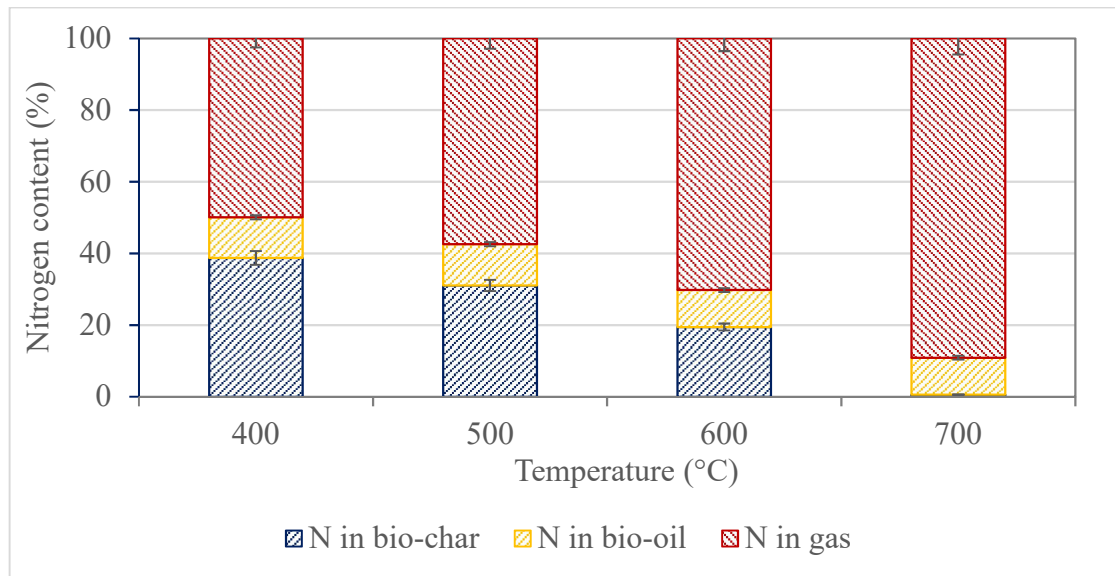
Figure 6-2 Nitrogen distribution in the products at different temperatures.

6.2.4 *GC-MS*

The collected bio-oil were analysed by GC-MS to establish their compositions. Table 6-3 shows the GC-MS bio-oil composition based on four main groups; aliphatic, aromatics, oxygenated compounds (including alcohols, ketones and aldehydes), and nitrogenated compounds. The table indicated that increasing the temperature resulted in increased aromatics content from 5.15% (400 °C) to 11.84% at 500 °C and decreased to 10.47% (700 °C). This can be partially attributed to thermal degradation of proteins. Some amino acids, such as tyrosine, can directly generate phenols through their decomposition (Lorenzetti *et al.*, 2016). Aromatics are mainly produced due to the presence of Brønsted and Lewis acid sites in the Li-LSX-zeolite, which enhances dehydration, decarbonylation and aromatisation reactions [2]. Also, low Si/Al ratio has been linked to maximum aromatic yield, due to enhanced concentration of acid sites in close proximity to one another (Du *et al.*, 2013b). The same trend was observed by Wang et al. (2013) on catalytic pyrolysis of *Chlorella vulgaris* using HZSM-5 where aromatic carbon yield increased with increasing temperature, from 14% at 400 °C to 16.7% at 800 °C (Wang & Brown, 2013).

Meanwhile, pyrolysis of the fatty acids led to the formation of a large fraction of aliphatic, mostly alkanes. The increase in temperature does not change the aliphatic compounds in the bio-oils range between ~20-23%. Hydrocarbon compounds are desirable fractions since they are chemicals with high commercial value. Other compounds such furans and phenols are stable compounds with high energy value and have been widely used as chemical additives or fuel substitutes (Imran *et al.*, 2016).

Nitrogenated compounds identified include amines, amides, pyridines, nitriles and indoles. Linear amides may have been formed from primary protein decomposition or from amines in amino acids that reacted with carboxylic acids to produce amides and water, while cyclic amides such as 2-pyrrolidone may have been formed from protein and amino acid intramolecular cyclisation (Harman-Ware *et al.*, 2013). Pyrazines and pyridines are produced from primary and secondary decomposition, cracking and/or intramolecular cyclisation of proteins and N-containing bio-char (Harman-Ware *et al.*, 2013). Indoles may be produced from decomposed tryptophan amino acids (Li *et al.*, 2015). Indoles were the most abundant nitrogenates in the N-compound group at 500 and 600 °C when the catalyst was used, while their presence was not detected at 400 °C, where amines were more abundant. With the increase in temperature to 600 °C, indole was completely removed in the presence of Li-LSX-zeolite and pyridine and nitrile were the most abundant compounds. Dehydration of amides intermediates produced nitriles compounds while the scission of ketones and other nitrogen compounds lead to the cyclisation and formation of pyridine (Chen *et al.*, 2017a). It can be seen that as temperature increases, less nitrogenated compounds appear in the bio-oils. Some of the complex nitrogen compounds were broken and released into gaseous phase. This finding is consistent with the Figure 6-2 (Nitrogen distribution) where most of the N compounds were released as gaseous phase.

Table 6-3 GC-MS bio-oil composition based on groups at different temperatures.

Group families	c (rel.%)			
	Temperature (°C)			
	400	500	600	700
Alcohol	2.12	2.93	2.54	2.20
Aldehydes	4.25	0.73	0.00	0.00
Aliphatic	21.77	23.13	20.9	19.44
Aromatics	5.15	11.84	11.46	10.47
Carboxylic acids	2.18	2.07	1.91	1.93
Esters	2.73	3.25	2.78	1.29
Ethers	0.39	1.31	0.93	0.64
Ketones	3.29	3.43	3.25	2.72
Nitrogen compounds	6.65	5.52	4.61	1.73

6.2.5 *Gas analyses*

Table 6-4 shows the gas compositions obtained from the pyrolysis at the different temperatures. Increasing temperature cracks low molecular compounds into other products such as CO, CO_2, CH_4, H_2 and other small paraffins. For example, at 600°C, the amount of H_2 and olefins increased sharply to 2.3 wt.% and 33.44 wt.% (from 0.11 wt.% and 29.17 wt.% at 400 °C). Other than that, nitrogen in gaseous form were released as HCN and NH_3 compounds, with the largest amount released at 700 °C, 13.7 wt.%.

A study conducted on the catalytic pyrolysis of *Isochrysis zhangjiangensis* at various temperature using catalyst ZSM-5 (Dong *et al.*, 2014). The trend on CO and CO_2 are almost similar with this study where the product increased with increasing temperature.

For example, CO_2 distribution increased from 42.5 to 54.5% when temperature increased from 550 °C to 650 °C.

Table 6-4 Gas product distributions at different temperatures.

Gas compounds	C (wt.%)			
	Temperature (°C)			
	400	500	600	700
H_2	0.11	0.91	2.28	1.77
CO	7.03	8.12	8.78	8.87
CO_2	0.41	0.87	0.49	0.7
CH_4	0.48	1.17	1.2	1.54
H_2O	19.66	19.74	18.39	14.91
HCN, NH_3	9.69	12.05	13.63	13.71
Olefins (C_2H_4, C_2H_3, C_3H_6, C_4H_8)	29.17	26.98	33.44	38.23
Alkanes (C_3H_8, C_2H_6, C_4H_{10}, C_5H_{12})	14.38	8.63	11.68	10.23

6.3 Effect of catalyst: microalgae ratio

For heterogenous catalytic systems, the contact between catalyst and biomass/vapour is an important issue and poses practical challenges. The contact can be improved by increasing the catalyst to biomass ratio. A different catalyst: microalgae ratio either led to an increase in the bio-oil yield or gas production.

6.3.1 *Pyrolysis yield and mass balance*

The effect of catalyst to biomass ratio was investigated by varying the amount of Li-LSX-zeolite catalyst. Based on the results reported in the previous subchapter, 500 °C was chosen as pyrolysis temperature in this series of experiments. A catalyst: microalgae weight ratio of 0.5:1, 1:1 and 3:1 was used in each experiment, and the results were compared to those yielded using the non-catalytic pyrolysis. Figure 6-3 shows the products distribution obtained by catalytic pyrolysis with the different catalyst: microalgae ratios.

There was a significant reduction in the bio-oil production compared to the non-catalytic tests, with the bio-oil yield decreased from 37 wt.% (non-catalytic) to 30 wt.% (0.5:1), 29 wt.% (1:1) and 23 wt.% (3:1), respectively. In parallel, a linear increase in gas yield can be observed with increasing catalyst ratio, with a maximum of 43 wt.% obtained using a ratio of 3:1. The use of larger amounts of zeolite led to a reduction in the bio-oil yield due to the increase in the production of non-condensable gaseous, primarily hydrocarbons. High catalyst ratio increased the activity of the catalyst by cracking most of the long-chain aliphatic compounds (mainly from fatty acids) generating light olefins and alkanes in the gas phase. Meanwhile, the amount of solid residue in the catalytic pyrolysis did not vary significantly with increasing catalyst: microalgae ratio which range about 34.5 to 36.6 wt.%.

Results showed in this study agree with Zeng et al. (2013) on catalytic pyrolysis of natural algae from water bloom over nickel phosphide catalyst (Zeng *et al.*, 2013). The bio-oil yield decreased as the catalyst: microalgae ratio increased from 0.0: 1.0 to 2.0: 1.0, from 22 wt.% to 12 wt.%. The gas distributions exhibit an increasing trend from 26 wt.% to 33 wt.% when the catalyst: microalgae ratio increasing.
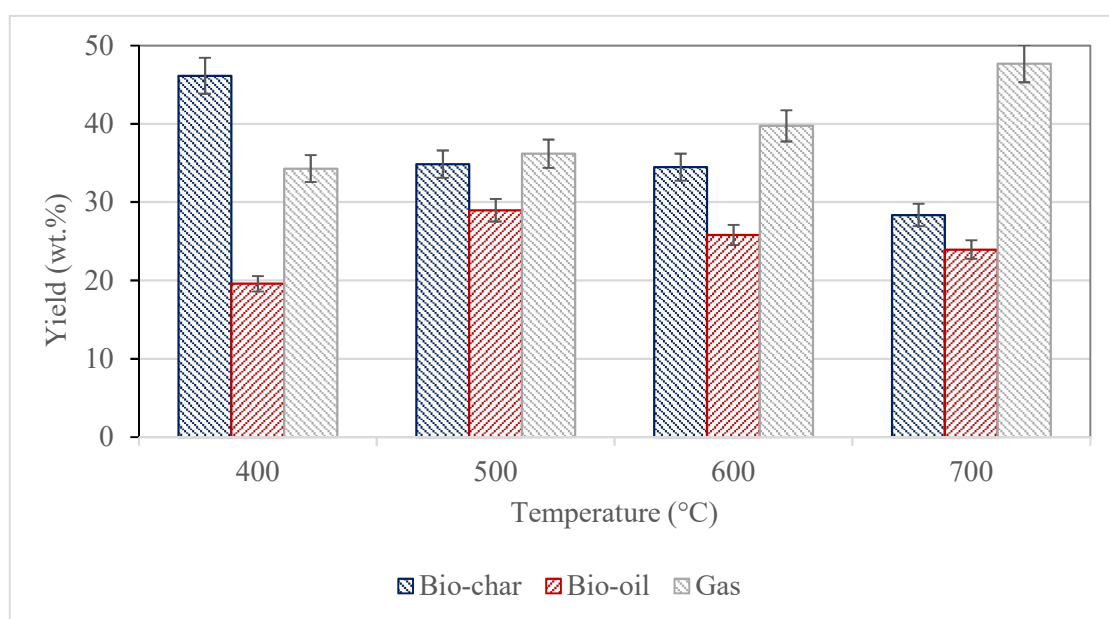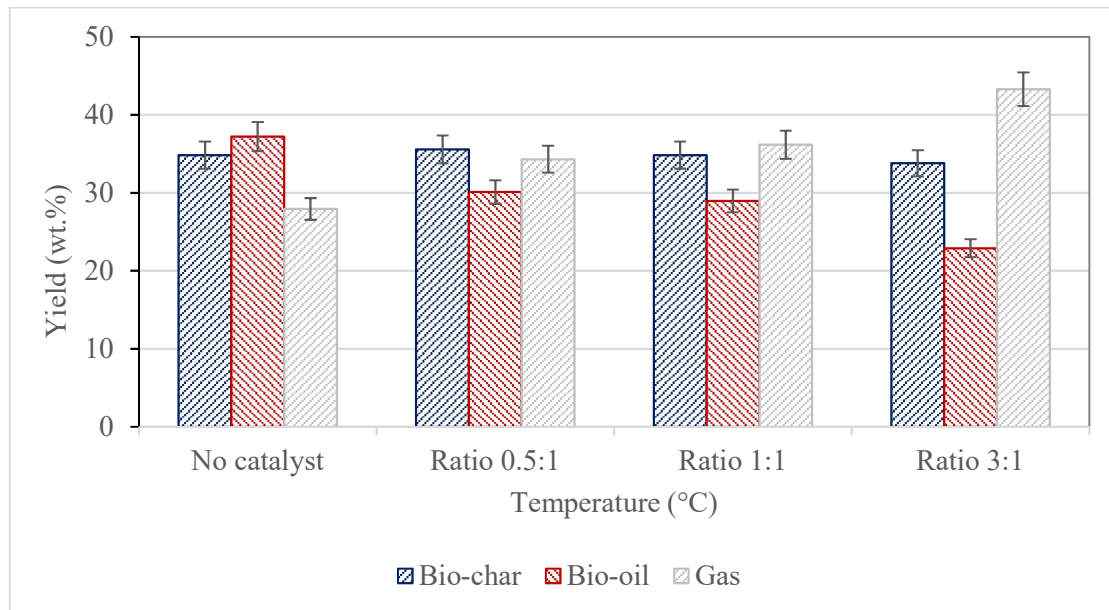
Figure 6-3 Product distribution from catalytic pyrolysis of *Isochrysis* sp. at different catalyst ratio.

6.3.2 *Elemental analyses*

A detailed elemental analysis of the bio-chars and bio-oils from the different catalyst: microalgae ratio is presented in Table 6-5, where the elemental composition and higher heating value of both products were given on a dry basis. Li-LSX-zeolite had a clear effect on the distribution of C, N, H and O in the solid and liquid products. The bio-chars were enriched in C and H with increased the presence of catalyst, while O content decreased denoting an increasing aromatisation degree.

In this study, N content of bio-oil reduced drastically from 3.89 wt.% to 0.79 wt.%, when the catalyst: microalgae ratio was increased from 0.5:1 to 3:1. This is in agreement with Gopakumar et al. (2012) where nitrogen content in the bio-oil was reduced when the catalyst load increase four times of biomass. The authors remarked that by increasing catalyst ratio N content can be reduced (Thangalazhy-Gopakumar *et al.*, 2012). The highest HHV of bio-oils (36.81 MJ/kg) was obtained with catalyst ratio 0.5:1, followed

by both ratios with HHV of 36.32 MJ/kg. However, the N content in the bio-oil represent hindrance for further implementation.

Table 6-5 Elemental analysis, H/C and O/C molar ratios and HHV of bio-chars and bio-oils obtained at different catalyst ratios.

	Catalyst: Microalgae ratio			
Elemental analysis	No catalyst	0.5:1	1:1	3:1
Bio-chars				
Carbon	45.41	47.41	52.00	64.60
Hydrogen	2.91	3.61	7.36	8.99
Nitrogen	3.41	4.36	4.72	4.56
Oxygen	48.24	44.62	35.91	21.86
H/C molar ratio	0.77	0.91	1.70	1.67
O/C molar ratio	0.80	0.71	0.52	0.25
HHV (MJ/kg)	14.25	16.13	23.04	30.81
Bio-oils				
Carbon	71.69	75.57	74.77	73.99
Hydrogen	10.01	9.84	9.86	10.23
Nitrogen	3.89	3.87	2.11	0.79
Oxygen	14.41	10.72	13.26	14.99
H/C molar ratio	1.68	1.56	1.58	1.66
O/C molar ratio	0.15	0.11	0.13	0.15

HHV (MJ/kg)	35.27	36.81	36.32	36.32

6.3.3 *Nitrogen distribution*

A detailed nitrogen distribution among the pyrolysis products is illustrated in Figure 6-4. About 27% of nitrogen remained in the bio-oil during non-catalytic pyrolysis. Meanwhile, in the presence of the Li-LSX-zeolite, only 3-22 wt.% of nitrogen was retained in the bio-oil, as most was released in the gas phase or retained in the bio-char. The use of 3 times as much catalyst than the microalgae was also effective in reducing the oxygen content in the bio-oil to ~11 wt.%.
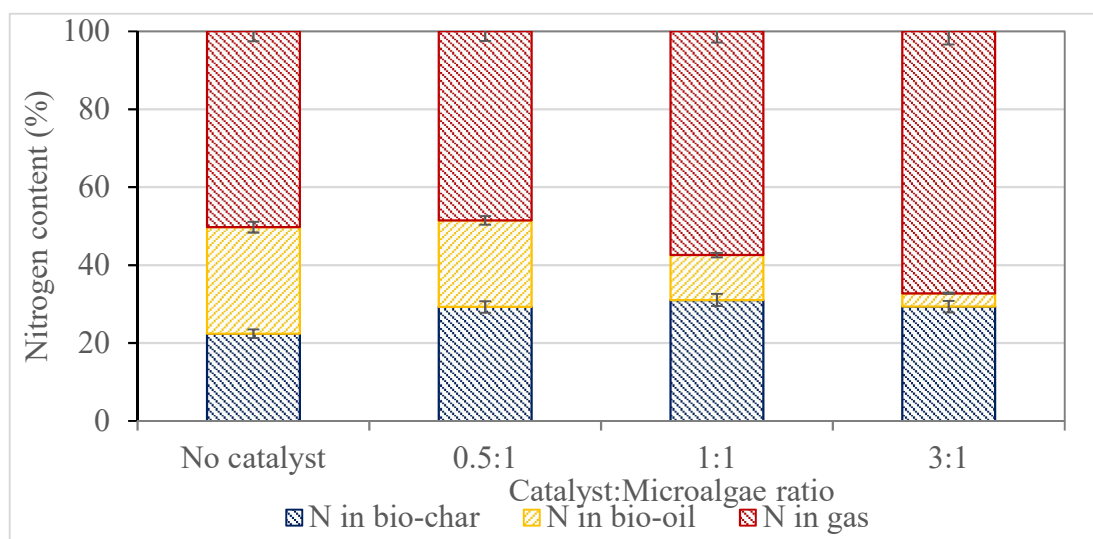
Figure 6-4 Nitrogen distribution in the products using different catalyst ratios.

6.3.4 *GC-MS*

The individual chemical compounds contained in the bio-oils from microalgae pyrolysis were identified by GC-MS and grouped based on their functionalities as shown in Table 6-6. It was estimated that only 44% of the bio-oil compounds can be detected by the GC-MS. Initially, the bio-oil contained about 45.5% oxygenated compounds and 17.1% nitrogen compounds. When the catalyst was added into the system with 3:1 ratio, the

oxygen and nitrogen compounds reduced to 10.6% and 3.8% respectively. This indicates that the bio-oil suffered a strong deoxygenation and denitrogenation while increasing the catalyst ratio, as confirmed by the EA analysis. Zeng et al. reported similar trend where the O and N compounds in bio-oil reduced as the catalyst: microalgae ratio increased (Zeng *et al.*, 2013). The O-compounds reduced from 58% to 20% when the catalyst: microalgae ratios increased, 0.5:1 to 2:1.

An opposite trend emerged with aromatic compounds, where their yield rose as the catalyst ratio increased to 3 to 1. Aromatic hydrocarbons were the abundance products (15.18%) along with aliphatic (14.51%), when the 3:1 ratio was used. Aromatic compounds such as benzene, toluene, naphthalene, indene was formed from the thermal and catalytic reaction of algae fatty acids, proteins and carbohydrates. Monoaromatics were formed by the diffusion of the cracked hydrocarbon pool into the catalyst pores where they underwent a series of dehydration, decarbonylation, decarboxylation, isomerisation, oligomerisation reactions. Larger aromatic compounds such as naphthalene, trimethyl naphthalene or dimethyl benzene were formed through secondary alkylation of smaller aromatics or likely formed on the catalyst surface (Jae *et al.*, 2011; Carlson *et al.*, 2009). Increasing the catalyst ratio resulted in a large fraction of polyaromatics compounds (PAH) such as phenanthrene, chamazulene, azulene.

Table 6-6 GC-MS bio-oil based on groups at different catalyst ratios.

Group families	c (rel.%)			
	Catalyst: microalgae (g/g)			
	No catalyst	0.5:1	1:1	3:1
Alcohol	12.35	5.36	2.93	1.1
Aldehydes	1.67	0.71	0.73	0.53
Aliphatic	26.49	22.34	23.13	15.18
Aromatics	2.89	7.85	11.84	14.51

Carboxylic acids	2.27	0.99	2.07	1.84
Esters	3.67	7.42	3.25	1.63
Ethers	0.84	2.56	1.31	2.2
Ketones	9.33	3.26	3.43	3.28
Nitrogen compounds	12.42	4.37	5.52	3.82

6.3.5 *Gas analyses*

Details on the gas product distributions are reported in Table 6-7. A high catalyst/biomass ratio enhanced the secondary cracking of the oil vapours and promoted the formation of hydrocarbon gaseous (Paasikallio *et al.*, 2017). During catalytic de-oxygenation of bio-oil vapours, the oxygen was released through different reaction: decarboxylation, decarbonylation and dehydration leading to the formation of CO_2, CO and H_2O. Increasing the catalyst concentration resulted in higher deoxygenation degree. The light olefins selectivity from catalytic pyrolysis showed a similar trend at different catalyst ratio ~26-33.6 wt.%. Meanwhile, alkanes compounds such as C_3H_8, C_2H_6, C_4H_{10}, C_5H_{12} increased when the catalyst ratio was increased from 0.5:1 to 3:1, suggesting that cracking activity to CO and CO_2 increases with higher catalyst concentration. A strong denitrogenation can be achieved at 1:1 catalyst ratio, where about 12.05 wt.% of NH_3 and HCN was released, compared to 1.57 wt.% released at catalyst: microalgae ratio of 0.5:1.

Pan et al. (2012) studied on catalytic pyrolysis of *Nannochloropsis* sp. varying catalyst: microalgae ratio using HZSM-5 at 400 °C (Pan *et al.*, 2010). As catalyst: microalgae ratio increased from 0.2:1 to 1:1, the amount of CO_2 in gaseous products increased from 18.3 wt.% to 20.40 wt.%. Meanwhile, H_2, CO and CH_4 distributions are fluctuating when the catalyst: microalgae ratio increased.

Table 6-7 Gas compositions at different catalyst ratio.

Gas compounds	C (wt.%)			
	Catalyst: microalgae (g/g)			
	No catalyst	0.5:1	1:1	3:1
H_2	0.11	1.42	0.91	1.38
CO	5.22	8.49	8.12	9.33
CO_2	1.26	0.93	0.87	0.97
CH_4	0.87	1.5	1.17	1.02
H_2O	12.93	22.9	19.74	20.22
HCN, NH_3	1.63	1.57	12.05	9.55
Olefins (C_2H_4, C_2H_3, C_3H_6, C_4H_8)	17.14	26.08	26.98	33.6
Alkanes (C_3H_8, C_2H_6, C_4H_{10}, C_5H_{12})	3.56	8.14	8.63	10.99

6.4 Effect of sweep gas flow rate

The sweep gas flow determines the reaction time during the pyrolysis process of microalgae. The higher the gas flow rates, the shorter the time for the decomposition reaction. Insufficient reaction time may lead to an incomplete conversion process, while excessive reaction time can result in decomposition of desirable products (Pütün, 2010; Sanchez-Silva et al., 2013; Campanella & Harold, 2012; Hu et al., 2013). The ideal process to produce biofuels and biochemicals from biomasses would be a single step reactor where solid biomass directly converted into bio-fuel at shorter residence times (Bridgwater, 2012; Cheng & Huber, 2012; Carlson et al., 2011).

6.4.1 *Pyrolysis yield and mass balance*

To study the effect of sweep gas flow rate on product yield, catalytic pyrolysis with different nitrogen gas flows; 1250, 345 and 210 ml/min were conducted, and the experimental results are summarised in Figure 6-5. Bio-oil yields in the absence of catalyst increased with the sweep gas flow rate up to 345 ml/min, from 35.2 wt.% to 37.2 wt.% and reduced when the sweep gas flow rate was 200 ml/min with 28.2 wt.% yield.

A different trend was obtained from the catalytic pyrolysis, where the bio-oil yields increased with increasing sweep gas flow rate, from 24.0 wt.% to 37.8 wt.%. The effect of sweep gas flow rate (or nitrogen flow rate) was studied by Z. Hu et al. on non-catalytic pyrolysis of blue-green algae blooms (BGAB) (Hu *et al.*, 2013). The results show bio-oil yield reached maximum yield (54.9 wt.%) at 100 mL/min and then declined to 37.9 wt.% when the gas flow rate was increased to 400 mL/min. In this work, a similar trend was observed with the highest bio-oil yield obtained at N_2 flow rate 210 ml/min, compared to the one obtained at 1250 ml/min.

Meanwhile, the bio-char yield increased from 31.4 wt.% to 45.8 wt.% with increasing sweep gas flow rate, regardless of the absence / presence of the catalyst. The slow sweep gas flow rate (200 ml/min) resulted in increased bio-char yield due to the secondary reactions such as oligomerisation and condensation of volatiles formed during the primary pyrolysis reactions. High gas yield obtained with high sweep gas flow rate (1250 ml/min) that swept the products more quickly from the hot zone, avoiding secondary reactions between the char and the gas species. From the results, it can be concluded that the optimum sweep gas flow rate for pyrolysis is 345 ml/min, where the highest bio-oil yield of 37 wt.% (without catalyst) and 28 wt.% (with catalyst).
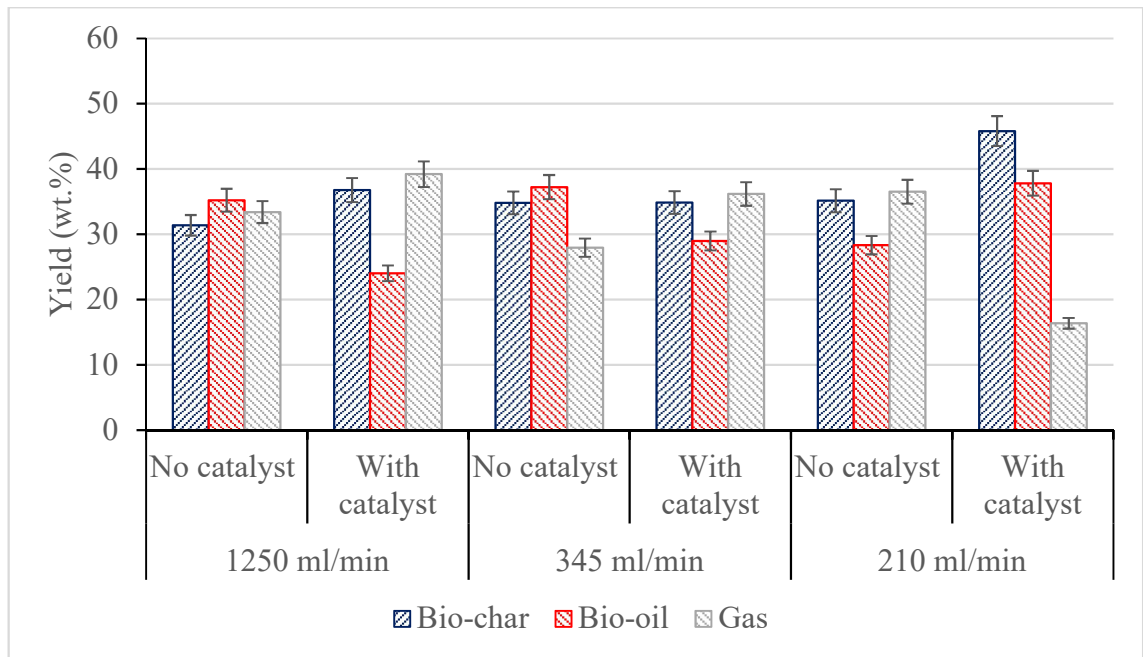
Figure 6-5 Effects of the sweep gas flow rates on product yields from catalytic pyrolysis of *Isochrysis* sp.

6.4.2 *Elemental analyses*

Table 6-8 shows the elemental analyses from the different of sweep gas flow rate as well as H/C, O/C ratios and HHV of bio-char and bio-oils obtained with and without the catalyst. From the figure, the C and H content of the bio-char in the presence of the catalyst is higher than the non-catalytic ones, with the fast sweep gas flow rate (1250 ml/min) presenting the highest C and H content (53.9% and 7.7%). This also suggests coking reactions taking place on the surface of the catalyst. Similarly, the C content of the bio-oil obtained using Li-LSX-zeolite, was the highest with flow rate of 1250 and 345 ml/min contained ~74.7 wt.% C, while N content was the lowest with ~2.1 wt.%. The presence of catalyst enhanced the bio-oil quality by reducing the N and O content in the bio-oils and increased its C content and HHV.

Table 6-8 Elemental analysis, H/C and O/C molar ratios and HHV of bio-chars and bio-oils obtained at different sweep gas flow rate.

Sweep gas flow rate	1250 ml/min		345 ml/min		210 ml/min	
Elemental analysis	No catalyst	With catalyst	No catalyst	With catalyst	No catalyst	With catalyst
Bio-chars						
Carbon	46.89	53.85	45.41	52.00	44.10	48.76
Hydrogen	1.71	7.70	2.91	7.36	1.79	6.35
Nitrogen	3.31	4.84	3.41	4.72	3.50	3.86
Oxygen	48.09	33.62	48.24	35.91	50.61	41.03
H/C molar ratio	0.44	1.72	0.77	1.70	0.49	1.56
O/C molar ratio	0.77	0.47	0.80	0.52	0.86	0.63
HHV (MJ/kg)	12.12	23.97	14.25	23.04	10.95	19.68
Bio-oils						
Carbon	70.57	74.46	71.69	74.77	66.82	70.96
Hydrogen	10.10	9.25	10.01	9.86	8.49	8.14

Nitrogen	4.28	2.16	3.89	2.11	3.75	2.53
Oxygen	15.05	14.13	14.41	13.26	20.94	18.37
H/C molar ratio	1.63	1.49	1.68	1.58	1.52	1.38
O/C molar ratio	0.11	0.14	0.15	0.13	0.25	0.20
HHV (MJ/kg)	35.15	35.72	35.27	36.32	31.10	32.51

6.4.3 *Nitrogen distribution*

The nitrogen distribution of the different sweep gas flow rate with and without catalyst in the products yield is illustrated in Figure 6-6. As already mentioned, the N content in the products comes from the large protein content in the *Isochrysis* sp. microalgae. The largest fraction of nitrogen was found in the gas phase, especially in the presence of Li-LSX-zeolite where, only 9.8 to 11.4% of nitrogen was retained in the bio-oils, while it raised to 20.1 to 28.4 % N in non-catalytic reaction. This clearly indicates that the Li-LSX-zeolite is effective in denitrogenating the bio-oils by removing most of the N content into gaseous phase, in particular at the slow sweep gas flowrate.
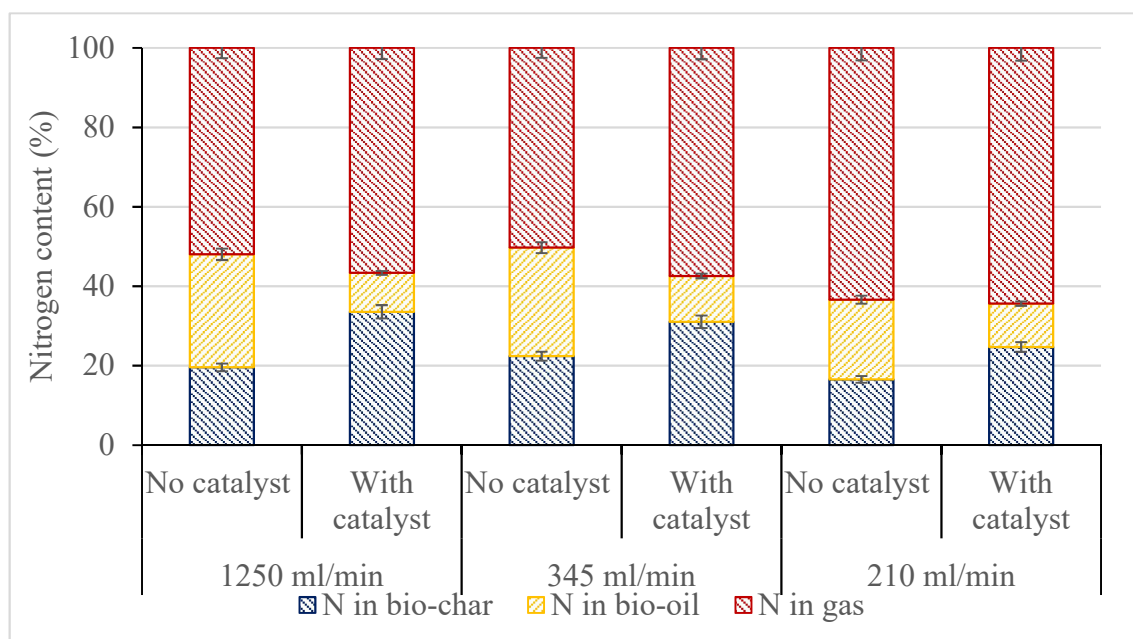
Figure 6-6 Nitrogen distribution in the products at different sweep gas flow rate.

6.4.4 *GC-MS*

The compounds identified in the bio-oils obtained at different sweep gas flow rate were divided into different groups. Table 6-9 shows the total relative abundance in percentage

of the four groups present in the bio-oil. The description of the different compounds grouped by their functionalities can be seen in Table3-1. The most abundant compounds among all conditions observed were the aliphatic compounds. The aliphatic compounds, which were derived from the deoxygenation of the microalgae fatty acids mainly contained dodecane, hexadecane, and 5-eicosene. Aliphatic fraction in the presence of Li-LSX-zeolite catalyst were lower compared to the non-catalytic ones. The catalyst cracked the aliphatic compounds, mostly long-chained hydrocarbons, forming gas species such as olefins and CO, CO_2 and aromatic compounds. A clear increase in aromatic compounds can in fact be observed in the presence of catalyst. The aromatic compounds mainly consisted of phenols, alkylated benzenes and polyaromatics such as p-xylene, 2-methyl naphthalene, and p-Cresol. The highest aromatic compounds were produced at the slowest gas flow rate of 210 ml/min (13.3 %), as compared to 345 ml/min (11.84%) and 1250 ml/min (10.05%). Polyaromatic compounds like indene, naphthalene and phenanthrene were increased in content at high flow rate (1250 ml/min), whereas benzene and phenols were identified with high concentration at slow sweep gas, 210 ml/min. This can be due to the compounds having enough time for secondary reactions where cracking and aromatisation/condensation reactions took place forming PAH compounds.

Other products were mainly oxygenated and nitrogenated compounds such as 9-Octadecenal, 2-Nonadecanone, phytol, pyrrole, indole and Olea nitrile. A great deoxygenation and denitrogenation power can be observed in the presence of Li-LSX-zeolite, where both chemical classes reduced about half than the non-catalytic reactions. The presence of catalyst improved the bio-oil compositions by reducing oxygen and nitrogen content. The results of GC-MS analysis showed that there were significant differences between different gas flow rate in chemical component. Slow flow rate (210 ml/min) produced high aromatic compounds and reduced oxygenated and nitrogenated compounds. These data are in agreement with the product distribution reported in Figure 6-7, where it can be observed that the bio-oil yield with Li-LSX zeolite increases at 1250 ml/min, mainly by formation of aromatics and in particular PAH. Also, the dramatic increase in secondary reactions and condensation reactions led to formation of large

156

condensation products in the biochar/coke at the expenses of all the other functionalities (such as oxygenate and nitrogenates).

Table 6-9 GC-MS bio-oil based on groups at different sweep gas flow rate.

Group families	c (rel.%)					
	Sweep gas flow rate					
	1250 ml/min		345 ml/min		210 ml/min	
	No catalyst	With catalyst	No catalyst	With catalyst	No catalyst	With catalyst
Alcohol	14.34	2.93	12.35	2.93	13.79	3.32
Aldehydes	1.49	0.65	1.67	0.73	0.88	0.50
Aliphatic	32.3	32.6	26.49	23.13	33.14	29.88
Aromatics	2.31	10.05	2.89	11.84	2.9	13.32
Carboxylic acids	3.09	3.01	2.27	2.07	2.56	1.37
Esters	4.86	3.57	3.67	3.25	4.98	3.70
Ethers	1.08	1.32	0.84	1.31	1.72	1.00
Ketones	17.74	2.96	9.33	3.43	19.52	4.02
Nitrogen compounds	15.79	10.91	12.42	5.52	11.51	6.41

6.5 In-situ vs Ex-situ catalytic pyrolysis

Depending upon the method of contacting catalysis and pyrolysis vapours, the process is classified as either in-situ or ex-situ catalytic pyrolysis. For the former, the catalyst is

mixed with the biomass to be pyrolysed where the Li-LSX-zeolite was mixed directly with the catalyst at the ratio of 1:1. For ex-situ catalytic pyrolysis, the biomass samples and catalyst were separated with quartz wool between them, to avoid mixing. The samples were placed on top of the catalyst during the pyrolysis. A detailed description of the ex-situ pyrolysis scheme can be found in Figure 3-13.

6.5.1 *Pyrolysis yield and mass balance*

To compare in-situ and ex-situ catalytic pyrolysis, both configurations were performed in the same reactor system, at 500 °C with catalyst: microalgae ratio of 1:1. Product distributions for both configurations are illustrated in Figure 6-7. In-situ catalytic pyrolysis produced slightly more bio-oils than the ex-situ, 28.9 wt.% compared to 26.7 wt.%. In comparison, ex-situ catalytic pyrolysis promoted the formation of gaseous products, 39.6 wt.% vs 36.2 wt.%. The main difference between the two configurations is the enlarged gas yield when the microalgae and catalyst are not in direct contact. Ex-situ pyrolysis seems to be more effective in cracking the vapours/aerosols formed during the primary pyrolysis reactions into smaller MW species. One explanation can be related to the formation of char in proximity of the Li-LSX-zeolite pores openings in the in-situ mode, which obstacles/slow down the diffusion in and out of the gas species resulting in slow gas flow rate and condensation reactions, rather than cracking to smaller MW species. This is supported by the contradict results of char yield and increase in gas yield when an ex-situ configuration is used. Additional information about the formation of solid carbonaceous deposits, or known as coke, are discussed in the next chapter.
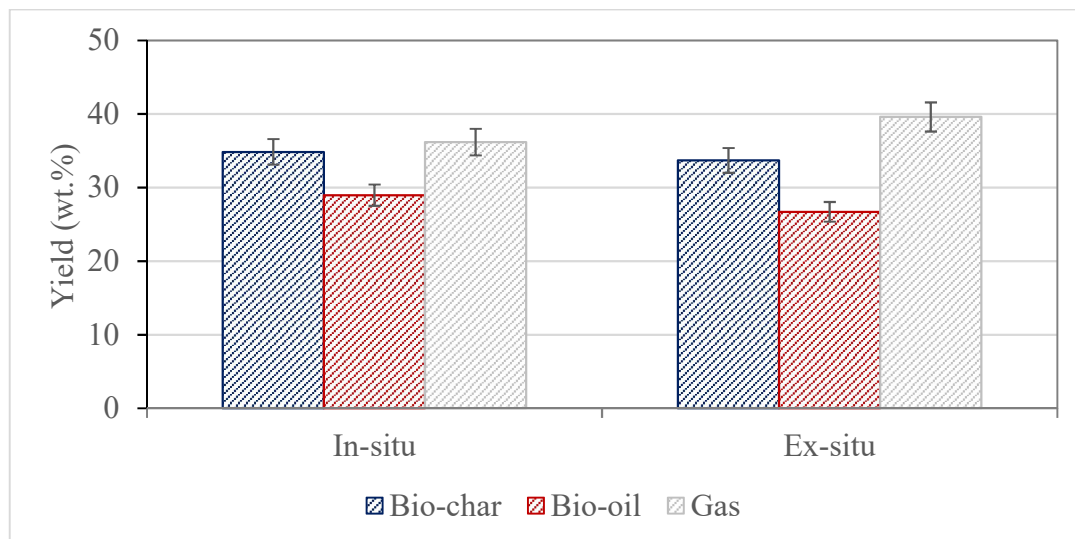
Figure 6-7 Comparison of in-situ vs ex-situ on product yields from catalytic pyrolysis of *Isochrysis*.

6.5.2   *Elemental analyses*

The elemental analyses of the bio-chars and bio-oils obtained by in-situ and ex-situ pyrolysis are reported in Table 6-7. Overall, the two configurations did not show major differences in terms of elemental distribution. The only significant difference can be attributed to the enhanced H content in the bio-char after the ex-situ pyrolysis (10 wt.% vs7.4 wt.%). Other than that, the bio-oils have very similar C, H, N and O contents. Therefore, these results suggest that different pyrolysis configuration does not change the EA of the pyrolysis products.

Table 6-10 Elemental analysis, H/C and O/C molar ratios and HHV of bio-chars and bio-oils obtained at different reactor configuration.

Elemental analysis	In-situ	Ex-situ	In-situ	Ex-situ
	Bio-chars		Bio-oils	
Carbon	52.00	53.69	74.77	74.20
Hydrogen	7.36	10.03	9.86	10.10
Nitrogen	2.72	2.75	2.11	2.89
Oxygen	37.91	33.53	13.26	12.81
H/C molar ratio	1.70	2.24	1.58	1.63
O/C molar ratio	0.52	0.47	0.13	0.13
HHV (MJ/kg)	22.63	27.26	36.74	36.83

6.5.3 *Nitrogen distribution*

Nitrogen distribution on the product compositions is shown in Figure 6-9. For ex-situ arrangement, most of N was released as gaseous products (68%). Meanwhile, for in-situ setup, 57.4% of N goes to gas phase. This data is in agreement to those reported in Figure 6-7, which shows that ex-situ pyrolysis increases the gas yield.
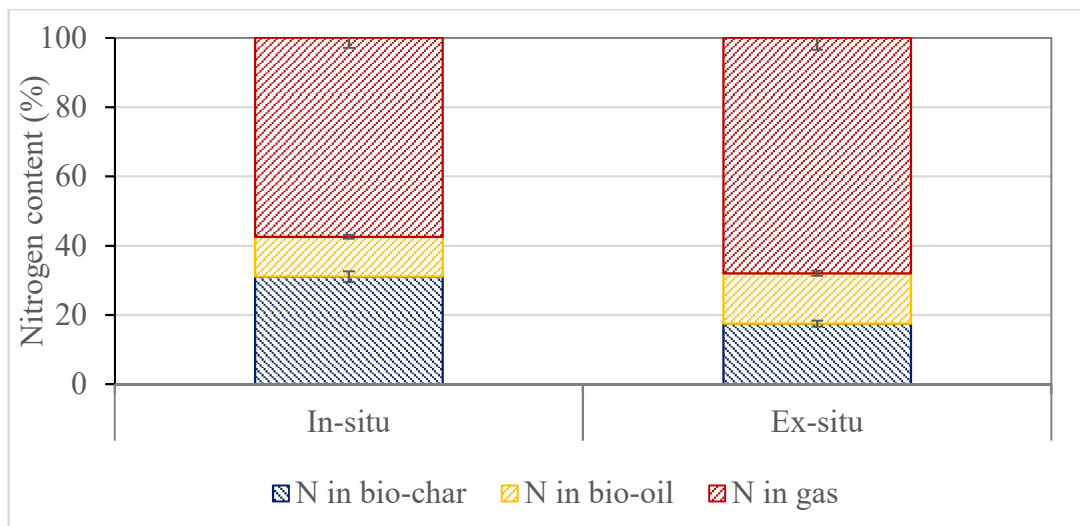
Figure 6-8 Nitrogen distribution using different setup of catalytic pyrolysis.

6.5.4 *GC-MS*

The products distributions from the in-situ and ex-situ configurations are summarised in Table 6-11. In-situ catalytic pyrolysis generated remarkably more aromatic hydrocarbons than did ex-situ catalytic pyrolysis. At 500 °C, carbon yield of aromatics for in-situ was 11.84% compared to only 10.3% for ex-situ catalytic pyrolysis. However, the aliphatic yield from both configurations were similar ~ 23%. A recent study by Carlson et al. (Carlson, 2010) on the conversion of furan over HZSM-5 showed that a higher yield of aromatics was obtained for in-situ catalysis using with a pyro probe set-up compared to ex-situ pyrolysis in a fixed bed reactor. Other than that, there were no differences between these two set-ups in terms of nitrogenated compounds and carboxylic acids distribution.

The differences in yields of aliphatic and aromatics for in-situ and ex-situ can be assigned to the differences in the gas flow, between these two set-ups. For in-situ catalytic pyrolysis, the microalgae were directly mixed with the catalyst. Thus, the catalyst was exposed to a concentrated pyrolysis vapour. In comparison, with ex-situ, the pyrolysis vapours were mixed with the sweep gas before contacting with the catalyst. Therefore, in the latter configuration, the vapours were diluted and had a shorter contact time with the

catalyst, compared to the in-situ catalytic pyrolysis. As a result, the vapours in in-situ reaction had longer reaction time and provide more opportunity for the small olefins formed by cracking, to oligomerise forming larger aromatic compounds in the catalyst pores Bronsted and Lewis acid sites, while small molecular weight aliphatic compounds were not re-arranged in PAH in ex-situ configuration. This resulted in the ex-situ catalytic pyrolysis to produce more monoaromatics such as benzene and relatively small PAH such as naphthalene, compared to the in-situ catalytic pyrolysis, where most of the aromatics produced were polyaromatic compounds such as chamazulenes, phenanthrenes, and anthracenes.

Table 6-11 GC-MS bio-oil based on groups at different reactor setups.

Group families	c (rel.%)	
	Reactor setup	
	In-situ	Ex-situ
Alcohol	2.93	3.21
Aldehydes	0.73	0.43
Aliphatic	23.13	23.01
Aromatics	11.84	10.33
Carboxylic acids	2.07	2.53
Esters	3.25	3.69
Ethers	1.31	1
Ketones	3.43	2.66
Nitrogen compounds	5.52	6.14

6.5.5 *Gas analyses*

Table 6-12 reports the gas products distribution when using the two different reactor set-ups. Different trends can be observed from both set-ups. In terms of deoxygenation, ex-situ pyrolysis promoted the production of CO_2, CO, olefins and alkanes, which is about 33.2% higher than in-situ (28.3%). These results tally with the product distribution (Figure 6-7) where ex-situ configuration tends to produce more gaseous compared to the in-situ.

Table 6-12 Gas compositions using different reactor setups.

Gas compounds	C (wt.%)	
	Reactor configurations	
	In-situ	Ex-situ
H_2	1.39	0.97
CO	8.12	15.81
CO_2	0.87	5.59
CH_4	1.17	1.6
H_2O	19.26	11.84
HCN, NH_3	4.97	3.86
Olefins (C_2H_4, C_2H_3, C_3H_6, C_4H_8)	26.98	33.43
Alkanes (C_3H_8, C_2H_6, C_4H_{10}, C_5H_{12})	8.63	13.6

6.6   Summary

The effect of pyrolysis temperature, catalyst loading, sweep gas flow rate and reactor configuration on microalgae *Isochrysis* were investigated. The results indicated that pyrolysis temperature had effect on the catalytic pyrolysis, where the product distribution depended on the temperature. High temperature led to gaseous formation, while low temperature produced high bio-char. Moderate temperature (500-600 °C) produced the highest bio-oil yield. Catalyst to biomass ratio of 0.5:1 produced high bio-oil yield than ratio 1:1, 34.3 wt.% compared to 28.9 wt.%. High catalyst ratio produced more gas due to the high amount of catalyst presence during the reaction. However, optimum aliphatic and aromatics produced in bio-oil can be achieved with catalyst: biomass ratio of 1:1.

Sweep gas flow rate affected the product distributions as well, where the maximum bio-oil yield was obtained at slow gas flow rate, 210 ml/min. Despite that, the bio-oil obtained at 1250 ml/min sweep gas flow rate had low HHV compared to the 345 ml/min, 32.5 MJ/Kg compared to 36.7 MJ/kg, proving that gas flow rate at 345 ml/min are the optimum flowrate. At slow flow rate (210 ml/min), mainly aromatics and in particular PAH were formed due to the increase in condensation reactions at the expenses of all the other functionalities (for example; oxygenate and nitrogenates).

Further, different pyrolysis configurations were evaluated, to compare the effectiveness of pyrolysis reaction of microalgae when in contact or separated from the catalyst. A marginal higher yield of bio-oil was obtained through in-situ pyrolysis (28.7 wt.%) compared to the ex-situ pyrolysis (26.7 wt.%). However, ex-situ pyrolysis was more effective in cracking the vapours/aerosols formed during the primary pyrolysis reactions into smaller MW species, which resulted in decreased char yield at the expenses of formation of monoaromatics, alkanes, olefins and CO_2. Instead, in-situ pyrolysis formed a large amount of PAH and other condensed products.

Overall, the outcomes in this Chapter indicate that the optimum condition for pyrolysing *Isochrysis* sp. microalgae using Li-LSX-zeolite include temperatures close to 500 °C, sweep gas flow rate of 345 ml/min and a biomass catalyst ratio of 1:1. The use of an ex-situ configuration resulted more effective in reducing the molecule weight of the volatile matter and increase the content of monoaromatics and short chain aliphatic compounds. However, the experiments highlight that the yield of the microalgae derived bio-oil are lower when compared to lignocellulosic bio-oils. This can be related to the high alkali metals content in the microalgae, which act as catalyst in the pyrolysis reactions. Therefore, the removal of alkali metals by specific pre-treatment can be beneficial in enhancing the bio-oil yield and potentially reducing the deactivation of the catalysts when cyclically used. Next chapter will discuss on the effect of chemical pre-treatment on microalgae demineralisation.

Chapter 7

Effect of chemical pre-treatment on pyrolytic bio-oil from microalgae

7.1 Introduction

Microalgae contain significant levels of macro-minerals (Na, K, Ca, P) and trace elements (Al, Cu, Fe and Mn) compared to non-marine biomasses such as wood, straws, *miscanthus* and willow coppice (Chen *et al.*, 2014; Bi & He, 2013; Ross *et al.*, 2008). It is well established that alkali and alkaline metals in biomass affect the mechanism of pyrolysis and decrease the pyrolysis oil yield by catalysing gasification reactions (Fahmi *et al.*, 2008; Ross *et al.*, 2008). Moreover, ash content affects the pyrolysis process design and operations (causing fouling, slagging and corrosion in the reactors), as well as the product purification process. As a result, the removal of inorganics from microalgae would benefit their intrinsic quality and reduces operating issues.

Microalgae can be treated in three different ways: physical, biological and chemical (Chen *et al.*, 2014; Ross *et al.*, 2008; Harun & Danquah, 2011; Du *et al.*, 2012). The chemical pathway involves the use of either mild solutions of acids (hydrochloric acid and sulphuric acid) or bases (lime and sodium hydroxide), which present minimal toxicity in the applied mild concentrations (Harun & Danquah, 2011). For example, acid treatment is typical in fermentation processes to disrupt cell walls and to release the entrapped carbohydrates in the microalgae. Other than that, chemical treatment with mild acid has been proposed as a method to reduce the amount of inorganics in microalgae (Choi *et al.*, 2014).

This chapter investigates the influence of the chemical pre-treatment on catalytic pyrolysis products. Microalgae *Isochrysis* sp. was chemically treated with three different chemicals; Acid, Base and deionised water. After pre-treatment, the samples were characterised by XRF, ICP-MS, EA and FT-IR to assess the demineralisation effect.

Then, fast pyrolysis experiments were performed with untreated and pre-treated *Isochrysis* sp in the presence of Li-LSX-zeolites. The pyrolysis test was carried out using horizontal reactor as explained in section 3.5.1. The pyrolysis products underwent several analyses for characterisation such as EA, GC-MS, FTIR and NMR.

This chapter explores the effects of the chemical treatments on the ash content as well as on improving the thermal decomposition of wet biomass and the recovery of valuable compounds in the liquid product. Besides, this chapter compares the pyrolysis results obtained from untreated and pre-treated microalgae, in terms of pyrolysis products yields and chemical distribution on bio-oil.

7.2 Characterisation of treated microalgae

Microalgae *Isochrysis* sp. underwent different chemicals pre-treatment to analyse the effect of pre-treatment on fast pyrolysis. After washing, the treated samples were dried in the oven at 60 °C for 24h, and then stored in airtight bags for further analyses. The identification of each sample and actions performed are listed in Table 7-1.

Table 7-1 Identification on each pre-treated sample.

		Action performed	
No.	Sample identification	Leaching agent	Concentration (%)
1	R	Raw *Isochrysis* sp.	
2	A01		0.4
3	A1	Acid (H_2SO_4)	1
4	A4		4
5	B01	Base (NaOH)	0.4

6	B1		1
7	B4		4
8	W	Water	W

7.2.1 *ICP-OES analysis of wastewater*

After the pre-treatment with the different chemicals, the wastewater obtained was sent for ICP-OES analyses for determine metals. The concentration of the alkali and alkaline metals in the wastewater left after the algae pre-treatment is shown in Table 7-2. Typically, Na, K, Ca and Mg are present in microalgae as salts of alginic acids (anionic polysaccharides) (Bi & He, 2013; Ross *et al.*, 2009). Also, these metals exist partly as salts (for example; oxide, carbonate, oxalate and chloride) ionically bound to the membrane cells. For example, magnesium (Mg) is bound as the central atom in chlorophyll and enables plants to convert light into energy. Meanwhile, potassium (K) is required by microalgae for growth and reproduction, as well as helping the photosynthesis process (Ross *et al.*, 2008).

Initially, the non-treated microalgae (R) contained high amount of alkali metals, as listed in Table 7-2. The various pre-treatment processes removed a significantly different proportion of the alkali metals from the microalgae. In the presence of H_2SO_4, the increase in alkali metal concentration in the wastewater was due to exchanging metal cations with protons from sulphuric acid and formation of inorganic salt species. Overall, the pre-treatment efficiency in removing the alkali metals followed the order: H_2SO_4 > water > NaOH. The highest sulphuric acid concentration (4%), A4 leached the highest fraction of K, Na, Mg and Ca, respectively. On the contrary, the base (B) treatment was not able to leach out Mg, K and Na or the leaching products (hydroxides) precipitated out from the solution and could not be detected in the treated solutions. Previous work showed that acid and water treatment removed polysaccharides such as fucoidan and mannitol from the microalgae structure (Ross *et al.*, 2009). In this work, the acid treatment resulted the most effective in decreasing inorganic content in *Isochrysis* sp.

168

Table 7-2 ICP analysis of wastewater after chemical pre-treatment.

	Concentration (ppm)							
Elements	R	A01	A1	A4	B01	B1	B4	W
Ca	607	2	9	47	0	0	13	4
Mg	745	45	48	74	0	3	2	24
K	2565	323	310	418	26	19	6	148
Na	19500	6374	6778	9151	0	1140	1160	4640

7.2.2 *XRF analysis of the acid treated microalgae.*

XRF analysis of the raw microalgae and of those treated with 1% and 4% H_2SO_4 are reported in Table 7-3. As can be seen, the XRF results confirm those obtained by ICP-MS (waste-water after pre-treatment) indicating that about 76 wt.% of Na and about 16 wt.% of K were removed using 4% H_2SO_4. The removal % showed by the XRF resulted higher than those shown by ICP-MS (50% for Na), which may be related to a non-complete dissolution of the oxide species in the waste-water previous ICP-MS tests. XRF confirms that the acid pre-treatment is very effective in removing Na and P and in minor extent K, but at the same time other species are increased in % (Ca, S), most likely due to the combination of leached species (Cs) with S and the re-precipitation of $CaSO_4$.

Table 7-3 XRF analysis of microalgae after chemical pre-treatment.

Samples	Weight (Wt.%)							
	Na	Si	P	S	K	Ca	Fe	Zn
R	8.944	0.026	1.055	0.485	0.672	0.384	0.045	0.005
A1	3.702	0.036	0.323	1.239	0.411	0.576	0.029	0.138
A4	2.162	0.087	0.389	7.458	0.456	0.455	0.031	0.0075

7.2.3 *FT-IR spectroscopy*

The chemical functionalities evaluation of biomass is frequently studied using near infrared spectroscopy. In this study, FTIR technique was used to investigate the impacts of chemical pre-treatment on biomass chemical composition. Figure 7-1 shows the various FT-IR spectra of between different chemical pre-treatment and untreated samples, H_2SO_4 and NaOH treated biomass samples. The pre-treatment decreases the polymerisation degree of carbohydrates and can solubilise certain proteins. These chemical structure changes were detected by FTIR. The intensity of some functional groups was decreased with the acid and water pre-treatment. The broad band at 3500-3200 cm^{-1} can be assigned to the O-H stretching vibrations of hydroxyl functional groups of alcohols after pre-treatment, the stretching decreased compared to the raw materials (R). The bands between 3100 and 3010 cm^{-1} and between 2950 and 2850 cm^{-1} are attributed to C-H stretching vibration of alkenes and alkanes, respectively. A change in both bands can be observed with an increased transmittance following the order: A4 > W > B4. The peak at 1730 cm^{-1} corresponds to C=O stretching vibration of free carbonyl group associable to ketones (1750-1680 cm^{-1}), aldehydes (1740-1690 cm^{-1}) and carboxylic acids (1780-1710 cm^{-1}). The next peaks from 1700 to1500 cm^{-1} can be associated to C=C bending vibrations of aromatics. As shown in Figure 7-1 (A), while aromatic band (e) increased in both A4 and B4 pre-treatments, the transmittance peak

associated to esters (d) increases after the treatment with 4% H_2SO_4 (A4). Transmittance bands at the frequency range of 1200-1100 cm^{-1} and 988.4 cm^{-1} are assigned to asymmetric SO_4 stretching (g) and symmetric stretching of SO_4 groups (h), respectively. Clearly, the Figures suggest that sulphates are present in the A4 and B4 cases, suggesting precipitation of metal sulphates during the pre-treatment.
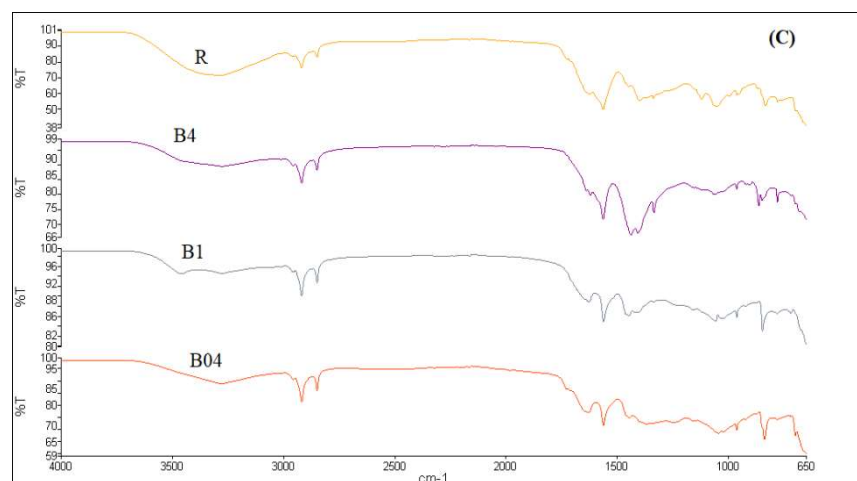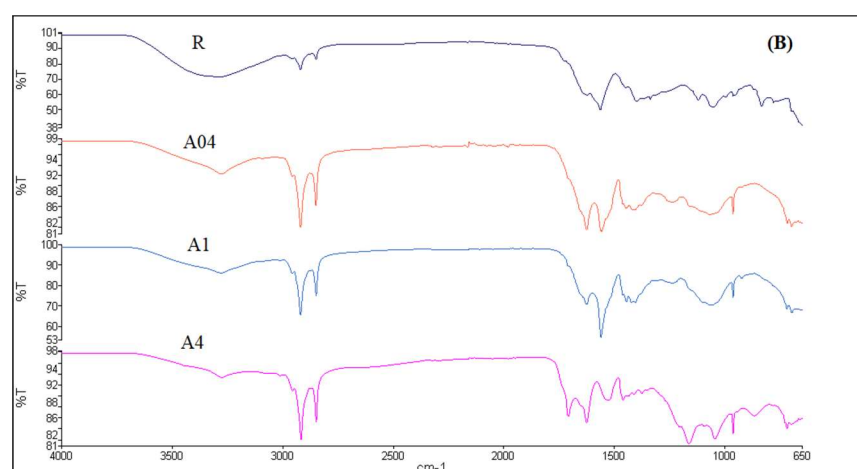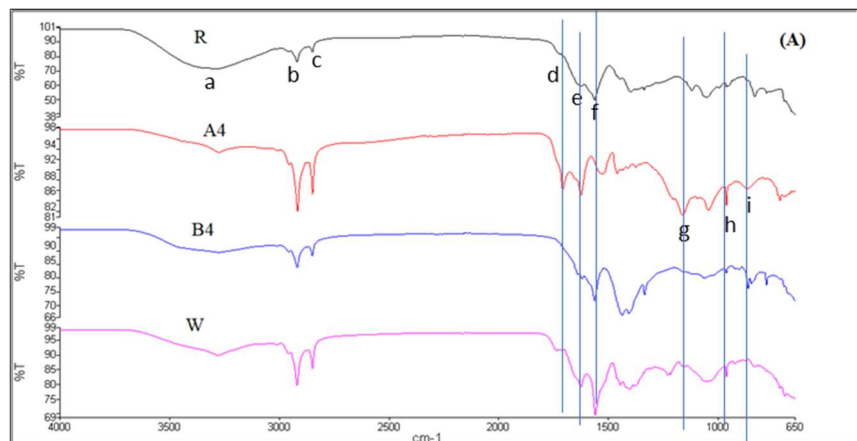
Figure 7-1 FTIR spectra (A) Raw and pre-treated samples (B) Raw and H2SO4 treated samples (C) Raw and NaOH treated samples. a-alcohol, b- alkene, c- alkane, d- ester, e- aromatic, f- alkene.

7.2.4 *Thermogravimetric analyses*

Thermogravimetric analysis was carried out to find the effect of the different chemical treatments on the volatilisation of *Isochrysis* microalgae. Figure 7-2 shows the TGA profiles of the raw and treated microalgae. Three stages in all the curves can be observed. The first stage, between 25 to 105 °C, was assigned to water evapouration. The second stage, between 110 to 550 °C, was attributed to decomposition of organic material (VM) and the final stage (temperature above 550 °C), shows the solid residue decomposition. According to Figure 7-2, it was found that the strong acid treatment (A4), reduced the solid residue (from 24% to 14%) and increased the volatile matter (71.7 wt.%) more than the treatment with water, W (63.7 wt.%). Meanwhile, base treatment (B) was not able to increase the volatiles (45.3%) compared to the non-treated microalgae (48.8%), suggesting precipitation of metal salts during the pre-treatment.
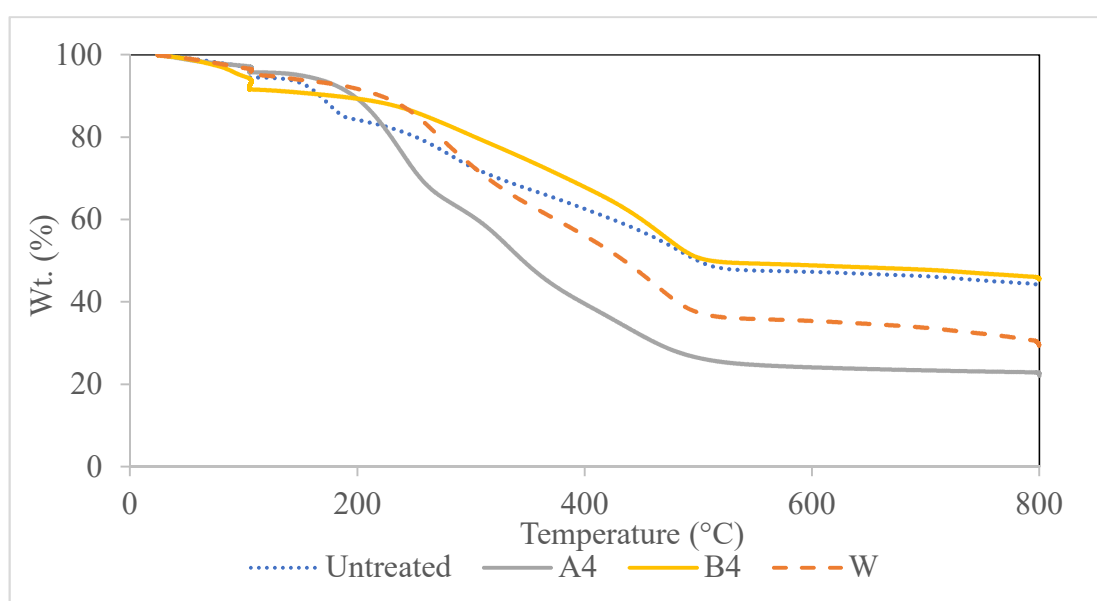
Figure 7-2 Mass loss (TG) curves of treated and untreated samples.

Figure 7-3 shows the DTG of the raw and treated *Isochrysis*. Significant differences in the DTG trends were shown by the different treatments. DTG profiles suggest a higher decomposition rate for all the treated microalgae compared to the non-treated ones. In the

173

presence of both H$_2$SO$_4$ acid (4%) and NaOH (4%), there was the disappearance of the peak between 180 and 210 °C, which is associated to devolatilisation of low molecular weight compounds, possibly branches of amino acids. The decomposition rate of the peaks associated to proteins (250-400°C) and fatty acids (430-490°C) was increased from 0.18 and 0.17 %/°C (non-treated algae) to 0.26 and 0.22 %/°C by acid treatment. This can be associated to the "softening" of the microalgae cell structure, where AAEM, that acts as catalyst during pyrolysis, have been removed through acid treatment. Meanwhile, there were no significant changes in the pyrolysis rate in the presence of B4 as shown in Figure 7-1. Moreover, the decomposition in the presence of 4% acid treated microalgae shifted the decomposition peaks at lower temperatures.
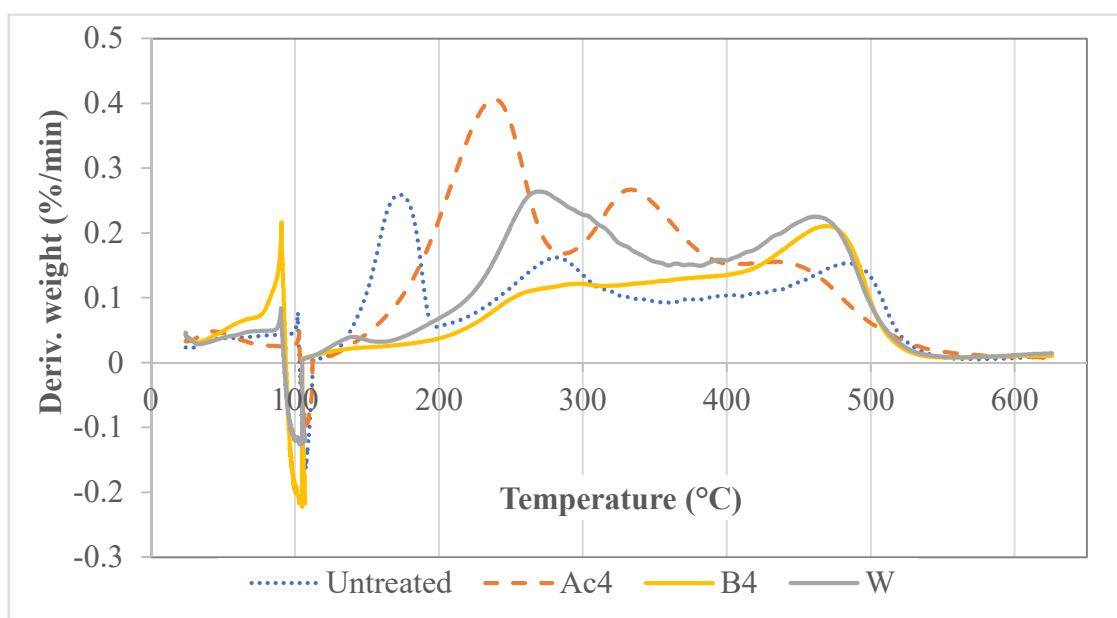
Figure 7-3 DTG pyrolysis of treated and untreated Isochrysis sp. with Li-LSX-zeolites at 500 °C.

7.2.5 *Ash percentage*

The ash contents of the treated microalgae are shown in Figure 7-3. The ash content decreased drastically from 20.8 wt.% (untreated algae) to 8-11 wt.% after acid treatment.

The lowest ash content (8.2 wt.%) was obtained by treating the microalgae with strong acid, A4. Strong acid hydrolysed the carbohydrates as well as other compounds, namely proteins and lipids. On the other hand, ash content increased to 25.6 wt.% when the microalgae were treated with 4% NaOH (B4) solution. The B01 and B1 were able to reduce the ash content to 14.4-17 wt.%. In the meantime, washing the microalgae with water (W) able to reduce the ash content to 10.5 wt.%, that is beneficial for the pyrolysis conversion as well as being cost effective. Hyung et al. (2014) reported that the treatment of *S. Japonica* with 98 wt.% bioethanol solution by reflux reduced ash from 22.9% to 17.9%, while ash content decreased to 1.5% after acid treatment with 5 wt.% H_2SO_4 solutions at 100 °C for 500 min (Hyung, Chul & Jin, 2014). The findings imply that the strength of the acid has an increased effect on deashing the microalgae, while the base strength had an inverse trend, with the most effective being the less concentrated solution.
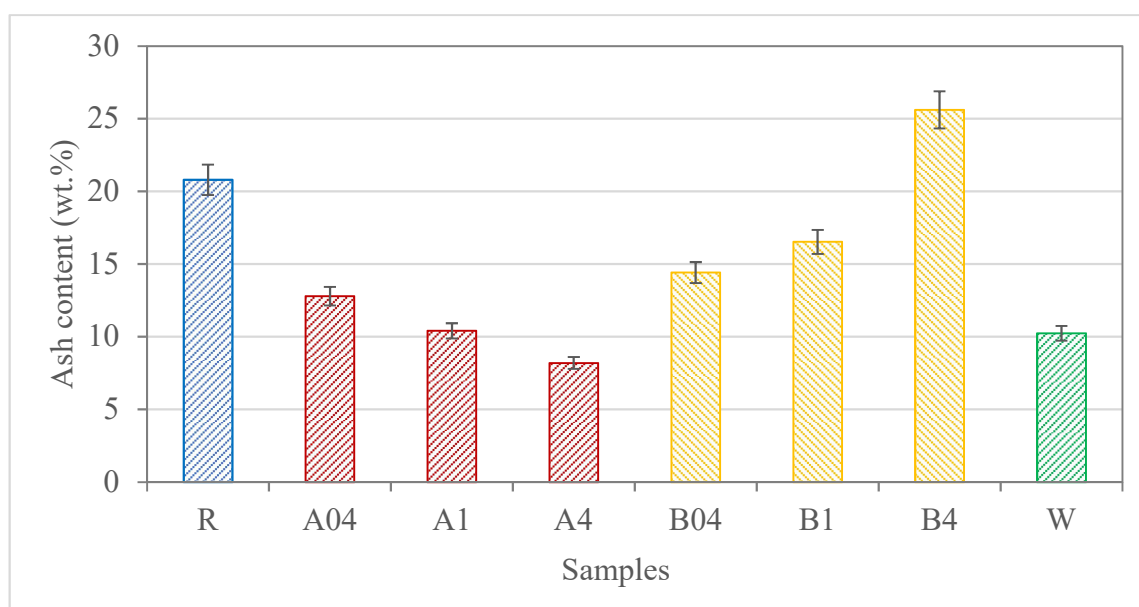
Figure 7-4 Ash content (wt.%) of pre-treated and untreated microalgae.

7.2.6 *Elemental analysis*

The EA and HHV analysis of the raw and treated *Isochrysis* sp. are summarised in Table 7-3. The results show that the carbon content increased after all the treatments (48-52%)

compared to the non-treated microalgae (38%). Nitrogen content after pre-treated increased due to the hydrolysis of proteins and nucleic acid. Based on the elemental composition, the microalgae high heating value were increased after treatment (20.6 – 23.6 MJ/kg), mostly due to the removal of oxygen and the enrichment in C and H. Despite this, the studied pre-treatments were less effective than hydrothermal treatment. For example, hydro-treated *Nannochloropsis oculata* showed C contents increase from 39.9% to 67.5% and HHV increase from 16.8 MJ/kg to 32.7 MJ/kg at 225 °C for 60 minutes (Du *et al.*, 2012).

Table 7-3 Elemental analysis and heating value of the treated and untreated *Isochrysis* sp.

	Samples							
Elemental analysis	R	A01	A1	A4	B01	B1	B4	W
Carbon	45.58	53.11	49.44	51.96	50.84	50.26	48.45	50.74
Hydrogen	5.84	7.27	6.73	7.36	6.94	6.95	6.75	7.03
Nitrogen	4.77	6.73	6.00	5.25	6.19	6.05	4.36	5.95
Oxygen	43.8	32.89	37.82	35.42	36.03	36.74	40.45	36.29
H/C molar ratio	1.54	1.64	1.63	1.70	1.64	1.66	1.67	1.66
O/C molar ratio	0.72	0.46	0.57	0.51	0.53	0.55	0.63	0.54
HHV (MJ/kg)	18.19	23.61	21.19	23.07	22.11	21.84	20.62	22.15

7.3 Catalytic pyrolysis products distribution

The yield of bio-oil and other products from the catalytic pyrolysis of the differently treated microalgae are shown in Figure 7-5. The values are based on ash free (daf) basis. High char yield is due to high presence of inorganic, which leads to condensation and polymerisation reactions. After the treatment with 4% acid (A4), the bio-oil yield increased to 38.33 wt.%, while the char yield was efficiently reduced to 24.20 wt.% (from

49.35 wt.%). Decreasing the strength of the acid from 4% to 1% (from A4 to A1) resulted in a bio-oil yield of 32 wt.%. A clear trend is visible with bio-oil yield increasing with increasing acid strength. The same trend was found in the pyrolysis of cotton stalk pre-treated with phosphoric acid, H_3PO_4 (Li *et al.*, 2013). Pyrolysis of treated biomass with acid caused the liquid oil yield to increase gradually until maximum of 37.8 wt.%. Biochar gradually increased meanwhile gas yields decreased when the acid concentration was increased.

The variation of product distribution caused by the introduction of H^+ ions and the disruption of the component structure such as lipid. H^+ provided by H_2SO_4 promoted dehydration reaction and disrupt the microalgae structure during pre-treatment. The influence became stronger as the acid concentration increasing, from 0.4% to 4%.

A different trend was shown after the treatment with NaOH, where a large yield of gas was produced rather than bio-oil. As can be seen in Figure 7-5, the gaseous obtained from base treated solution was up to 61 wt.% when treated with 0.4% and 1% of base (B01 and B1). The increase in the base concentration led to an increase in the bio-char yield, as shown with B4. The char yield increased to 50 wt.% compared to only 34 wt.% when treated with B01. This is probably due to the presence of Na^+ after the treatment, which enhanced secondary reactions that produces gas rather than bio-oil (Babich *et al.*, 2011). Also, NaOH had strong catalytic effect for condensation reactions, thus forming high molecular weight compounds in chars. Finally, the products distribution after water treatment did not differ much from that of the non-treated microalgae. Choi et al. (2014) reported that the oil yield was reduced from 37.9% to 33.3% after acid treatment of *Saccharina Japonica*. In this work, the acid pre-treatment in the presence of LSX-Zeolite increased the bio-oil yield after the removal of a fraction of the alkali species (Choi *et al.*, 2014).
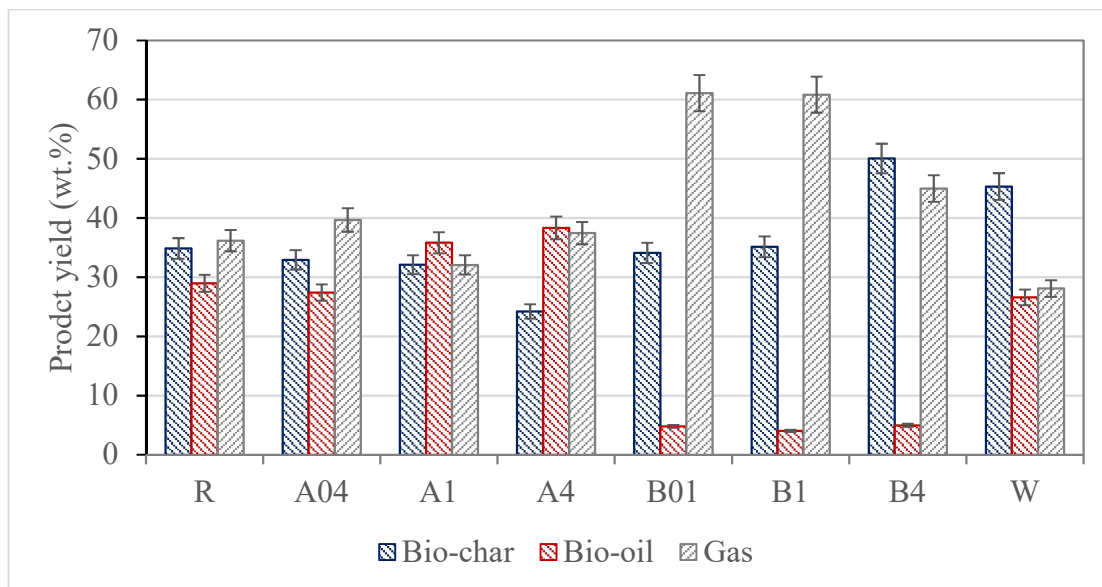
Figure 7-5 Pyrolysis products distribution (ash free).

7.4 Characterisation of pyrolysis products

7.4.1 *Bio-oil characterisation*

The bio-oils obtained from the catalytic pyrolysis of *Isochrysis* sp. were analysed by EA, GC-MS and NMR. Details of the analyses are explained below.

7.4.1.1 *Elemental analyses and HHVs of bio-oils*

The HHV and elemental analysis of the bio-oils from non-treated and treated microalgae are reported in Table 7-4. As expected, there was a modification of the material properties in comparison to the starting microalgae, R (see Table 7-3). The carbon(C) and hydrogen (H) contents resulted as those of R even after acid pre-treatment (A01, A1 and A4) (range around C: 74-75%; H: 10-10.1%), meanwhile, both C and H were reduced after the treatment with NaOH and water (C: 56-70%; H: 7.5-9%). Initially, the starting *Isochrysis* microalgae contained high nitrogen content (3.99%). Following the pyrolysis, the

nitrogen content in non-treated bio-oil was reduced to 2.11%. This can be ascribed to the zeolite denitrogenation effect. As expected, the treated microalgae did not result in lower N content in the bio-oils. This is due to the decomposition of protein chain during pre-treatment, released more N during decomposition of microalgae and trapped in the bio-oils.

The oxygen content decreased in the bio-oils t after 4% acid treatment (13%) compared to the bio-oil obtained without algae pre-treatment. The decrease in oxygen content in the bio-oils can be attributed to deoxygenation reactions such as decarbonylation, decarboxylation and dehydration. On the other hand, water and base treated consistently increased oxygen content up to 21% -33.9%. The basic pre-treatment resulted in a clear deterioration of the quality of the pyrolysis oils.

Table 7-4 HHV and elemental analysis bio-oil of *Isochrysis* sp. through catalytic pyrolysis.

	Samples							
Elemental analysis	R	A01	A1	A4	B01	B1	B4	W
Carbon	74.77	71.00	73.70	74.83	60.09	56.35	69.87	67.48
Hydrogen	9.86	9.59	10.11	10.04	8.08	7.49	9.06	9.10
Nitrogen	2.11	2.49	2.04	2.14	1.78	2.25	2.45	2.14
Oxygen	13.26	16.92	14.15	12.99	30.05	33.91	18.62	21.28
H/C molar ratio	1.58	1.62	1.65	1.61	1.61	1.60	1.56	1.62
O/C molar ratio	0.13	0.18	0.14	0.13	0.38	0.45	0.20	0.24
HHV (MJ/kg)	36.32	34.30	36.15	36.58	27.36	24.96	33.10	32.05

7.4.1.2 ^{1}H NMR analysis of bio-oils

To evaluate whether a chemical transformation occurred, the ^{1}H NMR analysis of the bio-oils were carried out. The percentage of the proton types, calculated on the basis of the ^{1}H NMR chemical shifts are reported in Table 7.5, showing important information about the effect of different chemical pre-treatment on catalytic pyrolysis. Overall, the protons adjacent to aliphatic (0.0 – 1.6 ppm) represents the majority in all the bio-oils (61-74%) with the highest aliphatic found after mild (0.4-1% NaOH) base pre-treatment, ranging from 70% to 73.5%. Inversely, the acid treatment increased the aliphatic protons according to the acid pre-treatment strength, resulting in less aliphatic protons than the non-treated case. For the next region, which includes protons on carbon atoms next to aliphatic alcohol/ether or a methylene group joining two aromatic rings (spectra 1.6 - 2.2 and 2.2 – 4.2 ppm), a sudden decrease is reported after base and water treatment. The treatment with 4% H_2SO_4 resulted in an increase in protons in the region of 2.2-3 ppm, denoting an increase in methylated aromatics, ethers and N-heterocyclic compounds. The region between 4.2 and 6.4 ppm represents the aromatic ether protons such as methoxy phenols and hydrogen atoms of carbohydrates molecules. The percentages of protons in this region were found to be in small amounts, ~1.39% in non-treated bio-oils and increasing after acid and water pre-treatment at ~4.15 to 6.59%. This indicate the pre-treatment hydrolyse carbohydrates and converted them into different classes of compounds. The aromatic regions of the spectra (6.4 – 6.8 and 6.8 – 8 ppm) initially (R) contained about 12.9% of the protons in the bio-oils. After strong acid treatment (A4), the protons attached reduced to 6.95%, while they increased to 13.8% after strong base treatment, B4.

Table 7-5 ^{1}H NMR results of bio-oils of different pre-treatment on catalytic pyrolysis at 500 °C.

Chemical shift region (ppm)	Type of protons	Hydrogen content (% of all hydrogen)							
		R	A01	A1	A4	B01	B1	B4	W
0.0 - 1.6	CH3. -CH2-	67.43	64.04	65.00	60.89	73.51	70.05	69.90	64.45
1.6 - 2.2	-CH2-, aliphatic OH	10.01	12.22	9.67	10.88	4.39	6.69	5.98	9.02
2.2 - 3.0	-CH3OC, -CH3-Ar, -CH2Ar	6.01	5.30	5.57	9.03	3.05	4.84	4.08	5.45
3.0 - 4.2	CH3O-, -CH2O-, =CHO	1.74	2.38	4.11	4.71	2.72	2.39	2.57	3.64
4.2 - 6.4	=CHO, ArOH, HC=C (nonconjugated)	1.35	4.15	5.19	6.59	2.90	3.44	3.20	5.98
6.4 - 6.8	HC=C (nonconjugated)	0.61	0.03	0.31	0.59	0.12	0.39	0.29	0.48
6.8 - 8.0	ArH, HC=C (conjugated)	13.66	11.41	9.98	6.95	13.10	11.15	13.81	10.63
8.0 - 10.0	-CHO, -COOH, downfiled ArH	0.13	0.47	0.17	0.36	0.21	0.51	0.17	0.35

7.4.1.3   GC-MS

The main chemical compounds contained in the bio-oils were identified by GC-MS and grouped by functional groups, as shown in Figure 7-6. These samples exhibit a range of functionalities such as carboxylic acids, aliphatic hydrocarbons and esters (mainly from lipids), aromatics, aldehydes, phenols and phytols. Prominent amongst these are nitrogen containing compounds such as amides, N-heterocyclic compounds, nitriles, amines formed by the cracking of proteins and chlorophylls ($C_{55}H_{72}O_5N_4Mg$) found in the algae (Miao, Wu & Yang, 2004). The formation of these compounds takes place with simultaneous dehydration, depolymerisation, decarboxylation, decarbonylation, denitrogenation, dehydrogenation, demethylation and cyclisation reactions.

After *Isochrysis* sp. was treated with 1% (A1) and 4% acid (A4), the bio-oil contained a large amount of aliphatic (42.29 -50.05%) followed by aromatics (15.3-21.1%). Therefore, the pyrolysis after acid treatment was effective in cracking down the algae macromolecules and increased the aromatisation process, compared to the pyrolysis of the non-treated algae. On the other hand, the use of mild 0.4% H_2SO_4 solutions (A01) resulted in an increase in the nitrogenates (0.4% H_2SO_4) and decreased the aromatics compound (both), compared to all the other runs. The treatment with the basic solutions led to high PAH content and N-compounds. In general, NaOH treatments resulted in condensation and aromatisation reactions that led to large yield of gas and char/coke. Pre-treatment with B4 produced 21.1% of aromatics, followed by B1 (18.2%) and B01 (17.52%).

Ketones and alcohols were presented in the bio-oils produced (A01) after treatment with 0. 1% acids and disappeared when the 4% and 1% H_2SO_4 acid solution (A1 and A4) was used in the pre-treatment. Other than that, carboxylic acid decreased from 11.1% to 4.3% when the acid concentration was increased from 0.4% to 4%. This can be related to carboxylic acids cracking via decarboxylation (producing CO_2) and decarbonylation (CO).

Interesting information on the catalytic activity were obtained when evaluating the mono-aromatics (MA) and poly-aromatic hydrocarbons (PAH) distribution in the bio-oils. Compounds derived from the decomposition of proteins, such as benzene sulphonamide ($C_6H_7NO_2S$) and other benzene substitutes decreased in yield at the increase in the acid strength used in the pre-treatment, passing from 2.1% (A01) to 1.5% (A1) and 0.3% (A4). This suggests that after treatment with 4% H_2SO_4, the protein fraction of the microalgae is cracked down and N is released in the gas phase, possibly as NH_3. In addition, cellulose dehydration products such as 2H-pyran started to be detected after 4% H_2SO_4 pre-treatment. The use of 4% NaOH and water resulted in low level of MA compounds.

The yield of PAH was very high when the *Isochrysis* microalgae were treated with 4% H_2SO_4, with 14% naphthalene substitutes, 2.5% phenanthrene, 1.9% indene, 1.5% azulene, 0.9% chamazulene and 0.5% anthracene. The production of PAH decreased with H_2SO_4 acid strength of 1% (4.5% naphthalene, 0.95 phenanthrene, 0.7% indene) and almost disappeared when the acid strength used was 0.4% (1% naphthalene, 0.2% phenanthrene, 0.2% anthracene). Study shown that H^+ provided by H_2SO_4 could promote the oligomerisation and cyclisation reaction of intermediate polymer short chains to form benzene ring, which further undergo condensation forming polycyclic aromatics hydrocarbons (PAH) (Jae *et al.*, 2011). Based on the properties of the pre-treated bio-oils, it appears that a pre-treatment with H_2SO_4 concentration between 0.4 and 1wt% H_2SO_4 would be the most beneficial and balanced treatment, which would be able to reduce the PAH and increase aliphatic compounds. The use of 4% NaOH also resulted in a bio-oil rich in PAH (11% naphthalene, 2.7% anthracene, 2.5% azulene).

Mild acid treatment is inexpensive and can be performed at low temperature. However, the process becomes expensive at high temperature or in the presence of strong acid solutions due to high energy input and the need for specific reaction vessels, which must be resistant to high temperature and corrosion (Behera *et al.*, 2014). On the contrary, although NaOH is inexpensive, downstream processing costs are high, thus making it a costly process.
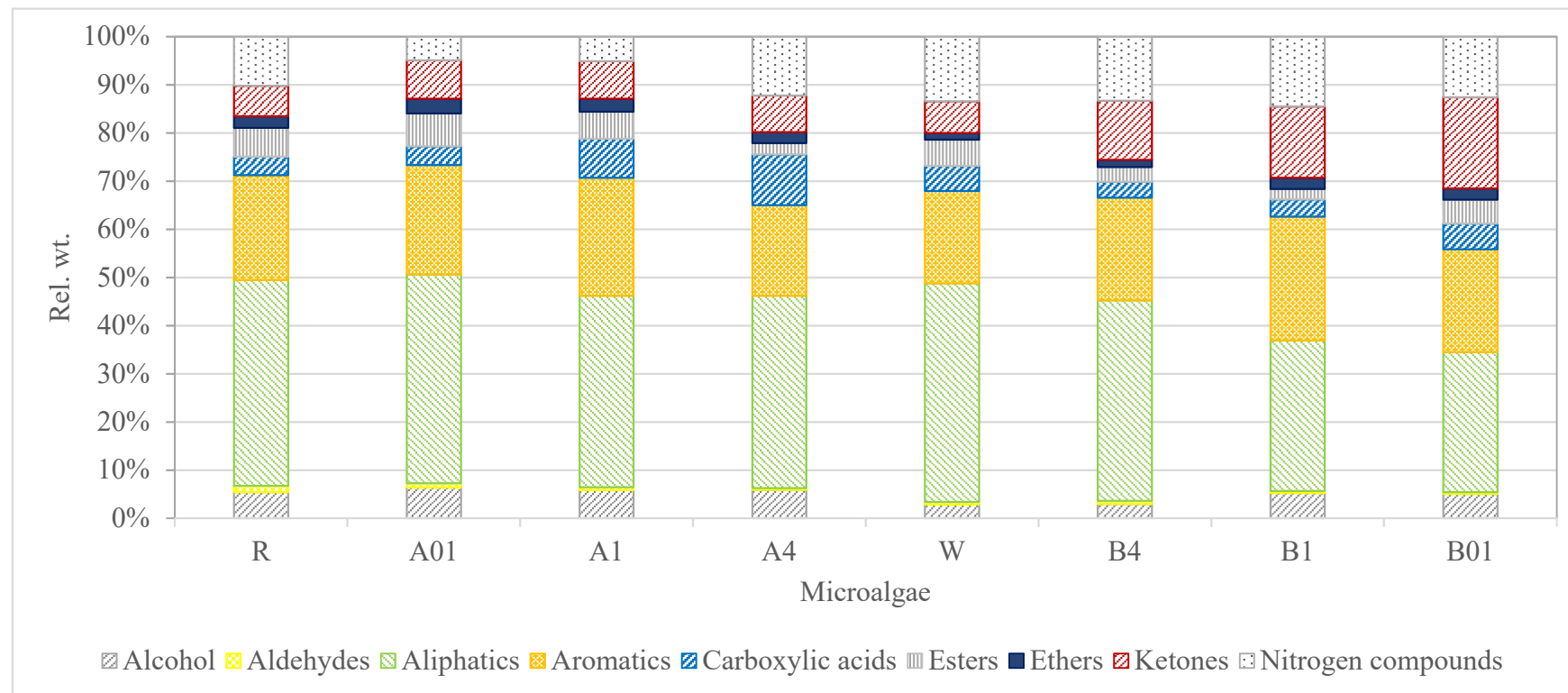
Figure 7-6 GC-MS relative content of different groups in catalytic pyrolysis bio-oils.

7.4.2   *Bio-char characterisation*

The visual observation of the *Isochrysis* bio-chars indicated a bulky and sintered non-treated (R) bio-char, while the treated bio-chars were made of small loose particles. The absence of sintering after pre-treatment can be linked to the removal of alkali species.

7.4.2.1   *Elemental analyses*

The elemental analysis of the bio-char from *Isochrysis* microalgae are shown in Table 7-6. After acid treatment, the algae structures were disrupted and dissociated enhancing volatilisation to gas/oil species and consequently reducing C and H in the bio-chars, which resulted in low H/C and high O/C ratios, compared to the non-treated microalgae. On the contrary, nitrogen contents increased after the pre-treatments, making the bio-chars suitable for soil amendment purposes.

Table 7-6 HHV and elemental analysis bio-char of Isochrysis sp. through catalytic pyrolysis.

Elemental analysis	Samples							
	R	A01	A1	A4	B01	B1	B4	W
Carbon	52.00	46.60	53.07	49.25	44.52	44.04	47.46	46.44
Hydrogen	7.36	6.21	6.32	4.56	6.05	6.11	6.04	5.63
Nitrogen	4.72	4.02	4.70	2.56	3.11	3.03	3.56	4.00
Oxygen	35.91	43.17	35.92	43.63	46.31	46.82	42.93	43.92
H/C molar ratio	1.70	1.60	1.43	1.11	1.63	1.67	1.53	1.46
HHV (MJ/kg)	23.04	13.35	14.98	12.99	11.98	11.84	13.02	12.34

7.4.2.2 FT-IR spectroscopy

FT-IR was employed to distinguish the chemical shift that took place after pre-treatment. Figures 7-7 and 7-8 show the absorbance spectra of bio-chars according to their treatment. A remarkable trend can be seen for the C-H bending linked to aromatics (880, 780, 680 cm^{-1}), which is not present only in the bio-char after 4% acid treatment (A4), but also very evident in the rest of the bio-chars. This suggests that the treatment with 4% acid drastically reduced the formation of highly condensed char species. Aliphatic C-H bonds (2950-2850 cm^{-1}) were not present in any of the bio-chars, as small/medium condensable/incondensable organic species were released in gas phase during the microalgae catalytic cracking. A clear trend was shown for the aromatic C=C bending (1500-1700 cm^{-1}), whose absorbance intensity decreased in the following order: Base > Water > Raw > Acid.

Aromatic containing nitrogen could be linked to the presence of N-H bend of amides (1530 cm^{-1}) and $-NO_2$ in aromatics (1490-1550 cm^{-1}). An interesting observation (see Figure 7-8) is that the biochar/catalyst remaining after the 4% acid treatment exhibit less functionalities (only aromatic C=C and C-H bending) compared to the chars obtained in the presence of 1% and 0.4% acid. This may be related to the higher leaching activity of the 4% acid solutions, which helped the decomposition of the algae structure during pyrolysis (see also Figure 7-2). Figure 7-8 also indicates that the intensity of the peaks in the region 1400-1700 cm^{-1} increased according to the increase in the NaOH solution strength, which suggest larger char yield under those conditions. This is in agreement with the pyrolysis products distribution shown in Figure 7-4. Figure 7-8 also shows that the intensity of the same peaks was lower when the acid solutions were used, which indicates lower char formation in their presence. The small peak at 1340-90 cm^{-1} could be ascribed to N-O (nitro compounds) or C-H form methyl groups. This band is well represented in the 0.4% acid bio-char, while is much less marked or absent in the other bio-chars. Finally, the characteristic peak near 750 cm^{-1} can be attributed to the Si-O-Si stretching vibration and Al-O. The broadband between 950 and 1100 cm^{-1} can be assigned to the asymmetric stretching vibrations of the Si-O bonds of the silica alumina catalyst.

Also, silica is an important constituent of microalgae (Jindo *et al.*, 2014). In Figure 7-7, a loss of SiO_2 can be appreciated by the decrease of intensity of the peaks after the pre-treatment compared to the non-treated one and the starting catalyst.
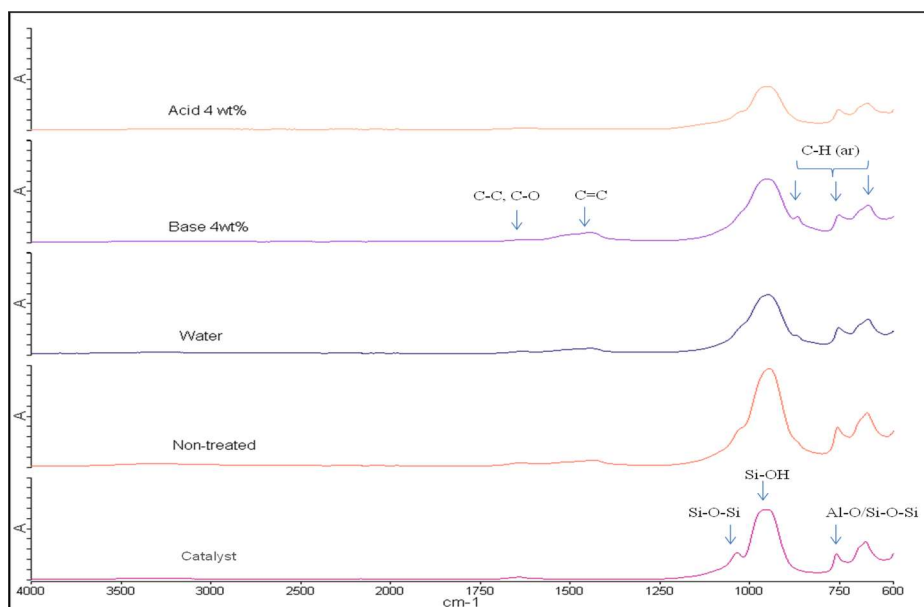
Figure 7-7 Comparison of FT-IR of bio-chars of different pre-treated microalgae.
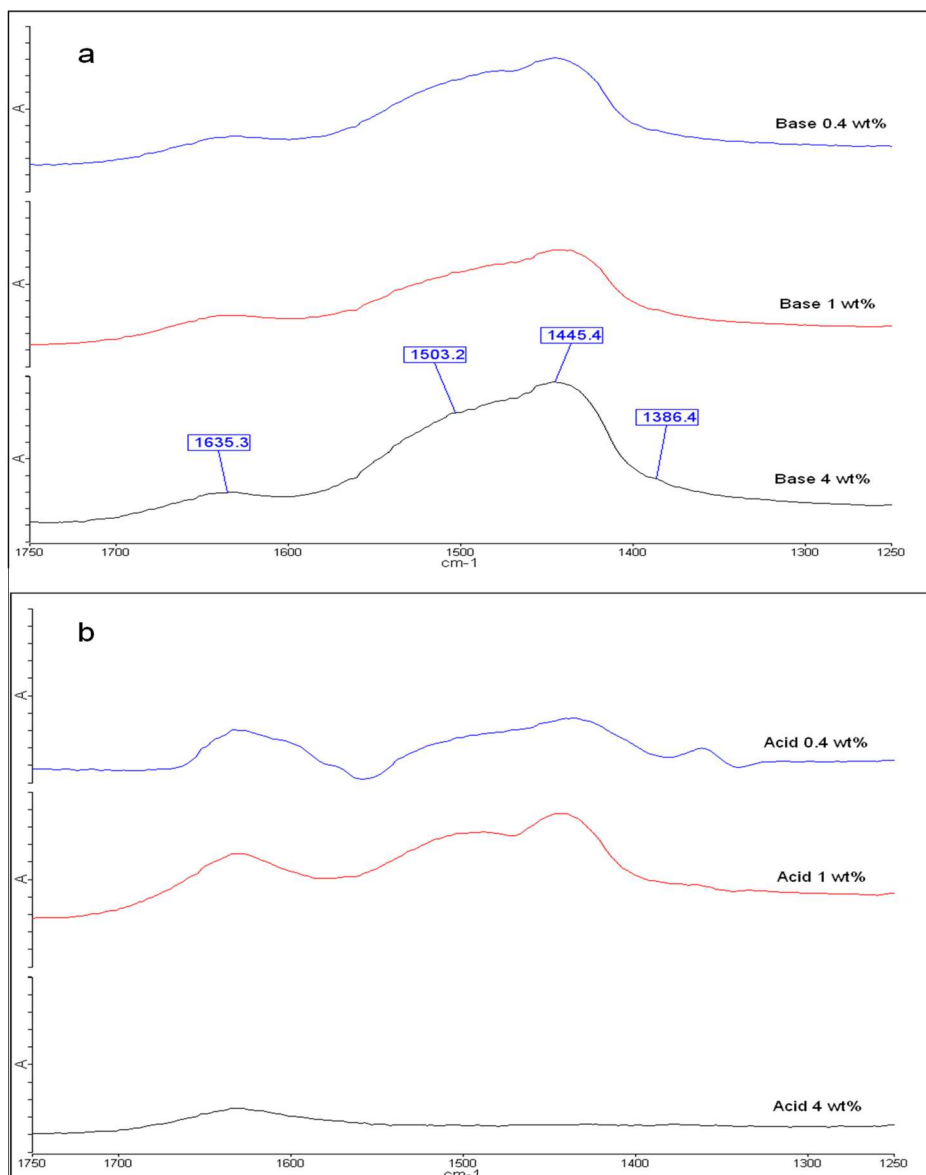
Figure 7-8 FT-IR of bio-chars: wavelengths of the 1300-1800 cm^{-1} region after pre-treatment (a) NaOH; (b) H_2SO_4 of different concentration.

7.5 Summary

Microalgae contain a high K and Na content, which may cause fouling problems during pyrolysis as well affecting the product distribution. Chemical pre-treatment of *Isochrysis* microalgae was performed in an effort to reduce the amount of inorganic species in the microalgae, towards enhanced bio-oil yield and quality. Pre-treatment of the algae in H_2SO_4 leached out over 53% of the Na and a large proportion of Ca, Mg and K. Meanwhile, pre-treatment in water leached around 24% of the Na and about 3-6% of Ca, Mg and K. While pre-treatment with NaOH was unsuccessful due to re-precipitation of Na salts.

Acid pre-treatment increased the yields of bio-gas and bio-oil, which presented a good potential for the bio-oil production. The bio-oil yield increased after H_2SO_4 treatment compared to the non-treated. The quality after acid treatment featured increased C contents and decreased O content, as compared to the non-treated *Isochrysis*. However, the HHVs of bio-oil remained unchanged with the non-treated bio-oil. Pyrolytic bio-oil after 1% H_2SO_4 solution treatment resulted in a decreased content in aromatics, while dominated by aliphatic hydrocarbons. The production of aromatics could be tuned by using strong (4 wt.% H_2SO_4) acid solution. Meanwhile, pyrolysis of microalgae after NaOH pre-treated had increased the gas production greatly. The highest gas yield obtained with weak base (0.4%) and reduced the bio-oil yield to the lowest. Most of the gaseous were released in forms of CO_2 when acid pre-treatment was used.

Chapter 8

Catalytic pyrolysis of non-treated and pre-treated *Isochrysis* sp. microalgae: Li-LSX-zeolite activity and regeneration

8.1 Introduction

In the previous chapters, the catalytic pyrolysis of pre-treated microalgae in the presence of Li-LSX-zeolite was described. The presence of Li-LSX-zeolite catalyst plays different roles such as a more effective depolymerisation of the microalgae, the promotion of deoxygenation and denitrogenation reactions and the enhanced formation of C-C bonds in the produced bio-oil.

A wide variety of heterogeneous catalysts have been studied in the literature, but acidic zeolite catalysts such as H-ZSM-5 are the most employed in this process due to their high deoxygenation and aromatisation activity. Acidic zeolites promote a series of reactions, such as secondary cracking, oligomerisation, cyclisation, aromatisation, and/or polymerisation reactions, among others, leading to partial deoxygenation of the pyrolysis vapours through the formation of CO, CO_2, and H_2O. Nevertheless, it is important to control such acid properties, since highly acidic zeolites promote polymerisation reactions, yielding higher amounts of coke and polyaromatic hydrocarbons (PAHs), which decrease the bio-oil yield dramatically and it is environmentally undesirable. Catalyst deactivation occurs due to coke formation and strong adsorption of oxygenates components on the surface of the catalyst support and represents one of the main limitations for ZSM-5 and other acidic zeolites.

In the previous chapter, microalgae *Isochrysis* sp. was treated to reduce the amount of inorganic species in the microalgae, towards the enhancement of the bio-oil yield and quality. The acid pre-treated microalgae increased the yield for bio-gas and bio-oil, showing good potential for catalytic pyrolysis. Also, as compared to the non-treated

microalgae, the treated microalgae produced higher aromatics, carboxylic acids as well as nitrogenated compounds.

This chapter investigates the use of Li-LSX-zeolite catalyst over several regeneration cycles on non-treated and treated *Isochrysis* sp. microalgae to evaluate the stability over cycles of this material and how its activity varies after a number of cycles, as it may affect the process viability. The pyrolysis experiments and their interpretation are reported in the first part of this chapter. The second section focuses on the characterisation of the reaction products to establish the regenerated catalyst contribution on yield and quality of the bio-oil. Finally, the catalyst characterisation is discussed in the last part.

8.2 Catalytic activity and regeneration

The catalytic pyrolysis runs were carried out using treated and non-treated microalgae to investigate the effect of catalyst regeneration on the yield and quality of the pyrolysis products. The pyrolysis of *Isochrysis* sp. were run at 500 °C using a fixed bed reactor using a catalyst: biomass ratio of 1: 1. Three catalytic regeneration cycles were carried out for both the pre-treated and not pre-treated microalgae in an ex-situ pyrolysis configuration.

The product yields distribution for the three cycles are summarised in Figure 8-1. On one hand, for the non-treated microalgae, the gas yield increased as the cycle number increased, passing from 39.6 wt.% (1st cycle) to 42.4 wt.% after the 3rd cycle. On the other hand, an opposite trend resulted with the pyrolysis of the treated microalgae, where the gas conversion decreased cycle after cycle (from 30.2 wt.% to 24.7 wt.%), while the bio-oil yield increased from 35.5 wt.% (1st cycle) to 42.6 wt.% (3rd cycle).

This is due to the removal of alkali metals in the pre-treated microalgae that catalyse gasification reactions. By comparing to the previous chapter, the 1% treated microalgae produced the same yield of bio-oil, ~34 to 35 wt.% showing that the reactor setup does

not affect the products distribution. However, the compositions of bio-oil and gaseous were different and are discussed in subchapter 8-3. Clearly, the pre-treatment affected the activity of the Li-LSX-zeolite in terms of the distribution of the reaction products, as discussed later in this chapter. Nevertheless, the change in catalytic activity can also be evaluated from the Li-LSX zeolite degree of deoxygenation and denitrogenation of the bio-oil.

The bio-char yield remained constant in the non-treated catalytic pyrolysis, while slightly decreased in the 2nd and 3rd cycles, when the pre-treated microalgae were used, suggesting that the partial hydrolysis of the macro-polymers and the removal of the alkali species resulted in lower coking. Moreover, this could be related to acidity decrease in the catalyst surface. The regenerated catalyst produced a similar yield to the fresh catalyst, showing the possibility of regeneration and the effectiveness of the process.
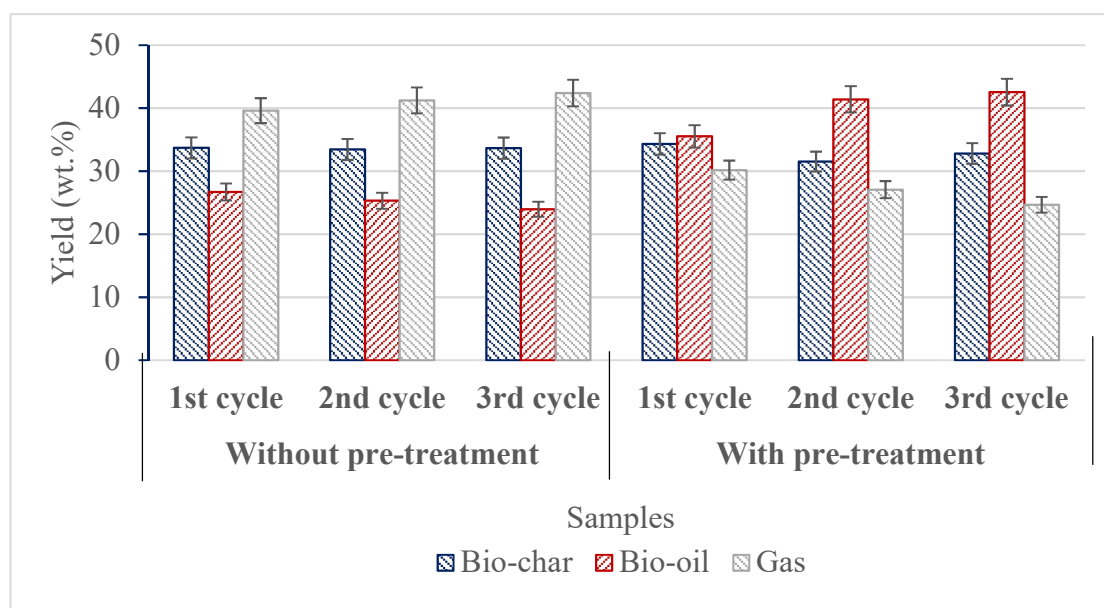
Figure 8-1 Products yield distribution with and without pre-treatment over 3 cycle catalyst regeneration.

8.3   Characterisation of pyrolysis products

8.3.1   *Elemental analyses of bio-chars and bio-oils*

A further indication of the activity of the catalyst can be extrapolated from the EA and HHV data. Table 8-1 reports the elemental analyses and high heating value (HHV) of the bio-chars and bio-oils obtained from the pyrolysis after regeneration at 500°C. The EA data indicate that the char formation was lower when the non-treated microalgae were used in the three cycles. Moreover, an increase in H and N and a decrease of C resulted in the increase in the cycles for the non-treated microalgae. The chars were consistently enriched in C, H and N and depleted in oxygen when the pre-treated microalgae were used instead of the non-treated ones. This suggests that the pre-treatment, when coupled to the catalytic pyrolysis in the presence of Li-LSX-zeolite, led to coking reactions and condensation of N-heterocyclic species that were only partially removed during the regeneration stage.

Initially, the bio-char contained 69.8 wt.% C and 6.94 wt.% N. After the third pyrolysis cycle, C and N contents increased to 72.5 wt.% and 8.02%. This showed that the Li-LSX-zeolite catalytic activity decreased according to the number of cycles and was not be able to remove the nitrogen in the gas phase. The bio-char from pyrolysis contains hydrogen and oxygen whereas coke that forms on acidic zeolites surfaces consists of polyaromatic structures (Paasikallio *et al.*, 2017). The HHV of the bio-chars obtained using the pre-treated microalgae were relatively high, ranging from 27.5 to 27.8 MJ/kg and also, both C and N resulted good for soil amendment application (Grierson, Strezov & Shah, 2011).

The bio-oils from the pyrolysis of the non-treated microalgae contained high C and H content, which further increased after the 3rd cycle (76.0 wt.% and 10.3 wt.%, respectively). The catalyst also maintained an excellent deoxygenation activity during the three cycles. In the presence of Li-LSX zeolite, the oxygen is removed through several reactions such as decarboxylation, decarbonylation and dehydration, resulting in a high

gas yield and a low aromatic-rich bio-oil yield. This study shows that for the catalytic pyrolysis of the pre-treated microalgae, both C and H decreased when compared to that associated with the non-treated ones, while the oxygen content of the bio-oil increased. Therefore, the pre-treatment led to an inhibition of the deoxygenation activity and lower C content denoting deactivation of the catalyst.

The nitrogen content of the bio-oils decreased according to the increase in the cycle for both the pre-treated and not ones, indicating that also the denitrogenation activity was inhibited. Overall, the HHV of the bio-oils were higher when the non-treated microalgae were used and improved after the third cycles recording the highest HHV, 37.95 MJ/kg for the non-treated ones.

Table 8-1 Elemental analysis, H/C and O/C molar ratios and HHV of bio-chars and bio-oils obtained from treated and non-treated microalgae pyrolysis.

Elemental analysis (wt.%)	Without pre-treatment			With pre-treatment		
	1st cycle	2nd cycle	3rd cycle	1st cycle	2nd cycle	3rd cycle
Bio-chars						
Carbon	53.69	62.32	58.61	69.79	71.28	72.50
Hydrogen	10.03	1.68	1.56	5.25	4.65	4.14
Nitrogen	2.75	4.99	4.73	6.94	8.91	8.02
Oxygen	33.53	31.01	35.10	18.02	15.16	15.33
H/C molar ratio	2.24	0.32	0.32	0.90	0.78	0.69
O/C molar ratio	0.47	0.37	0.45	0.19	0.16	0.16
HHV (MJ/kg)	27.26	19.20	17.32	27.79	27.62	27.45

Bio-oils

Carbon	74.20	75.63	75.99	64.51	68.59	69.17
Hydrogen	10.10	10.42	10.29	8.87	9.60	9.75
Nitrogen	2.89	3.08	3.89	2.62	3.07	3.06
Oxygen	12.81	10.87	9.83	24.00	18.74	18.02
H/C molar ratio	1.63	1.65	1.62	1.65	1.68	1.69
O/C molar ratio	0.13	0.11	0.10	0.28	0.20	0.20
HHV (MJ/kg)	36.83	37.95	37.93	30.58	33.52	34.00

The nitrogen distribution in the products of the catalytic pyrolysis of treated and non-treated microalgae is shown in Figure 8-2. The use of Li-LSX-zeolite and the non-treated microalgae resulted in nitrogen content in the bio-oils of about 14.6%-17.5%, while most of N was removed in the gaseous phase (73.3% to 79.8%). When the *Isochrysis* sp. microalgae were treated with 1% H_2SO_4 solution, the fraction of N in the bio-char and bio-oil increased to the expenses of the N removed to gas. The increase in N in bio-char and bio-oil cycle after cycle can be directly linked to the catalyst deactivation.
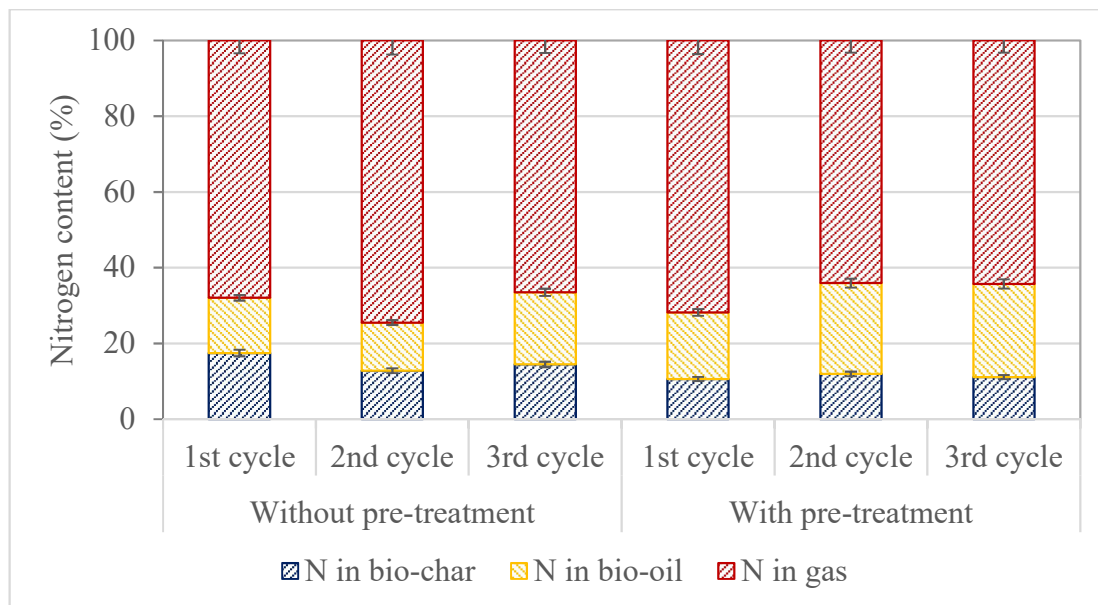
Figure 8-2 Nitrogen distribution in the pyrolysis products.

8.3.2 *Bio-oil characterisation*

The bio-oil obtained from the catalytic pyrolysis of treated and non-treated *Isochrysis* sp. after the catalyst regeneration at 500°C were submitted for further analyses, namely GC-MS and NMR. Details of the analyses are explained below.

8.3.2.1 *^{1}H NMR*

NMR analyses are of great importance since it gives an overview of the chemical functionalities present in the bio-oils. Table 8-2 reports the integration of the ^{1}H NMR spectra of the treated and non-treated *Isochrysis* bio-oils obtained from the three cycles of pyrolysis/catalyst regeneration. The ^{1}H NMR suggests that there are clear differences in the overall chemical composition of the bio-oils in the presence of catalyst after three cycles of pyrolysis/regeneration. From the NMR spectra, the most up-field region 0.0 to 1.6 ppm, represents aliphatic protons that are attached to carbon atoms, at least two bonds. This region was shown to be more populated for all the bio-oil obtained from the pre-

treated microalgae. The aliphatic protons in the bio-oils from non-treated microalgae showed a decrease in intensity with the increase in the cycle number. Therefore, the pre-treatment led to a more aliphatic bio-oil. The integrated region from 1.6 to 2.2 ppm and 2.2 to 3.0 ppm represent protons on aliphatic carbon atoms bonded to C=C double bond (aromatic or olefinic) or C two bonds away from heteroatom. The percentage of this group increased after the second and the third cycle of regeneration for the no-treated microalgae but remained constant for the pre-treated ones, showing that heteroatoms increased after the catalyst deactivation. The next integrated region of the spectra (3-4.2 ppm) represents protons on carbon atoms next to aliphatic alcohol/ether/ester, or methylene group joining two aromatic rings. The highest percentage of protons was observed after the third cycle, in both cases.

The region between 4.2 to 6.4 ppm represents oxygenated compounds such as carbohydrates, phenolic OH or olefinic protons. In this region the lowest proton percentage was observed for the bio-oil from the non-treated microalgae. This may be because before being able to remove oxygenated compounds from the bio-oils, the catalyst already lost its capacity after deactivation. Next regions between 6.4 and 6.8 and from 6.8 to 8.0 were assigned to aromatic protons. From Table 8-2, it is shown that the non-treated microalgae produced high aromatics compounds in the bio-oil compared to the pre-treated microalgae. Moreover, the deactivation of the catalyst coincides to the decreased abundance of aromatics in the bio-oil. Aldehydes and carboxylic acids (8 – 10 ppm) were less present compared to other functional groups. Overall, the proton NMR analyses indicate that higher percentage of the aliphatic protons (compounds) exist in the bio-oils, especially when the microalgae were pre-treated, while aromatics are enhanced when the microalgae are processed as they are. Based on the results from SEM-EDS, EA and BET analysis, the NMR support the fact that the catalyst is partially deactivated in terms of deoxygenation and aromatic productions after three cycles and that the pre-treatment completely changes the chemical functionalities of the bio-oil.

Table 8-3 ^{1}H NMR integrations of treated and non-treated *Isochrysis* pyrolysis bio-oils versus specific chemical shift ranges.

		Hydrogen content (% of all hydrogen)					
		Without pre-treatment			With pre-treatment		
Chemical shift region (ppm)	Type of protons	1st cycle	2nd cycle	3rd cycle	1st cycle	2nd cycle	3rd cycle
0.0 - 1.6	CH3. -CH2-	69.23	61.11	57.02	70.68	69.08	69.04
1.6 - 2.2	-CH2-, aliphatic OH	7.57	15.06	15.69	12.37	13.15	11.99
2.2 - 3.0	-CH3OC, -CH3-Ar, -CH2Ar	3.17	6.21	7.33	6.68	6.98	6.73
3.0 - 4.2	CH3O-, -CH2O-, =CHO	1.95	1.60	3.91	0.13	0.48	1.37
4.2 - 6.4	=CHO, ArOH, HC=C (nonconjugated)	4.48	4.56	4.88	2.31	3.42	4.40
6.4 - 6.8	HC=C (nonconjugated)	0.00	0.14	0.24	0.36	0.57	0.47
6.8 - 8.0	ArH, HC=C (conjugated)	13.41	13.20	10.57	7.39	6.14	5.66
8.0 - 10.0	-CHO, -COOH, downfiled ArH	0.23	0.12	0.36	0.08	0.18	0.34

8.3.2.2   GC-MS analyses

GC-MS analyses were carried out to evaluate if the organic compounds present in the bio-oils suffered any modification after the pyrolysis/regeneration cycles at 500°C. The compounds present in the bio-oils were identified and divided into nine groups; alcohols, aldehydes, aliphatic, aromatics, carboxylic acid, esters, ethers, ketones and nitrogen compounds. Accordingly, the results are illustrated in Figure 8-3. Most of the compounds present in bio-oils were aliphatic, followed by aromatic groups. The presence of aliphatic confirmed the ^{1}H NMR results in Table 8-3, where aliphatic were also the most abundant compounds in the bio-oils. The aliphatic compounds were reduced after the second and the third cycle in both cases, but the proton NMR suggests that aliphatic are maintained at almost constant rate when the microalgae were previously pre-treated. Three types of compounds were identified in the aliphatic group: n-alkanes, alkenes and branched hydrocarbons. Most of the chain alkanes were distributed in the range from C_9 to C_{22}. Among the alkane, nonadecane, hexadecane, cyclo-hexadecane and docosane were the most abundant. Alkenes such as octadecene, heptadecene, hexadecene were also identified. Though alkenes were present in the bio-oils, n-alkanes were dominant.

Aromatic hydrocarbons were also identified in the bio-oils for both the treated and non-treated microalgae. Monoaromatics such as benzene and polyaromatics such as naphthalene were the most abundant in the bio-oils. In agreement to the NMR, the percentage of aromatics was reduced after the second and the third cycles, due to the poisoning on the catalyst surface, which blocked the acid sites access. Carbonyl groups such as ketones and aldehydes are oxygenated compounds that affect the stability and heating value of the bio-oils. Furthermore, the presence of acids in bio-oil is undesirable due to its corrosive nature. The presence of Li-LSX-zeolite catalyst during pyrolysis reduced the oxygenated compounds for both the pre-treated and non-treated microalgae, however, the percentage increased after three cycles.

198

A study investigated the catalytic pyrolysis of biomass over fresh (FZ), spent (SZ) and regenerated (RZ) of ZSM-5 catalyst (Zhang *et al.*, 2015). The bio-oils from the spent catalyst (SZ) contained high hydrocarbons compared to the regenerated and fresh catalyst. The hydrocarbons selectivity was in the order: SZ>RZ>FZ. Due to the low catalyst acidity, SZ converted more primary fast pyrolysis gaseous into hydrocarbons, followed by RZ (moderate acidity) and fresh catalyst (high acidity). Another study reported there are no changes in the carbon yield after three cycles of regeneration using ZSM-5 catalyst, indicating that the thermal regeneration does not affect the catalyst stability even after three cycles (Li *et al.*, 2014b). This finding contradicts with the findings of this study.

The nitrogen compounds in bio-oils such as indole, nitriles, pyridines and pyrimidines, which derived from the degradation of microalgae proteins, consistently increased with the increase in the pyrolysis cycle in the presence of both non- and pre-treated microalgae, indicating deactivation of the denitrogenation activity. The amount of nitrogenated compounds in bio-oil increased in the case of non-treated microalgae, from 6.1% to 10.9%, while for the treated microalgae, N compounds increase from 10.3% to 26.3%. The results confirmed the EA analyses, where N content increased after the second and third cycles.
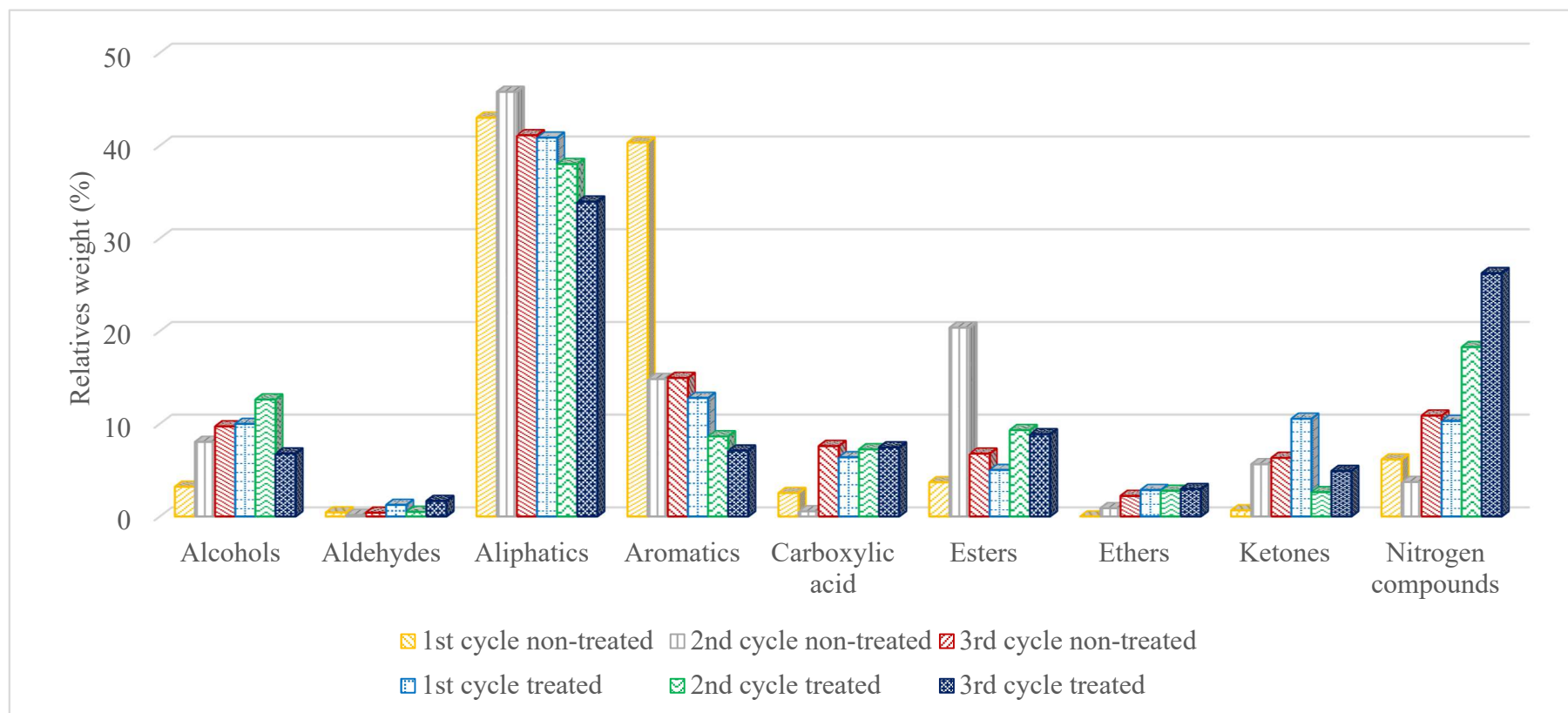
Figure 8-3 GC-MS bio-oil based on groups for catalyst regeneration of treated and non-treated microalgae.

8.3.3 *Bio-char characterisation*

Figure 8-4 shows the FT-IR spectra of the non-treated and pre-treated bio-chars after three cycles of catalyst regeneration. As expected, after 2nd and 3rd cycles, significant changes occurred in both the bio-chars chemical and structural compositions. In both the non-treated and pre-treated samples, the presence of a distinctive O-H group at between 3300 and 3200 cm^{-1} can be associated with N-H$_2$ and N-H stretches and to O-H stretching in alcohols. The O-H stretching vibration band almost disappeared for bio-chars obtained after the third cycle compared to the 1st and 2nd cycle. This indicates that during the 3rd cycle, most of the -OH was released into the gaseous phase. This is supported by Table 8-3, which suggests that high water was released during the third cycles. The absorbance peaks between 2970 and 2950 cm-1 and between 2880 to and 2860 cm-1 indicate saturated aliphatic hydrocarbons (C-H stretching vibrations). Despite of not being very different between pre-treated and non-treated bio-chars, a decrease in saturated aliphatic is shown after three cycles. At the same time, the peaks representing for aromatic carbon, such as C=O stretching (1700 cm-1), C=C (1380 cm-1 to 1450 cm-1) appeared more clearly, in particular for the non-treated (1st cycle) and the pre-treated ones (1st and 2nd cycles).

After each cycle of regeneration, there were a number of bands whose intensity increased. For instance, the 832 and 700 cm^{-1} (aromatic C-H deformation modes), the 1600 cm^{-1} band (aromatic C=C stretching and C=O stretching modes of conjugated ketones), and the 1400 cm^{-1} band (C-C stretching vibrations in the aromatic rings). These findings show that more aromatics were formed in the bio-chars after three cycles of catalyst regeneration, for the pre-treated microalgae. Finally, sulphides were detected at 710 cm^{-1}, with silicates also represented between 1040 to 1100 cm-1. Research on FT-IR of bio-chars from different feedstocks (lignocellulose biomasses) from pyrolysis at different temperature reported that SiO$_2$ appeared in all bio-chars increased from 400 to 800 °C. This show that bio-char getting stable at high temperature due to the silicon-carbon framework (Jindo *et al.*, 2014). Silica is an important component in plants that protect

them from degradation. Overall, the FT-IR spectrums show that the bio-chars obtained from pyrolysis are mainly composed of aromatic and aliphatic compounds.
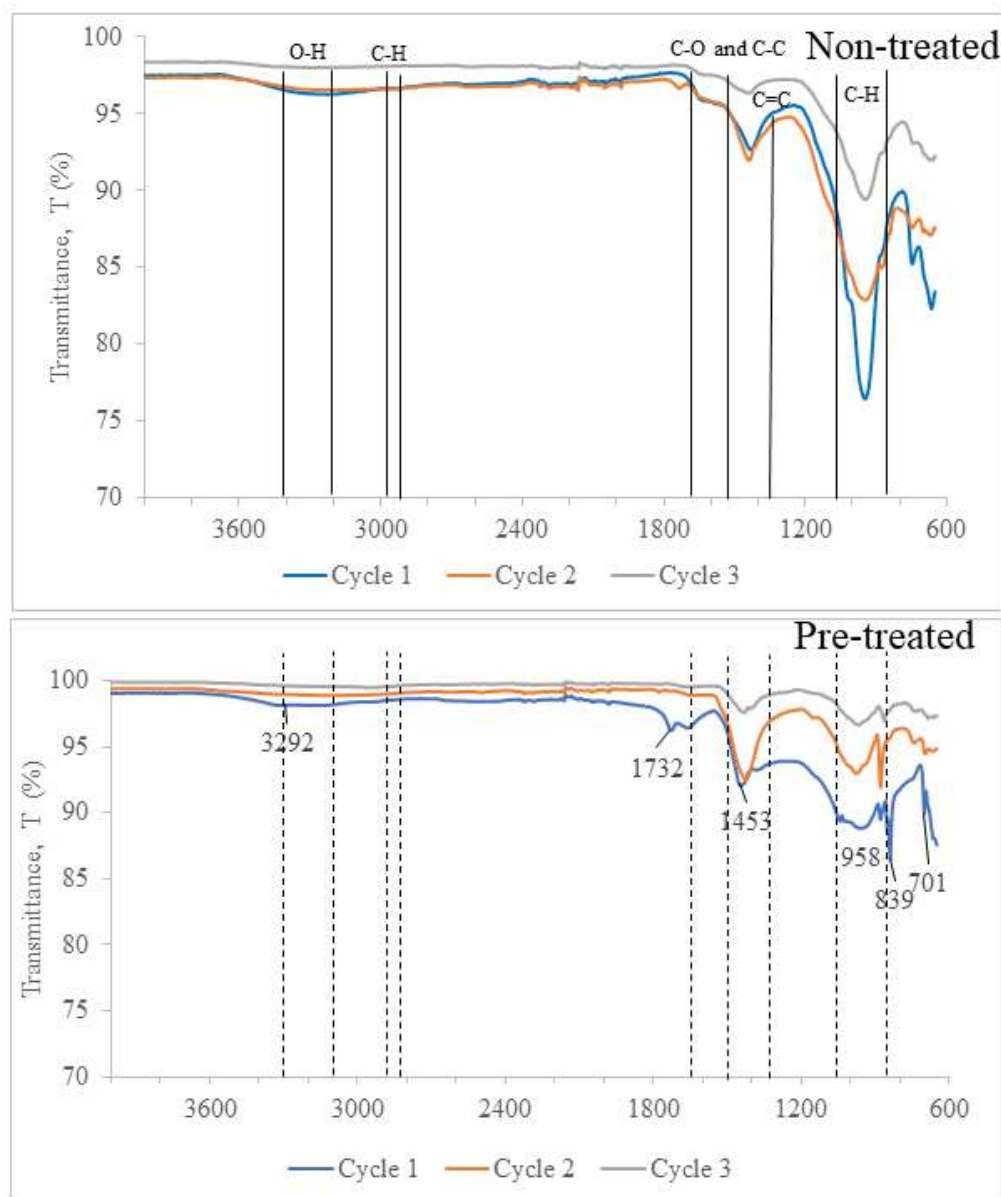
Figure 8-4 FT-IR of non-treated and pre-treated derived bio-chars after catalyst regeneration.

8.3.4 *Gaseous analyses*

The analyses of the composition of gas fractions obtained from the catalytic pyrolysis of treated and non-treated of *Isochrysis* at 500°C is presented in Table 8-2. For the non-treated microalgae, the gas yield was in the range 39.6 to 42.4 wt.%, which was higher compared to the pre-treated microalgae, 24.7 to 30.2% (see Figure 8-1).

Overall, the regenerated catalyst behaved differently in the non-treated and pre-treated microalgae cases. For the non-treated microalgae, the hydrogen content increased with increasing regeneration cycles, from 0.96 to ~1.9%. The same trend was observed with the pre-treated microalgae. The CO and CO_2 content remained almost unchanged with the non-treated microalgae, while both gas species decreased in content when the pre-treated ones where used, suggesting strong deactivation of the acid sites in the Li-LSX-zeolite. The zeolite produced less olefins and higher yields of hydrocarbons (C1-C4 alkanes) with the increased regeneration cycles, indicating a change in the catalytic activity from that related to the acid sites in the catalyst pores to crack reactions occurring on acid sites on the zeolite surface. The same trend for both non-treated and pre-treated microalgae can be observed with the nitrogenated compounds such as HCN and NH_3, where the distribution lessens with the increase in the regeneration cycles. This is to confirm that the catalyst experienced poisoning and deactivation.

The conversion of the oxygen in the pyrolysis vapours to CO, CO_2 and H_2O has been reported as the primary conversion of oxygen species for catalytic upgrading. The main aim of the catalysis of biomass pyrolysis is to upgrade the highly oxygenated pyrolysis vapours by oxygen removal to produce hydrocarbon product. Figure 8-5 illustrates the deoxygenation activity with catalyst regeneration cycles. It is clearly seen that the main deoxygenation pathways are dehydration reactions, by releasing water to the gas followed by decarbonylation then decarboxylation.

Table 8-2 Gas product distributions with catalyst regeneration cycles.

Gas product distribution (wt.%)	Non-treated			Pre-treated		
	1st cycle	2nd cycle	3rd cycle	1st cycle	2nd cycle	3rd cycle
H_2	0.96	1.43	1.88	0.96	1.29	1.11
CO	19.68	18.96	20.87	18.75	15.60	17.42
CO_2	1.55	1.63	1.29	2.57	1.87	1.08
CH_4	4.57	3.13	2.83	4.58	9.10	7.82
H_2O	11.78	16.31	17.07	11.80	11.97	17.03
HCN, NH_3	1.87	1.37	2.38	1.86	0.58	0.88
Olefins (C_2H_4, C_2H_3, C_3H_6, C_4H_8)	43.34	44.77	42.99	43.26	24.27	25.85
Alkanes (C_3H_8, C_2H_6, C_4H_{10}, C_5H_{12})	13.61	10.02	8.52	13.55	33.67	26.68
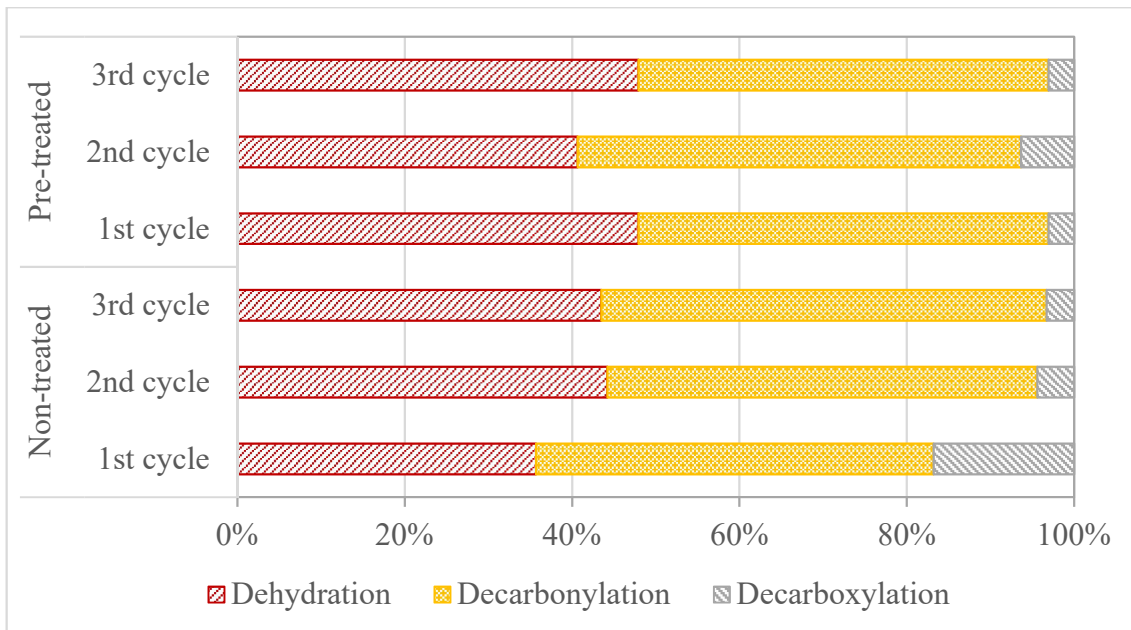
Figure 8-5 Catalytic deoxygenation activity with catalyst regeneration.

8.4 Catalyst characterisation

Catalyst samples were collected and characterised after each cycle of pyrolysis and regeneration. Prior to the characterisation, the catalyst samples were sieved to remove the accumulated free ash (from the coke in the regeneration step). The sieved samples then thoroughly characterised and used again for the next cycle of ex-situ catalytic pyrolysis. By sieving the catalyst samples, it was excluded any possible effect of the free ash on the properties of catalyst and its activity.

8.4.1 *BET analyses*

The impact of the pre-treatment of microalgae on the catalyst Li-LSX-zeolite after three cycles of regeneration is presented in Table 8-3. Initially, the BET surface area of the raw Li-LSX-zeolites was 662.0 m^2/g. After the 1st cycle of pyrolysis of both the treated and non-treated microalgae, the BET surface area was reduced to 336.6 m^2/g (non-treated

205

microalgae) and 409.1 m^2/g (pre-treated microalgae), respectively. Increasing exposure to biomass vapours/gas species resulted in a noticeable gradual reduction of the total surface area of the catalyst. The catalyst surface area was drastically reduced after the 2nd, and the 3rd cycles, with the smallest surface area, recorded after the 3rd cycle with the pre-treated microalgae, 121.5 m^2/g.

The same trend is shown by the micropore volume and surface. The fresh catalyst had a micropore volume of 0.31 cm^3/g. After the third cycle, the micropore volume was reduced to less than half of the start value (0.10 cm^3/g). Similarly, the catalyst from the non-treated microalgae pyrolysis showed a gradual decrease in the pore volume to 0.05 cm^3/g after the third cycle. The reduction of BET surface area and micropores volume and surface was probably due to the accumulation of carbon or inorganic deposits on the surface of the Li-LSX zeolite, which obstacle the further diffusion of gas/vapour species in the catalysts micropores. If the reduced surface area led to decrease bio-oil yield for the non-treated algae, as can be observed in Figure 8-1, a different trend resulted for the pre-treated microalgae, with the bio-oil yield increasing despite the decreased surface available. This suggests that the decreased acid-related cracking occurring in the Li-LSX-zeolite pores decreased, but in the same time, some other activity was taking place on the remaining micropores, on the catalyst surface that resulted in enhanced bio-oil yield. This phenomenon is discussed in the next sub-chapter (8.4.4), where the SEM-EDS analysis of the Li-LSX zeolite after the three cycles were carried out.

Table 8-3 The physicochemical properties of Li-LSX-zeolites before (raw) and after catalytic pyrolysis and regeneration cycles (at 500°C).

		BET Surface area (m^2/g)	Micropore volume (cm^3/g)	Micropore area (m^2/g)	External surface area (m^2/g)
Raw		662.02	0.31	620.27	41.76
Catalyst without pre-treatment	1st cycle	336.58	0.16	302.40	50.88
	2nd cycle	316.10	0.14	265.22	34.18
	3rd cycle	229.05	0.10	197.48	31.57
Catalyst with pre-treatment	1st cycle	409.08	0.18	339.48	69.60
	2nd cycle	176.16	0.07	122.78	53.38
	3rd cycle	121.48	0.05	98.43	23.05

8.4.2 *Elemental analyses*

The results reported in the sections above clearly suggest that the calcination at 500°C is not able to remove all the carbon deposits and the catalysts are deactivated. Therefore, a set of calcination experiments were carried out at higher temperature to establish the optimal calcination temperature. Elemental analyses were therefore used to evaluate the coking reactions that took place during pyrolysis and carried out using Elemental Analyser CHN400.

Table 8-4 shows the composition of C, H and N deposited on the catalyst surfaces. The non-treated spent catalyst showed a high carbon deposited on the catalyst surface (C: 5.9 – 6.4 wt.%). The same trend can be observed with the treated catalyst, where about 6.4 to 7.3 wt.% of C is presence on the catalyst surfaces. A small amount of H and N was also detected in the range 0.4-2.2 wt.% and 0.45-0.86 wt.%, respectively. Most of the C, H and N deposits were removed after calcination at 700 °C and completely disappeared at 950 °C, showing that the latest temperature would be ideal for the complete removal of the coke. However, it has to be noticed that previous studies suggest that the structure of Li-LSX zeolite is retained unchanged up to 700°C, so that the benefits in terms of complete carbon deposit removal, of calcining at 950°C cannot be reached without damaging the catalyst (Kodasma, Fermoso & Sanna, 2019). Therefore, the "optimal" removal of the whole N and almost all the C is achieved at 700 °C after three cycles, with no differences between the presence of treated and non-treated microalgae.

Table 8-4 Elemental analysis of spent and regenerated catalyst at 700 and 950 °C.

Samples	%C	%H	%N		%C	%H	%N
NT1	5.89	2.20	0.45	TR1	6.41	2.06	0.60
NT2	6.82	1.94	0.59	TR2	7.05	1.80	0.75
NT3	5.10	1.83	0.52	TR3	7.30	1.39	0.86
After calcination 700 °C				After calcination 700 °C			
NT17	0.34	1.61	0.00	TR17	0.16	1.64	0.00
NT27	0.32	1.52	0.00	TR27	0.16	1.00	0.00
NT37	0.14	1.62	0.00	TR37	0.15	0.40	0.00
After calcination 950 °C				After calcination 950 °C			
NT195	0.00	0.00	0.00	TR195	0.00	0.00	0.00
NT295	0.00	0.00	0.00	TR295	0.00	0.00	0.00
NT395	0.00	0.00	0.00	TR395	0.00	0.00	0.00

The header spans "Weight (wt.%)" across the value columns. Left side rows grouped under rotated label "Non-treated microalgae (NT)"; right side rows grouped under rotated label "Treated microalgae (TR)".

8.4.3 *TGA*

TGA of coked catalysts was carried out in air of 70 mL/min, with the weight loss between 20 and 700 °C being associated to coke deposits. Figure 8-6 shows the derivative thermogravimetry (DTG) curves of the coked regenerated catalysts over three cycles. Figure 8-6 gives three stages of mass loss: 20-258, 258-400 and 400-600 °C for the treat microalgae with peaks at 320 and 460°C; while only two stages (20-258 and 258-600°C) are associated to non-treated microalgae. The first peak is associated to release of moisture, while the other peaks are attributed to coke. This suggests that the coke is multi-composition, where the weight loss at moderate temperature indicates the soft coke, while peaks at higher temperatures indicate hard coke. The DTG results also indicate that the

coke formation remains the same after three cycles of regeneration at 500 °C, which is consistent to the information reported in Section 8.4.1.
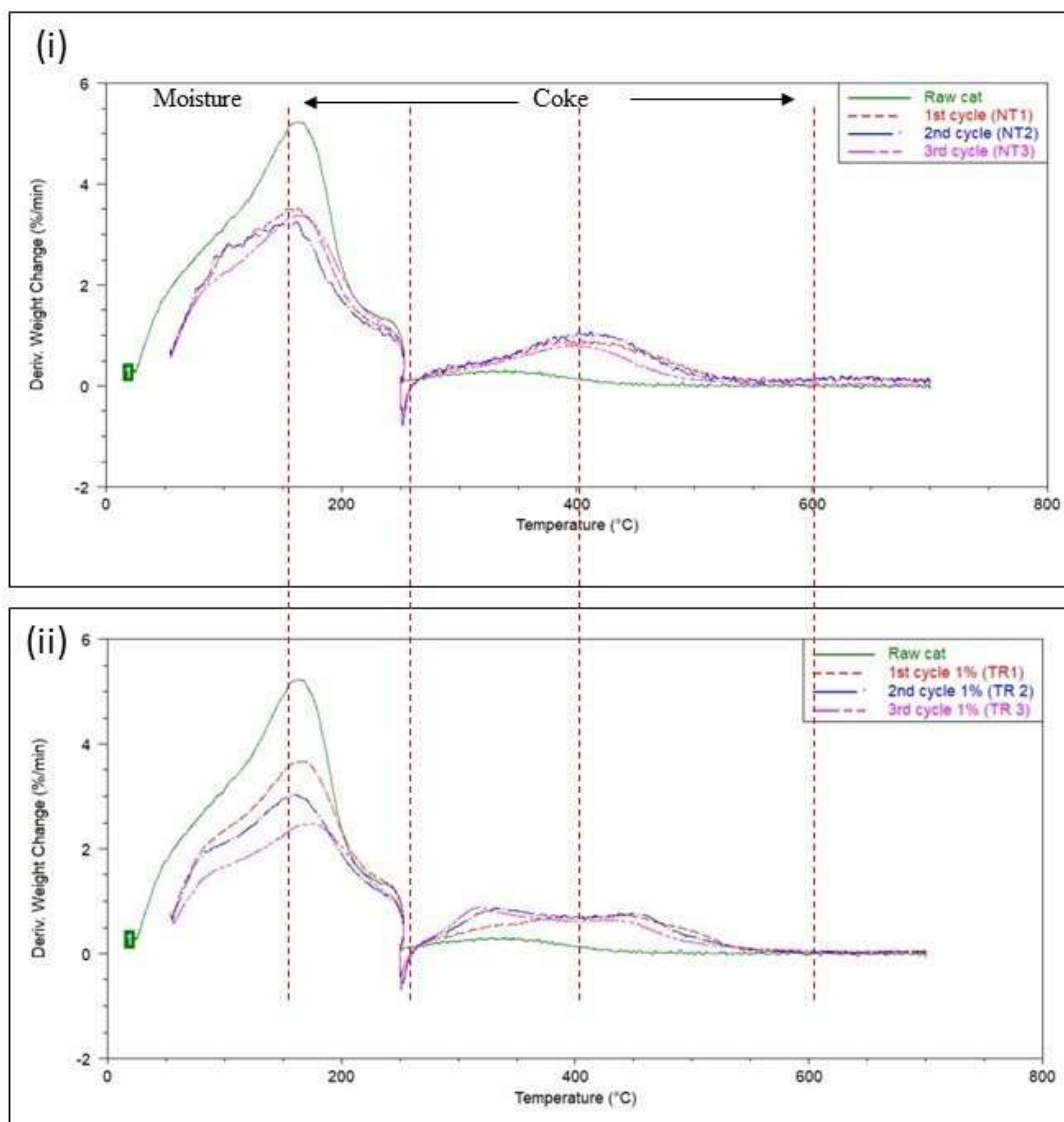
Figure 8-6 DTG of Li-LSX-zeolite catalyst regeneration of (i) non-treated and (ii) treated microalgae pyrolysis.

The amount of coke formed on samples was calculated by the TGA plots and reported in Table 8-5. Total coke formation for each cycle varies from 5.62% to 9.11%. The deviation of coke removal during the process might happen due to the presence of impurities or

disturbance during the experiment were carried out. The coke formation in Li-LSX-zeolite from non-treated microalgae average of 8% while from treated microalgae average of 8.01%. Hernando et al. investigate on coke formation of MCM-22 zeolite during the catalytic pyrolysis of wheat straw. The study showed that coke deposited range between 3.9 to 5.2 wt.% respected to the biomass feed (Hernando *et al.*, 2017a). Meanwhile, another study comparing two catalysts on fast pyrolysis of glucose. The results show that MCM-22 produced high coke compared to H-ZSM-5 due to the porous structure of MCM-22 that provide space for coke accumulations (Jae *et al.*, 2011). These data indicate that higher calcination temperature is required for the regeneration of Li-LSX-zeolite.

Table 8-5 Coke removal (%) of catalyst regeneration at different cycles.

Samples	Total coke (%)
NT1	8.81
NT2	8.61
NT3	5.62
TR1	7.99
TR2	9.11
TR3	7.92

8.4.4 *SEM-EDX*

The SEM pictures of the fresh, spent and regenerated (at 700 °C) zeolite are presented in Figure 8-7 to verify the potential sintering of the catalyst particles and the effect of thermal regeneration on the removal of deposited coke.

The EDS of the calcined Li-LSX-zeolite (Figure 8-7) present remarkable changes compared to the fresh catalyst, when the pre-treated microalgae were used. First, the EDS analyses indicate a much more dramatic decrease in Al, Si and O content in the catalyst

surface and second, it further reveals that other elements such as Ca (in less extent), Na, C, P and S increased double fold or more compared to the fresh catalyst. Therefore, the presence of clusters of deposits on the catalyst surface (see Figure 8-8) before regeneration can be referred to the formation of sulphate species (for example; Ca/Na$_2$SO$_4$), phosphorus species and carbonaceous species (coke). It seems that the sulphur from the sulphuric acid solution reacted to the Na+ (removed from the microalgae structure during the acid leaching) forming Na2SO4, which precipitated and therefore was recovered together to the leached microalgae. Similarly, phosphorus species accumulated by the pre-treated microalgae.
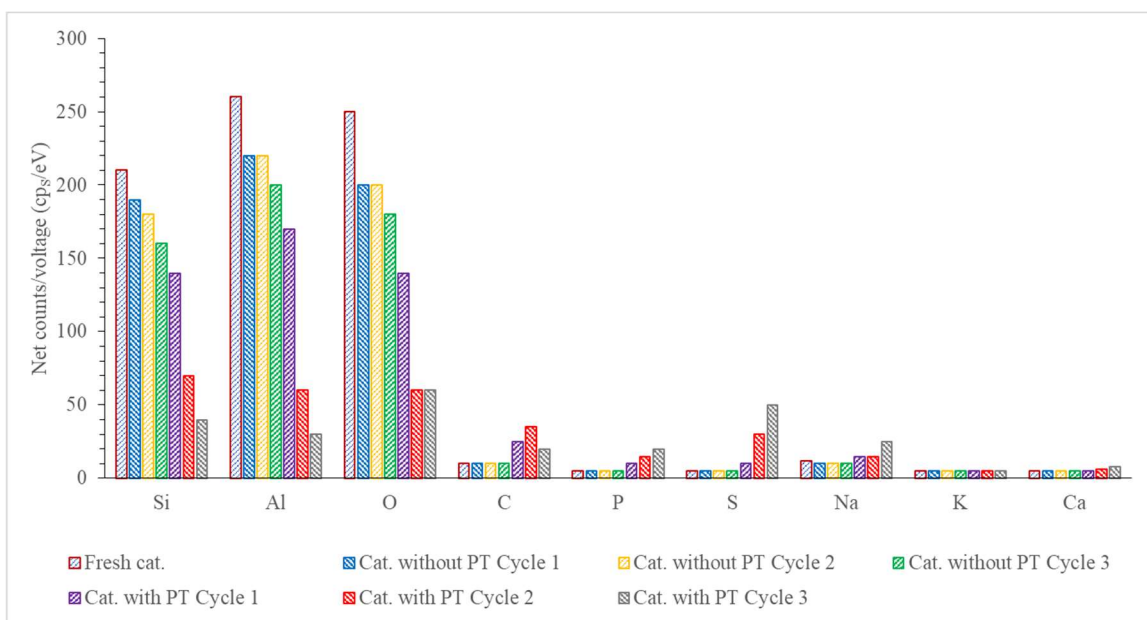
Figure 8-7 EDS of spent catalysts after the regeneration step at 500 °C.

Figure 8-8 shows the Li-LSX zeolite after the calcination at 700°C that the fresh Li-LSX zeolite is formed by uniform crystals with sizes within the size of 500–600 nm. Large particles can be observed in the calcined zeolite as a consequence of some sintering. On the contrary, the SEM photograph of the regenerated zeolite is very similar to that of the fresh one, which indicates that it recovers its textural appearance after the regeneration process at 700°C. Although SEM image shows some disruption of original sphere shape

structure in the regeneration catalyst, which is an indication of a partial collapse in the catalyst morphology, this observation could be responsible for the reduction in surface and pore characteristics recorded.

A quantitative analysis of EDX demonstrated a different elemental surface composition before and after the regeneration of Li-LSX-zeolite as summarised in Table 8-2. The presence of carbon, oxygen, silicon, sodium and aluminium were analysed. The carbon content was remarkably reduced indicating that most of the coke was removed after regeneration at 700°C. The Si/Al ratio remained unchanged after regeneration, showing that the change in catalyst acidity cannot be linked to the yield of bio-oil from pyrolysis. Hernando et al. discussed that low Si/Al ratio of catalyst promotes non-desired reactions; enhanced the production of gaseous and coke formation (Hernando *et al.*, 2017b). The changes observed in the catalyst properties after regeneration, particularly the surface area, which is directly proportional to the number of active sites, can be attributed to the declined performance recorded after each cycle. The increased presence of Na after the thermal regeneration can be linked to the decreased surface available.

Table 8-6 EDX results of Li-LSX-zeolite catalyst before and after regeneration at 700°C.

Weight (wt.%)						
Element	C	O	Al	Si	Na	Si/Al
NT1	24.34	55.06	10.05	9.71	0.42	0.97
NT2	23.74	56.04	10.06	12.90	0.49	1.28
NT3	22.06	57.67	9.77	10.12	0.38	1.04
After regeneration at 700 °C						
NT170	12.36	54.59	16.11	16.84	0.10	1.05
NT270	9.71	56.17	16.08	17.10	0.68	1.06

NT370	3.97	57.07	18.85	18.81	0.43	1.00
TR1	27.17	54.62	8.74	8.61	0.86	0.99
TR2	26.14	49.04	8.43	9.10	2.85	1.08
TR3	21.28	52.85	10.18	10.55	3.49	1.04
After regeneration at 700 °C						
TR170	13.31	54.23	14.52	15.03	1.43	1.04
TR270	11.01	56.03	14.86	15.36	1.87	1.03
TR370	10.45	49.98	12.96	12.73	2.51	0.98

	Fresh catalyst	Spent catalyst (Without pre-treatment)	Regenerated catalyst (Without pre-treatment)	Spent catalyst (With pre-treatment)	Regenerated catalyst (With pre-treatment)
1st cycle					
2nd cycle					
3rd cycle					
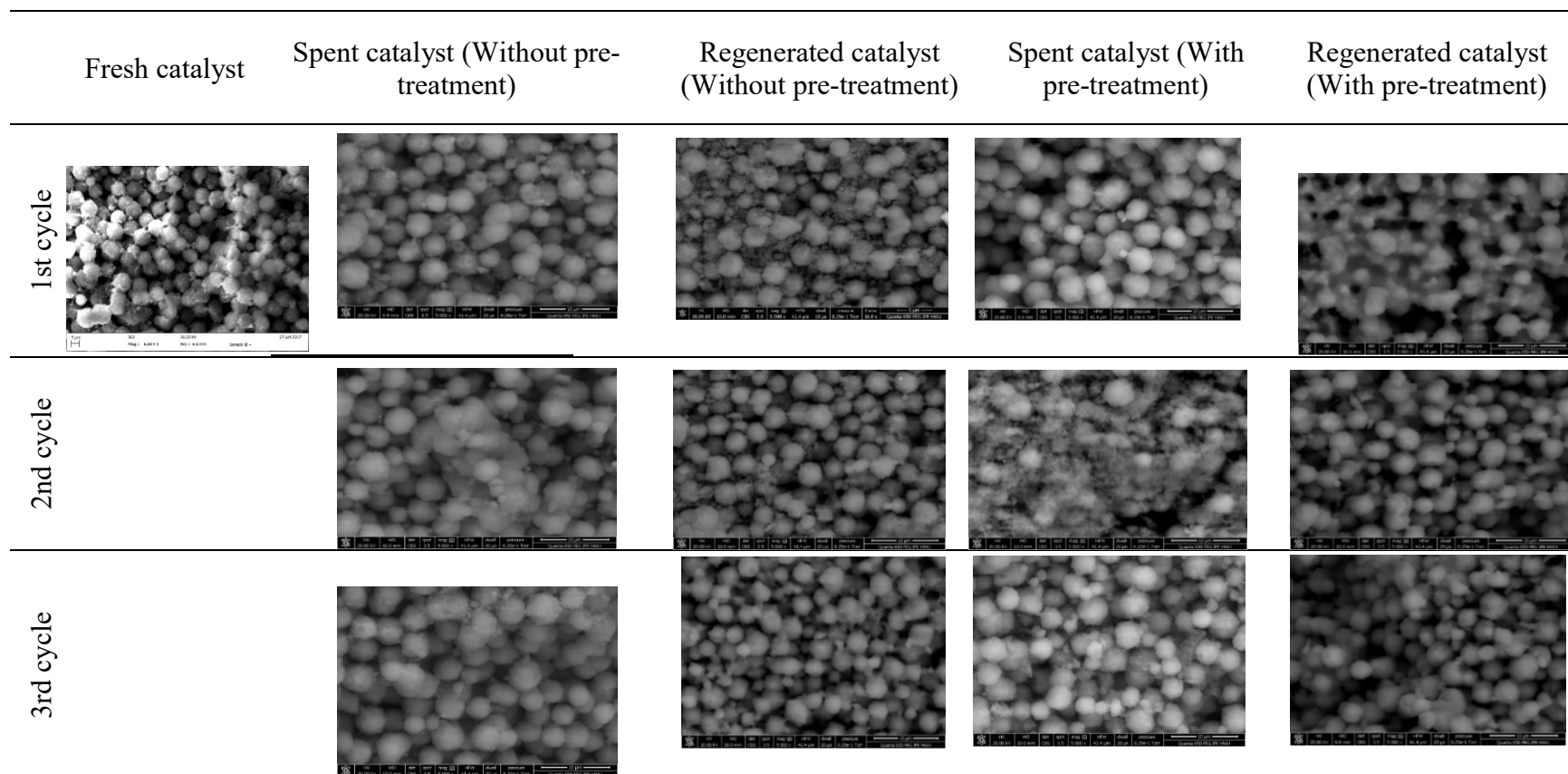
Figure 8-8 SEM-EDX of raw, spent and regenerated catalyst from treated and non-treated pyrolysis at 700 °C.

8.4.5 *XRD*

The XRD patterns of the regenerated catalysts at the two different temperatures were collected after 1st, 2nd and 3rd regeneration cycles in the presence of treated and non-treated microalgae (Figures 8-9). Differently, the XRD patterns of the Li-LSX regenerated at 700 °C do not present significant differences with the fresh Li-LSX-zeolite, confirming that the crystalline structure was retained after the thermal treatment and did not differ as the catalyst was regenerated three times. This indicates that the crystallite particles remain the same during the successive cycles. However, there is a slight increased peak for the regenerated catalyst from the treated microalgae (Figure 8-9 (b, c)) at 23° 2-theta, in particular after the 3rd cycle. This indicates carbon deposition after three cycles, which correlates well with data reported in Table 8-1.
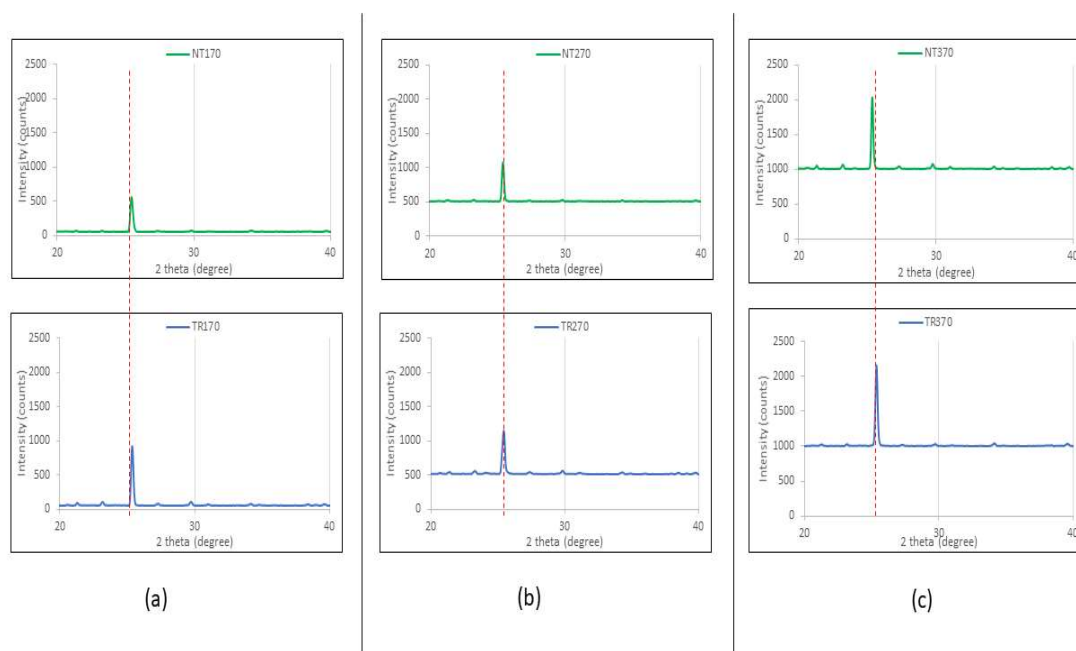
Figure 8-9 XRD patterns of Li-LSX-zeolite catalyst after 1 (a), 2 (b) and 3 (c) regeneration cycles at 700 °C.

The catalysts regenerated at 950 °C (not shown in the figure) instead presented completely different XRD patterns compared to the fresh Li-LSX zeolite suggesting a modification of the crystalline structure. This is corroborated by the previous work, where the thermal stability of this material was reported up to 700 °C (Kodasma, Fermoso & Sanna, 2019). The XRD patterns indicate the presence of SiO_2 (26 2-theta) and Al_2O_3 phases in the annealed material.

8.4.6 *FT-IR of regenerated catalysts*

To further investigate the effect of the catalyst regeneration using Li-LSX-zeolite, FTIR was performed to the different catalyst remaining after the three pyrolysis cycles. Figure 8-10 illustrated the FTIR spectra of the Li-LSX-zeolite catalysts when the treated and non-treated microalgae were used. Several absorption bands can be found between 500 and 4000 cm^{-1}, from which the different characteristics of the spent catalyst can be found. As expected, catalyst samples behave in a similar way regarding each cycle, presenting small difference after the pyrolysis. Peaks between 3400 to 3600 cm^{-1} are assigned to hydroxyl (OH) stretching. It shows that there are slight changes between the cycles showing the interaction or displacement of hydroxyl groups with the adsorbed NO_x^- species. However, the difference is too small to define. C-C stretching vibrations between 1450 and 1650 cm^{-1} indicate the presence of aromatic structures, probably trapped in the catalyst pores, which were not completely removed in the regeneration stage. A study on characterisation of coke deposit from catalytic pyrolysis of biomass derivates using FTIR were carried out. Their work indicates that the coke formation increases according with the temperature increase (Zhang *et al.*, 2014). The bands that appears at frequencies lower than 700 cm^{-1} can be attributed to the vibration of Si-O-or Al-O symmetric stretching vibration of the zeolite structure (Chumee & Materials, 2013). There are no clear changes between the cycles, indicating that the Si-O-Al structure are not deteriorated after several cycles.
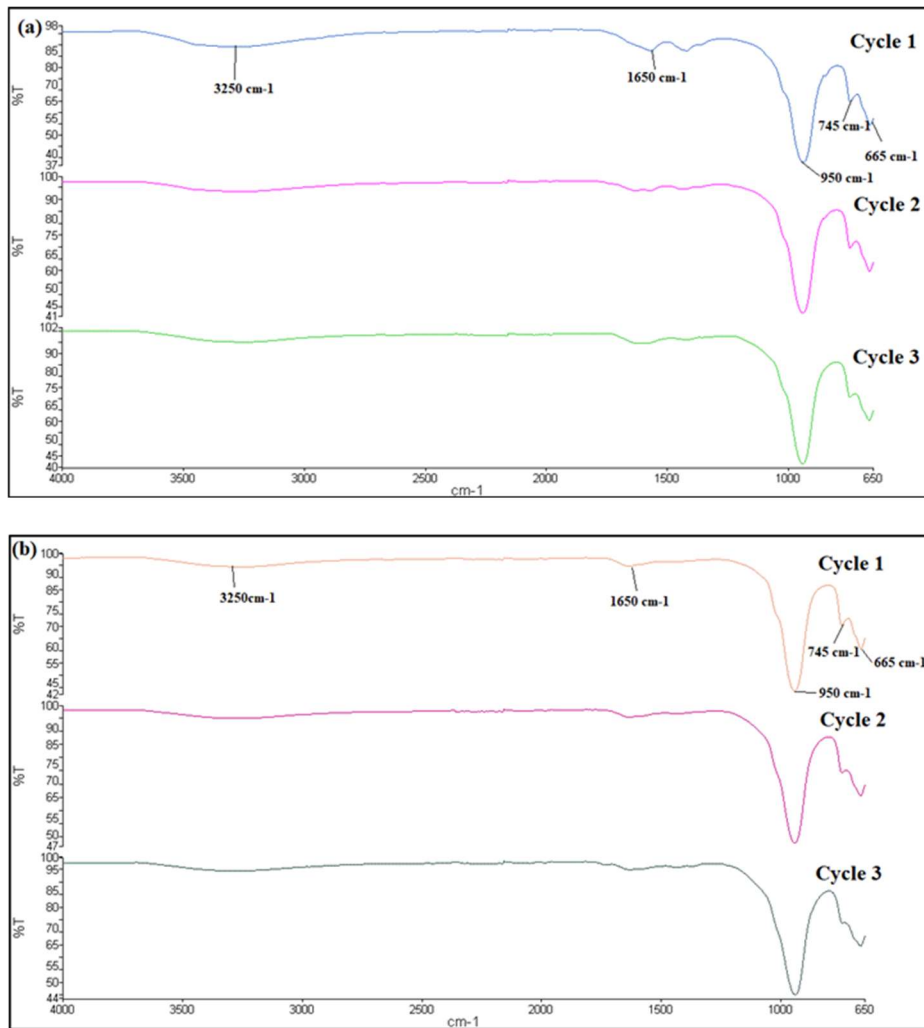
Figure 8-10 FT-IR catalysts from pyrolysis of (a) non-treated microalgae (b) treated
microalgae after three cycles of catalyst regeneration.

8.5 Summary

The Li-LSX-zeolite catalyst was used on pyrolysis of non-treated and treated microalgae
and regenerated for three cycles. Overall, a very different behaviour was noticed in the
pyrolysis process when non- or pre-treated microalgae where used. For the pyrolysis of
non-treated microalgae, the bio-oil yield slightly decreased, and the gaseous yield
increased after three cycles, while the bio-oil yield increased for the treated microalgae at
the expenses of gas.

The products distribution and the BET analysis show that the catalyst can maintain a reasonable catalytic activity for cracking over three cycles in the presence of non-treated microalgae; however, strong deactivation occurred in the three cycles when pre-treated microalgae were processed. Despite this, the regeneration process resulted in a modified catalyst that was able to enhance the bio-oil yield and shift the bio-oil composition from aromatic to aliphatic-rich.

The BET measurements show a decrease in surface area from the first to the third cycles, especially on the catalyst when treated microalgae where used. The surface decrease was of 30% for the non-treated microalgae and 70% for the treated ones. A severe deactivation was observed for the catalyst used with pre-treated microalgae, where materials were deposited and agglomerated on the catalyst surface after the regeneration, showing that the catalyst structure was modified. A trace amount of P, S, Na (for example; Na_2SO_4) appeared to deposit on the regenerated catalyst. This indicate that the mineral in the microalgae did not poison the catalyst. Instead, it was the mineral accumulation from the pre-treatment reactions that poisoned the catalyst.

Coke formation influenced not only on the catalyst activity but also the product distribution. The degree of aromatisation depends on the catalyst acidity that decreased after the third cycle of regenerations. Carbonyl and nitrogenated groups increased after the third cycles related to the decreased in the catalyst activity, especially with the acid leached microalgae. The BET, NMR, GC-MS and EA results suggest that the Li-LSX-zeolite catalyst lose its function after three cycles, due to the carbon deposition and sodium sulphate (for the pre-treated microalgae) and is not able to efficiently denitrogenate the bio-oil. The results discussed in this chapter suggest that the pre-treatment significantly affect the catalyst activity resulting in a very different catalytic activity that enhanced the bio-oil yield and changed the composition of the bio-oil to a more aliphatic one. However, the deoxygenation and the denitrogenation capacity were greatly lowered. To reduce the catalyst deactivation, a regeneration temperature of 700 °C was found to be effective.

Chapter 9
Conclusions and recommendations

9.1   Conclusions

The aim of this research was to convert microalgae using pyrolysis into bio-oil and adding catalyst to enhance the quality of the bio-oil produced for fuels and chemicals production. This work aimed to address some of the limitations that hinder microalgae as replacement for fossil fuels.

The technical viability of converting *Isochrysis* sp. microalgae into bio-oil by catalytic pyrolysis in presence of Li-LSX-zeolite was proved. Li-LSX-zeolite was able to greatly reduce the nitrogen content in the bio-oil and form aromatic compounds thanks to its acidity and pores size. Mild acid pre-treatment could be used to enhance the bio-oil yield, but at expenses to the denitrogenation activity of Li-LSX-zeolite. To reduce the effect of coking on Li-LSX zeolite, the catalytic must be regenerated at 700°C.

The following sections summarise the conclusions drawn from each chapter.

9.1.1   *Characterisation and pyrolysis of microalgae for biofuel production*

Three species of microalgae were assessed for bio-fuel production; *Isochores*, *Nannochloropsis* and *Tetraselmis*. The aim of this work was to establish if any of the selected microalgae could be used as a source for bio-fuels through thermo-chemical processing and also to evaluate their potential direct upgrading by catalytic pyrolysis. These three species contain high carbon content and their decomposition profiles are suitable for bio-oil production by pyrolysis. Among the three species, *Isochrysis* sp. produced the largest bio-oil fraction (37.2 wt.%) during pyrolysis, indicating a good suitability of this species as transportation fuel feedstock. *Tetraselmis* sp. was found to be less suitable for production of bio-oil, mostly due to the low oil yield and the large

retention of nitrogen in the bio-oil (42%). This was correlated to the large protein content in *Tetraselmis* sp., which resulted in charring reactions. Moreover, bio-oil produced from *Isochrysis* contained high abundance of aliphatic compounds (derived mostly form the lipids), lower aromatics and N-compounds compared to the other microalgae bio-oils, which was linked to the low starting protein content of *Isochrysis*. Therefore, the composition of the different microalgae play an important role for define their best pathway to produce transportation fuels. *Isochrysis* sp. was selected for further work on its catalytic upgrading for bio-oil quality enhancement. Another important aspect that clearly affected the retention of carbon in the bio-oil was the abundant presence of alkali and alkaline earth metals, which catalyse cracking reaction and led to large gas yield. In view of this, the demineralisation of *Isochrysis* was defined as a potential strategy for enlarge the organic retained in bio-oil.

9.1.2 *Catalytic pyrolysis of microalgae Isochrysis sp.to fuels and chemicals*

This chapter investigated on the effect of addition of Li-LSX-zeolite (zeolite), micro-powder SiO_2 Na-FA and Na-Li-FA catalysts for the pyrolysis of microalgae. The screening of the catalysts over microalgae pyrolysis was conducted with an in-situ fixed bed configuration at 500 °C using a catalyst: microalgae ratio of 1:1. The product yields, bio-oil properties and composition and net energy content were compared to those obtained with non-catalytic pyrolysis. Overall, the addition of catalysts reduced the bio-oil yield of about 16-26 % compared to the non-catalytic pyrolysis bio-oil yield. The strong acid catalyst (Li-LSX-zeolite) and the weak acid catalyst (micro-silica) favoured the cracking of microalgae and produced large fraction of gaseous products (~36-37 wt.%). Most of the N-compounds were released into gaseous form (NH_3 and HCN) by using Li-LSX-zeolite, meanwhile the remnant catalyst retained N-compounds in the bio-oil. This behaviour was confirmed by the bio-oils characterisation, which showed that Li-LSX-zeolite was able to reduce the nitrogen content of about 46% of the non-catalytic run. All the catalysts used enlarged the fraction of aliphatic compounds in the bio-oil, but only Li-LSX-zeolite promoted the formation of aromatics compounds, which passed from 3.4 rel.% (non-catalytic) to ~20 rel.%. In the presence of catalyst, the oxygen was

eliminated by decarbonylation, followed by dehydration and decarboxylation reaction. Therefore, this study showed that Li-LSX-zeolite catalyst is a promising catalyst for the in-situ removal of N from microalgae bio-oil and for the production of a mixture of aliphatic and aromatics for bio-fuel applications.

9.1.3 *Optimisation studies on catalytic pyrolysis of Isochrysis sp. using Li-LSX-zeolite catalyst*

This chapter investigated the effects of process parameters such as temperature, catalyst: biomass ratios, sweep gas flow rate and reactor configuration on the pyrolysis products distribution and composition of *Isochrysis* sp. microalgae. Catalytic pyrolysis of *Isochrysis* sp. was conducted using fixed bed reactor at 400 to 700 °C, with different catalyst: biomass ratio (varied from 0.5:1, 1:1 and 3:1), sweep gas flow rate (1250, 345 and 210 ml/min) and reactor configurations (in-situ vs ex-situ).

At 500 °C, 11.8% aromatics and 23.1% aliphatic were produced. The increase in temperature led to the transfer of C to the gas phase, coke formation on the catalyst surface and decrease in N-compounds in the bio-oil. Increasing the catalyst to biomass ratio reduced the bio-oil yield and promoted cracking generating light alkenes and olefins in the gaseous phase. In particular, the increase in the catalyst to biomass ratio from 0 to 3 to 1 resulted in the aromatics being five-fold those non-catalytically obtained and in a higher cracking power that reduced the bio-oil to 23% at expenses of olefins rich gas. At the same time, the increase in the catalyst to microalgae ratio resulted in an increase production of PAH compounds, so that the optimum aliphatic and aromatics compounds can be achieved with ratio of 1:1. This shows that the products composition can be obtained by tuning the catalyst: microalgae ratio.

The investigation of the pyrolysis sweep gas flow rate into the reactor indicated that the maximum bio-oil yield can be obtained at low flow rate, 210 ml/min (37.9 wt.%), while the high flow rate (1250 ml/min) produced larger fraction of gas (~39.1 wt.%).

The reactor configuration affected the composition of the bio-oil, with increased abundance of short chain aliphatic and monoaromatics produced with the ex-situ configuration. The ex-situ configuration also increased the gas yield and maximised the removal of N in gas phase to 68%. The formation of char in proximity of the Li-LSX-zeolite pores openings in the in-situ mode, can obstruct/slow down the diffusion in and out of the cracked primary species resulting in less secondary cracking/molecules rearrangement to olefins and monoaromatics and enhanced condensation reactions.

As a conclusion, the optimum condition for pyrolysing Isochrysis sp. microalgae using Li-LSX-zeolite include temperatures close to 500 °C, sweep gas flow rate of ~345 ml/min, microalgae: catalyst ratio of 1:1 and an ex-situ configuration, towards a low N content bio-oil and olefins rich gas phase.

9.1.4 *Effect of chemical pre-treatment on pyrolytic bio-oil from microalgae*

This chapter evaluates the effect of de-ashing microalgae biomass using different solvents via chemical pre-treatment. The demineralisation of *Isochrysis* was defined as a potential strategy for enlarge the organic retained in bio-oil as well as to reduce charring and gasification reactions. The solvents used were water, H_2SO_4 and NaOH with different concentrations (0.1%, 1% and 4%). The pre-treatment leached out alkali and alkaline-earth metals in the following orders: H_2SO_4> Water > NaOH. About 53% of Na were leached out using H_2SO_4, while 24% Na removal using water and no Na compounds were detected after NaOH pre-treatment due to re-precipitation of Na salts.

It was found that pre-treatment had a significant effect on the pyrolysis yields and products composition. The bio-oil yield was boosted using acid pre-treatment (from 29 to 38.3 wt.% with 4% H_2SO_4), while basic pre-treatment tailored gas formation (0.1 and 1% NaOH) and char (4% NaOH). This was linked to the leaching of alkali and alkaline-earth metals by the acid pre-treatment, and the simultaneous de-structuring on the microalgae main components (long chain fatty acids, proteins and carbohydrates) and the

re-precipitation of alkali salts when the base was used, which led to gasification and charring reactions.

However, the pre-treatment reduced the denitrogenation activity of the Li-LSX-zeolite. Pyrolysis of the acid treated microalgae altered the chemical compounds presence in the bio-oil produced, increasing the formation of aliphatic and aromatic compounds. Instead, the basic pre-treatment resulted in bio-oil rich in PAH and nitrogenates compounds. Overall, the mild acid pre-treatment (1%) should be preferred due to low-cost treatment, although the bio-oil composition can be tailored by tuning the concentration of the acids.

9.1.5 *Catalytic pyrolysis of non-treated and pre-treated Isochrysis sp. microalgae: Li-LSX-zeolite activity and regeneration*

This chapter investigates the use of Li-LSX-zeolite catalyst over several regeneration cycles on non-treated and treated *Isochrysis* sp. microalgae to evaluate the stability over cycles of this material and how its activity varies after number of cycles, as it may affect the process viability. Coke formation has been shown to be extremely high during the pyrolysis, suggest that the coke was formed from combination of graphitic carbon and aromatic hydrocarbon that condensed on catalyst surface.

The SEM-EDS analyses suggested that there were no changes on catalyst from non-treated microalgae while, the structure of catalyst from treated microalgae contained high clumped materials. The Li-LSX-zeolite in the presence of the pre-treated microalgae suffered strong deactivation due to deposition of Na_2SO_4 (formed during pre-treatment) and coke on the regenerated catalyst surface at 500°C. During catalytic pyrolysis, the non-treated microalgae showed a reducing trend for the bio-oil yield cycle after cycle. On contrary, bio-oil yield increased after three cycles of catalyst regeneration, when the pre-treated microalgae were processed. In this case, the removal of alkali metals and the reduced acidity of the regenerated catalyst (denoted by the reduced production of aromatics) aided the catalyst to react and produced more condensable volatiles

compounds compared to the non-treated microalgae. On the catalyst activity, pyrolysis of both treated and non-treated microalgae showed deactivation after three cycles. After three cycles, an increase in oxygenate and nitrogenate compounds was observed, as well as a reduction in the presence of aromatic compounds in the bio-oil. This suggests that the acidity of Li-LSX-zeolite was reduced after several cycles of regeneration, resulting in a higher bio-oil yield richer in aliphatic compounds. To avoid this, the regeneration of the catalyst was attempted at higher temperatures (700-950°C), with 700°C resulting effective in removing most of the coke deposits from the catalyst, without modifying its structure.

9.2   Recommendations and future work

The utilisation of microalgae to produce bio-oil via catalytic pyrolysis was investigated in this work. Although this research has reached its aims, some works can be extended. Despite the effects of operating conditions including temperature, sweep gas flow rate and the effects of different catalyst on product yields and qualities were investigated, there are still many unexplored areas under this research topic. More studies are needed in the future in order to improve the conversion efficiency, bio-oil quality and finally, to understand the detailed reaction mechanisms.

9.2.1   *Microalgae Improvement/Modification*

Despite *Isochrysis* and *Nannocloropsis* sp. microalgae being shown to be good feedstock for biofuels production, the seasonal variability of their composition has to be taken into account. The variability may result in undesirably high content of alkali/alkaline earth metals and low content in fatty acids. Therefore, methods such as genetic modifications and/or controlled growth environment should be pursued to enhance the production of fatty acids and to reduce the ash content. Moreover, cost-effective separation of the microalgae cells from the water media represents a key aspect for the future success of the "dry" thermochemical conversion of microalgae to transportation fuels.

9.2.2 *Selection of catalysts and reactors for microalgae pyrolysis*

This study proved the ability of the Li-LSX-zeolite catalyst to enhance the quality of bio-oil by reducing the O and (mostly) N-compounds presence in the bio-oil, and that it can be tuned to produce compounds compatible with gasoline and diesel. However, this study also shows that the catalyst lose activity over three cycles due to coking and metal contamination. The regeneration study showed that regeneration at 700 °C was able to remove most of the coke deposits, suggesting that the catalyst activity could be retained operating at this temperature. To confirm this, a set of experiments towards the evaluation of the products yield/quality should be carried out with catalyst regeneration at 700 °C instead of 500 °C. Moreover, the catalyst can be impregnated with noble metals such palladium, rhodium and gallium or nickel to find the best catalytic system towards products selectivity and reduced deactivation. These noble metals promote Brønsted acid sites on the zeolites network and tailored the acidity of the catalyst. Therefore, in addition to metal impregnation method, the catalyst can be prepared with different method, either sol-gel or ion-exchange method. The catalyst preparation can give differences in the properties of bifunctional catalysts.

The reactor used in this work was a single fixed bed reactor with different configurations. Further catalytic work could investigate the combination of two or more secondary fixed bed reactor systems that can be set-up at different conditions, instead of one, to evaluate the progression of coking over time. Configurations that enable to recover the catalyst in a more precise way for further evaluation and characterisation should be accounted. Also, the microalgae species investigated in this work should be processed using reactors with continuous feeding such as fluidised beds or auger reactors for future larger scale upgrading of the bench scale unit to an industrial unit. In addition, larger scale catalytic experiments should be performed to produce bio-oil in large quantities. This will enable the application of further analysis such as viscosity test, which was not possible in the present study due to the low quantities of bio-oil.

9.2.3 *Life cycle assessment (LCA)*

Although microalgae are treated as one of the most popular feedstocks for producing next generation of biofuel, the study on the economical and energy recovery produce large amounts of algal biomass for biofuel production has not been achieved yet. Therefore, no matter what technologies are selected as the conversion process, a comprehensive life cycle assessment (LCA) is essential to evaluate the feasibility of the system. The LCA process should covered from the upstream processes including algae growing, harvesting and dewatering, and the downstream processes, including bio-crude oil upgrading or refining. In other words, the boundary of LCA must cover the whole processes (upstream and downstream) to evaluate whether this approach is economically and energetically favourable.

References

Abd Rahman, N.A., Fermoso, J. & Sanna, A. (2017) Effect of Li-LSX-zeolite on the in-situ catalytic deoxygenation and denitrogenation of Isochrysis sp. microalgae pyrolysis vapours. *Fuel Processing Technology*. 173 (January), 253–261.

Ahmad, a. L., Yasin, N.H.M., Derek, C.J.C. & Lim, J.K. (2011) Microalgae as a sustainable energy source for biodiesel production: A review. *Renewable and Sustainable Energy Reviews*. 15 (1), 584–593.

Amin, S. (2009) Review on biofuel oil and gas production processes from microalgae. *Energy Conversion and Management*. 50, 1834–1840.

Aysu, T., Abd Rahman, N.A. & Sanna, A. (2016) Catalytic pyrolysis of Tetraselmis and Isochrysis microalgae by nickel ceria based catalysts for hydrocarbon production. *Energy*. 103, 205–214.

Aysu, T., Maroto-Valer, M.M. & Sanna, A. (2016) Ceria promoted deoxygenation and denitrogenation of Thalassiosira weissflogii and its model compounds by catalytic in-situ pyrolysis. *Bioresource Technology*. 208 (May), 140–148.

Aysu, T., Ola, O., Maroto-Valer, M.M. & Sanna, A. (2017a) Effects of titania based catalysts on in-situ pyrolysis of Pavlova microalgae. *Fuel Processing Technology*. 166, 291–298.

Aysu, T., Ola, O., Maroto-Valer, M.M. & Sanna, A. (2017b) Effects of titania based catalysts on in-situ pyrolysis of Pavlova microalgae. *Fuel Processing Technology*. 166, 291–298.

Aysu, T. & Sanna, A. (2015) Bioresource Technology Nannochloropsis algae pyrolysis with ceria-based catalysts for production of high-quality bio-oils. *Bioresource Technology*. 194, 108–116.

Babich, I. V., van der Hulst, M., Lefferts, L., Moulijn, J.A., et al. (2011) Catalytic pyrolysis of microalgae to high-quality liquid bio-fuels. *Biomass and Bioenergy*. 35, 3199–3207.

Bae, Y.J., Ryu, C., Jeon, J.-K., Park, J., et al. (2011) The characteristics of bio-oil produced from the pyrolysis of three marine macroalgae. *Bioresource technology*. 102 (3), 3512–3520.

Bartholomew, C.H. (2001) Mechanisms of catalyst deactivation. *Applied Catalysis A: General*. 212 (1–2), 17–60.

Beer, L.L., Boyd, E.S., Peters, J.W. & Posewitz, M.C. (2009) Engineering algae for biohydrogen and biofuel production. *Current Opinion in Biotechnology*.

Behera, S., Arora, R., Nandhagopal, N. & Kumar, S. (2014) Importance of chemical pretreatment for bioconversion of lignocellulosic biomass. *Renewable and*

Sustainable Energy Reviews. 36, 91–106.

Bi, Z. & He, B. (2013) Characterization of microalgae for the purpose of biofuels production. *Trans. ASABE*. 56 (4), 1529–1539.

Brennan, L. & Owende, P. (2010) Biofuels from microalgae—A review of technologies for production, processing, and extractions of biofuels and co-products. *Renewable and Sustainable Energy Reviews*. 14 (2), 557–577.

Bridgwater, a. V. (2012) Review of fast pyrolysis of biomass and product upgrading. *Biomass and Bioenergy*. 38, 68–94.

Bridgwater, T. & Watkinson, I. (2015) *Biomass and Waste Pyrolysis A Guide to UK Capabilities*.

Bu, Q., Lei, H., Ren, S., Wang, L., et al. (2012) Production of phenols and biofuels by catalytic microwave pyrolysis of lignocellulosic biomass. *Bioresource Technology*. 108, 274–279.

Campanella, A. & Harold, M.P. (2012) Fast pyrolysis of microalgae in a falling solids reactor: Effects of process variables and zeolite catalysts. *Biomass and Bioenergy*. 46, 218–232.

Campanella, A., Muncrief, R., Harold, M.P., Griffith, D.C., et al. (2012) Thermolysis of microalgae and duckweed in a CO_2-swept fixed-bed reactor: bio-oil yield and compositional effects. *Bioresource technology*. 109, 154–162.

Carlson, T.R. (2010) *Catalytic Fast Pyrolysis of Biomass for the Production of Fuels and Chemicals*. University of Massachusetts - Amherst.

Carlson, T.R., Cheng, Y.-T., Jae, J. & Huber, G.W. (2011) Production of green aromatics and olefins by catalytic fast pyrolysis of wood sawdust. *Energy & Environmental Science*. 4 (1), 145.

Carlson, T.R., Tompsett, G. a., Conner, W.C. & Huber, G.W. (2009) Aromatic Production from Catalytic Fast Pyrolysis of Biomass-Derived Feedstocks. *Topics in Catalysis*. 52 (3), 241–252.

Chaiwong, K., Kiatsiriroat, T., Vorayos, N. & Thararax, C. (2013) Study of bio-oil and bio-char production from algae by slow pyrolysis. *Biomass and Bioenergy*. 56, 600–606.

Channiwala, S.A. & Parikh, P.P. (2002) A unified correlation for estimating HHV of solid, liquid and gaseous fuels. *Fuel*. 81 (8), 1051–1063.

Chen, M. qiang M. gong, Wa, J., Zhang, M. xu, Chen, M. qiang M. gong, et al. (2008a) Catalytic effects of eight inorganic additives on pyrolysis of pine wood sawdust by microwave heating. *Journal of Analytical and Applied Pyrolysis*. 82 (1), 145–150.

Chen, M. qiang, Wang, J., Zhang, M. xu, Chen, M. gong, et al. (2008b) Catalytic effects of eight inorganic additives on pyrolysis of pine wood sawdust by microwave heating. *Journal of Analytical and Applied Pyrolysis*. 82 (1), 145–150.

Chen, M., Wa, J., Zhang, M., Chen, M., et al. (2008c) *Journal of Analytical and Applied Pyrolysis Catalytic effects of eight inorganic additives on pyrolysis of pine wood sawdust by microwave heating*. 82, 145–150.

Chen, W.-T., Ma, J., Zhang, Y., Gai, C., et al. (2014) Physical pretreatments of wastewater algae to reduce ash content and improve thermal decomposition characteristics. *Bioresource technology*. 169, 816–820.

Chen, W., Yang, H., Chen, Y., Xia, M., et al. (2017a) Algae pyrolytic poly-generation: Influence of component difference and temperature on products characteristics. *Energy*. 131 (May), 1–12.

Chen, W., Yang, H., Chen, Y., Xia, M., et al. (2017b) Transformation of nitrogen and evolution of N-containing species during algae pyrolysis. *Environmental Science & Technology*. (June), acs.est.7b00434.

Cheng, S., Wei, L., Zhao, X. & Julson, J. (2016) Application, Deactivation, and Regeneration of Heterogeneous Catalysts in Bio-Oil Upgrading. *Catalysts*. 6 (12), 195.

Cheng, Y.-T. & Huber, G.W. (2012) Production of targeted aromatics by using Diels–Alder classes of reactions with furans and olefins over ZSM-5. *Green Chemistry*. 14 (11), 3114–3125.

Cheng, Y.T., Jae, J., Shi, J., Fan, W., et al. (2012) Production of renewable aromatic compounds by catalytic fast pyrolysis of lignocellulosic biomass with bifunctional Ga/ZSM-5 catalysts. *Angewandte Chemie - International Edition*. 51 (6), 1387–1390.

Chiaramonti, D., Prussi, M., Buffi, M., Casini, D., et al. (2015) Thermochemical Conversion of Microalgae: Challenges and Opportunities. *Energy Procedia*. 75, 819–826.

Chisti, Y. (2007) Biodiesel from microalgae. *Biotechnology advances*. 25 (3), 294–306.

Choi, J.J.-W.W., Choi, J.J.-W.W., Suh, D.J., Ha, J.-M.M., et al. (2014) Production of brown algae pyrolysis oils for liquid biofuels depending on the chemical pretreatment methods. *Energy Conversion and Management*. 86, 371–378.

Chumee, J. & Materials, A. (2013) *Enhanced Quality of Zeolite LSX : Studying Effect of Crystallized Containers*. 380–382.

DEFRA: Department for Environment Food & Rural Affairs (2017) *Crops Grown For Bioenergy in England and the UK: 2016*. (December), 1–2.

Demirbaş, A. (2001) Yields of hydrogen-rich gaseous products via pyrolysis from selected biomass samples. *Fuel*. 80 (13), 1885–1891.

Demirbas, M.F. (2011) Biofuels from algae for sustainable development. *Applied Energy*. 88 (10), 3473–3480.

Derrien, A., Coiffard, L.J.M., Coiffard, C. & De Roeck-Holtzhauer, Y. (1998) Free amino acid analysis of five microalgae. *Journal of Applied Phycology*. 10 (2), 131–134.

Dickerson, T. & Soria, J. (2013) Catalytic fast pyrolysis: A review. *Energies*. 6 (1), 514–538.

Dillon, H. (2009) Algae : fuel of the future ? *Environmental Science and Technology*. (10), 7160–7161.

Dong, W., Shen, Z., Peng, B., Gu, M., et al. (2016) Selective Chemical Conversion of Sugars in Aqueous Solutions without Alkali to Lactic Acid Over a Zn-Sn-Beta Lewis Acid-Base Catalyst. *Scientific Reports*. 6 (January), 26713.

Dong, X., Chen, Z., Xue, S., Zhang, J., et al. (2013) Catalytic pyrolysis of microalga Chlorella pyrenoidosa for production of ethylene, propylene and butene. *RSC Advances*. 3 (48), 25780.

Dong, X., Xue, S., Zhang, J., Huang, W., et al. (2014) The production of light olefins by catalytic cracking of the microalga Isochrysis zhanjiangensis over a modified ZSM-5 catalyst. *Chinese Journal of Catalysis*. 35 (5), 684–691.

Du, Z. (2013) *THERMOCHEMICAL CONVERSION OF MICROALGAE FOR BIOFUEL PRODUCTION*. University of Minnesota.

Du, Z., Hu, B., Ma, X., Cheng, Y., et al. (2013a) Catalytic pyrolysis of microalgae and their three major components: Carbohydrates, proteins, and lipids. *Bioresource Technology*. 130, 777–782.

Du, Z., Ma, X., Li, Y., Chen, P., et al. (2013b) Production of aromatic hydrocarbons by catalytic pyrolysis of microalgae with zeolites: Catalyst screening in a pyroprobe. *Bioresource Technology*. 39, 397–401.

Du, Z., Mohr, M., Ma, X., Cheng, Y., et al. (2012) Hydrothermal pretreatment of microalgae for production of pyrolytic bio-oil with a low nitrogen content. *Bioresource Technology*. 120, 13–18.

Energy and Climate Change Committee (2016) *2020 renewable heat and transport targets Second Report of Session 2016–17*. 7.

Fahmi, R., Bridgwater, A.V., Donnison, I., Yates, N., et al. (2008) The effect of lignin and inorganic species in biomass on pyrolysis oil yields, quality and stability. *Fuel*. 87 (7), 1230–1240.

Fermoso, J., Coronado, J.M., Serrano, D.P. & Pizarro, P. (2017a) *Pyrolysis of microalgae for fuel production*. Elsevier Ltd.

Fermoso, J., Pizarro, P., Coronado, J.M. & Serrano, D.P. (2017b) Advanced biofuels production by upgrading of pyrolysis bio-oil. *Wiley Interdisciplinary Reviews: Energy and Environment*. (February), 1–18.

Ferrell, J. & Sarisky-Reed, V. (2010) National Algal Biofuels Technology Roadmap. *U.S. Department of Energy*. (May), 140.

Foley, P.M., Beach, E.S. & Zimmerman, J.B. (2011) Algae as a source of renewable chemicals: opportunities and challenges. *Green Chemistry*. 13 (6), 1399.

Foster, A.J., Jae, J., Cheng, Y.T., Huber, G.W., et al. (2012) Optimizing the aromatic yield and distribution from catalytic fast pyrolysis of biomass over ZSM-5. *Applied Catalysis A: General*. 423–424, 154–161.

French, R. & Czernik, S. (2010) Catalytic pyrolysis of biomass for biofuels production. *Fuel Processing Technology*. 91 (1), 25–32.

Gable, K. (2013) *FTIR instrumentation and theory*. 2013. Http://Chemistry.Oregonstate.Edu/Courses/Ch361-464/Ch362/Irinstrs.Htm.

Gai, C., Zhang, Y., Chen, W.T., Zhang, P., et al. (2013) Thermogravimetric and kinetic analysis of thermal decomposition characteristics of low-lipid microalgae. *Bioresource Technology*. 150, 139–148.

Gouveia, L. (2011) Microalgae as a feedstock for biodiesel. *SpringBriefs in Microbiology*. 25 (1), 31–43.

Grierson, S., Strezov, V., Ellem, G., Mcgregor, R., et al. (2009) Thermal characterisation of microalgae under slow pyrolysis conditions. *Journal of Analytical and Applied Pyrolysis*. 85 (1–2), 118–123.

Grierson, S., Strezov, V. & Shah, P. (2011) Properties of oil and char derived from slow pyrolysis of Tetraselmis chui. *Bioresource Technology*. 102 (17), 8232–8240.

Hannon, M., Gimpel, J., Tran, M., Rasala, B., et al. (2010) Biofuels from algae: challenges and potential. *Biofuels*. 1 (5), 763–784.

Harman-Ware, A.E., Morgan, T., Wilson, M., Crocker, M., et al. (2013) Microalgae as a renewable fuel source: Fast pyrolysis of Scenedesmussp. *Renewable Energy*. 60, 625–632.

Harun, R. & Danquah, M.K. (2011) Influence of acid pre-treatment on microalgal biomass for bioethanol production. *Process Biochemistry*. 46 (1), 304–309.

Hernando, H., Fermoso, J., Moreno, I., Coronado, J.M., et al. (2017a) Thermochemical

Fermoso, J., Coronado, J.M., Serrano, D.P. & Pizarro, P. (2017a) *Pyrolysis of microalgae for fuel production*. Elsevier Ltd.

Fermoso, J., Pizarro, P., Coronado, J.M. & Serrano, D.P. (2017b) Advanced biofuels production by upgrading of pyrolysis bio-oil. *Wiley Interdisciplinary Reviews: Energy and Environment*. (February), 1–18.

Ferrell, J. & Sarisky-Reed, V. (2010) National Algal Biofuels Technology Roadmap. *U.S. Department of Energy*. (May), 140.

Foley, P.M., Beach, E.S. & Zimmerman, J.B. (2011) Algae as a source of renewable chemicals: opportunities and challenges. *Green Chemistry*. 13 (6), 1399.

Foster, A.J., Jae, J., Cheng, Y.T., Huber, G.W., et al. (2012) Optimizing the aromatic yield and distribution from catalytic fast pyrolysis of biomass over ZSM-5. *Applied Catalysis A: General*. 423–424, 154–161.

French, R. & Czernik, S. (2010) Catalytic pyrolysis of biomass for biofuels production. *Fuel Processing Technology*. 91 (1), 25–32.

Gable, K. (2013) *FTIR instrumentation and theory*. 2013. Http://Chemistry.Oregonstate.Edu/Courses/Ch361-464/Ch362/Irinstrs.Htm.

Gai, C., Zhang, Y., Chen, W.T., Zhang, P., et al. (2013) Thermogravimetric and kinetic analysis of thermal decomposition characteristics of low-lipid microalgae. *Bioresource Technology*. 150, 139–148.

Gouveia, L. (2011) Microalgae as a feedstock for biodiesel. *SpringBriefs in Microbiology*. 25 (1), 31–43.

Grierson, S., Strezov, V., Ellem, G., Mcgregor, R., et al. (2009) Thermal characterisation of microalgae under slow pyrolysis conditions. *Journal of Analytical and Applied Pyrolysis*. 85 (1–2), 118–123.

Grierson, S., Strezov, V. & Shah, P. (2011) Properties of oil and char derived from slow pyrolysis of Tetraselmis chui. *Bioresource Technology*. 102 (17), 8232–8240.

Hannon, M., Gimpel, J., Tran, M., Rasala, B., et al. (2010) Biofuels from algae: challenges and potential. *Biofuels*. 1 (5), 763–784.

Harman-Ware, A.E., Morgan, T., Wilson, M., Crocker, M., et al. (2013) Microalgae as a renewable fuel source: Fast pyrolysis of Scenedesmussp. *Renewable Energy*. 60, 625–632.

Harun, R. & Danquah, M.K. (2011) Influence of acid pre-treatment on microalgal biomass for bioethanol production. *Process Biochemistry*. 46 (1), 304–309.

Hernando, H., Fermoso, J., Moreno, I., Coronado, J.M., et al. (2017a) Thermochemical

valorization of camelina straw waste via fast pyrolysis. *Biomass Conversion and Biorefinery*. (May).

Hernando, H., Fermoso, J., Ochoa-Hernández, C., Opanasenko, M., et al. (2017b) Performance of MCM-22 zeolite for the catalytic fast-pyrolysis of acid-washed wheat straw. *Catalysis Today*. (April).

Hu, Z., Zheng, Y., Yan, F., Xiao, B., et al. (2013) Bio-oil production through pyrolysis of blue-green algae blooms (BGAB): Product distribution and bio-oil characterization. *Energy*. 52, 119–125.

Huang, F.-Y. (2012) Thermal Properties and Thermal Degradation of Cellulose Tri-Stearate (CTs). *Polymers*. 4 (2), 1012–1024.

Huang, F., Tahmasebi, A., Maliutina, K. & Yu, J. (2017) Formation of nitrogen-containing compounds during microwave pyrolysis of microalgae: Product distribution and reaction pathways. *Bioresource Technology*. 245 (July), 1067–1074.

Huber, G.W. & Corma, A. (2007) Synergies between bio- and oil refineries for the production of fuels from biomass. *Angewandte Chemie (International ed. in English)*. 46 (38), 7184–7201.

Hyung, J., Chul, H. & Jin, D. (2014) Pyrolysis of Seaweeds for Bio-oil and Bio-char Production. *Chemical Engineering Transaction*. 37, 121–126.

Imran, A., Bramer, E.A., Seshan, K. & Brem, G. (2016) Catalytic flash pyrolysis of biomass using different types of zeolite and online vapor fractionation. *Energies*. 9 (3), 1–17.

Jae, J., Tompsett, G. a., Foster, A.J., Hammond, K.D., et al. (2011) Investigation into the shape selectivity of zeolite catalysts for biomass conversion. *Journal of Catalysis*. 279 (2), 257–268.

Jahirul, M., Rasul, M., Chowdhury, A. & Ashwath, N. (2012) Biofuels Production through Biomass Pyrolysis —A Technological Review. *Energies*. 5 (12), 4952–5001.

Jindo, K., Mizumoto, H., Sawada, Y., Sanchez-Monedero, M.A., et al. (2014) Physical and chemical characterization of biochars derived from different agricultural residues. *Biogeosciences*. 11 (23), 6613–6621.

Jones, C.S. & Mayfield, S.P. (2012) Algae biofuels: versatility for the future of bioenergy. *Current opinion in biotechnology*. 23 (3), 346–351.

Kodasma, R., Fermoso, J. & Sanna, A. (2019) Li-LSX-zeolite evaluation for post-combustion CO2 capture. *Chemical Engineering Journal*. 358 (October), 1351–1362.

Kumar, G., Shobana, S., Chen, W.-H., Bach, Q.-V., et al. (2017) A review of thermochemical conversion of microalgal biomass for biofuels: chemistry and processes. *Green Chem.* 19 (1), 44–67.

Laird, D.A. (2010) *Chapter 16 Pyrolysis and Biochar-Opportunities for Distributed Production and Soil Quality Enhancement*. (Figure 1), 257–281.

Laskar, D.D., Tucker, M.P., Chen, X., Helms, G.L., et al. (2014) Noble-metal catalyzed hydrodeoxygenation of biomass-derived lignin to aromatic hydrocarbons. *Green Chemistry*. 16 (2), 897.

Lee, A.F. & Wilson, K. (2014) Recent developments in heterogeneous catalysis for the sustainable production of biodiesel. *Catalysis Today*.

Lehto, J., Oasmaa, A., Solantausta, Y., Kytö, M., et al. (2014) Review of fuel oil quality and combustion of fast pyrolysis bio-oils from lignocellulosic biomass. *Applied Energy*. 116, 178–190.

Li, H., Liu, Z., Zhang, Y., Li, B., et al. (2014a) Conversion efficiency and oil quality of low-lipid high-protein and high-lipid low-protein microalgae via hydrothermal liquefaction. *Bioresource Technology*. 154, 322–329.

Li, J., Li, X., Zhou, G., Wang, W., et al. (2014b) Catalytic fast pyrolysis of biomass with mesoporous ZSM-5 zeolites prepared by desilication with NaOH solutions. *Applied Catalysis A: General*. 470, 115–122.

Li, L.L., Zhang, R., Tong, D.M. & Hu, C.W. (2015) Fractional Pyrolysis of Algae and Model Compounds. *Chinese Journal of Chemical Physics*. 28 (4), 525–532.

Li, P., Wang, X., Gong, W., Yang, H., et al. (2013) Effects of metal salt additives on biomass microwave pyrolysis characteristic. *Nongye Jixie Xuebao/Transactions of the Chinese Society for Agricultural Machinery*. 44 (6), 162–167.

López, A., de Marco, I., Caballero, B.M., Adrados, A., et al. (2011) Deactivation and regeneration of ZSM-5 zeolite in catalytic pyrolysis of plastic wastes. *Waste Management*. 31 (8), 1852–1858.

Lorenzetti, C., Conti, R., Fabbri, D. & Yanik, J. (2016) A comparative study on the catalytic effect of H-ZSM5 on upgrading of pyrolysis vapors derived from lignocellulosic and proteinaceous biomass. *Fuel*. 166 (October), 446–452.

Luque, R., Editors, G., Jang, B.W., Gläser, R., et al. (2010) Fuels of the future. *Energy & Environmental Science*. 3 (3), 253.

Maity, J.P., Bundschuh, J., Chen, C.-Y. & Bhattacharya, P. (2014) Microalgae for third generation biofuel production, mitigation of greenhouse gas emissions and wastewater treatment: Present and future perspectives – A mini review. *Energy*. 78, 104–113.

Mayer, Z. a., Apfelbacher, A. & Hornung, A. (2012) A comparative study on the pyrolysis of metal- and ash-enriched wood and the combustion properties of the gained char. *Journal of Analytical and Applied Pyrolysis*. 96, 196–202.

McKendry, P. (2002) Energy production from biomass (part 2): Conversion technologies. *Bioresource Technology*. 83 pp.47–54.

Miao, X., Wu, Q. & Yang, C. (2004) Fast pyrolysis of microalgae to produce renewable fuels. *Journal of Analytical and Applied Pyrolysis*. 71, 855–863.

Micromeritics (2012) *Gas sorption Analyses*. 1–6.

Mohan, S.V., Devi, M.P., Subhash, G.V. & Chandra, R. (2014) *Algae Oils as Fuels.*. Elsevier B.V.

Mortensen, P.M., Grunwaldt, J.-D., Jensen, P. a., Knudsen, K.G., et al. (2011) A review of catalytic upgrading of bio-oil to engine fuels. *Applied Catalysis A: General*. 407 (1–2), 1–19.

Naik, S.N., Goud, V. V., Rout, P.K. & Dalai, A.K. (2010) Production of first and second generation biofuels: A comprehensive review. *Renewable and Sustainable Energy Reviews*. 14 (2), 578–597.

O'neil, G.W., Carmichael, C. a., Goepfert, T.J., Fulton, J.M., et al. (2012) Beyond fatty acid methyl esters: Expanding the renewable carbon profile with alkenones from Isochrysis sp. *Energy and Fuels*. 26, 2434–2441.

O'Neil, G.W., Knothe, G., Williams, J.R., Burlow, N.P., et al. (2014) Synthesis and analysis of an alkenone-free biodiesel from isochrysis sp. *Energy and Fuels*. 28 (4), 2677–2683.

Olivares-Marin, M., Drage, T.C. & Maroto-Valer, M.M. (2010) Novel lithium-based sorbents from fly ashes for CO2 capture at high temperatures. *International Journal of Greenhouse Gas Control*. 4 (4), 623–629.

Paasikallio, V., Kalogiannis, K., Lappas, A., Lehto, J., et al. (2017) Catalytic Fast Pyrolysis: Influencing Bio-Oil Quality with the Catalyst-to-Biomass Ratio. *Energy Technology*. 5 (1).

Pan, P., Hu, C., Yang, W., Li, Y., et al. (2010) The direct pyrolysis and catalytic pyrolysis of Nannochloropsis sp. residue for renewable bio-oils. *Bioresource Technology*. 101, 4593–4599.

Parikh, J., Channiwala, S. & Ghosal, G. (2005) A correlation for calculating HHV from proximate analysis of solid fuels. *Fuel*. 84 (5), 487–494.

Park, J.H., Choppala, G., Lee, S.J., Bolan, N., et al. (2013) Comparative sorption of Pb and Cd by biochars and its implication for metal immobilization in soils topical

collection on remediation of site contamination. *Water, Air, and Soil Pollution*. 224 (12).

Patil, V., Tran, K.Q. & Giselrød, H.R. (2008) Towards sustainable production of biofuels from microalgae. *International Journal of Molecular Sciences.*. 9 pp.1188–1195.

Phukan, M.M., Chutia, R.S., Konwar, B.K. & Kataki, R. (2011) Microalgae Chlorella as a potential bio-energy feedstock. *Applied Energy*. 88 (10), 3307–3312.

Phusunti, N. (2012) *Pryolytic and kinetic study of Chlorella Vulgaris under isothermal and non- isothermal conditions*. Aston University.

Pütün, E. (2010) Catalytic pyrolysis of biomass: Effects of pyrolysis temperature, sweeping gas flow rate and MgO catalyst. *Energy*. 35 (7), 2761–2766.

Pütün, E., Serrano-ruiz, J.C., Luque, R., Campelo, J.M., et al. (2014) Green Chemistry – Guidelines for Referees Green Chemistry publishes high quality research and reviews. *Bioresource Technology*. 4 (1), 1944–1957.

Raheem, A., Wan Azlina, W.A.K.G., Taufiq Yap, Y.H., Danquah, M.K., et al. (2015) Thermochemical conversion of microalgal biomass for biofuel production. *Renewable and Sustainable Energy Reviews*. 49, 990–999.

Raveendran, K., Ganesh, A., Khilar, K.C., Mukarakate, C., et al. (2017) Catalytic Pyrolysis of Biomass in a Fluidized Bed Reactor Cristina Gonzalez-Fernandez and Rau´ l Mun˜oz (ed.). *Bioresource Technology*. 9 (1), 473–480.

Rogers, K.A. & Zheng, Y. (2016) Selective Deoxygenation of Biomass-Derived Bio-oils within Hydrogen-Modest Environments: A Review and New Insights. *ChemSusChem*. 9 (14), 1750–1772.

Ross, a. B., Anastasakis, K., Kubacki, M. & Jones, J.M. (2009) Investigation of the pyrolysis behaviour of brown algae before and after pre-treatment using PY-GC/MS and TGA. *Journal of Analytical and Applied Pyrolysis*. 85 (1–2), 3–10.

Ross, a, Jones, J., Kubacki, M. & Bridgeman, T. (2008) Classification of macroalgae as fuel and its thermochemical behaviour. *Bioresource Technology*. 99 (14), 6494–6504.

Sacha Alberici and Gemma Toop (2013) *UK biofuel industry overview*. (Department for Transport (DfT) UK).

Sanchez-Silva, L., López-González, D., Garcia-Minguillan, A.M. & Valverde, J.L. (2013) Pyrolysis, combustion and gasification characteristics of Nannochloropsis gaditana microalgae. *Bioresource Technology*. 130, 321–331.

Sanna, Aimaro, Maroto-Valer, M. (2016) CO 2 capture at high temperature using fly ash-derived sodium silicates. *Industrial & Engineering Chemistry Research*. 55, 4080–

4088.

Sanna, A. (2013) Advanced Biofuels from Thermochemical Processing of Sustainable Biomass in Europe. *BioEnergy Research*. 7 (1), 36–47.

Sanna, A. & Abd Rahman, N.A. (2015) Conversion of Microalgae Bio-oil into Bio-diesel. In: A. Prokop et Al. (ed.). *Algal Biorefineries*. Springer International Publishing Switzerland. pp. 493–510.

Sanna, A., Ramli, I. & Mercedes Maroto-Valer, M. (2015) Development of sodium/lithium/fly ash sorbents for high temperature post-combustion CO2 capture. *Applied Energy*. 156, 197–206.

Sawangkeaw, R. & Ngamprasertsith, S. (2013) A review of lipid-based biomasses as feedstocks for biofuels production. *Renewable and Sustainable Energy Reviews*. 25, 97–108.

Sawant, S.D., Baravkar, A.A. & Kale, R.N. (2011) FT-IR spectroscopy: Principle, technique and mathematics. *International Journal of Pharma and Bio Sciences*. 2 (1), 513–519.

Scott A Speakman (2009) *Basic X-ray Powder Diffraction (XRPD)*. [Online]. 2009. Available from: https://serc.carleton.edu/research_education/geochemsheets/techniques/XRD.html.

Serrano-ruiz, J.C. & Dumesic, J.A. (2012) Catalytic Production of Liquid Hydrocarbon Transportation Fuels. *Catalysis for Aternative Energy Generation*. 29–57.

Serrano-Ruiz, J.C., Luque, R., Campelo, J.M. & Romero, A. a. (2012) Continuous-Flow Processes in Heterogeneously Catalyzed Transformations of Biomass Derivatives into Fuels and Chemicals. *Challenges*. 3 (2), 114–132.

Shao, S., Zhang, H., Xiao, R., Li, X., et al. (2018) Controlled regeneration of ZSM-5 catalysts in the combined oxygen and steam atmosphere used for catalytic pyrolysis of biomass-derivates. *Energy Conversion and Management*. 155 (October 2017), 175–181.

Shin, H.Y., Lim, S.M., Bae, S.Y. & Oh, S.C. (2011) Thermal decomposition and stability of fatty acid methyl esters in supercritical methanol. *Journal of Analytical and Applied Pyrolysis*. 92 (2), 332–338. A

Singh, J. & Gu, S. (2010) Commercialization potential of microalgae for biofuels production. *Renewable and Sustainable Energy Reviews*. 14 (9), 2596–2610.

Spolaore, P., Joannis-Cassan, C., Duran, E. & Isambert, A. (2006) Open Archive Toulouse Archive Ouverte (OATAO) Commercial Applications of Microalgae. *Journal of Bioscience and Bioenginering*. 101, 87–96.

Suan, N.H., Juan, J.C., Show, P.L., Yap, J.Y., et al. (2017) Microalgae biorefinery: High value products perspectives. *Bioresource Technology*. 229 (January), 53–62.

Suganya, T., Varman, M., Masjuki, H.H. & Renganathan, S. (2016) Macroalgae and microalgae as a potential source for commercial applications along with biofuels production: A biorefinery approach. *Renewable and Sustainable Energy Reviews*. 55.

Thangalazhy-Gopakumar, S., Adhikari, S., Chattanathan, S.A. & Gupta, R.B. (2012) Catalytic pyrolysis of green algae for hydrocarbon production using H+ZSM-5 catalyst. *Bioresource technology*. 118, 150–157.

Thompson, M. (2008) CHNS elemental analysers. *AMC Technical briefs*. (29), 1–2.

Wang, J., Zhang, M., Chen, M., Min, F., et al. (2006) Catalytic effects of six inorganic compounds on pyrolysis of three kinds of biomass. *Thermochimica Acta*. 444 (1), 110–114.

Wang, K. & Brown, R.C. (2013) Catalytic pyrolysis of microalgae for production of aromatics and ammonia. *Green Chemistry*. 15 (3), 675.

Wang, X., Zhao, B., Tang, X. & Yang, X. (2015) Comparison of direct and indirect pyrolysis of micro-algae Isochrysis. *Bioresource Technology*. 179, 58–62.

Wijffels, R.H., Barbosa, M.J., Oswald, W.J., Golueke, C.G., et al. (2010) An outlook on microalgal biofuels. *Science (New York, N.Y.)*. 329 (5993), 796–799.

Xiu, S. & Shahbazi, A. (2012) Bio-oil production and upgrading research: A review. *Renewable and Sustainable Energy Reviews*. 16 (7), 4406–4414.

Yu, K.L., Lau, B.F., Show, P.L., Ong, H.C., et al. (2017) Recent developments on algal biochar production and characterization. *Bioresource Technology*. 246 (June), 2–11.

Yue, D., You, F. & Snyder, S.W. (2014) Biomass-to-bioenergy and biofuel supply chain optimization: Overview, key issues and challenges. *Computers & Chemical Engineering*. 66, 36–56.

Zainan, N.H., Srivatsa, S.C. & Bhattacharya, S. (2015) Catalytic pyrolysis of microalgae Tetraselmis suecica and characterization study using in situ Synchrotron-based Infrared Microscopy. *Fuel*. 161 (May 2016), 345–354.

Zanota, M.-L., Heymans, N., Gilles, F., Su, B.-L., et al. (2011) Thermodynamic study of LiNaKLSX zeolites with different Li exchange rate for N2/O2 separation process. *Microporous and Mesoporous Materials*. 143 (2–3), 302–310.

Zeng, Y., Zhao, B., Zhu, L., Tong, D., et al. (2013) Catalytic pyrolysis of natural algae from water blooms over nickel phosphide for high quality bio-oil production. *RSC Advances*. 3 (27), 10806.

Zhang, B., Zhong, Z.P., Wang, X.B., Ding, K., et al. (2015) Catalytic upgrading of fast pyrolysis biomass vapors over fresh, spent and regenerated ZSM-5 zeolites. *Fuel Processing Technology*. 138, 430–434.

Zhang, H., Shao, S., Xiao, R., Shen, D., et al. (2014) Characterization of coke deposition in the catalytic fast pyrolysis of biomass derivates. *Energy and Fuels*. 28 (1), 52–57.

Zhang, H., Xiao, R., Jin, B., Xiao, G., et al. (2013) Biomass catalytic pyrolysis to produce olefins and aromatics with a physically mixed catalyst. *Bioresource technology*. 140, 256–262.

Appendices

Appendix A
Mass balance data

Example of data collected for a pyrolysis experiment. Run at T=500 °C

	Without cat		With cat	
Experiment	No 5001	No 5002	5001	5002
Date				
Algae	1.503	1.510	1.510	1.507
Cat	0.000	0.000	1.509	1.505
Total algae + cat.	1.509	1.510	3.041	3.015
Char + cat.	0.519	0.530	2.038	2.028
Bottle before 1	158.491	158.640	158.495	151.918
Bottle before 2	148.792	148.772	148.769	158.389
Bottle before 3	193.022	193.056	193.019	192.482
Bottle after 1	158.786	158.922	158.650	152.070
Bottle after 2	148.830	148.826	148.849	158.451
Bottle after 3	193.248	193.282	193.230	192.696
Bio-oil 1	0.295	0.282	0.155	0.152
Bio-oil 2	0.038	0.054	0.080	0.062

Bio-oil 3	0.226	0.226	0.211	0.214

Yield

Bio- char	0.519	0.530	0.529	0.523
Bio-oil	0.559	0.562	0.446	0.428
Gas	0.425	0.418	0.535	0.556

(wt.%)

Bio- char	34.53	35.10	35.03	34.70
Bio-oil	37.19	37.22	29.54	28.40
Gas	28.28	27.67	35.43	36.89

AVG

Bio-char	34.83	34.85
Bio-oil	37.22	28.97
Gas	27.94	36.18

Appendix B
GC-MS data analysis

Below are reported two examples of the GC-MS spectra for he -oils from pyrolysis (with and without catalyst) run at 500 °C.

Typically, the reading of the GC-MS data was taken until retention time 55.0 minutes. Since the compounds identified after 55 minutes were assigned to contamination (plasticizers). The compounds present in the bio-oil were divided into different groups. Table A2 shows some of the compounds present in the different functional groups of the bio-oils.

Alcohol	Carboxylic acid
Nonadecanol	Benzyl oxy tridecanoic acid
Octadecanol	n-Hexadecanoic acid
Tridecen-1-ol	Tetradecanoic acid
Benzenemethanol	Carbamic acid
Aldehyde	**Ester**
Octadecenal	Dodecanoic acid, 2,4,5-trichlorophenyl ester
Pentanal, 2-methyl-	Fumaric acid, butyl 1-naphthyl ester
7-Tetradecenal	Pentafluoropropionic acid, decyl ester
Aliphatics	6-Bromohexanoic acid, 4-hexadecyl ester
Docosane	Butanal, 2-methyl- Propanoic acid
Tridecane	**Ether**
Tetradecene	Methylnonadecanoate

|	
Pentadecane	Z-4-Tridecen-1-yl acetate
Hexadecene	Methyl tetradecanoate
Octadecene	**Ketone**
Hexane	Pentadecanone
Cyclohexane	Hexadecanone
Cyclopentane	Heneicosanone
Aromatics	Nonadecanone
Phenol	**Nitrogen compounds**
Chamazulene	Hexadecanamide
Naphthalene	Oleanitrile
Phenanthrene	3-Methylcarbazole
Thymol	Propanamide
p-Cresol	Dodecanamide
Toluene	Pyridine
Benzene	1H-Indole

Appendix C

¹H NMR spectra
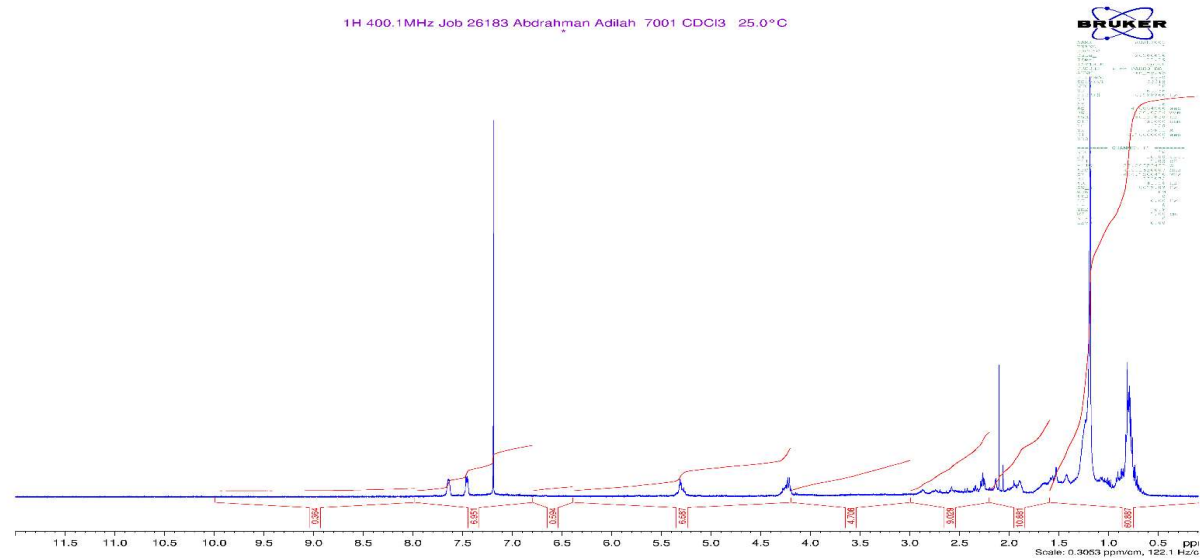
Figure A-1 Proton NMR integrations.